THE UNIVERSITY
of LIVERPOOL

The Effects of Mitochondria-Targeted Antioxidant Mitoquinone on Pancreatic Acinar Cells

Thesis submitted in accordance with the requirements of the University of Liverpool for the degree of Doctor in Philosophy

By

Nicole Joanne Cash

September 2015

Abstract

While oxidative stress has been repeatedly implicated in the pathogenesis of acute pancreatitis (AP), recent clinical evidence has found little benefit of general antioxidant therapy. The actions, however, of newer mitochondria-targeted antioxidants such as MitoQ, have yet to be determined in AP. A recently undertaken *in vivo* study by our group has highlighted mixed effects of MitoQ treatment in caerulein-induced AP (CER-AP) and no protection against bile acid-induced AP (TLCS-AP).

Therefore, the *in vitro* effects of MitoQ against toxin-induced pathophysiological effects of bile acid taurolithocholic acid-3-sulphate (TLCS) and caerulein analogue CCK hyperstimulation were determined. Furthermore, the effects of MitoQ on pancreatic acinar cell physiology and cell death were evaluated and compared to non-antioxidant analogue DecylTPP (dTPP). Additional investigations assessed the potential protective capabilities of MitoQ against non-oxidative ethanol metabolite palmitoleic acid ethyl ester (POAEE)-, ethanol- and H_2O_2-induced effects. These experiments were carried out alongside a more detailed assessment of H_2O_2-induced effects in isolated pancreatic acinar cells.

Key Findings

- MitoQ and non-antioxidant analogue dTPP caused predominantly adverse effects on pancreatic acinar cell responses, in a concentration-dependent manner. These effects are likely due to the targeting component of both TPP^+ derivatives.
- *In vitro*, MitoQ did not protect against bile acid TLCS- and CCK hyperstimulation-induced effects on mitochondrial membrane potential ($\Delta\Psi m$), NAD(P)H levels, cytosolic Ca^{2+} concentration ($[Ca^{2+}]_c$), cellular apoptosis or necrosis.
- CCK and TLCS treatment *in vitro*, led to differing levels and mode of cell death. CCK induced substantial apoptosis and necrosis, the latter in a biphasic pattern. In contrast, the predominant mode of cell death with TLCS treatment was necrosis. These results mirror *in vivo* results in AP models demonstrating a more severe AP pathophysiology with TLCS-induced AP than CCK/caerulein-induced AP.
- MitoQ had no effects on POAEE- and ethanol-induced cellular necrosis. In contrast, MitoQ provided a mild inhibition of apoptosis in a concentration-dependent manner, consistent with a proposed role of reactive oxygen species (ROS) to promote apoptosis in these cells.
- H_2O_2 induced concentration-dependent effects on levels of ROS, NAD(P)H/FAD^+, $[Ca^{2+}]_c$, $\Delta\Psi m$, cellular apoptosis and necrosis. Low micromolar concentrations favoured apoptosis and high millimolar concentrations necrosis.
- MitoQ effectively inhibited H_2O_2-induced ROS increases. However, MitoQ exacerbated H_2O_2-induced effects on NAD(P)H/FAD^+ levels and provided no protection against high micromolar and millimolar H_2O_2-induced cell death.

These results enhance our understanding of the ROS balance in pancreatic acinar cells. The findings of this study emphasize the unsuitability of the use of targeted antioxidant therapy in the treatment of AP.

The novel effects of H_2O_2 on mitochondrial metabolism, observed at low micromolar concentrations, highlight our incomplete understanding of the role of ROS in cellular function and warrant further investigation.

Acknowledgements

Firstly, I wish to thank my supervisors Dr David Criddle and Professor Robert Sutton for their continued support, advice and encouragement. A special thank you to Dr David Criddle for his patience and guidance during this PhD project, which would not have been possible without his support.

I would like to thank Professor Alexei Tepikin for the help and guidance provided during my time in the laboratory. A thank you to Mischa Chvanov for providing me with invaluable and continuous advice, technical expertise and kindness.

Thank you to David Collier, Tony Parker and Dayani Rajamanoharan for their friendship and constant support.

Thank you to my mentor Professor David Edgar for his unwavering belief in me and Svetlana Voronina for always being available to provide any help needed.

A further thank you to all the members of Blue Block/the PBRU especially Yulin Ouyang, Li Wen, Wei Huang and Jane Armstrong for an array of things and also Mark Houghton, Marie Johnson and Helen Davies.

I would also like to thank everyone else who has been a big support and encouraged me throughout this PhD. Thank you to the BBSRC for funding this project and making this thesis possible.

A huge thank you to my parents, family and friends for their faith, encouragement, love, and putting up with me.

Abbreviations

ACh	Acetyl Choline
ADH	Alcohol dehydrogenase
ALDH	Aldehyde dehydrogenase
ADP	Adenosine diphosphate
cADPr	Cyclic ADP ribose
Akt	Protein kinase B
ALI	Acute lung injury
ANT	Adenine nucleotide translocase
AP	Acute pancreatitis
AP-1	Activator protein 1
ARDS	Acute respiratory distress syndrome
AR42J	Pancreatic tumoural cell line
ASK1	Apoptosis signal regulating kinase 1
ATP	Adenosine triphosphate
BAE	Bovine aortic endothelial
BAPTA	(1,2-bis(o-aminophenoxy)ethane-N,N,N',N'-tetraacetic acid)
BAX	bcl-2-like protein 4
3-BCP	3-benzyl-6-chloro-2-pyrone
BKA	Bongkrekic acid
Ca^{2+}	Ca^{2+} (generic)
$[Ca^{2+}]_c$	Cytosolic Ca^{2+} concentration
$[Ca^{2+}]_m$	Mitochondrial Ca^{2+} concentration
CAT	Catalase
CD38	Cluster of differentiation 38
CEL	Carboxylester lipase
CEM	Human leukemic cell line
CER-AP	Caerulein-stimulated acute pancreatitis model
CypD	Cyclophilin D
CYP2E1	Cytochrome p450 2E1
CCCP	Carbonyl cyanide m-chlorophenlyhydrazone
CCK	Cholecystokinin

Abbreviations

CM-H_2DCFDA	5-(and-6)-chloromethyl-2',7'-dichlorodihydrofluorescein diacetate
CsA	Cyclosporin A
DAG	diacylglycerol
DBTC	dibutyltin-dichloride
DCFDA	Dichlorofluorescin diacetate
DEB025	D-MeAla3-EtVal4-cyclosporine (Alisporivir)
ddH_2O	Double distilled water
DHE	Dihydroethidium
DHR	Dihydrorhodamine-123
dTPP	Decyltriphenylphosphonium bromide
dUb	Decylubiquinone
$\Delta\Psi m$	Mitochondrial membrane potential
DMN	2,4-dimethoxy-2-methylnaphthalene
DMSO	Dimethyl sulphoxide
DPI	Diphenylene iodonium
EGF	Epidermal growth factor
EGR1	Early growth response protein 1
EGTA	Ethylene glycol tetraacetic acid
ER	Endoplasmic reticulum
ERCP	Endoscopic retrograde cholangiopancreatography
ERK	Extracellular-signal-regulated kinase
ESR	Electron spin resonance
ETC	Electron transport chain
EtOH	Ethanol
F_1F_o-ATP synthase	ATP synthase/complex V
$FADH_2$/FAD^+	Flavin adenine dinucleotide (reduced/oxidised)
FA	Fatty acid
FAEE	Fatty acid ethyl ester
FCCP	Carbonyl cyanide-4-(trifluoromethoxy)phenylhydrazone
F/F_o	Fluorescence intensity normalised to the initial intensity
GI	Gastrointestinal
GPCR	G-protein-coupled receptor
GPBAR1	G-protein-coupled bile acid receptor 1
GPx	Glutathione peroxidase
cGMP	cyclic guanosine-3',5' –monophosphate

Abbreviations

GSH	Glutathione
GSSG	Glutathione disulphide
HEK 293T cells	Human Embryonic Kidney 293 cells
HEPES	4-(2-hydroxyethyl)-1-piperazineethaqnesulphonic acid
H_2O_2	Hydrogen peroxide
ICAM	Intercellular Adhesion Molecule 1
I_{CRAC}	Ca^{2+}-release-activated Ca^{2+} current
IκBα	IkappaBalpha
IL-1β	Interleukin-1 beta
IL-6	Interleukin-6
IMM	Inner mitochondrial membrane
IP_3	Inositol 1,4,5 trisphosphate
IP_3R	Inositol 1,4,5 trisphosphate receptor
IRS-1	Insulin receptor substrate 1
JNK	c-Jun N-terminal kinase
α-KGDH	α-ketoglutarate dehydrogenase
KO	Knockout
M40401	SOD mimetic
MAO	Monoamine oxidases
MAPK	Mitogen-activated protein kinases
MCU	Mitochondrial Ca^{2+} uniporter
MDA	Malondialdehyde
MICU1	Mitochondrial Ca^{2+} uptake 1
ΔΨm	Mitochondrial membrane potential
MitoQ	Mitoquinone
MnSOD	Manganese superoxide dismutase
MPTP	Mitochondrial permeability transition pore
MPO	Myeloperoxidase
NAADP	Nicotinic acid adenine dinucleotide phosphate
NADH/NAD^+	Nicotinamide adenine dinucleotide (reduced/oxidised)

Abbreviations

NAC	N-acetylcysteine
NADPH	Nicotinamide adenine dinucleotide phosphate
NCLX	Na^{+}/Ca^{2+} exchanger
ND-07	2-acetoxy-5-(2-4-(trifluoromethyl)-phenethylamino)-benzoic acid
NF-κB	Nuclear factor kappa B
NLRP3	NACHT, LRR and PYD domains-containing protein 3
$NO^{\bullet}$	Nitric oxide
NOX	NADPH oxidase
NQO1	NAD(P)H quinone oxidoreductase 1
$O_2^{\bullet-}$	Superoxide anion
$OH^{\bullet}$	Hydroxyl radical
$ONOO^{-}$	Peroxynitrite
Orai1	Ca^{2+} release-activated Ca^{2+} channel protein 1
PA	Palmitic acid
PAC	Pancreatic acinar cell
PD	Parkinson's disease
PDAC	Pancreatic ductal adenocarcinoma
PDH	Pyruvate dehydrogenase
PEG	Polyethylene glycol
PI	Propidium iodide
PKC	Protein kinase C
PKD	Protein kinase D
Pi	Inorganic phosphate
PI3K	Phosphoinositide 3-kinase
PIP_2	Phosphatidylinositol 4,5-bisphosphate
PLC	Phospholipase C
PM	Plasma membrane
PMA	Phorbol myristate acetate
PMCA	Plasma membrane Ca^{2+}-ATPase

Abbreviations

PMN	Polymorphonuclear leukocyte
POA	Palmitoleic acid
POAEE	Palmitoleic acid ethyl ester
PP2A	Protein phosphatase 2A
$Ppif^{-/-}$	Peptidylprolyl isomerase F (Knockout of cyclophilin D)
Prx1	Peroxiredoxin detoxification enzyme
PSTI	Pancreatic secretory trypsin inhibitor
PTP1B	Protein-tyrosine phosphatase 1B
RNS	Reactive nitrogen species
ROS	Reactive oxygen species
$[ROS]_i$	Intracellular reactive oxygen species
$[ROS]_m$	Mitochondrial reactive oxygen species
RyR	Ryanodine receptor
SAPK	Stress-activated protein kinases
SDH	Succinate dehydrogenase
SERCA	Sarcoplasmic/endoplasmic reticulum Ca^{2+}-ATPase
SkQ1	Plastoquinonyl-decyl-triphenylphosphonium
SIRS	Systemic inflammatory response syndrome
SOCE	Store-operated Ca^{2+}-entry
SOD	Superoxide dismutase
STAT3	Signal Transducer and Activator of Transcription 3
STIM1	Stromal interaction molecule 1
TBARS	Thiobarbituric acid reactive substances
TCA	Tricarboxylic acid
TFB2M	Transcription Factor B 2 (mitochondrial)
TLCS	Taurolithocholic acid -3-sulphate
TLCS-AP	TLCS-stimulated acute pancreatitis model
TMRM	Tetramethyl rhodamine methyl ester
TNF-α	Tumor necrosis factor alpha
TPC	two-pore channel

Abbreviations

TPP^+	(2-Hydroxyethyl)triphenylphosphonium bromide
TRO40303	3,5-Seco-4-nor-cholestan-5-one oxime-3-ol
VDAC	Voltage-dependent anion channel
VIP	Vasoactive intestinal peptide
WT	Wild-type
XOD	Xanthine oxidase
XOH	Xanthine dehydrogenase
Zn/Cu SOD	Zinc/Copper superoxide dismutase

Table of Contents

CHAPTER 2:

Chapter 1

Introduction

The Exocrine Pancreas: Physiological Function

The pancreas is a long, narrow gland located on the left side of the abdominal cavity. It lies posterior and inferior to the stomach, and has a head, tail and body. The widest region of the organ is the head of the pancreas, which connects to the duodenum. Extending laterally, the pancreas narrows slightly to form the body of the pancreas and tapers near the spleen to form the tail region. The organ is dual functioning of both digestive and endocrine systems. Functioning as an endocrine gland, the pancreas produces the hormones insulin and glucagon responsible for glucose homeostasis.

Ninety-nine percent of the pancreas mass, functions as the exocrine gland and is responsible for the production and secretion of digestive enzymes trypsin, amylase, lipase, chymotrypsin, carboxypeptidase and elastase, including bicarbonate from ductal cells. The exocrine pancreas is arranged into acini, clusters of acinar cells surrounding a duct, which converge until the large pancreatic duct. Digestive enzymes secreted into the pancreatic duct are delivered to the duodenum for the digestion of fats, carbohydrates and proteins. The precursor trypsinogen is activated in the duodenum by enteropeptidase to produce trypsin, which then activates further trypsinogen, chymotrypsinogen, procarboxypeptidase and proelastase. The pancreas is controlled by the autonomic nervous system, both sympathetic and parasympathetic. The exocrine pancreatic secretion is regulated primarily by neurotransmitter acetylcholine (ACh), produced by parasympathetic

fibres of the vagus nerve, and circulating gastrointestinal hormone cholecystokinin (CCK). ACh predominantly stimulates pancreatic enzyme secretion with minimal effects on fluid and bicarbonate secretion. CCK on the other hand causes both substantial enzyme and electrolyte secretion. Gastrointestinal (GI) hormone secretin stimulates secretion of bicarbonate from pancreatic and biliary ducts and duodenal Brunner's glands while also acting to potentiate the action of CCK on pancreatic acinar cells (PACs) (Pandol 2010). Vasoactive intestinal polypeptide (VIP) is a structurally similar hormone to secretin, although stimulates a weaker pancreatic response (Rhoades et al. 2009). Secretion of enzymes from the PAC is induced through stimulation of Ca^{2+} release from intracellular stores.

Pancreatic Acinar Cell

PACs are a polarised cell type, the main constituent and workhorse of the exocrine pancreas. They form berry like clusters called acini and surround a small duct (Petersen 1992; Petersen et al. 1999). Close to the ductal lumen, dense core secretary granules containing zymogen are found on the apical side of the cell. These are clearly visible in light microscopy and are secreted via fusion to the apical membrane (Jamieson et al. 1971; Case 1978). The mitochondria are predominantly distributed in the perigranular, perinuclear and subplasmalemmal regions, with the highest density in the Ca^{2+} perigranular region (Jamieson et al. 1971; Tinel et al. 1999; Park et al. 2001; Johnson et al. 2003). There is a dense endoplasmic reticulum

(ER) network extended through the basolateral and perinuclear region (Petersen et al. 1999; Gerasimenko et al. 2002). The nucleus is located at the basal region of the cell, close to the golgi apparatus, a 5 stack structure at the edge of the granular region (Dolman et al. 2005). PACs retro-differentiate into more-duct like cells whilst still retaining the capability for acinar-specific antigen expression (De Lisle et al. 1990). Therefore, primary isolated PACs are most commonly used for experimental investigations *in vitro*.

Ca^{2+} Signalling

The majority of Ca^{2+} in the human body is located in the calcified matrix of bone. The remaining 0.9% acts as an integral and diverse signalling messenger, pivotal to processes such as muscle contractility, stimulating exocytosis of secretory vesicles and gene transcription (Petersen 1992; Berridge et al. 2003; Clapham 2007). Physiological stimulation of PACs causes Ca^{2+} changes of an oscillatory manner. An effect enabled due to low cytosolic concentrations of Ca^{2+} and high buffering capacity of Ca^{2+}-binding proteins and other chelating cytosolic components. Diverse signalling is possible, through varying the frequency, amplitude and distribution of these Ca^{2+} oscillations, enabling the transmission of physiologically relevant information (Berridge et al. 2000). The binding of agonists such as ACh, CCK and secretin/VIP, stimulate enzyme secretion via the activation of specific plasma membrane (PM) receptors (Palade 1975). ACh through the

activation of muscarinic receptors on the basolateral membrane and CCK through the activation of guanine nucleotide-binding protein G protein-coupled receptors (GPCR's) type A and B (Rosenzweig et al. 1983; Ashby et al. 2003; Murphy et al. 2008). Bile acid taurolithocholic acid 3-sulphate (TLCS) induces effects on cytosolic Ca^{2+} release also through the activation of a GPCR, which will be discussed in more detail later in this chapter (Perides et al. 2010). TLCS has been established as the most potent releaser of Ca^{2+} among bile acids tested on PACs to date (Voronina et al. 2002).

Acetylcholine and CCK receptors are both seven transmembrane domain receptors coupled to G proteins. Receptor activation leads to phospholipase C (PLC) cleavage of phosphatidylinositol 4,5-bisphosphate (PIP_2) and mobilisation of secondary intracellular messengers inositol 1,4,5 trisphosphate (IP_3) and diacyl-glycerol (DAG) (Berridge 1981). DAG elicits cellular responses through the activation of protein kinase C (PKC) and protein kinase D (PKD). PKC can also phosphorylate and activate PKD. IP_3 directly interacts with the IP_3 receptor (IP_3R) (Streb et al. 1983) located on the ER intracellular Ca^{2+} store membrane, stimulating release of Ca^{2+} and initiation of intracellular Ca^{2+} signalling. The IP_3R is further stimulated by this Ca^{2+} release and Ca^{2+} sensitive ryanodine receptors (RyR) are activated in a positive feedback loop, leading to propagation of a global Ca^{2+} rise (Adkins et al. 1999; Straub et al. 2000). CCK receptor activation also stimulates adenosine diphosphate (ADP)-ribosyl cyclase activity leading to the synthesis of Ca^{2+} mobilising secondary messenger's cyclic ADP ribose (cADPr) and nicotinate-adenine dinucleotide phosphate (NAADP). The molecular mechanism for CCK-stimulated

NAADP formation is not completely understood, although evidence suggests a role for the enzyme cluster of differentiation 38 (CD38) (Fukushi et al. 2001). On the other hand, ACh stimulation of PACs does not result in detectable accumulation of NAADP (Yamasaki et al. 2005). Ca^{2+} oscillations are maintained by prolonged cADPr elevation which specifically acts upon RyRs to sensitise them to Ca^{2+}-induced channel opening (Galione et al. 1991). NAADP acts upon RyRs, IP_3Rs (Cancela et al. 2000; Gerasimenko et al. 2003) and the two-pore channel (TPC) family of proteins primarily expressed in acidic lysosomal/endosomal compartments (Yamasaki et al. 2004). NAADP plays an important role in the initiation of a Ca^{2+} response, with the rapid production of NAADP preceding the Ca^{2+} signal onset (Cancela et al. 1999; Cancela 2001; Patel et al. 2001). Bile acid TLCS simulates Ca^{2+} release through both IP_3Rs and RyRs; RyRs through the activation of NAADP but not cADPr pathway (Gerasimenko et al. 2006).

PACs are non-excitable and rather than induce Ca^{2+} signals by depolarising the plasma membrane as in excitable cells, Ca^{2+} signals are generated by Ca^{2+} release from intracellular stores as described above (Streb et al. 1984). The main Ca^{2+} pool responsible for Ca^{2+} release, whether a global rise or oscillatory in nature is the ER (Streb et al. 1984; Yule et al. 1988). Hyperstimulation with agonists CCK/ACh and toxic insult with bile acids and non-oxidative fatty acid metabolites, induce a sustained global elevation of cytosolic Ca^{2+} (Kim et al. 2002; Voronina et al. 2002; Criddle et al. 2004; Criddle et al. 2006). The maintenance of cytosolic Ca^{2+} concentration ($[Ca^{2+}]_c$) rises, is dependent on Ca^{2+} entry into the cell. The influx of Ca^{2+} through store-operated Ca^{2+} entry (SOCE), is induced by a lowered ER luminal

Ca^{2+} concentration (Putney 1986). The Ca^{2+} sensor, stromal interaction molecule 1 (STIM1) (Liou et al. 2005; Roos et al. 2005; Zhang et al. 2006) is an integral ER membrane protein. STIM1 senses ER Ca^{2+} depletion, through the disassociation of Ca^{2+} from the ER hand, leading to the translocation and aggregation of STIM1 at ER sites close to the PM (Lur et al. 2009). STIM1 then physically gates the plasma membrane pore-forming Orai1, which mediates Ca^{2+} influx, leading to Ca^{2+}-release-activated Ca^{2+} current (I_{CRAC}) (Feske et al. 2006; Prakriya et al. 2006; Gwack et al. 2007; Hong et al. 2011). As Ca^{2+} influx is critical to the maintenance of Ca^{2+} oscillations and sustained Ca^{2+} rises (Huang et al. 2006), the absence of a functional Na^{+}/Ca^{2+} exchanger renders PACs crucially reliant upon adenosine triphosphate (ATP) levels for Ca^{2+} homeostasis (Muallem et al. 1988).

In PACs, cytosolic Ca^{2+} clearance occurs via plasma membrane ATP dependent Ca^{2+}-ATPase pumps, the plasma membrane Ca^{2+}-ATPase (PMCA) and sarco-endoplasmic reticulum Ca^{2+}-ATPase (SERCA). The majority of PMCAs are located in the apical region of the cell (Lee et al. 1997) correlating with the level of Ca^{2+} extrusion in this region (Belan et al. 1996; Belan et al. 1997). Disruption to normal Ca^{2+} signalling occurs early in murine models of AP (Ward et al. 1996) and is responsible for premature enzyme activation and necrosis (Duchen 1999; Raraty et al. 2000; Gukovskaya et al. 2002).

Figure 1.1

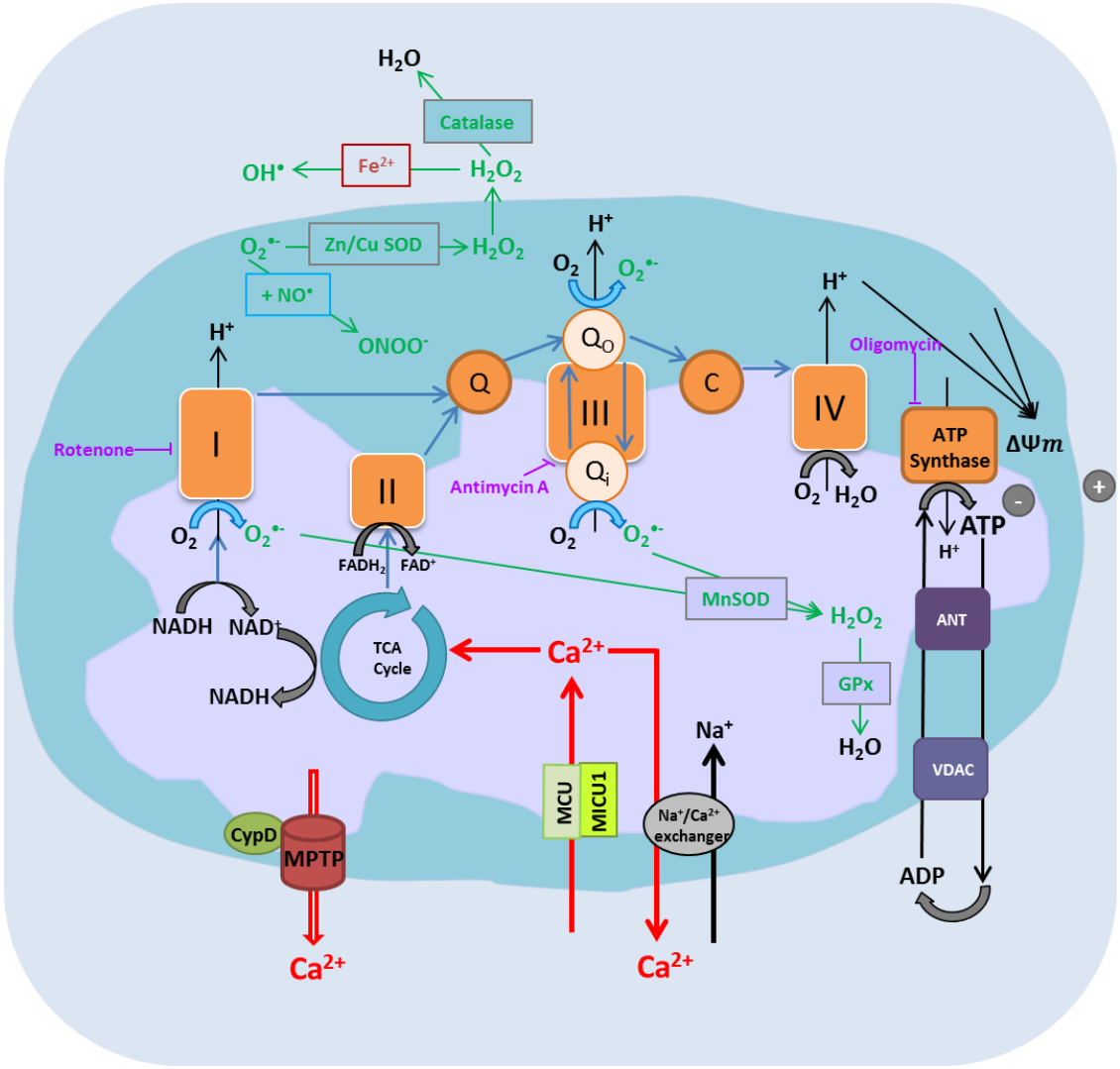

Figure 1.1 Mitochondrial Ca^{2+} transport and reactive oxygen species (ROS) production. Ca^{2+} import occurs via the MCU/MICU1. The calcium exchangers are responsible for Ca^{2+} export and the MPTP facilitates free diffusion of solutes less than 1.5kDa when open. Ca^{2+} influx activates the TCA cycle leading to increased production of nicotinamide adenine dinucleotide (NADH) that fuels the ETC through an initial donation of electrons to complex I. Protons pumped into the intermembrane space generate the mitochondrial membrane potential (ΔΨm) used by complex V to generate ATP. ROS superoxide is produced at complex I of the ETC into the mitochondrial matrix and complex III into both matrix and intermembrane space. $O_2^{\bullet-}$ is dismutated to H_2O_2 by superoxide dismutases (SOD) manganese SOD (MnSOD) in the matrix and zinc/copper (Zn/Cu) SOD in the cytosol. H_2O_2 is then converted to H_2O by matrix glutathione peroxidase (GPx) and cytosolic catalase. ETC electron flow is illustrated with dark blue arrows and arrows in pale blue the electron flow involved in ROS production. Common ETC complex inhibitors are shown in pink. Adapted from Viola et al. (2010) ©.

Ca^{2+} and Mitochondrial Physiology

In PACs, as mentioned, mitochondrial distribution is perigranular, perinuclear and subplasmalemmal with the greatest density found in the perigranular region. Mitochondria are a critical component of all cells and are frequently described as the powerhouse, generating ATP through oxidative phosphorylation and approximately 90% of the total ROS generation in healthy cells (Herst et al. 2004). The process of ATP synthesis by F_1F_o-ATP synthase (ATP synthase/complex V) involves oxidation of metabolites in the tricarboxylic acid (TCA) cycle. Nicotinamide adenine dinucleotide (NADH) and flavin adenine dinucleotide ($FADH_2$) are produced and supply electrons to the electron transport chain (ETC) at complexes I and II (Brand et al. 1987). Ubiquinone connects complexes I and II to complex III through accepting NADH and $FADH_2$-derived electrons. Complexes I, III and IV function as proton pumps, transferring protons across the inner membrane. The accompanying drop in redox potential generates the mitochondrial membrane potential ($\Delta\Psi m$) of around 150–180 mV, which is critical to mitochondrial ATP generation. Mitochondrial ROS are predominantly generated at ETC complexes I, involving NADH dehydrogenase, and III (cytochrome b) (Boveris et al. 1976; Fleury et al. 2002; Ueda et al. 2002). ROS production is a fine balancing act of aerobic metabolism, reducing O_2 to H_2O, maximising ATP synthesis and maintaining the levels of ROS required for cell signalling, which will be discussed in more detail later in this chapter (Inoue et al. 1999; Brookes et al. 2002). Elevated levels of ROS, damage cellular components such as proteins, lipids and DNA through irreversible oxidative modifications (Letko et al. 1991; Kadlubar et al. 1998; Palmieri et al. 2007). The

distinct mitochondrial genome (mtDNA) is much more sensitive to ROS-induced damage than nuclear DNA, leading to ΔΨm depolarisation, increased ROS production, activation of signal transduction pathways and programmed cell death (Yakes et al. 1997; Halangk et al. 1998; Heerdt et al. 1998; Weber et al. 1998; Kamata et al. 2005; Dios 2010). The mitochondria also play an important role in regulating cell death via the release of cytochrome c and opening of the mitochondrial permeability transition pore (MPTP) (Liu et al. 1996; Loeffler et al. 2000; Criddle et al. 2007).

In the perigranular region, the mitochondria form a belt, which regulates Ca^{2+} wave propagation. This is described as a "buffer barrier" or "firewall" in isolated PACs. When the $[Ca^{2+}]_c$ is elevated in close proximity to the mitochondria, the mitochondria uptake Ca^{2+} during ER refilling, which acts to buffer signals from entering the nucleus in the basolateral region (Tinel et al. 1999; Park et al. 2001). The nucleus is therefore protected from undesirable effects of unwanted Ca^{2+} signals, and has been proposed to retain the capacity to confine nuclear Ca^{2+} signals (Petersen 2012). Ca^{2+} uptake by the mitochondria has been demonstrated to up-regulate the activity of Krebs cycle dehydrogenases, leading to an increase in levels of NAD(P)H, fuelling ETC ATP production (Hajnóczky et al. 1995; Voronina et al. 2002). The main pool of NAD(P)H in the cell is mitochondrial, with minor sources provided by cytosolic glycolytic enzymes. Mitochondria not only shape and define cytosolic Ca^{2+} elevations to modulate metabolism and respond to cellular ATP demands, but functionally adapt in response to cellular signals, a phenomena

dependent on the region of mitochondrial distribution (Park et al. 2001; Soubannier et al. 2009). This buffering capability of the mitochondria is reliant on a high Ca^{2+} loading capacity.

The mitochondria accumulate Ca^{2+} in response to both physiological Ca^{2+} signals (Rizzuto et al. 2000; Johnson et al. 2002) and global Ca^{2+} waves (Hajnóczky et al. 1995). Ca^{2+} import into the mitochondria occurs primarily due to the mitochondrial Ca^{2+} uniporter (MCU) which relies on the ΔΨm to drive transport. The MCU is a high capacity, low affinity sensitive channel located in the inner mitochondrial membrane (Kirichok et al. 2004), which enables rapid Ca^{2+} uptake into the mitochondria. This is important for the regulation of mitochondrial respiration, through the activation of Ca^{2+}-sensitive dehydrogenases of the TCA cycle, such as pyruvate dehydrogenase (PDH), as mentioned earlier. Influx of Ca^{2+} into the mitochondria is also essential for MPTP opening (Pan et al. 2013). Mitochondrial Ca^{2+} uptake 1 (MICU1) is a key regulator of the MCU and senses mitochondrial matrix Ca^{2+} levels via its EF-hand domains. (Perocchi et al. 2010). In an open state, outer membrane voltage-dependent anion channels (VDAC) are responsible for ATP/ADP exchange and is the predominant route for ATP efflux from the mitochondria (Schmid et al. 1998; Gincel et al. 2001).

Efflux and clearance of Ca^{2+} from the mitochondria occurs via the mitochondrial Na^{+}/Ca^{2+} exchanger (NCLX) (Palty et al. 2010; Nita et al. 2015). In

response to pathological Ca^{2+} overload the MPTP opens, permeabilising the mitochondrial membrane and providing rapid extrusion of Ca^{2+} and other mitochondrial contents of less than 1.5kDa. The MPTP is a non-specific pore in the mitochondrial membrane playing a major role in mitochondrial permeabilisation leading to equilibration of H^+ across the inner membrane, dissipation of ΔΨm and cessation of ATP production (Leist et al. 1997; Giacomello et al. 2007; Kroemer et al. 2007; Baines 2009; Baumgartner et al. 2009). This MPTP permeabilisation also leads to depletion of ATP, which is a central trigger for necrosis in PACs (Nakagawa et al. 2005; Mukherjee et al. 2015). ATP is essential for activation of apoptotic caspases, therefore, ATP depletion due to MPTP opening prevents apoptosis and leads to a necrotic mode of cell death.

The MPTP is a multi-protein complex, which is thought to form within the inner mitochondrial membrane (IMM) at the interface between adjacent F_0 sectors of F_0F_1-ATP synthase complex dimers (Strauss et al. 2008; Bernardi 2013; Giorgio et al. 2013). Matrix cyclophilin D (CypD), a peptidylprolyl isomerase F (Ppif) gene product, regulates MPTP opening and is not a structural pore component. CypD binds to the F_0F_1-ATP synthase lateral stalk, an action requiring inorganic phosphate (Pi) (Bernardi 2013; Giorgio et al. 2013). MPTP formation and opening is prevented in cells without CypD ($Ppif^{-/-}$) and by applying CypD inhibitor cyclosporin A (CsA) (He et al. 2002; Baines et al. 2005; Basso et al. 2005). Cells from CypD knockout (KO) mice are protected against Ca^{2+} overload- and ROS-induced ΔΨm depolarisation and necrosis, although the mechanisms are still under investigation

(Baines et al. 2005; Shalbueva et al. 2013). MPTP opening has been predominantly associated with the induction of necrosis, and apoptosis not considered a defining feature of MPTP-induced effects. However, the MPTP could be a gatekeeper for both modes of cell death and more recently, there is evidence that MPTP opening also may also play a role in programmed necrosis (necroptosis) (Nakagawa et al. 2005; Kinnally et al. 2011; Karch et al. 2015). Evidence suggests that transient MPTP opening may enable apoptosis through maintenance of ATP production (Crompton 1999; Kroemer et al. 2000). Our group has demonstrated that menadione- and TLCS-induced increases in ROS levels can lead to apoptosis (Criddle et al. 2006; Booth et al. 2011). Elevated levels of ROS led to Ca^{2+}-dependent opening of the MPTP, an action which was inhibited by non-targeted thiol-containing antioxidant N-acetylcysteine (NAC) (Gerasimenko et al. 2002; Baumgartner et al. 2009). In summary, MPTP opening is dependent on elevated levels of mitochondrial Ca^{2+} which can be further promoted by increases in ROS (Petronilli et al. 1994; Kroemer et al. 2007; Rasola et al. 2011).

Opening of the MPTP has also been demonstrated in an ethanol (EtOH)-induced AP model. An action that was effectively ameliorated using a knockout of cyclophilin D (Schild et al. 1999; Gukovskaya et al. 2002; Shalbueva et al. 2013). MPTP inhibition has now been assessed using known inhibitors CsA and bongkrekic acid alongside cyclophilin D knockout in multiple AP models - hyperstimulation, bile acid, alcoholic and choline-deficient ethionine-supplemented. Results demonstrated a dramatic improvement to all pathological responses authenticating the MPTP as a

drug target for AP (Mukherjee et al. 2015). Treatment with mitochondria-targeted antioxidant Mitoquinone (MitoQ), reduced levels of mitochondrial ROS leading to diminished frequency of cytosolic Ca^{2+} waves and inhibition of MPTP opening in mouse hearts (Davidson et al. 2012). These results mirrored those results seen with NAC and Ca^{2+} chelator BAPTA-AM in human leukemic cell line (CEM) (Lu et al. 2007). Inhibition of MPTP opening could provide a potential therapeutic target, however, little is known yet of the physiological effects of ROS, including H_2O_2, on $Ppif^{-/-}$ PACs resistant to MPTP opening. As the mitochondria play a critical regulatory role in both physiological and pathophysiological cell function, dysfunction is central to the development and progression of diseases such as acute pancreatitis and requires further investigation.

Reactive Oxygen Species (ROS): Production

The majority of all primary cellular ROS is produced in the mitochondria (Boveris et al. 1973). Reduction of O_2 in the mitochondria during normal oxidative phosphorylation produces partly reduced intermediates termed reactive oxygen species (ROS) including superoxide anion ($O_2^{\bullet-}$), hydroxyl radical $OH^{\bullet}$ and the non-radical hydrogen peroxide (H_2O_2) a small, uncharged, diffusible molecule. The principal oxidant produced by mitochondria is $O_2^{\bullet-}$. $O_2^{\bullet-}$ is formed largely at ETC complex I and released into the mitochondrial matrix, and the complex III coenzyme Q10 Q cycle, which releases superoxide into both the matrix and intermembrane

space (Turrens 2003; O'Malley et al. 2006; Davidson 2010). $O_2^{\bullet-}$ is dismutated to H_2O_2 by superoxide dismutase (SOD) manganese SOD (MnSOD) which then exits the mitochondria, or Zinc/Copper SOD (Zn/Cu SOD) in the intermembrane space. MnSOD(-/-) are more susceptible to oxidative stress in comparison to the wild type (WT) mice and die soon after birth due to extensive damage to the mitochondrial DNA (Li et al. 1995). On the other hand, mice which are deficient in Cu/ZnSOD develop normally but exhibit elevated cell death (Reaume et al. 1996). H_2O_2 can undergo an iron catalysed Fenton reaction to produce $OH^{\bullet-}$ leading to a lipid peroxidation chain reaction and DNA damage (Sutton et al. 1984; Braughler et al. 1986; Winterbourn 1987). H_2O_2 is widely known to induce detectable increases in cellular ROS in various cell types (Rigoulet et al. 2011; Mankad et al. 2012; Osera et al. 2015).

ROS can also be produced by α-ketoglutarate dehydrogenase (α-KGDH) of the TCA cycle and monoamine oxidases (MAOs) found in the mitochondrial outer membrane (Starkov et al. 2004; Tretter et al. 2004; Andreyev et al. 2005). ROS produced by xanthine oxidase (XOD) has been proven to contribute to both local effects and systemic organ failure in AP in caerulein-stimulated PACs, *in vivo* and *in situ* (Nonaka et al. 1989; Nonaka et al. 1990; Cassone et al. 1991; Suzuki et al. 1993; Folch et al. 1998; Telek et al. 2001). Transmembrane multiunit enzyme nicotinamide adenine dinucleotide phosphate (NADPH) oxidase (NOX), uses NAD(P)H as an electron donor to catalyse $O_2^{\bullet-}$ production (Chan 2009). This increases the production of secondary ROS such as H_2O_2 which again in turn can stimulate NOX (Babior 1995; Lambeth et al. 2000; Cheng et al. 2001; Yu et al. 2005). NOX is

strongly expressed in inflammatory cells and more recently, there is growing evidence for a role in the pathogenesis of acute pancreatitis. Expression of cytosolic and membrane bound key NOX subunits and NOX1 have been found to be constitutively expressed in pancreatic acinar AR42J cells. There is also evidence of NOX expression in human pancreatic islets (Rebelato et al. 2012). However, there is no evidence for NOX isoforms so far in primary acinar cells (Gukovskaya et al. 2002).

H_2O_2

It has been shown that in PACs, H_2O_2 has effects on both cellular Ca^{2+} signalling and mitochondrial membrane potential. Oxidative stress induced by 1mM H_2O_2 can lead to a release of Ca^{2+} from cytosolic stores and Ca^{2+} overload. These stores include the ER and also the mitochondria, demonstrated by prior depletion of the ER Ca^{2+} store (Pariente et al. 2001). It was concluded that these effects were likely mediated by Ca^{2+}-ATPase sulfhydryl group oxidation by H_2O_2. Concentrations of <100µM can alternatively induce Ca^{2+} oscillations (Granados et al. 2006) and lead to a faster propagation of CCK-induced Ca^{2+} waves (Granados et al. 2007). Ca^{2+} released into the cytosol is subsequently up-taken by the mitochondria, leading to increases in FAD^{+} levels and $\Delta\Psi m$ depolarisation (Gonzalez et al. 2005). The application of H_2O_2 concentrations of >50µM caused a concentration-dependent inhibition of plasma membrane Ca^{2+}-ATPase (PMCA) activity and ATP depletion via independent actions. Insulin has been demonstrated to protect against these effects by switching metabolism to glycolysis and fuelling the PMCA, even when the

mitochondria were impaired (Bruce et al. 2007; Baggaley et al. 2008; Mankad et al. 2012). These results showed that H_2O_2-induced oxidative stress at concentrations greater than 50µM can play a role in modulating Ca^{2+} overload, a major driver of necrosis, via PMCA inhibition (Bruce et al. 2007; Baggaley et al. 2008). H_2O_2 can also inhibit CCK-induced amylase release (Rosado et al. 2002) suggesting a regulatory role in PACs. In several cell types H_2O_2 has been demonstrated to have submillimolar and millimolar concentration-dependent effects on NAD(P)H, FAD^+, ROS levels and a variety of signalling pathways, which will be discussed in more detail later in this chapter (Chinopoulos et al. 1999; Tretter et al. 2000; Nulton-Persson et al. 2001; Gonzalez et al. 2005; Gerich et al. 2009).

Not only ROS but also reactive nitrogen species (RNS) such as nitric oxide ($NO^{\bullet}$) have physiological roles in the cell, such as signal transduction (Finkel 1998; Finkel et al. 2000; Droge 2002) and modulation of mitochondrial function (Cleeter et al. 1994; Brookes et al. 2002; Brookes et al. 2002). $NO^{\bullet}$ is produced in the cell by nitric oxide synthase, catalysing the oxidation of L-arginine to citrulline and $NO^{\bullet}$, requiring cofactors NADPH and O_2. The primary pancreatic source of $NO^{\bullet}$ are neurons and vascular endothelium, playing a role in the control of pancreatic blood flow (Konturek et al. 1993; Kirchgessner et al. 1994). The mitochondrial respiratory chain is also capable of producing $NO^{\bullet}$ (Giulivi et al. 1998; Castello et al. 2006) and the combination of $NO^{\bullet}$ with $O_2^{\bullet-}$ forms the strong oxidant peroxynitrite ($ONOO^-$) (Moncada et al. 1991; Radi et al. 1991; Packer et al. 1996). Excessive accumulation of ROS and/or reactive nitrogen species and the unregulated oxidation of cellular

components such as DNA, proteins and lipids are collectively known as oxidative stress.

The potential dangers of ROS received great attention in a plethora of diseases and there is substantial evidence of ROS-induced acinar cell damage during the early development of acute pancreatitis (Sanfey et al. 1984; Tsai et al. 1998; Schulz et al. 1999). However, conflicting evidence has shown that antioxidant treatment is only partially effective in models of AP, reducing oedema but not acinar cell damage (Steer et al. 1991; Sato 1995; Esrefoglu 2012; Armstrong et al. 2013). The ability of ROS to induce alterations to Ca^{2+} homeostasis, particularly causing sustained increases in $[Ca^{2+}]_c$ is considered an important contributing factor, not only in the pathogenesis of pancreatitis but also in chronic pancreatitis, diabetes and cardiac function and warrants further investigation (Niederau et al. 1991; Schoenberg et al. 1994; Ward et al. 1995; Weber et al. 1998; Ho et al. 1999; Viola et al. 2010).

Oxidative stress

A role for ROS was proposed in the development of AP, due to an elevated oxidative status/reduced antioxidant capacity observed in the clinic and in experimental animal models (Hackert et al. 2011). For example, increased superoxide, hydrogen peroxide and lipid peroxide levels and diminished antioxidant status were present in the blood of AP patients in comparison to healthy controls (Tsai et al. 1998). Oxidative stress occurs early in the progression of acute

pancreatitis and the disease severity is dependent on the imbalance between oxidant levels and endogenous antioxidant defences (Tsai et al. 1998). Clinically, ROS cannot be detected directly due to their short half-lives. Therefore, it is generally acceptable to measure stable metabolites as indicators of oxidative stress. These include by-products of lipid peroxidation, malondialdehyde (MDA) and thiobarbituric acid reactive substances (TBARS). Parameters of the oxidant-antioxidant balance can be determined by including measurements of reduced glutathione (GSH) with the oxidative stress markers listed above or in conjunction with oxidized glutathione (GSSG) (Schulz et al. 1999; Dziurkowska-Marek et al. 2004; Pérez et al. 2015).

Oxidative stress, can be detected not only by measuring accumulation of ROS-mediated lipid peroxidation products (Nonaka et al. 1989; Guyan et al. 1990) but also through fluorescence (Urunuela et al. 2002), and protein modification (Reinheckel et al. 1998). Further methods include detection of antioxidant depletion (Rau et al. 2001; Rahman et al. 2004) and cerium perhydroxide (Telek et al. 2001). Programmed cell death can be induced by H_2O_2, through oxidative activation of p53, kinases, caspases, apoptosis signal regulating kinase 1 (ASK1), p38 mitogen-activated protein kinase (p38 MAPK) and c-Jun N-terminal kinases (JNKs) (Ueda et al. 2002; Gough et al. 2011). In contrast, severe oxidative stress predominantly leads to induction of necrosis, due to the extent of cellular damage to proteins, nucleic acids and lipid membranes. Damage to membranes such as the mitochondrial membrane by lipid peroxidation, would lead to ATP depletion, cellular rupture and dispersal of intracellular contents (Higuchi 2004). The extent of

apoptosis and necrosis has been suggested to have a pivotal role in the development of acute pancreatitis (Herrera et al. 2001; Martindale et al. 2002; Bhatia 2004; Fulda et al. 2010; Weber et al. 2013). The balance between the two modes of cell death, in response to low and high oxidant treatment has not been investigated yet in PACs.

ROS Signalling

Oxygen radicals such as H_2O_2 have been traditionally viewed from the perspective of the damage they may impart. For example, in AP due to ROS-induced effects including Ca^{2+} overload and up-regulation of pro-inflammatory cytokines leading to a more severe pathophysiological response (Folch et al. 2000; Baggaley et al. 2008; Dios 2010; Yu et al. 2014). However, as introduced earlier, mitochondrial ROS can also act as signal-transducing molecules and can play an important regulatory role in both the pancreas and AP (Escobar et al. 2012; Pérez et al. 2015).

Many clinical attempts to regulate oxidative stress have encountered a reduction in biomarkers with little or no therapeutic benefit. Therefore, further assessment is required of the cellular effects and signalling pathways managed by ROS, such as H_2O_2, alongside the role of ROS in AP cell death and the inflammatory response. This thesis has investigated the cellular effects of ROS H_2O_2, and protective capabilities of mitochondria-targeted antioxidant MitoQ in PACs. ROS, in

particular H_2O_2, can bring about reversible protein oxidation at low concentrations and undergo concentration changes in response to physiological stimuli (Weber et al. 1998; Nulton-Persson et al. 2001; Granados et al. 2004; Rigoulet et al. 2011). These responses satisfy certain prerequisites of signalling molecules (Trimm et al. 1986; Suzuki et al. 1997; Denu et al. 1998; Finkel et al. 2000; Pelletier et al. 2012; Pérez et al. 2015). The rapid and reversible oxidation of proteins is crucial to ROS mediated modulation of cell signalling and ROS compartmentalisation can enable regulation of specifically targeted cellular effects (Pietraforte et al. 2014).

Figure 1.2

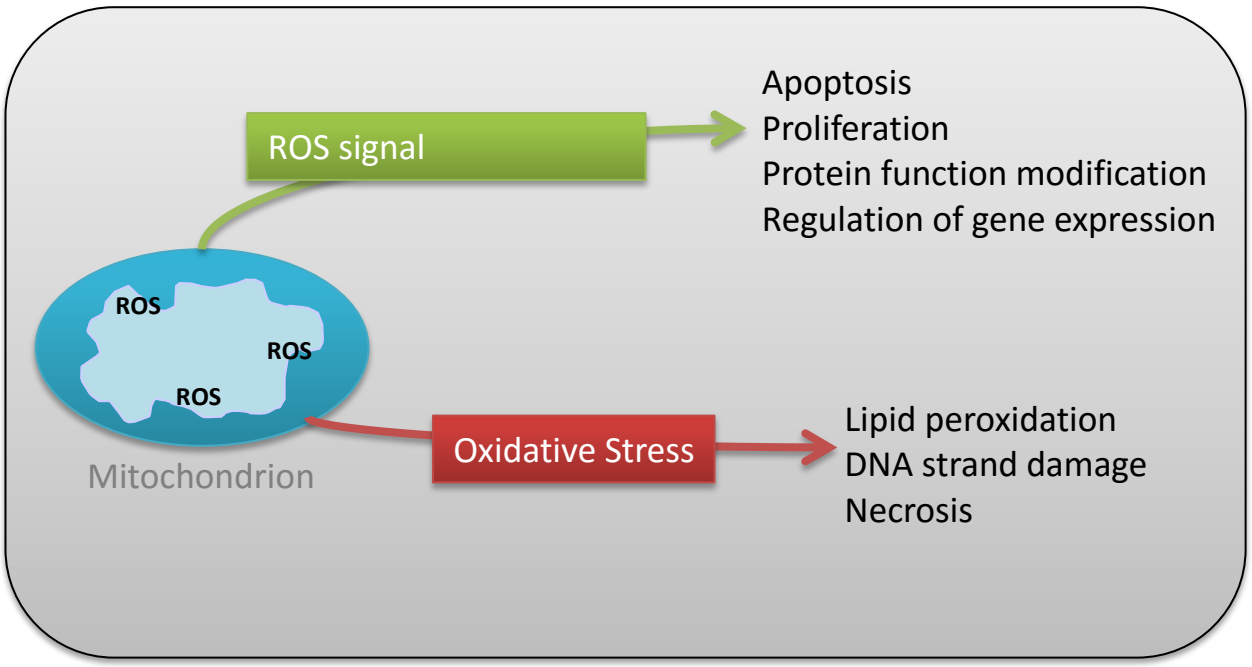

Figure 1.2 The two heads of mitochondrial ROS production. ROS produced during mitochondrial respiration is crucial to cell survival and protective mechanisms such as proliferation and apoptosis. Elevated ROS production and/or an imbalance in ROS levels/antioxidant capabilities of the cell lead to lipid peroxidation, DNA strand damage and necrosis.

In this study, we focus on reactive oxygen species H_2O_2, which is considered an important secondary messenger in the AP inflammatory response (Escobar et al. 2012). Hydrogen peroxide applied exogenously is commonly the oxidant of choice in redox studies because of its continuous production in the mitochondria and lack of charge, enabling it to diffuse relatively easily across cellular membranes (Chance et al. 1979). The specific mechanisms for H_2O_2 participation in cell signalling are still under investigation. Accumulated research into specific signalling pathways and oxidation targets are outlined below. H_2O_2 are thought to mediate cell-signalling pathways through reversible oxidation of redox-sensitive cysteine residues (sulfhydryl groups) on target proteins, such as protein tyrosine phosphatases (PTPs) (Finkel 2011; Klomsiri et al. 2011). However, with excessive levels of ROS, these modifications are irreversible and lead to cell death. There is evidence that H_2O_2 compartmentalisation can maintain specific oxidation effects through localised inactivation of a peroxiredoxin detoxification enzyme Prx1. Therefore restricting low concentrations of H_2O_2 to the specific cellular sub-domains of a signalling site (Toledano et al. 2010; Woo et al. 2010).

In PACs, millimolar H_2O_2 concentrations lead to Ca^{2+} release from the ER and mitochondria and overload in an IP_3 independent mode (Pariente et al. 2001). This effect was believed to occur through irreversible oxidisation of Ca^{2+}-ATPase sulfhydryl groups of agonist-sensitive stores (Granados et al. 2006; Baggaley et al. 2008). Alternately, at concentrations of <100µM, H_2O_2 has been shown to stimulate cytosolic Ca^{2+} oscillations, and inhibit CCK-induced amylase secretion (Granados et

al. 2006). In tumourigenic pancreatic cell line AR42J, H_2O_2 caused partial depolarisation of the ΔΨm, and 10μM but not 1μM induced apoptosis through cytochrome c release and caspase 3 activation (Morgado et al. 2008). These results provide insight into the dose dependent cellular effects of H_2O_2 which have yet to be fully investigated in primary PACs (Nulton-Persson et al. 2001). H_2O_2 has further demonstrated the capacity to mimic insulin signalling in the pancreas via sulfhydryl oxidation (Czech et al. 1974) and play a role in mammalian cell proliferation (Burdon et al. 1989).

ROS can mediate neutrophil infiltration of the pancreas through activation of oxidant-sensitive nuclear transcription factor, nuclear factor kappa B (NF-κB), and up-regulation of lung P-selectin (Folch et al. 2000; Blanchard Ii et al. 2001). Furthermore ROS can initiate pro-inflammatory cytokine transcription and induction of apoptosis, dependent on the level of oxidant (Kim 2008). Although NOX isoforms have not been found in PACs, a variety of studies have investigated NOX enzyme derived H_2O_2, which has furthered our knowledge of the physiological roles for endogenous H_2O_2 (Burdon et al. 1989). NOX derived H_2O_2, mediates signal transduction pathways via activation of proteins such as MAPKs, tyrosine kinases and Ras proteins (Wu et al. 2010). In PACs, CCK and TLCS have both been shown to induce the production of ROS (Granados et al. 2004; Booth et al. 2011), such as H_2O_2, which can lead to the activation of MAPKs, extracellular-signal-regulated kinases (ERK), JNK/ stress-activated protein kinases (SAPK) and p38 MAPKs in a PKC-independent manner (Dabrowski et al. 1996; Dabrowski et al. 2000; Graf et al.

2002). MAPK signalling is involved in diverse processes from cell survival to cell death (Son et al. 2011). The modulation of MAPK activation by ROS occurs through reversible oxidation of cysteine residues leading to the inhibition of MAPK phosphatases (Pérez et al. 2015). The activation of pro-inflammatory cytokines such as interleukin-1 beta (IL-1β), interleukin 6 (IL-6) and tumour necrosis factor alpha (TNF-α) in the pancreas are responsible for the aggravation of both local and systemic manifestations of AP (Tracey et al. 1992; Viedma et al. 1992; Sameshima et al. 1993; Kim 2008). IL-6 can been used as a severity indicator as it elevates leukocyte adherence and plays an important role in multiple organ failure (Schirmer et al. 1989; Tracey et al. 1992; Heath et al. 1993; Kishimoto et al. 1994; McKay et al. 1996). Additionally, ROS signalling in the inflammatory cascade may play a role in the regulation of histone deacetylases for example via redox-sensitive serine/threonine protein phosphatase PP2A (Yang et al. 2006; Escobar et al. 2012; Pérez et al. 2015). Histone deacetylases have been shown to regulate trypsin activation, inflammation, and tissue damage in AP (Hartman et al. 2015).

It is also important to briefly mention reactive nitrogen species $NO^{\bullet}$, which acts a messenger molecule in signalling pathways via cyclic guanosine-3',5' – monophosphate (cGMP), nitrosylation of regulatory thiols (Blaise et al. 2005) and Ca^{2+} influx in PACs (Gukovskaya et al. 1994). Several protective effects of $NO^{\bullet}$ have been demonstrated. These include inhibition of ultrastructural degenerative alterations generated by caerulein-induced AP (Andrzejewska et al. 1999), and decreased neutrophil accumulation in the pancreas (Inagaki et al. 1997). In contrast,

high intracellular $NO^{\bullet}$ can irreversibly bind to NADH and succinate, leading to inhibition of mitochondrial respiration (Brown 1995). In combination with $O_2^{\bullet-}$, $NO^{\bullet}$ forms the powerful oxidant $ONOO^-$, involved in lipid peroxidation, DNA strand damage and necrosis (Xia et al. 1997; Szabo 2003). Hydrogen peroxide and nitric oxide are now not only recognised for the damaging effects at high concentrations, but also as an important part of redox sensitive signalling pathways leading to the activation and inhibition of oxidant sensitive components (Suzuki et al. 1997; Finkel 1998; Goldkorn et al. 1998; Maechler et al. 1999; Gabbita et al. 2000; Fleury et al. 2002; Moncada et al. 2002; Ueda et al. 2002; Rigoulet et al. 2011).

ROS and Ca^{2+}

There is substantial evidence for a close "push-pull" relationship between ROS and Ca^{2+} signalling, both Ca^{2+}-induced ROS increases and ROS-induced changes in Ca^{2+} levels. High levels of ROS as mentioned earlier, can induce Ca^{2+} overload, and in turn elevated cytosolic levels of Ca^{2+} can lead to increased ROS production (Gonzalez et al. 2002; Granados et al. 2004; Gonzalez et al. 2005). While Ca^{2+} plays a critical physiological role in ATP synthesis and mitochondrial function it can also stimulate pathological ROS generation, cytochrome c release due to disassociation with cardiolipin, and apoptosis (Brookes et al. 2004).

Ca^{2+} stimulation of mitochondrial ROS production occurs through activation of the TCA cycle and oxidative phosphorylation, enhancing respiratory chain

electron flow. There is a strong correlation between mitochondrion metabolic rate and levels of ROS production. High Ca^{2+} concentrations lead to MPTP opening, which can be sensitised by oxidation of MPTP components (Chernyak et al. 1996; Szalai et al. 1999; Criddle et al. 2007). Menadione-induced ROS increases can cause elevated $[Ca^{2+}]_c$ leading to partial ΔΨm, MPTP opening, cytochrome c release and apoptosis. These actions can be inhibited with Ca^{2+} chelator BAPTA-AM. Thus, it was concluded that elevated Ca^{2+} concentrations coupled with increased ROS production can lead to oxidant stress-induced apoptosis through MPTP opening (Gerasimenko et al. 2002; Gerasimenko et al. 2002; Criddle et al. 2006; Baumgartner et al. 2007; Criddle et al. 2007). MitoQ inhibited these actions in intact mouse hearts (Davidson et al. 2012).

ROS, including H_2O_2, affects Ca^{2+} homeostasis via oxidation of ROS sensitive cysteine residues on IP_3R and RyR, and also Orai1, as demonstrated in T-cells (Favero et al. 1995; Eu et al. 2000; Sun et al. 2001; Meissner 2002; Meissner 2010). ROS-induced activation of IP_3R and RyR receptors enhances ER Ca^{2+} release and can prevent inhibition of IP_3R by calmodulin. SERCA Ca^{2+}-ATPase oxidation occurred at cysteine residue Cys674 and led to enhanced pump activity in cardiac, skeletal and vascular smooth muscle. Continued oxidant exposure led to irreversible SERCA inhibition and therefore Ca^{2+} overload (Grover et al. 1988; Suzuki et al. 1992; Adachi et al. 2004). As introduced earlier, in PACs high concentrations of ROS H_2O_2 led to the irreversible inhibition of Ca^{2+}-ATPase PMCA, likely through oxidation of critical thiol groups. PMCA inhibition prevents Ca^{2+} removal from the cytosol and leads to

Ca^{2+} overload and necrosis. On the other hand low micromolar concentrations of oxidant H_2O_2 simulated Ca^{2+} oscillations (Granados et al. 2006; Baggaley et al. 2008). These results demonstrate a modulating role of mitochondrial ROS on Ca^{2+} pools.

The involvement of ROS in AP is complex and poorly defined. Despite the strong evidence demonstrating oxidative stress in AP, there has been an apparent translational gap, with results from randomised clinical trials for antioxidant therapy so far discouraging (Uden et al. 1990; Du et al. 2003; Katsinelos et al. 2005; Bjelakovic et al. 2007; Siriwardena et al. 2007; Besselink et al. 2008; Sateesh et al. 2009; Bansal et al. 2011).

ROS: Cellular Defences

A network of antioxidant strategies have been developed by the cell to manage cellular levels of ROS and minimise the irreversible oxidation of cellular molecules, proteins, lipids and DNA. Management of ROS levels is also critical to maintain the narrow concentration ranges of H_2O_2 and $NO^{\bullet}$ required for involvement in cell signalling pathways (Pelletier et al. 2012). Enzymes SOD (metaloenzyme family) and glutathione peroxidase (GPx), and reductants NADH, ubiquinol and reduced glutathione, operate to limit harmful effects of elevated ROS. In the mitochondrial matrix, GPx scavenges H_2O_2 and is regulated by selenium. In the cytosol, catalase (CAT) converts H_2O_2 into H_2O and $O_2^{\bullet-}$. $O_2^{\bullet-}$ is generally an unreactive and stable radical at neutral pH, until conversion into ROS such as $ONOO^-$

and H_2O_2, which can then be further converted to the more reactive radical $OH^{\bullet-}$. $O_2^{\bullet-}$ can undergo a slow spontaneous dismutation to H_2O_2, although SOD is responsible for the enzymatic conversion of $O_2^{\bullet-}$ to H_2O_2. In caerulein-induced pancreatitis for example, SOD levels are diminished (Dabrowski et al. 1988; Nonaka et al. 1990; Esrefoglu et al. 2006), demonstrating an imbalance in cellular oxidant-antioxidant status. The majority of $O_2^{\bullet-}$ is released into the mitochondrial matrix and eliminated by manganese SOD (MnSOD). $O_2^{\bullet-}$ can reduce transition metals such as Fe^{2+} and generate $NO^{\bullet}$ from H_2O_2, and $ONOO^-$ through interaction with $OH^{\bullet-}$.

Mitochondrial glutathione, ascorbate (Vitamin C) and lipophilic antioxidant vitamin E levels are elevated in comparison to the cytosol. Ascorbate in its active form, Glut1, and glutathione are actively transported into the mitochondria to manage levels of mitochondrial ROS (Kc et al. 2005; Zechmann et al. 2008; James et al. 2009; Marí et al. 2009). Glutathione (GSH) is a key pancreatic cytoprotectant (Neuschwander-Tetri et al. 1997) with a high metabolic rate of turnover only lower than that found in the liver and kidneys (Neuschwander-Tetri et al. 1997). GSH is synthesised from precursor n-acetyl cysteine (NAC) and oxidised to glutathione disulphide (GSSG) (Winterbourn 2008). GSH consists of glutamate, cysteine and glycine, the central thiol group accounting for the reducing capabilities. NAD(P)H produced within the TCA cycle is responsible for providing electron donation for the turnover between reduced and oxidised forms. Glutathione, however has a low reactivity with H_2O_2 and requires GSH peroxidise to reduce H_2O_2 to H_2O. NAD(P)H quinone oxidoreductase 1 (NQO1), a FAD containing flavoprotein, is ubiquitously expressed in all tissues and expression is up-regulated in AP (Hammons et al. 1995;

Dinkova-Kostova et al. 2000; Lyn-Cook et al. 2006). NQO1 uses NAD(P)H as a reducing cofactor to maintain reduced coenzyme Q10, directly scavenges superoxide and acts to stabilise p53 (Beyer et al. 1996; Siegel et al. 1997; Asher et al. 2002; Siegel et al. 2004). NQO1 inhibition dramatically increased menadione-induced ROS in PACs (Criddle et al. 2006). This evidence demonstrates that in general the pancreas is well equipped to deal with mild oxidative stress.

Acute Pancreatitis

Acute pancreatitis (AP) is a severe inflammatory condition of the exocrine pancreas caused primarily by gallstones and excess alcohol (Frossard et al. 2008; Banks et al. 2013; Yadav et al. 2013). There is a progressively increasing incidence, currently at ~30/100,000 per year in the United Kingdom (Roberts et al. 2013). Most patients have a mild and self-limiting clinical course irrespective of triggers (Tenner et al. 2013). Roughly 15-20% of cases involve potentially lethal complications such as persistent organ failure and infected pancreatic necrosis (Petrov et al. 2012), resulting in a heavy socio-economic burden (Peery et al. 2012). Despite increased understanding of the complex pathophysiology of this disease in the last two decades and a large number of clinical trials, a specific therapy for AP is lacking (Tenner et al. 2013).

The initial site of damage in AP is considered the pancreatic acinar cell, which exhibits many pathological features. These include premature activation of digestive enzyme precursors, inhibition of apical secretion, disordered autophagy

and lysosomal degradation, mitochondrial dysfunction and release of inflammatory cytokines (Lerch et al. 2013). Diverse experimental AP precipitants include bile acids, cholecystokinin hyperstimulation and non-oxidative ethanol metabolites. These induce Ca^{2+} overload, increased ROS production, mitochondrial dysfunction and loss of ATP that results in acinar cell necrosis (Booth et al. 2011). The extent of which determines outcome in a clinical setting. Genetic alterations can impair PAC function, such as mutations in the pancreatic secretory trypsin inhibitor gene (PSTI). In animal models, PSTI deletion led to PAC death and impaired regeneration, predisposing patients to pancreatitis (Witt et al. 2000; Nathan et al. 2005; Ohmuraya et al. 2005). Deletion of cathepsin B gene can reduce the severity of experimentally introduced pancreatitis, through preventing intrapancreatic activation of trypsinogen. However, deletion of the cathepsin gene does not alter the extent of inflammation (Halangk et al. 2000). AP can be initiated in patients with gain-of-function mutations which lead to the genetic activation of the NF-κB pathway and elevated Ras signalling (Chen et al. 2002; Ji et al. 2009; Ji et al. 2009), both play a role in the pathogenesis of AP (Yu et al. 2015). NF-κB acts as an inflammatory mediator, up-regulating pro-inflammatory cytokine expression and leading to the recruitment of neutrophils, macrophages, monocytes, and lymphocytes, to the pancreas (Gukovsky et al. 2013). Ras signalling also plays a role in the development of local and systemic inflammation, and the activation in PACs is also believed to be linked to the development of pancreatic ductal adenocarcinoma (PDAC) (Ji et al. 2009; Logsdon et al. 2009; Yu et al. 2015). Early growth response protein 1 (EGR1) and several other novel genes have also been suggested to play a role in AP development and severity (Ji et al. 2003).

Extensive cellular necrosis is a key contributor to the severity of acute pancreatitis. In contrast, apoptosis is considered protective, in part by diverting cells from necrosis (Bhatia 2004; Criddle et al. 2006; Booth et al. 2011). Necrosis is associated with cell rupture and an inflammatory response in acute pancreatitis. Whereas apoptosis or programmed cell death, requires gene expression and results in cell shrinkage and nuclear fragmentation. Apoptosis leads to very little or no inflammation in AP (Wyllie et al. 1980; Cohen et al. 1984; Gerschenson et al. 1992; Kaiser et al. 1995; Bhatia et al. 1998; Bhatia 2004; Bhatia 2004).

Primary oxidant production elicits lipid peroxidation, oedema and diminishes endogenous antioxidant levels. Oxidant-sensitive transcription factor NF-κB can be activated by elevated levels of ROS and translocate into the nucleus, leading to pro-inflammatory chemokine and cytokine transcription (Kim 2008; Morgan et al. 2011). This results in a localised and systemic inflammatory response syndrome (SIRS). The features of AP progression include activation and infiltration of inflammatory cells into the pancreas, which provoke further ROS production and injury (Pandol et al. 2007). During the early stages of clinical acute pancreatitis, access to the organ and tissue of patients is very limited. Therefore, experimental models of pancreatitis are predominantly used to research mechanistic issues. Although many animal species have been employed in AP models, the mouse remains popular. It provides access to a variety of genetic manipulations, and has a relatively low maintenance cost (Dawra et al. 2007; Pandol et al. 2007). Non-invasive models include hormone-

induced, alcohol-induced, immune-mediated, diet-induced, gene knockout and L-arginine. Invasive models include closed duodenal loop, antegrade pancreatic duct perfusion, intraductal bile acid exposure, hyperstimulation, vascular-induced, ischaemia/reperfusion and duct ligation. The *in vivo* and *in vitro* effects of CCK and analogue caerulein, bile acid TLCS and ethanol/fatty acid ethyl ester (FAEE) palmitoleic acid ethyl ester (POAEE) will be outlined in this chapter.

CCK and Caerulein

Enzyme secretion in the pancreas is regulated by circulating gut hormone CCK and neurotransmitters ACh from cholinergic nerves, and VIP from pancreatic nerves. ACh and CCK both stimulate fluid and enzyme secretion. As early as the 19th century, it was recognised that the exocrine pancreas can be damaged by excessive neuronal stimulation (Mouret 1895). CCK and analogue caerulein stimulate increases in cytosolic Ca^{2+} and can induce AP in experimental models (Watanabe et al. 1984; Niederau et al. 1985; Sjödin et al. 1990). CCK naturally occurs in several molecular forms and the full-length form (CCK-58) has been demonstrated to be the principal circulating type of CCK in humans (Eberlein et al. 1987). CCK-8 has been most extensively studied and has essentially identical actions to CCK-58 (Gonzalez et al. 1997) including $[Ca^{2+}]_c$ elevations, mitochondrial dysfunction, digestive enzyme secretion and cellular damage (Saillan-Barreau et al. 1998; Criddle et al. 2009). Therefore, CCK-8 is the form applied in this work.

The mode of CCK action is biphasic. Low concentrations of the picomolar range are associated with physiological responses and activate high affinity receptors. Low-affinity receptors are activated by high concentrations of CCK and are associated with hyperstimulation and Ca^{2+} overload (Rosenzweig et al. 1983; Jensen R T 1994; Saillan-Barreau et al. 1998). For example, hyperstimulation with CCK in isolated PACs, can induce a large initial rise (or peak) in cytosolic Ca^{2+} followed by a prolonged plateau and depolarisation of the mitochondrial membrane (Raraty et al. 2000; Gukovskaya et al. 2002). Large sustained $[Ca^{2+}]_c$ rises induced by CCK-8 hyperstimulation cause acinar cell necrosis via premature intracellular digestive enzyme activation (Raraty et al. 2000). Supraphysiological concentrations of CCK-8 (>0.1nM) in rat PACs induced ΔΨm depolarisation, while activating cell death signalling pathways, including caspase activation and MPTP-dependent cytochrome c release (Smith et al. 2012). While in comparison, at physiological doses, CCK stimulation induced cytosolic Ca^{2+} oscillations and increased NAD(P)H levels via an increase in mitochondrial Ca^{2+}-sensitive dehydrogenase activity (Hajnóczky et al. 1995; Robb-Gaspers et al. 1998; Rizzuto et al. 2000; Voronina et al. 2002).

CCK acts via two known GPCRs, type A and type B. Type A is expressed in murine PACs with some species differences between the CCK-A receptor of rats and mice (Saillan-Barreau et al. 1998). CCK-A activation leads to MAPK activation in pancreatic AR42J acinar cells (Ji et al. 2000; Logsdon 2000). A study performed using

a transgenic mouse strain expressing the human CCK-B/gastrin receptor in the exocrine pancreas, demonstrated that the CCK-B/gastrin receptor mediates exocytosis in acinar cells and can couple to phospholipase C (Saillan-Barreau et al. 1998). Ca^{2+} oscillations induced by physiological picomolar concentrations of CCK are mediated by NAADP and cADPr (Petersen et al. 2006). On the other hand, CCK hyperstimulation leads to the activation of PLC, generation of IP_3 and changes associated with pancreatitis.

In response to CCK *in vitro* and caerulein *in vivo*, JNKs and MAPKs are rapidly activated (Dabrowski et al. 1996). CCK stimulated intracellular Ca^{2+} rises and PKC activation in turn induces NF-κB activation and elevated mob-1 chemokine expression, a downstream target of the Ras signalling pathway (Han et al. 1999; Han et al. 2000). CCK-8 and analogue caerulein induced similar dose-related increases of intracellular Ca^{2+} concentrations ($[Ca^{2+}]_i$) and amylase secretion through Ca^{2+}-mediated ROS generation (Sjödin et al. 1990; González et al. 2006). The plasmakinetics of caerulein and CCK-9 are also similar (Mossner et al. 1991). The CCK-8 elicited amylase secretion can be impaired by ethanol in mouse PACs (González et al. 2006) in a Ca^{2+} Ca^{2+}-dependent influx mechanism (González et al. 2006; Fernandez-Sanchez et al. 2009).

CCK analogue caerulein, is derived from the Australian tree frog *Litoria caerulea*. Caerulein-induced pancreatitis (CER-AP) in rodents is a non-invasive model of acute pancreatitis. It is well characterised and widely used to induce a mild, self-limited and reversible disease, in comparison to retrograde infusion of bile

acid TLCS. Caerulein benefits from a longer half-life in the body than CCK and improved stability against biological degradation. Therefore, caerulein is predominantly used in experimental models (Mossner et al. 1991). It is characterised by pancreatic oedema, premature zymogen activation and systemic inflammatory response (Lerch et al. 1994; Halangk et al. 2000; Lerch et al. 2002). CER-AP is one of the most commonly applied animal models of AP used by over 100 research groups and has contributed greatly to our understanding of AP. However, CER-AP has few clinical parallels (Lerch et al. 1994; Lerch et al. 2013). CER-AP, however, remains a convenient and reliable experimental model to induce a milder level of damage to the pancreas. The model has been utilised in many studies and groups to investigate oxidative stress in AP despite of the restricted pathophysiological relevance to the clinical situation. Caerulein generated ROS were proposed to play a role in the development of CER-AP, through activation of NF-κB. ROS scavengers may inhibit NF-κB activation and alleviate the inflammatory response in PACs (Yu et al. 2000). In CER-AP, treatment with free radical scavengers SOD and catalase inhibited lipid peroxidation, zymogen degranulation, ultra-structural and biochemical injury and tissue necrosis (Guice et al. 1986; Schoenberg et al. 1991). Caerulein pancreatitis can induce early SAPK activation, acinar glutathione depletion, diminished ATP and premature activation of digestive enzymes due to impaired cytoskeleton integrity (Luthen et al. 1995; Grady et al. 1996).

A study in the choline deficient ethionine-supplemented diet-induced model of acute haemorrhagic pancreatic necrosis and the supramaximal caerulein stimulation model of acute interstitial oedematous pancreatitis compared the effects of agents designed to reduce oxidative stress (Steer et al. 1991). In both models, only a decrease in the degree of pancreatic oedema was observed. Whereas, other markers of AP were unaffected, suggesting that ROS did not exert a pivotal role in the development of acinar cell damage.

Taurolithocholic acid 3-sulphate (TLCS)

The underlying cause of 60-75% of acute pancreatitis cases are gallstones or alcohol abuse. The gallbladder and pancreas share a draining duct, of which the exit (sphincter of Oddi) to the duodenum can become blocked by passing gallstones. This results in reflux of bile into the pancreatic duct leading to increased ductal pressure and direct effects on the pancreas. Bile acids induce a severe AP pathology characterised by tissue necrosis, leukocyte infiltration, oedema, and haemorrhage (Yagci et al. 2004). *In vivo*, experimental biliary acute pancreatitis can be induced by infusion of retrograde ductal taurocholate. Introduction of bile acids directly into the common bile duct is a more clinically representative surgical model of experimental AP, enabling the study gallstone obstruction associated AP, which accounts for 30-50% of AP cases. One of the most frequently used bile acids is sodium taurocholate. Infusion in rats has been used extensively to investigate AP

associated with multiple organ dysfunction, including lung injury, a major cause of early death in patients (Lichtenstein et al. 2000). The bile acid concentration utilised requires careful choice as excessive levels will produce extensive acinar cell damage that may be too rapid to provide a reliable representation of the disease (Su et al. 2006).

In isolated mouse PACs, bile acids such as natural bile acid TLCS, activate G-protein coupled bile acid receptor 1 (Gpbar 1) expressed at the apical pole of PACs, leading to Ca^{2+} release from intracellular stores and subsequent $[Ca^{2+}]_c$ elevation (Perides et al. 2010). Bile acids elicit Ca^{2+} overload via phosphoinositide 3-kinase (PI3K) activation (Fischer et al. 2007) and inhibition of the SERCA pump. This prevented Ca^{2+} clearance from the cytosol (Kim et al. 2002) and induced Ca^{2+} release from the ER via PLC activation (Lau et al. 2005). Bile acid provoked release of Ca^{2+} from the ER and apical acidic stores is dependent on both RyR's (and RyR activator cADPr) and IP_3R's (Gerasimenko et al. 2006; Lewarchik et al. 2014). A mode for TLCS-induced injury is via Ca^{2+}-dependent activation of serine/threonine phosphatase calcineurin. Activated calcineurin mediates intra-acinar protease activation through NF-κB nuclear translocation (Muili et al. 2013) and premature trypsinogen activation in the pancreatic acinar cell (Ma et al. 2013). Pancreatic acinar cell trypsinogen activation is involved in the early stages of pancreatic injury but not inflammation in experimental AP. Endogenously activated trypsinogen can induce acute but not chronic pancreatitis in transgenic mice (Dawra et al. 2011; Gaiser et al. 2011; Logsdon et al. 2013). Bile acid-induced toxic cytosolic Ca^{2+} rises

can be inhibited by depletion of ATP (Voronina et al. 2002; Barrow et al. 2008) and are mirrored by a rise in mitochondrial Ca^{2+} (Booth et al. 2011).

In PACs TLCS (500µM) has been shown to induce increased $[ROS]_M$ and $[ROS]_I$ via sustained cytosolic and mitochondrial Ca^{2+} elevations and a predominantly necrotic mode of cell death (Booth et al. 2011). In contrast, the lower concentration of 200µM had no detectable effects on ROS levels in DCFDA loaded cells (Booth et al. 2011). Bile acid treatment caused mitochondrial dysfunction and membrane depolarisation (Voronina et al. 2004). While mild cellular increases in ROS generally induce apoptosis, large, prolonged increases in cytosolic and mitochondrial Ca^{2+} combined with ATP depletion induced necrosis (Kim et al. 2002; Booth et al. 2011). The use of antioxidants could prevent ROS-induced apoptosis and the removal of this proposed protective mechanism may account for failure in clinical trials (Bhatia 2004; Bjelakovic et al. 2007; Siriwardena et al. 2007; Armstrong et al. 2013). Inhibition of NQO1, which is a protective cellular detoxifying mechanism, by 2,4-dimethoxy-2-methylnaphthalene (DMN) can potentiate menadione-induced ROS increases and promote apoptosis (Criddle et al. 2006; Booth et al. 2011). Levels of NQO1 are elevated in AP as well as pancreatic adenocarcinoma (Hammons et al. 1995; Ross 1997; Dinkova-Kostova et al. 2000; Lyn-Cook et al. 2006). The lower concentration TLCS treatment (200µM) induced detectable ROS increases upon inhibition of NQO1. This effect was unaffected by NADPH oxidase inhibitor, diphenyliodonium chloride. Furthermore, TLCS-induced ROS increases were completely abolished in cells pre-treated with BAPTA and $0Ca^{2+}$

in the extracellular media. Following pancreatic ductal taurocholate administration in rats, elevated markers of oxidative stress have been demonstrated (Telek et al. 1999; Rau et al. 2000; Yasar et al. 2002). The study of Rau and colleagues (Rau et al. 2000) however, indicated that whilst ROS may be mediators of tissue damage, their extracellular generation alone did not induce typical biochemical and morphological changes indicative of AP. This evidence could demonstrate a multi-faceted action of TLCS-AP. In contrast, while antioxidant NAC has demonstrated the ability to inhibit apoptosis regulated by NF-κB, NAC can also reduce tissue necrosis, leukocyte infiltration, oedema, and haemorrhage in a rat taurocholate AP model (Yagci et al. 2004; Pandol et al. 2007).

Ethanol and non-oxidative metabolite FAEE

A link between alcohol consumption and the pancreas has been reported since 1788 (Crawley 1788). In the USA, alcoholic pancreatitis is one of the predominant alcohol-related hospital diagnoses. Not all heavy drinkers develop AP, and while the reasons for this are not clear, the development is accelerated in those patients with a high fat diet and who are smokers (Dufour et al. 2003; Yang et al. 2008; Pandol et al. 2010). Elevated oxidative stress levels are found in alcoholic pancreatitis patients (Szuster-Ciesielska et al. 2001; Kamyar Shahedi 2013). PACs degrade alcohol via both oxidative and non-oxidative ethanol metabolism (Haber et al. 1998; Gukovskaya et al. 2002; Haber et al. 2004). The oxidative pathway

primarily involves oxidisation of alcohol to acetaldehyde by alcohol dehydrogenase (ADH) in the acini cytosol. Oxidative metabolism induces increased levels of ROS via cytochrome P450 2E1 (CYP2E1) production of H_2O_2, and acetaldehyde-induced depletion of glutathione (Apte et al. 2010; Ji 2012). Elevated CYP2E1 expression in the pancreas is induced in rats fed with alcohol. Long term ethanol consumption therefore sensitises the pancreas to developing acute pancreatitis by altering gene expression in rats (Kubisch et al. 2006).

Non-oxidative alcohol metabolism following ethanol ingestion, produces diverse fatty acid ethyl esters (FAEEs) via FAEE synthase, which can be detected in patient serum levels (Doyle et al. 1994). Ethanol in combination with saturated fatty acid palmitic acid (PA) is converted by palmitoleic acid ethyl ester (POAEE) synthase and acyl-coenzyme A: ethanol *O*-transferase to POAEE, which induces Ca^{2+} overload in PACs (Criddle et al. 2004; Samad et al. 2014). POAEE has been demonstrated to accumulate in the pancreas of alcoholic pancreatitis patients (Kaphalia et al. 2001). The metabolism of POAEE to palmitoleic acid (POA) by FAEE hydrolase is responsible for further toxic effects such as mitochondrial depolarization, ATP depletion, Ca^{2+} overload and necrosis (Criddle et al. 2004; Criddle et al. 2006). Inhibition of carboxylesterase prevented POAEE-induced necrosis in PACs (Criddle et al. 2006). In comparison to the liver the activity of FAEE synthase in the pancreas is larger and ADH activity lower (Gukovskaya et al. 2002). Inhibition of oxidative alcohol metabolism exacerbated FAEE levels and led to organ toxicity and inflammation (Werner et al. 2002). The combination of ethanol and unsaturated

fats, is thought to result in acinar cell injury from digestive enzyme activation and necrosis (Werner et al. 1997; Gukovskaya et al. 2002; Criddle et al. 2004; Criddle et al. 2006). Observations *in vivo* have indicated that the toxic effects of ethanol/palmitoleic acid (POA) are associated with the inhibition of oxidative alcohol metabolism and are proposed to be due to production of FAEEs via carboxylester lipase (CEL) (Huang et al. 2014).

The short term effects of ethanol on intracellular Ca^{2+} appear small (Criddle et al. 2004). However, through the non-oxidative ethanol metabolism pathway, FAEEs can induce pancreatic oedema, pancreatic trypsinogen activation, and vacuolization of acinar cells, (Werner et al. 2002; Lamarche et al. 2004). suggesting a central role for FAEEs in the development of alcoholic pancreatitis (Werner et al. 2002). It has also been suggested that toxic levels of EtOH may exacerbate PAC CCK-induced effects (Del Castillo-Vaquero et al. 2010). The use of ethanol in combination with POAEE has clinical parallels as intoxicated human blood FAEE concentrations have been reported up to 50µM and mirrored by the concentration of EtOH (Laposata et al. 1986; Werner et al. 1997; Soderberg et al. 2003). In summary, ethanol and POAEE studies indicate that alcohol-induced toxic effects are predominantly FAEE driven, which is of great clinical relevance in an organ with predominantly non-oxidative ethanol metabolism.

The effects of acute alcohol administration have been widely investigated in animals. However, a reliable model of AP has yet to be induced by ethanol alone

and to date, there is a lack of suitable models for alcoholic pancreatitis (Schneider et al. 2002; Wan et al. 2012; Huang et al. 2014). The mechanisms and pathogenesis of alcohol-induced pancreatitis are not yet fully understood, and therefore, a specific therapy is lacking. Ethanol administration has historically been combined with other factors such as CCK, secretin or pancreatic ductal obstruction to induce AP (Siech et al. 1991; Ponnappa et al. 1997; Siech et al. 1997; Pandol et al. 1999). Several studies have evaluated oxidative stress in alcohol AP models. For example, ethanol increased oxidative stress levels in the pancreas of animals injected with a dibutyltin-dichloride/ethanol combination (DBTC/EtOH) or ethanol alone. However, only animals treated with DBTC/EtOH rapidly exhibited morphological damage leading to full-blown AP (Weber et al. 1995). Furthermore, alcohol injection directly into the biliary duct of rats caused increased circulatory TBARS alongside decreased levels of GSH and elevated levels of nitric oxide associated with AP (Schneider et al. 2002; Andican et al. 2005). However, results should be treated with caution since direct fluid injection into the biliary duct may lead to pancreatic damage per se (Schneider et al. 2002). Using a different approach, a combination of ethanol with mild stimulation of the pancreas (CCK and secretin) and short-term ductal obstruction, induced AP within 24h and was associated with oxidative stress (Wittel et al. 2003).

Although these studies have used alcoholic induction of AP, the underlying pathophysiological mechanisms remain unclear and relevance to the clinic debatable, especially considering the relatively small proportion of alcoholics that develop AP. This highlights additional predisposing factors, such as a high fat diet

and smoking (Apte et al. 2010; Criddle 2015). Our group has made significant progress in the field, developing a promising novel model of alcoholic acute pancreatitis. This model is based on intraperitoneal injections of an ethanol POA combination (FAEE-AP). Biochemical markers were elevated and led to acute exocrine pancreatic damage and systemic inflammation. The FAEE-AP model demonstrated induction of extensive pancreatic necrosis, neutrophil infiltration and oedema. Importantly, the *in vitro* and *in viv*o pathological changes were mirrored, reliable and reproducible (Huang et al. 2014). This study showed that inhibition of oxidative ethanol metabolism and promotion of the non-oxidative pathway induced mitochondrial dysfunction in a Ca^{2+} dependent manner. Localisation of non-oxidative ethanol metabolites to the mitochondria led to release of fatty acids via hydrolysis. FAEE formation was prevented through inhibition of FAEE synthase carboxylester lipase (CEL) leading to alleviated effects of ethanol and FAEE *in vitro* and *in vivo*.

Antioxidant therapy

Reactive oxygen species received substantial attention over the decades for the potentially detrimental cellular effects they may impart. ROS have previously been viewed as purely unfortunate by-products of mitochondrial respiration. To further support this opinion, accumulating clinical data demonstrated elevated oxidant status and reduced antioxidant capacity such as Vitamin A and E and

carotenoid depletion (Curran et al. 2000). These effects were mirrored in experimental animal models and correlated to the severity of acute pancreatitis, however, the specific roles and ROS targets in AP are poorly understood (Schulz et al. 1999; Rau et al. 2000; Hackert et al. 2011). Evidence now points to the role of ROS particularly H_2O_2 and reactive nitrogen species nitric oxide as key signal transduction molecules essential for cellular processes such as growth, cytokine activation and protective mechanisms such as induction of apoptosis. It is understood that the cell delicately manages low levels of ROS to maintain signalling capacity without the potential damaging effects. In the development of oxidative stress-related diseases such as AP, increased ROS production and depleted endogenous antioxidant availability leads to an imbalance of these two components and oxidative stress. Elevated levels of ROS have been demonstrated to mediate pancreatic acinar cell necrosis and the release of inflammatory mediators in both pancreas and lungs. The following inflammatory response, includes recruitment of immune cells and development of pancreatic oedema. ROS increases associated with the disease progression have been demonstrated *in vitro* induced by caerulein hyperstimulation and bile acid and elevated markers of oxidative stress *in vivo* experimental models (Dabrowski et al. 1988; Sato 1995; Granados et al. 2004; Esrefoglu et al. 2006; Booth et al. 2011).

While increased ROS production has been demonstrated in response to a variety of stimuli and AP precipitants in the pancreatic acinar cell, the mechanisms are poorly characterised. Antioxidant therapy was introduced to reduce the levels

of oxidative stress observed in the clinical setting and cellular ROS increases in response to known experimental AP inducers. Many clinical attempts to regulate oxidative stress have encountered a reduction in biomarkers but with little or no therapeutic benefit (Halliwell 2000; Ueda et al. 2006; Bjelakovic et al. 2007; Iannitti et al. 2009). A meta-analysis indicated that antioxidant therapies such as β-carotene, vitamin A and vitamin E do not improve the outcome of a number of diseases and may actually be detrimental, causing an increase in mortality (Bjelakovic et al. 2007). Antioxidant therapy with intravenous selenium, NAC and ascorbic acid plus β-carotene and α-tocopherol resulted in restoring antioxidant levels and reduced oxidative stress biomarkers in severe AP. However, antioxidant therapy provided no improvement to the extent of organ dysfunction or patient outcome and elevated mortality (Virlos et al. 2003; Siriwardena et al. 2007).

Antioxidant therapy: Experimental AP findings

There have been a number of studies demonstrating pathological improvements in both experimental AP models and in the clinic. A large number of studies have evaluated the effects of antioxidant as a pre-treatment, which diminishes the clinical relevance. The majority of AP patients present after the initial pancreatic events, when the level of injury is progressing into the systemic phase. However, these studies can still contribute to our understanding of oxidative stress and antioxidant therapy in AP and it is important to outline key studies. One

such study of caerulein-induced AP in rats, applied lycopene pre-treatment, an antioxidant and anti-inflammatory carotenoid present in tomatoes. Lycopene inhibited decreases of GSH levels and increases of MDA while concurrently protecting against elevations of TNF-α , IL-1β, myeloperoxidase (MPO), amylase, lipase and histopathological damage (Ozkan et al. 2012). This reduction of oxidative damage may be linked to inhibition of neutrophil infiltration and subsequent lipid peroxidation, an aspect of AP in which antioxidant treatments might potentially minimise pancreatic damage. On the other hand, in another caerulein rat AP model, natural antioxidant resveratrol, encountered in red wine, ameliorated changes in biochemical AP markers and histological damage to the pancreas, but failed to improve the pancreatic antioxidant status (Szabolcs et al. 2006).

Beneficial effects of other natural antioxidants derived from plants, such as the flavonoid quercetin and α-/β-amyrin, have also recently been shown in the murine caerulein AP model (Carvalho et al. 2010; Melo et al. 2011), although both compounds were again administered as a pre-treatment rather than therapy. Prophylactic effects with other agents shown in the caerulein AP model include chondroitin-4-sulphate (Cuzzocrea et al. 2004; Campo et al. 2008), a novel agent ND-07 (Lee et al. 2012) and M40401, a SOD mimetic (Cuzzocrea et al. 2004). Interestingly, one study addressed the issue of prophylaxis versus treatment in the assessment of antioxidant efficacy in AP. The effects of NAC in the mouse caerulein AP model were compared when administered before and after the first caerulein injection (Demols et al. 2000). Only the prophylactic treatment was successful in

limiting the severity of experimental AP. Administration of probiotics can effectively reduce oxidative stress in a modified version of the caerulein model, in which AP was induced by intraductal glycodeoxycholate infusion and intravenous caerulein administration (Lutgendorff et al. 2008). These stimulated the biosynthesis of GSH while reducing pancreatic damage and inflammation. In comparison, a clinical study from the same group demonstrated that early administration of probiotics to severe AP patients more than doubled the relative risk of mortality (Besselink et al. 2008). These data clearly highlight that major gaps exist between experimental models and the clinic and that caution should be exercised in the extrapolation of preclinical findings to patient care.

More success has been observed in other experimental AP models, such as in taurocholate-induced experimental AP. ROS scavenger SOD prevented glutathione depletion and reduced the severity of pancreatic injury (Rau et al. 2000). Combined NAC, selenium and ascorbic acid treatment 12 hours post induction of L-arginine-induced experimental AP resulted in amelioration in pancreatic and remote organ injury (Hardman et al. 2005). The involvement of oxidative stress was initially evaluated in an acute necrotising AP rat model, induced by retrograde intraductal infusion of 3% sodium taurocholate (Rau et al. 2000). The study compared an oxidative stress treated group (XOD and hypoxanthine) with a ROS scavenger treated group (SOD/CAT) and showed a significant decrease in conjugated dienes (lipoperoxidation product), amelioration of acinar cell damage, and decreased number of inflammatory cells in the scavenger group. However, the

application of SOD/CAT had no discernible effect on MDA, GSH, amylase or lipase levels or on formation of oedema. The authors concluded that whilst ROS may be important mediators of tissue damage, extracellular generation alone did not induce typical biochemical and morphological changes indicative of AP, and suggested that factors other than ROS must be involved for triggering AP *in vivo*. An alternative approach of ductal obstruction was used to investigate oxidative stress in AP (Urunuela et al. 2002). This study showed increased levels of amylase, highest 6-12 h post ligation, MDA levels which peaked at 6 h and a decrease in GSH levels which troughed at 6 h post ligation. Dihydrorhodamine-123 (DHR) fluorescence was also used to measure oxidative stress in isolated acinar cells and results showed a progressive increase in ROS. The authors suggested that acinar cell ROS acted as signalling messengers to exacerbate disease, activating intracellular proteases, stellate cells and recruitment of immune cells to the pancreas (Urunuela et al. 2002). More recently, a study assessed oxidative stress 48 h post biliopancreatic ductal taurocholate administration to rats, and showed elevated MDA levels in pancreas and erythrocytes, with SOD activity significantly depressed (Yasar et al. 2002). An elevation of oxygen free radicals in taurocholate-induced AP in rats was shown using direct *in vivo* capture of cerium perhydroxide precipitates with confocal laser scanning microscopy (Telek et al. 1999; Telek et al. 2001), which colocalised with NF-κB activation, P-selectin and intercellular adhesion molecule 1 (ICAM) up-regulation (Telek et al. 2001).

In agreement with a role for oxidative stress in bile acid-induced AP, antioxidant pre-treatment with NAC, that has prevented oxidant-induced ROS increases in PACs (Criddle et al. 2006), reduced tissue necrosis, leukocyte infiltration, oedema and haemorrhage in taurocholate-induced AP in rats (Yagci et al. 2004). However, this occurred without concurrent induction of AP. Intravenous administration of a naturally occurring antioxidant, resveratrol, protected against oxidative stress in taurocholate-induced AP, reducing cellular oxidative damage and lipid peroxidation concurrent with lower serum amylase, reduced pancreatic lesions and neutrophil infiltration (Li et al. 2006).

Antioxidant therapy: Clinical experience

The investigation of antioxidant monotherapy in clinical AP has been undertaken in relatively few studies. Selenium supplementation in AP patients was associated with lower serum levels of MDA, but no change in SOD. However, this was a small limited study with only 16 patients (Wollschlager et al. 1997). A non-randomised series showed that introduction of selenium into a treatment protocol was associated with a reduction in mortality from AP; however, there were no severe AP patients included in this study (Kuklinski et al. 1992; Kuklinski et al. 1995). Subsequently, the therapeutic efficacy of high-dose (10 g/day) vitamin C was investigated in AP patients (Du et al. 2003). Compared with the normal group, vitamins C and E, β-carotene, whole blood GSH levels and erythrocyte SOD activity were significantly decreased and lipid peroxidation increased in AP patients,

especially so in severe cases. The results from this study appeared promising, with a significantly quicker recovery from clinical symptoms demonstrated in the high-dose group. Another study evaluated the efficacy of high-dose allopurinol, a XOD inhibitor that blocks generation of ROS, for prevention of post-ERCP AP (Katsinelos et al. 2005) in a prospective, double-blinded, placebo controlled trial. The frequency of AP was significantly lower in the allopurinol compared with the placebo group and mean duration of hospitalisation was significantly shorter, suggesting efficacy for post-endoscopic retrograde cholangiopancreatography (ERCP) pancreatitis.

An early, small, double-blinded trial in 20 patients indicated promise of antioxidant therapy in AP, using a combination of selenium, vitamins C and E, β-carotene and methionine. However, no severe AP patients were included (Uden et al. 1990). In contrast, subsequent studies have generally provided no supportive evidence for the use of antioxidant treatment in AP. For example, although a prospective randomised study AP patients demonstrated decreased oxidative stress in response to antioxidant treatment but no significant reductions of hospital stay or complication rates were detected (Sateesh et al. 2009). Similarly, an investigation in patients with predicted severe AP evaluating combined antioxidant therapy (intravenous NAC, selenium and ascorbic acid; nasogastric β-carotene and α-tocopherol), demonstrated that although vitamin C and selenium levels were significantly increased towards normal following treatment, in-hospital mortality was not reduced (Virlos et al. 2003).

More convincing evidence for a lack of efficacy of antioxidant treatment in AP has been provided by a randomised, double-blind placebo controlled trial of combined therapy (intravenous NAC, selenium and vitamin C) in predicted severe AP patients over a 3-year period (Siriwardena et al. 2007). This study showed that serum levels of antioxidants (ascorbic acid, selenium and GSH/GSSG ratio) rose whilst markers of oxidative stress fell during treatment. Importantly, no statistical difference in organ dysfunction, the primary end-point, or for any secondary end-point of organ dysfunction or patient outcome was detected; clearly indicating that the use of intravenous NAC, selenium and vitamin C combined therapy was ineffective in severe AP. Moreover, this study highlighted a trend towards a more deleterious outcome in patients given antioxidant therapy, which may reflect an ability of antioxidants to increase acinar cell necrosis (Booth et al. 2011; Booth et al. 2011). In agreement, a more recent study recruited 39 patients with severe AP, of which 19 were randomly assigned to antioxidant treatment (vitamin A, E and C), with 20 controls. There was no significant difference in organ dysfunction and length of hospital stay associated with treatment, although markers of oxidative stress (MDA, SOD and reduced GSH) were also not significantly different between the two groups at Day 7 (Bansal et al. 2011). Some antioxidant therapy was successful in the clinic; however, there is insufficient clinical data supporting the beneficial use of antioxidants alone or in combination therapy (Schulz et al. 1999; Banks et al. 2010; Armstrong et al. 2013; Murphy 2014). Since therapy of AP cannot be used prophylactically in the clinical setting, all therapeutic approaches are limited with regard to an inhibition of certain pathophysiological steps.

Antioxidant therapy: Targeted antioxidants

Although there was a lack of success of general antioxidant therapy, a role of ROS was still evident in the development of AP amongst many other oxidative stress-related diseases such as hypertension, atherosclerosis, diabetes and kidney disease. Therefore, antioxidants targeted to the mitochondria, the main source of cellular ROS, were developed for proposed improved efficiency, as most small molecule antioxidants are only taken up by the mitochondria in small amounts and are distributed around the body. Antioxidant targeting was accomplished through linking an antioxidant compound to a lipophilic cation triphenylphosphonium (TPP^+). (2-Hydroxyethyl)triphenylphosphonium bromide (TPP^+ henceforth) is the simplest derivative used in this study (Figure 1.3). TPP^+ is used as a control for more complex derivatives MitoQ and dTPP, alongside non-targeted ubiquinone Decylubiquinone (dUb) in order to rule out or confirm any biological effects of the TPP^+ moiety. Uptake utilises the mitochondrial membrane potential ($\Delta\Psi m$) for accumulation 100-500 fold inside the mitochondria in comparison to the cytosol, an action inhibited by carbonyl cyanide-4-(trifluoromethoxy)phenylhydrazone (FCCP) uncoupler-induced $\Delta\Psi m$ dissipation (Murphy et al. 2000; Kelso et al. 2001; Jauslin et al. 2003; James et al. 2005; Ross et al. 2005). Uptake into the cell is driven by the plasma membrane potential. These mitochondria targeted antioxidants include MitoQ (conjugated to the same ubiquinone as found in Coenzyme Q10) (Kelso et al. 2001), MitoE (conjugated to Vitamin E), MitoSOD (conjugated to superoxide dismutase) and MitoTEMPO, which has both superoxide and alkyl radical scavenging properties and more recently the development of TPP-conjugated caffeic acid (Teixeira et al.

2015). All TPP^+ derivatives can pass easily through phospholipid bilayers without the requirement for a specific uptake mechanism, as they are relatively lipid-soluble, despite their net positive charge (Ross et al. 2005; Murphy et al. 2007; Smith et al. 2008).

Figure 1.3

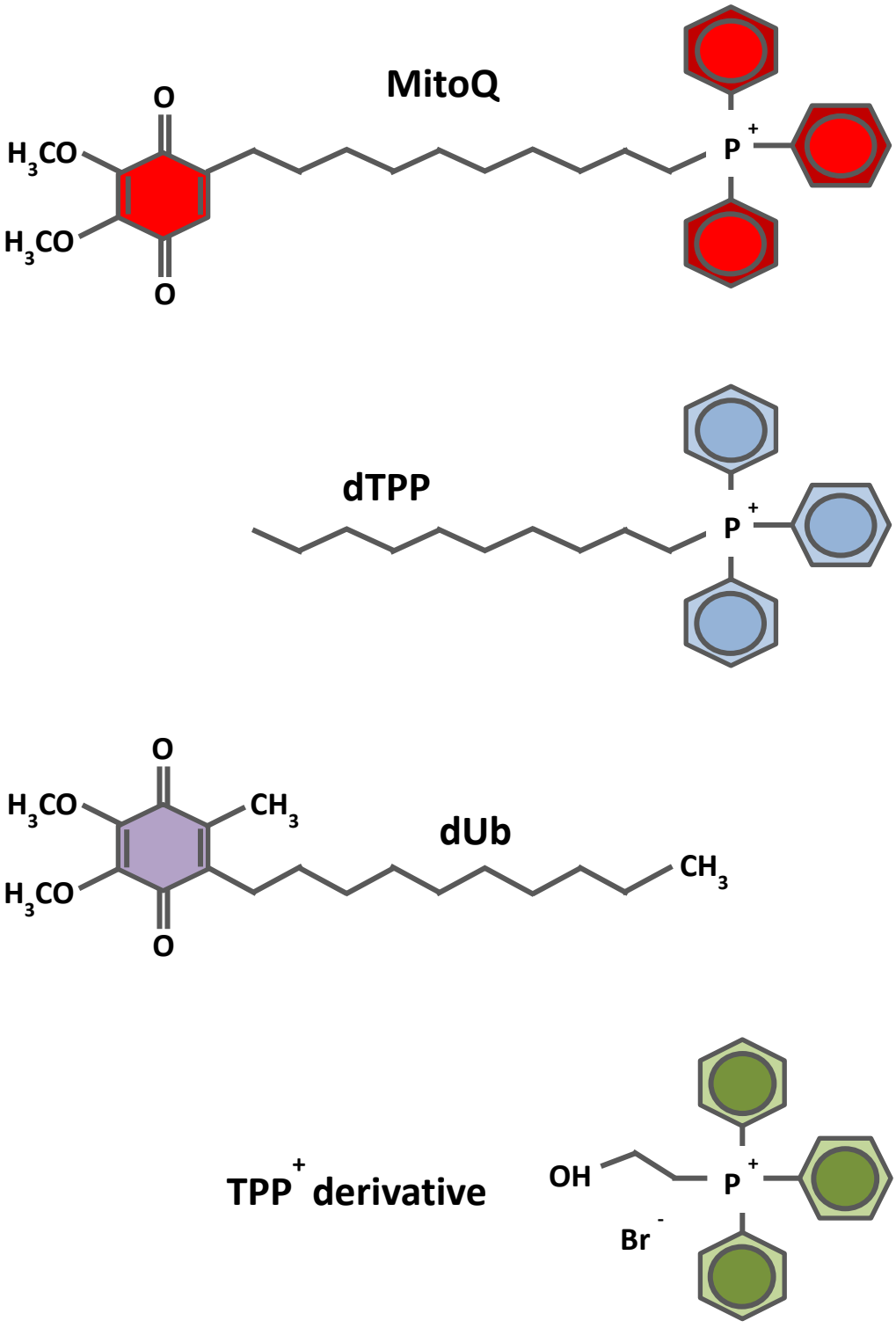

Figure 1.3 Structures of the antioxidant and TPP^+ compounds used in this thesis. MitoQ and dUb are shown in the oxidised forms. The simplest TPP^+ derivative used is one hydroxyl group attached to TPP^+ and has low hydrophobicity and a slower mitochondrial accumulation rate in comparison to the longer more hydrophobic TPP^+ molecules.

Figure 1.4

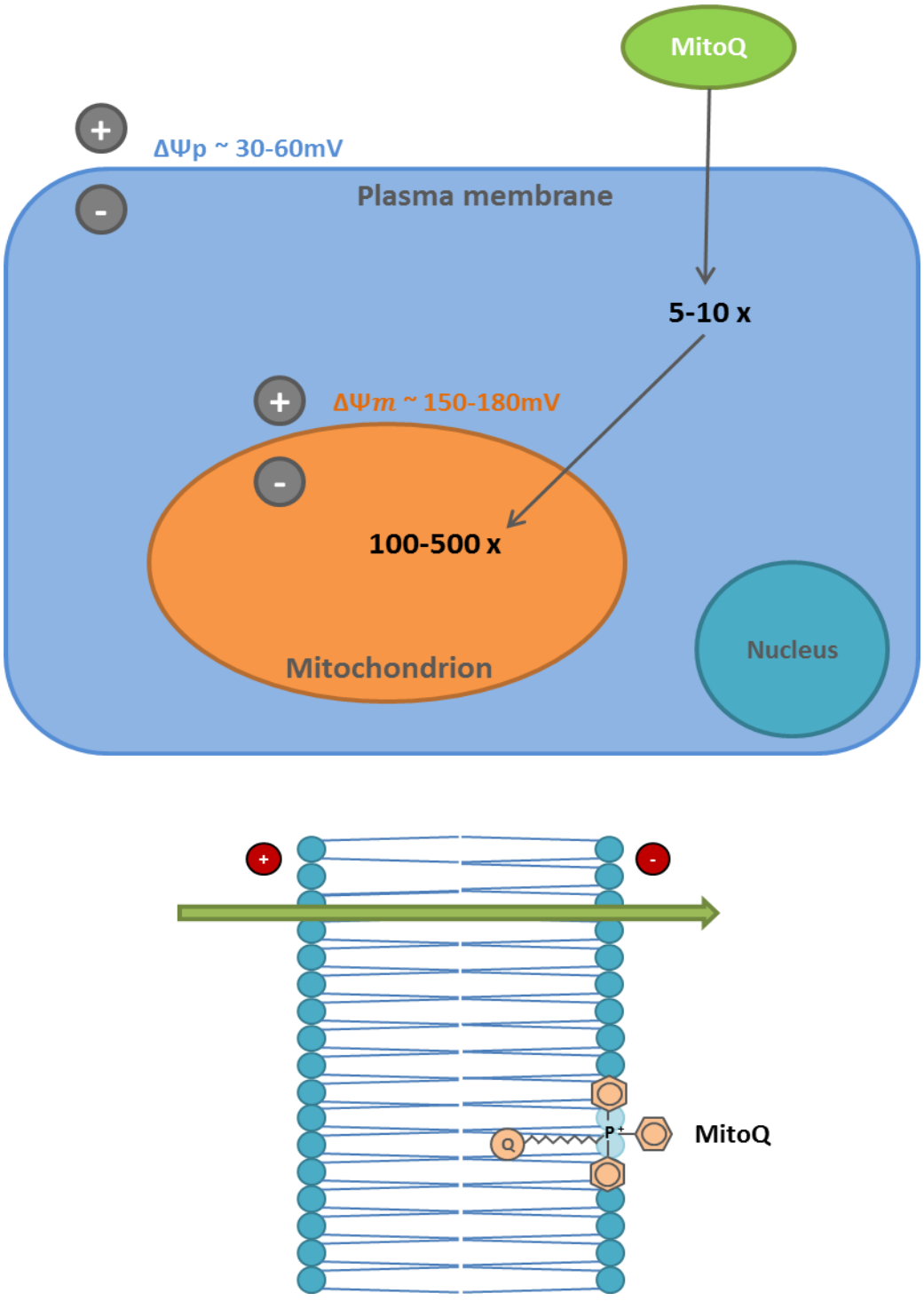

Figure 1.4 Uptake and accumulation of MitoQ and lipophilic cations. Driven by the plasma membrane potential (ΔΨp) MitoQ and lipophilic cations pass through the plasma membrane and accumulate in the cytosol 5-10 fold. Further accumulation of 100-500 fold inside the mitochondria in comparison to the cytosol, is driven by the mitochondrial membrane potential (ΔΨm). Once there, MitoQ is reduced to the active ubiquinol antioxidant by complex II of the electron transport chain. Adapted from Smith et al. (2003)© and Murphy et al. (2007).

Mitoquinone (MitoQ) is the best-characterised mitochondria-targeted antioxidant, designed to deliver a quinone antioxidant moiety to the mitochondria via a 10-carbon alkyl chain linked to the TPP lipophilic cation (Smith et al. 2010). The majority of MitoQ in the mitochondria is found adsorbed to the matrix surface of the inner membrane, sitting deeper into the phospholipid bilayer than the TPP^+ cation alone and (1-Decyl)triphenylphosphonium bromide (dTPP) (Ross et al. 2005). Once located in the mitochondria, MitoQ is continuously recycled by complex II of the electron transport chain to the active antioxidant quinol form. The rate of recycling is at a similar rate to non-targeted form dUb, but both compounds may still interact with superoxide in the quinone form (Kelso et al. 2001; Asin-Cayuela et al. 2004; James et al. 2005; James et al. 2007; Maroz et al. 2009).

Initial toxicity studies in mice showed MitoQ to be non-toxic at 750 nmol/mouse and toxic at 1,000 nmol/mouse with intravenous administration. Concentrations of up to 500µM were well tolerated by mice in drinking water over 4-6 months accumulating to ~113 pmol MitoQ/g in the heart, ~20 pmol MitoQ/g in the liver, and ~2 pmol/g in the brain (Smith et al. 2003; James et al. 2004). In young C57BL/6 mice fed MitoQ for 24-28 weeks there were decreases in the respiratory quotient, liver triglyceride content, plasma triacylglyceride content and white adipocyte size. Overall, there were small overall improvements in balance and motor coordination. There were no substantial differences in any further parameters measured such as O_2 consumption and bone mineral density. MitoQ therapy has shown success in animal models, initially showing to be protective against cardiac ischemia-reperfusion injury (Adlam et al. 2005). In humans, the oral

dosing of MitoQ resulting in a plasma peak concentration (33 ng/ml after ~1 h) is 80 mg (1 mg/kg) (Smith et al. 2010).

Successful studies have shown that MitoQ protects against many oxidative stress-induced conditions. These studies include in isolated mitochondria, cell lines and animal disease models such as sepsis (Lowes et al. 2008), cardiac ischemia-reperfusion injury (Adlam et al. 2005), alcoholic fatty liver disease (Chacko et al. 2011) and toxin-induced Parkinsonism (Ghosh et al. 2010). Further *in vivo* work has demonstrated neuroprotective effects in amyotrophic lateral sclerosis, ameliorated age-related arterial endothelial dysfunction in mice and suppressed NACHT, LRR and PYD domains-containing protein 3 (NLRP3) inflammasome-mediated inflammatory cytokines which ameliorated experimental mouse colitis (Dashdorj et al. 2013; Gioscia-Ryan et al. 2014; Miquel et al. 2014). MitoQ is an effective antioxidant against lipid peroxidation, peroxynitrite and superoxide and inhibiting CCK (10pM) induced ROS increases in PACs (Camello-Almaraz et al. 2006; James et al. 2007). However, in a TLCS-induced AP model MitoQ treatment was not protective and elevated lung myeloperoxidase and interleukin-6 in CER-AP (Huang et al. 2015).

The overall positive results in animal models led to the progression of MitoQ to the clinic and this drug has undergone a double blind, placebo-controlled study in Parkinson's disease. However, there was no improvement to the disease progression. This was proposed to be due to insufficient brain penetration (Snow et al. 2010). There were minimal effects of MitoQ on viral load in a phase II clinical trial

in hepatitis C patients, although there was an overall improvement to liver damage (Smith et al. 2010).

The mechanisms not only appear complex and lacking in definition but there is also evidence demonstrating adverse side effects of MitoQ (Leo et al. 2008; Fink et al. 2012; Reily et al. 2013; Huang et al. 2015; Trnka et al. 2015). All quinols can potentially produce superoxide, effects that were not measureable *in vivo* (James et al. 2004; Smith et al. 2010). MitoQ and other ubiquinol-targeted antioxidants have demonstrated the ability to act as a prooxidant *in vitro*, effects not mirrored by the non-targeted component (Echtay et al. 2002; James et al. 2004; James et al. 2005; O'Malley et al. 2006; Doughan et al. 2007). The efficient redox cycling (production of superoxide from molecular oxygen) capabilities of MitoQ have been compared to that of menadione, resulting in comparatively more superoxide production. In comparison, the non-targeted ubiquinone had little effect on ROS production (Doughan et al. 2007). Enhanced superoxide production via MitoQ redox cycling at ETC complex I, led to elevated levels of H_2O_2 through dismutation by MnSOD. This may alter H_2O_2 signal transduction (Lee et al. 2011). In contrast to the endogenous co-enzyme Q, MitoQ interacts weakly with complexes I and III (James et al. 2007). There is evidence that MitoQ can also be redox cycled at complex I of the ETC leading to increased superoxide production (Doughan et al. 2007; Reily et al. 2013). MitoQ can inhibit a number of H_2O_2 induced signalling pathways and lipid peroxidation in several cell types (Hwang et al. 2001; Echtay et al. 2002; Saretzki et al. 2003; Schäfer et al. 2003; Chen et al. 2004; Dhanasekaran et al. 2004; Ross et al. 2005). However, MitoQ does not react with H_2O_2 directly (Kelso et al. 2001; Asin-

Cayuela et al. 2004; James et al. 2005). Non-targeted antioxidants NAC and natural antioxidant cinnamtannin B-1 can also inhibit H_2O_2 or menadione-induced cell death (Karczewski et al. 2000; Niwa et al. 2003; Gonzalez et al. 2012). MitoQ has shown a number of limited protective capabilities against H_2O_2-induced effects such as mtDNA damage in HDFn cells (Oyewole et al. 2014). In pancreatic acini, the protective capabilities of MitoQ against H_2O_2 effects have yet to be assessed.

The likely reason for MitoQ as a poor substrate for complexes I and III, is the bulkiness of the TPP^+ moiety and interaction of the cation with phospholipid bilayers (Ross et al. 2005; James et al. 2007). MitoQ can not only increase forward transport derived superoxide production, as mentioned earlier, but also enhance ETC complex I expression (Lee et al. 2011). In contrast, MitoQ can block ROS produced from reverse electron transport, effects proposed to be occurring at one or more complex I Q binding sites and inhibitory effects on ETC complexes (Fink et al. 2009; Plecitá-Hlavatá et al. 2009; Lee et al. 2011; Fink et al. 2012). These combined antioxidant and prooxidant abilities have been shown to lead to decreased bioavailability of mitochondrial nitric oxide, which may have effects on nitric oxide signalling (James et al. 2005). The targeted component TPP^+ of the TPP derivatives, such as MitoQ, MitoTEMPOL and MitoE can both act as a mild uncoupler and inhibitor of the ETC (James et al. 2005; Plecitá-Hlavatá et al. 2009; Fink et al. 2012; Reily et al. 2013; Huang et al. 2015; Trnka et al. 2015). The TPP^+ moiety has been shown to have inhibitory effects on the HeLa cell mitochondrial

Na^+/Ca^{2+} exchanger resulting in accumulation of Ca^{2+} within the mitochondria following IP_3 receptor mediated Ca^{2+} release into the cytosol (Leo et al. 2008).

Aims and Objectives

Oxidative stress has been implicated in the pathogenesis of acute pancreatitis (AP), although recent clinical evidence has found no benefit of antioxidant therapy. However, the actions of newer mitochondria-targeted antioxidants in AP remain undetermined. Recent studies by our group using caerulein hyperstimulation and bile experimental models of AP showed MitoQ to have mixed effects in CER-AP providing no protection in TLCS-induced AP. The aim of this work was to evaluate the *in vitro* actions of MitoQ and analogues on mitochondrial function, ROS production, Ca^{2+} concentrations and cell death while furthering our understanding of the role of ROS such as H_2O_2 in PACs.

Chapter 2

Materials and Methods

Removal and Preparation of the Pancreas

6 to 8 week old male CD-1 and CypD knockout mice ($Ppif^{-/-}$ and C57BL/6) mice (Charles River Laboratories, Inc.) were killed by cervical dislocation, in accordance with Animal (Scientific Procedures) Act 1986. The animal was lain on its right side and 100% EtOH was used to wet the fur, and sterilise. A large incision was made through the skin and an incision was then made through the abdominal wall to gain access to the peritoneal cavity. Using forceps, the spleen was carefully lifted up and out of the abdominal and the pancreas cut away from the spleen with dissection scissors before being gently removed from the vicinity of the duodenum. The pancreas was then placed in a dish with ~8ml of NaHEPES buffered physiological saline, containing (mM): NaCl 140, KCl 4.7, $MgCl_2$ 1.13, HEPES 10, and glucose 10, $CaCl_2$ 1. The final pH of the solution was adjusted to pH 7.35 using NaOH. The extracted pancreas was gently washed in this solution in order to remove any excess blood and fluids and to provide the opportunity to discard any attached omentum, fur or spleen. The wash was then repeated and the pancreas transferred to a third dish, with care taken to drain off as much of the accompanying solution as possible.

Figure 2.1

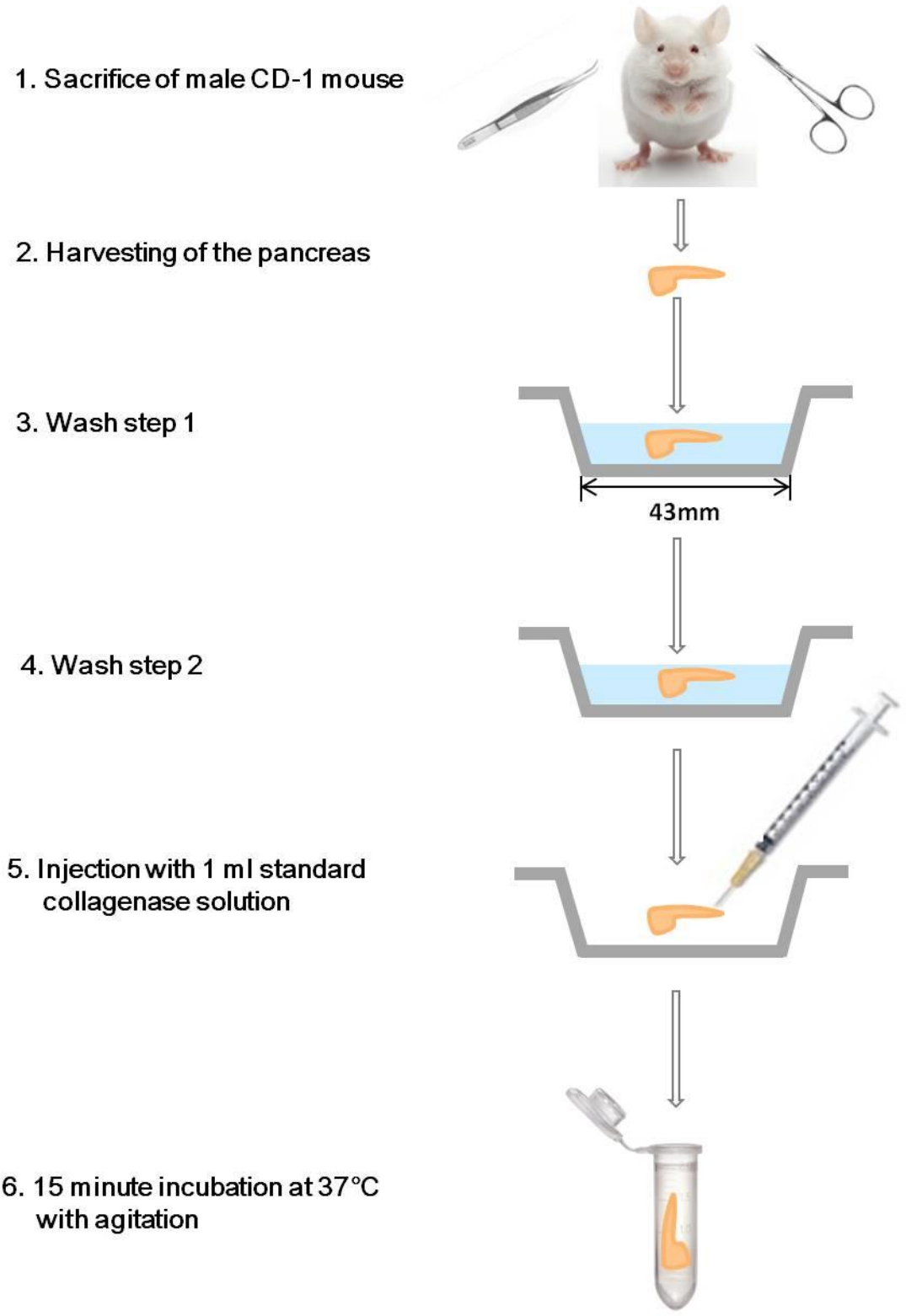
1. Sacrifice of male CD-1 mouse
2. Harvesting of the pancreas
3. Wash step 1
43mm
4. Wash step 2
5. Injection with 1 ml standard collagenase solution
6. 15 minute incubation at 37°C with agitation

Pancreatic Acinar Cell Isolation

The isolated pancreas was injected with 1 ml of standard collagenase solution at 37°C, ~220 units/ml in standard physiological saline (Worthington Biochemical Corporation Lakewood, NJ, USA) at multiple points with the aim to distribute the collagenase throughout. The pancreas and collagenase was transferred to a 1.5ml Eppendorf and incubated at 37°C in an agitating water bath for 15-20 minutes depending on collagenase batch variations. The pancreas was then transferred to a 15ml polycarbonate tube (Sarstedt, Leicester, UK) and ~5ml physiological saline added to dilute the collagenase and stop further substantial digestion. The pancreas was vigorously sucked in and out of a 1ml pipette tip cut diagonally to increase the diameter. The turbid supernatant formed was transferred into a fresh identical 15ml tube. This process was repeated a further three times, until a turbid supernatant was no longer obtained, using pipette tips cut with a progressively smaller tip diameter. The collected supernatant was centrifuged at 1000RPM for 1 minute. The pellet was resuspended in NaHEPES and filtered through a 70µM cell strainer (BD Biosciences) before repeating the centrifuge step. The pellet was then resuspended in a final solution NaHEPES to the cell density required.

Figure 2.2

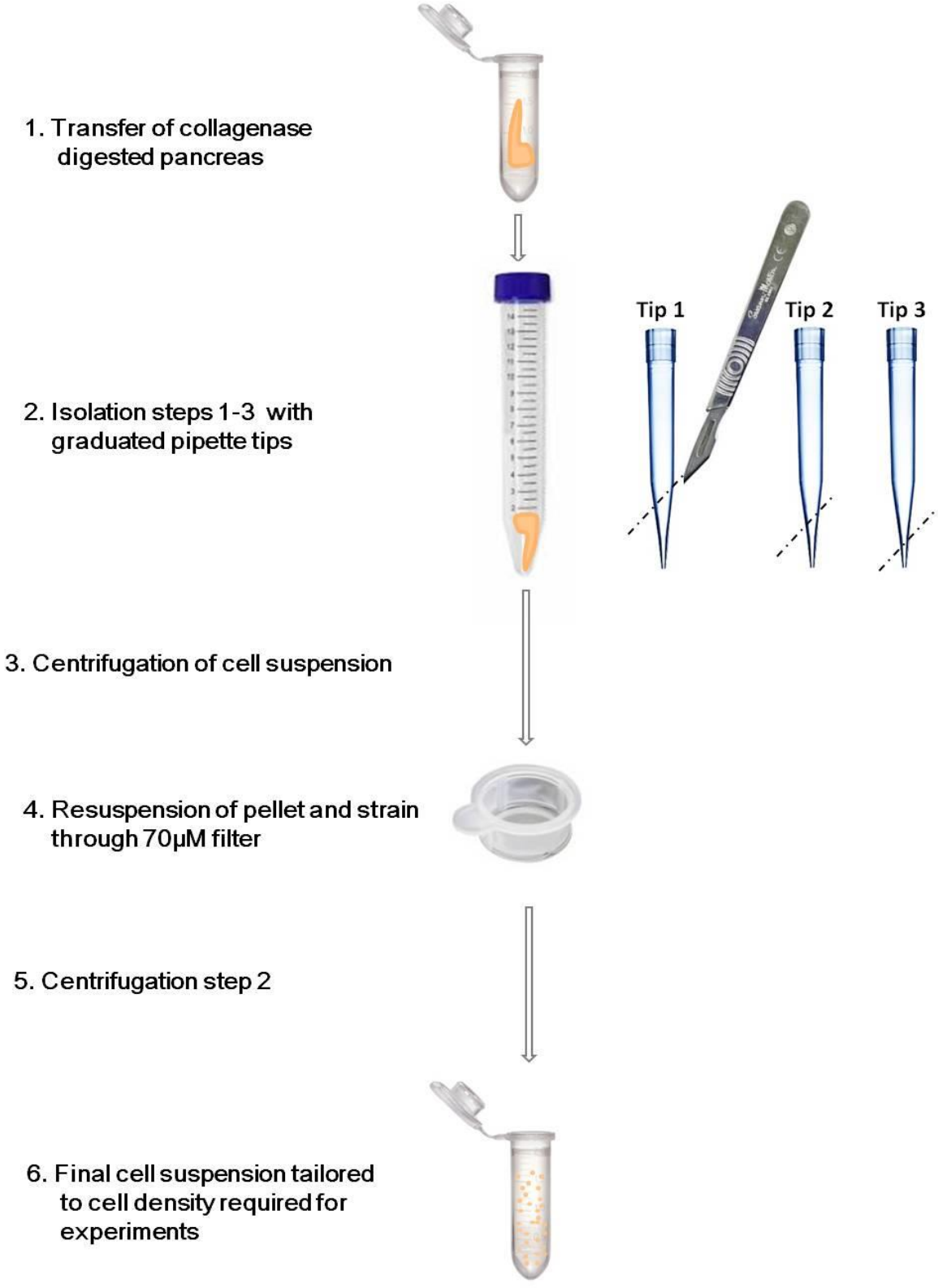
1. Transfer of collagenase digested pancreas
2. Isolation steps 1-3 with graduated pipette tips
Tip 1
Tip 2
Tip 3
3. Centrifugation of cell suspension
4. Resuspension of pellet and strain through 70µM filter
5. Centrifugation step 2
6. Final cell suspension tailored to cell density required for experiments

Loading Fluorescence Indicators

When a fluorescence indicator was required for confocal microscopy experiments, the dye was loaded for 30 minutes at room temperature in an agitating water bath. The cell suspension was then washed with 5-6ml of Na HEPES, centrifuged (as previously described) and resuspended in 1-2ml NaHEPES tailored to experimental requirements and cell density. When multiple pre-treatment groups were used, the cells were gently mixed to ensure homogeneity before being aliquoted into separate 1.5ml Eppendorf centrifuge tubes allocated per treatment group. The pre-treatment of pancreatic acinar cells would be performed for 30 minutes at room temperature prior to the experiment and washed again with NaHEPES to remove any compound not within the cells.

Experimental Procedures

All confocal experiments on isolated pancreatic acinar cells were performed at room temperature (23-25°C) and the cells were used no more than 4 hours after cell isolation was completed if not otherwise stated.

Materials and Reagents

Reagents, if not otherwise mentioned were all from Sigma-Aldrich. Mitoquinone (MitoQ) and its non-antioxidant moiety control, (1-Decyl)triphenylphosphonium bromide (dTPP) were synthesised in the Department of Chemistry, University of Octago, New Zealand. In the case of pre-treatment experiments with MitoQ, dTPP and for certain experiments Decylubiquinone (dUb) and (2-Hydroxyethyl)triphenylphosphonium bromide (referred to as TPP^+ henceforth), each compound was added from a 10µM stock diluted in NaHEPES.

Data Analysis

Data are presented as mean ± SEM. The mean for individual experiments was obtained from at least three repetitive experiments. Statistical analysis was performed using software packages Origin 9 and Excel for Windows, and paired t-test applied unless otherwise stated.

Confocal Microscopy

Microscope work was performed using either a Zeiss LSM510 confocal microscope (Carl Zeiss; Jena, Germany) or an Olympus IX71 imaging system (Olympus Corporation, Shinjuku, Tokyo, Japan).

Olympus IX71 Imaging System

The Olympus imaging system used a 10x/0.4 UPlanSApo dry objective and 1.5 aperture and was applied for imaging of both chloromethyl 2',7'-dichlorodihydrofluorescein diacetate (CM-H_2DCFDA) and Fura-2-AM (Fura-2 hereafter) fluorescence. To obtain maximum signal and minimal background for CM-H_2DCFDA imaging excitation was set at 450nm with a 15% band width. For the ratiometric dye Fura-2 excitation was set to 340/380 and emission 510nm.

Zeiss LSM510

Excitation lines and emission collection parameters were optimised to obtain minimum noise and maximal signal in accordance to the Excitation/Emission spectrum of the dyes or autofluorescence. The pinhole was adjusted to the requirements of the specific experimental set to allow for maximum light collection for each of the following parameters. NAD(P)H and FAD^+ (autofluorescence) and dyes Fluo-4, AM (Fluo-4 hereafter), Tetramethylrhodamine methyl ester (TMRM),

CM-H_2DCFDA, Mag-Fluo-4, AM (Mag-Fluo-4) and Rhod-2, AM (Rhod-2) were all purchased from Life Technologies (Carlsbad, CA, United States of America). Cells were visualised using a C-Apochromat 63x numerical aperture 1.2 water immersion objective, collecting fluorescence values every 3-10 seconds depending on experimental requirements. Fluo-4 measurements required a more rapid cycle time of ~4 seconds to enable effective monitoring of the more rapid changes in cytosolic Ca^{2+}, whereas detection of membrane depolarisation with TMRM ~5-6 second intervals were adequate. Autofluorescence measurements were more delicate and to avoid any laser-induced photo bleaching, a longer scanning interval of 6-7 seconds was used: this ensured stability of the measured trace. To avoid photo-activation of CM-H_2DCFDA, ~10 seconds cycle time was used. Whole cell imaging of NAD(P)H and FAD^+ autofluorescence, Fluo-4 and CM-H_2DCFDA required the pinhole at a maximum 18.21 Airy units (optical slice of 141µM) for optimum light intensity. The settings used for NAD(P)H were optimised to a fluorescence intensity >1100, maintaining as consistent levels of gain as possible between experiments. This enabled the selective avoidance of cells, which were not in optimum health, as they would typically exhibit initial fluorescence values of below 1000. This method was essential for providing reliable, reproducible results of maximum sensitivity. A similar approach was applied to FAD^+ measurements, however, as FAD^+ fluorescent values increase with treatment, the opposite strategy was applied and cells with lower intensity values were typically used. When working with CM-H_2DCFDA it was critical to the experiments to select cells with lower fluorescence intensity (but not too low as this can indicate poor loading of the dye). This enables effective monitoring of fluorescence increases particularly for longer experiments to avoid

saturation. For imaging of mitochondria with dyes TMRM and Rhod-2 the pinhole was set to an intermediary 2.5 Airy units (optical slice of 20µM). Care was taken to select cells with optimum loading and no indications of damage or onset of depolarisation (TMRM measurements).

Perfusion Systems

To maintain a constant presence of a solubilised compound cells were perfused using a gravity fed perfusion system with a six (Olympus Imaging System) or eight-way manifold (Zeiss 510) (Warner Instruments Inc.) with 15ml syringes to hold the solutions. Thin-walled silicone tubing (AlteSil High Strength Tubing, 0.5mm Bore, 0.25mm Wall; Altec Products Ltd., Bude, UK) was used for its flexibility and it is easier to clean away any salt deposit blockages with manual massage of the tube. A vacuum suction system was used to remove the perfused solutions and maintain a continuous flow. Tubing and flow was checked prior to each experiment to ensure absence of any blockage or bubbles. Each tube and tubing was washed with 70% ethanol and ddH_2O prior to and post experimental session to sterilised the system and to prevent build-up of any dust, debris or salt deposits. The glass slides used for the Zeiss 510 system were not coated and the cells loaded into the chamber perfused with NaHEPES within 1 minute. This helped to eliminate cells prior to the experiment, which may be easily disturbed during experimentation by the perfusion flow and cause loss of data. The Olympus imaging system had a slightly more rapid

perfusion rate therefore, poly-l-lysine coated slides (0.3% in ddH_2O) were used to promote adhesion. A schematic is shown in figure 2.3

Figure 2.3

Schematic representation of the gravity perfusion systems used. (A) A side view of the system showing 4 of 8 15ml syringes suspended to generate the perfusion flow, the location of solution input and exit via suction. (B) A cross-sectional view of the chamber providing a more detailed view.

Figure 2.3

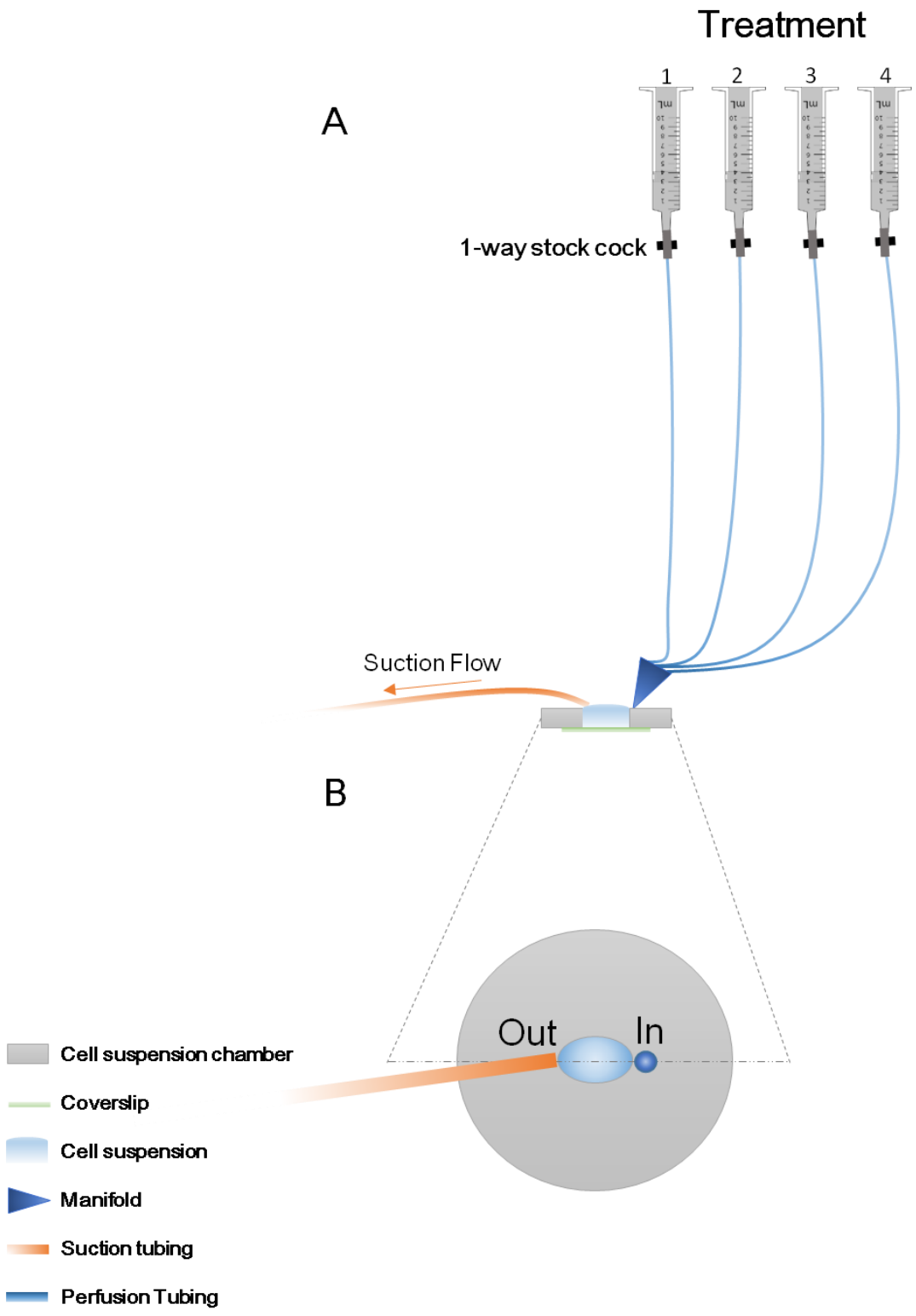
Treatment
1
2
3
4
A
1-way stock cock
Suction Flow
B
Out
In
Cell suspension chamber
Coverslip
Cell suspension
Manifold
Suction tubing
Perfusion Tubing

Imaging with and without Fluorescent Indicators

CM-H_2DCFDA

Experiments employed various different dyes. Cellular oxidative stress was assessed using CM-H_2DCFDA, (Life technologies). This chloromethyl derivative of H_2DCFDA provides improved retention. It passively diffuses into the cell, where its acetate groups are cleaved by intracellular esterases and its thiol-reactive chloromethyl group reacts with intracellular glutathione and other thiols. This allows for facilitation of longer experiments as the subsequent oxidation yields a fluorescent adduct which is trapped inside the cell. CM-H_2DCFDA is prepared at a concentration of 10mM in high-grade di-methyl sulfoxide and frozen in aliquots at -20˚C. This is added to 1ml of cell suspension to obtain a final concentration of 10µM. DMSO concentrations were kept below 0.1% at all times CM-H_2DCFDA was loaded in Corning® 15 ml centrifuge tubes (wrapped in aluminium foil to prevent light exposure) at room temperature with gentle agitation for 30 minutes. The cells were then washed in NaHEPES and re-suspended in 1-2ml, depending on experimental requirements. This methodology was maintained for other fluorescent indicators bar the final working concentration and these changes or any others are noted. The cells were excited with a 488nm argon laser line and emission collected between 505-550nm. Laser intensity was kept low (0.8-1%) and both detector gain and the scanning interval were also kept minimal for all experiments to minimise photoactivation of the indicator.

TMRM

Mitochondrial membrane potential was determined using the fluorescent dye TMRM. TMRM is a cell-permeant cation, which selectively and readily accumulates in the mitochondrial matrix. Pancreatic acinar cells were loaded with 37nM TMRM for 30 minutes at room temperature and processed as previously described. This was reduced down from 40nM to prevent over loading and dequenching. TMRM-loaded cells were excited with 543nm helium-neon laser and emitted fluorescence was captured between 560-650nm. Laser power used was 4-5%.

NAD(P)H autofluorescence

NAD(P)H autofluorescence was also visualised via excitation with both 351nm and 364nm coherent laser lines of the UV laser module and emission collected between 390-450nm. The 351nm laser line was used at a laser power of 1% and the 364nm at 2%. The pinhole was set at maximum, the amplifier offset adjusted slightly per experiment and amplifier gain set at an intermediary value. It was found that using both 351nm and 364nm laser lines provided exemplary NAD(P)H autofluorescence and the settings were optimised to provide minimal noise and enable visualisation of individual mitochondrial structures. The starting fluorescent values were maintained towards the higher range to enable detection of any small decreases if present.

FAD^+ autofluorescence

For determinations of FAD+ auto-fluorescence no dye was employed. The oxidized form FAD+ is auto-fluorescent and no dye loading of the cells is required. FAD^+ autofluorescence was visualised via excitation with a 458nm argon laser and emission collected between 505-560nm. The laser power was used at 20% with the pinhole set at maximum, the amplifier offset adjusted slightly per experiment and amplifier gain set at the maximum value. The settings were optimised to provide minimal noise and the starting fluorescent values were maintained towards the lower range to enable detection of small increases if present. Imaging both NAD(P)H and FAD^+ simultaneously provides a measure of cellular metabolism using the ratio of oxidation-reduction (redox) NAD(P)H/FAD^+ (Chance et al. 1979; Ostrander et al. 2010). This method provides a valuable tool to assess relative changes in the redox state without the application of exogenous stains or dyes. Fluorescence measurements were normalised and the NAD(P)H values divided by the FAD^+ values.

Fluo-4, AM

Cytosolic Ca^{2+} was imaged with the single wave, cell permeable acetoxymethyl ester (AM) form of Ca^{2+} indicator Fluo-4 (Life technologies), which is an analogue of Fluo-3. Fluo-4 has an increased fluorescence excitation to Fluo-3 and consequent increased fluorescent signal levels via the substitution of two chlorine

by two fluorine's. The AM-ester group results in an uncharged molecule that can permeate cell membranes. Once inside the cell, the acetoxymethyl group is removed by cellular esterases generating a charged form, which exhibits a slower leak rate from the cell in comparison to the parent compound. The affinity of Fluo-4 for Ca^{2+} is 345 nM, which is within the ideal range of $[Ca^{2+}]_c$ concentrations (50nM-5uM) encountered in the cytosolic compartment (Ward et al. 1995). Fluo-4 was loaded to obtain a final concentration of 5µM with excitation being with a 488nM laser line and emission collected between 505-530nM.

Fura-2, AM

Cytosolic Ca^{2+} was also imaged with ratiometric dye Fura-2. Pancreatic acinar cells were loaded with 5µM fura-2-AM (Life Technologies) as previously described and imaged using the Olympus Imaging system. Excitation was set at 340nm/380nm and collected at 510nm.

Rhod-2, AM

The Ca^{2+} sensitive rhodamine-derived indicator Rhod-2 (Invitrogen; Paisley, UK) was used to image mitochondrial Ca^{2+}. As with Fluo-4 and Fura-2, Rhod-2 was loaded in the cell permeable AM form, however in comparison, intracellular cleavage of the AM group yields a positive charge, promoting sequestration into the mitochondria via membrane potential-driven uptake. Rhod-2 was prepared and stored as with Fluo-4 and loaded at a final concentration of 5µM for 30 minutes at

room temperature as previously described for Fluo-4. A 543nM laser line was used for excitation and emission collected between 560-650nM. The low resting state fluorescence exhibited by Rhod-2 required careful imaging to avoid saturated readings as upon stimulation this fluorescence can increase >100.

Mag-Fluo-4, AM

Mag-Fluo-4, AM is an analogue of fluo-4 with a Kd for Mg^{2+} of 4.7 mM and a Kd for Ca^{2+} of 22 µM. This made it useful as a low-affinity Ca^{2+} indicator for measuring Ca^{2+} within the endoplasmic reticulum compartment. Care was taken to avoid the nucleus using a specific region of interest to take the fluorescence readings from during confocal experiments.

Plate Reader Cell Death Experiments

Basic Principles – Measurement of Apoptosis

CellEvent® Caspase-3/7 Green reagent is a four amino acid peptide (DEVD) conjugated to a nucleic acid-binding dye. The DEVD peptide sequence is a cleavage site for caspase-3/7 and the conjugated dye is non-fluorescent until the DEVD peptide is cleaved from the peptide and the free dye can bind DNA. A green fluorescence is generated at an emission wavelength of 530nm with the intensity being proportional to the level of activated caspase-3/7.

Figure 2.4

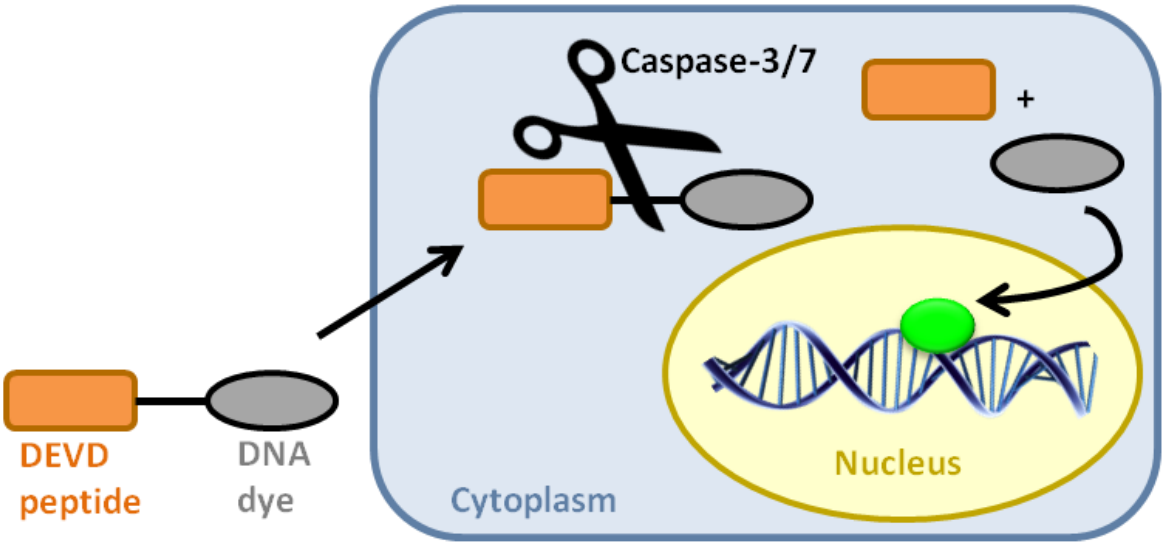

Basic Principles – Measurement of Necrosis

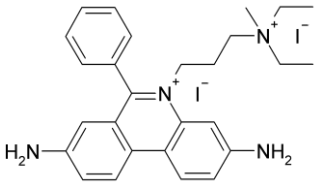

Propidium iodide (PI) dye is an ideal indicator of necrotic cells as it is a membrane impermeant and therefore excluded from viable cells. It binds to DNA (and RNA) by intercalating between base pairs with little or no sequence preference. Once the dye is bound it exhibits enhanced fluorescence of 20- to 30-fold. With an excitation maximum at 535 nm and emission maximum at 617 nm PI can be easily used in combination with CellEvent® Caspase-3/7 Green reagent to compare levels of apoptosis and necrosis.

Figure 2.5

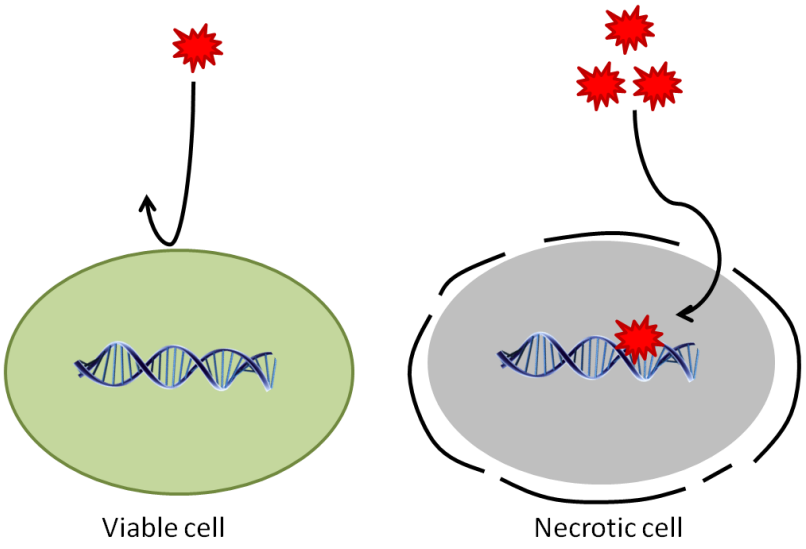

Reagents

Cholecystokinin (CCK)	10nM
Taurolithocholic acid-3-sulfate (TLCS)	500µM
Hydrogen peroxide	1µM, 5µM, 10µM, 500µM and 1mM
Palmitoleic acid ethyl ester (POAEE)	100µM
Ethanol	85mM and 850mM
Polyethylene glycol (PEG)	280mM
MitoQ/dTPP/dUb/TPP^+	0.1µM, 0.2µM, 0.5µM, 1µM

Methods

For detection of necrosis and apoptosis, POLARstar OMEGA fluorescence microplate reader (BMG labtech) was employed for time-course experiments at 37^0C. Flat bottomed 96-well microplates (Greiner Bio-One Ltd) were used to seed cells and measurements set to scan 1 cycle/100 seconds for a minimum of 450 cycles. Propidium Iodide (PI) was used to detect necrosis and was loaded at a final concentration of 10µg/ml. An additional wash step was included prior to adding PI to minimise any free nuclei present. Excitation was set at 520nm and emission collection at >590nm. For apoptosis measurements CellEvent® Caspase-3/7 Green Ready Probes® Reagent was added to the acinar cell suspension at 2 drops/ml (approximately 40 µl/ml). Excitation/Emission used was 485/530nm. The gain was set to an intensity of 900 in all experiments. Cells were prepared as described previously and filtered with a 70µm cell strainer, which helped to remove any

clumps of necrotic cells. The final preparation of cells was added after manual agitation to ensure homogeneity to each well of the 96-well microplate. MitoQ/dTPP/dUb/TPP^+ were added at this step for those groups receiving pre-treatment. The plate was then inserted into the microplate reader to establish a cell death baseline. Upon establishment of a baseline, the microplate was removed and the reagents, as detailed above, were added to the corresponding treatment groups. The plate was carefully sealed with a permeable membrane (Breathe-Easy® sealing membrane, Diversified Biotech, Dedham, United States) and reinserted for the remainder of the experiment. Cell free blanks were used (buffer and dye) and these values deducted from the fluorescent values generated. Normalisation was performed after subtraction of the background to the baseline/beginning of the experiment or to specific time points if required.

Chapter 3

The Effects of Mitoquinone on Murine Pancreatic Acinar Cells

Effects of MitoQ on Cellular ROS Levels

Pancreatic acinar cells were either continuously perfused with MitoQ and simultaneously monitored or pre-treated with MitoQ for 30 minutes. Experimental treatment was then commenced and compared to both the non-antioxidant analogue dTPP, which has similar hydrophobicity to MitoQ, and NaHEPES control (physiological saline).

Isolated cell suspensions were initially loaded for 30 minutes with 10µM general oxidative stress indicator CM-H_2DCFDA, washed and loaded onto the microscope stage to measure basal levels of reactive oxygen species (ROS). 1µM MitoQ and dTPP were continuously perfused over the cells. Basal $[ROS]_I$ levels were not affected by either compound in comparison to the NaHEPES control (Figure 3.1). 10µM MitoQ and dTPP treatment also did not show significant changes (Figure 3.2).

To assess the protective capabilities of MitoQ in comparison to the control compound (dTPP), a high concentration of exogenous oxidant H_2O_2 (1mM) was applied. The 1mM H_2O_2 treatment caused a steady rise of ROS in pancreatic acinar cells (positive control group) as reflected by increased intensity of CM-H_2DCFDA fluorescence. Cells pre-treated with 1µM MitoQ, exhibited reduced ROS levels compared with the positive control group and cells pre-treated with 1µM dTPP (Figure 3.3). Both MitoQ and dTPP pre-treatment at 10µM reduced 1mM H_2O_2 induced ROS increases (Figure 3.4).

Figure 3.1

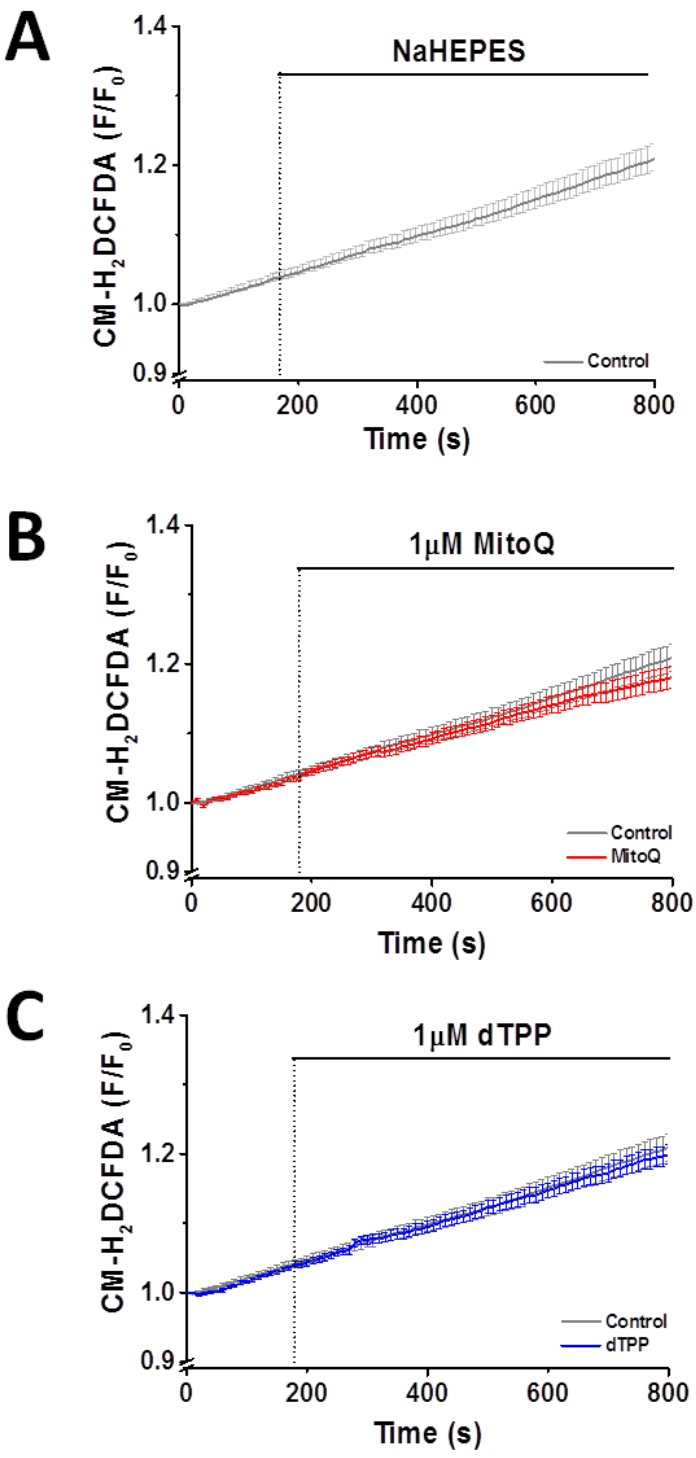

Figure 3.1. Basal levels of reactive oxygen species (ROS) are not affected by 1μM MitoQ and dTPP treatment. Basal ROS levels from CM-H_2DCFDA loaded cells were measured for 3 minutes prior to perfusion with **(A)** NaHEPES (Control), **(B)** MitoQ (1μM) or **(C)** dTPP (1μM). No significant changes were observed. Traces are averages of >65 cells from at least 3 animals. Data have been normalised to the initial fluorescence reading t=0 expressed as F/F_0. All data shown are mean ±SEM.

Figure 3.2

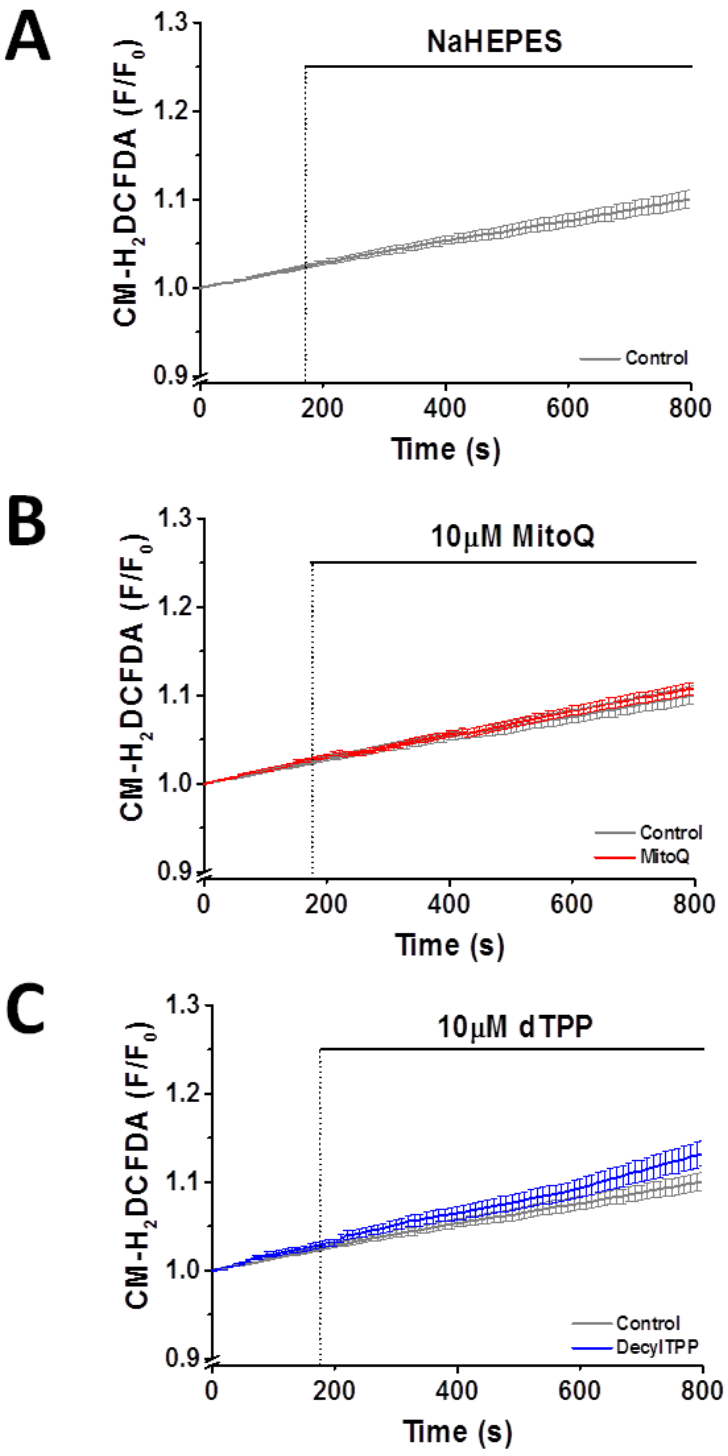

Figure 3.2. Basal levels of ROS are not affected by 10µM MitoQ and dTPP treatment. Basal ROS levels from CM-H_2DCFDA loaded cells were measured for 3 minutes prior to perfusion with **(A)** NaHEPES, **(B)** MitoQ (10µM) or **(C)** dTPP (10µM). No significant changes were observed. Traces are averages of >46 cells from at least 3 animals. Data have been normalised to the initial fluorescence reading t=0 expressed as F/F_0. All data shown are mean ±SEM. The slight increase seen with 10µM dTPP treatment did not reach significance of $p<0.05$ (paired ttest, one way ANOVA).

Figure 3.3

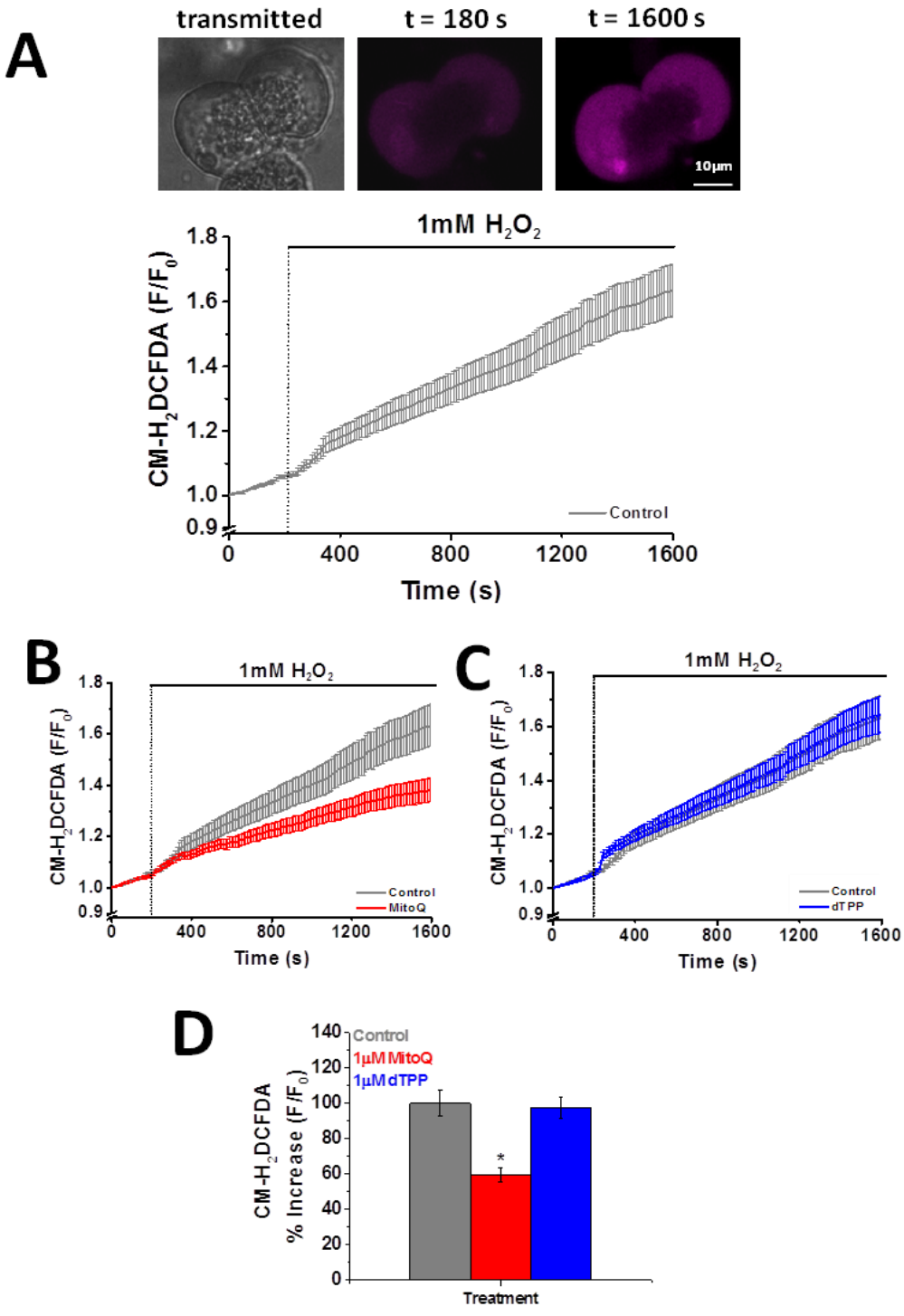

Figure 3.3. MitoQ inhibited 1mM H_2O_2-induced ROS increases. Pancreatic acinar cells pre-treated with **(A)** NaHEPES (Control), **(B)** MitoQ (1µM) or **(C)** dTPP (1µM) prior to treatment for 25 minutes with 1mM H_2O_2. **(D)** Data are expressed as percent increase of the mean fluorescence intensity during treatment with 1mM H_2O_2. Images show typical CM-H_2DCFDA fluorescence (scale bar 10µm). The data are averages of >87 cells from at least 3 animals and have been normalised to the initial fluorescence reading t=0 expressed as F/F_0. All data shown are mean ±SEM. * $p<0.05$ vs untreated control.

Figure 3.4

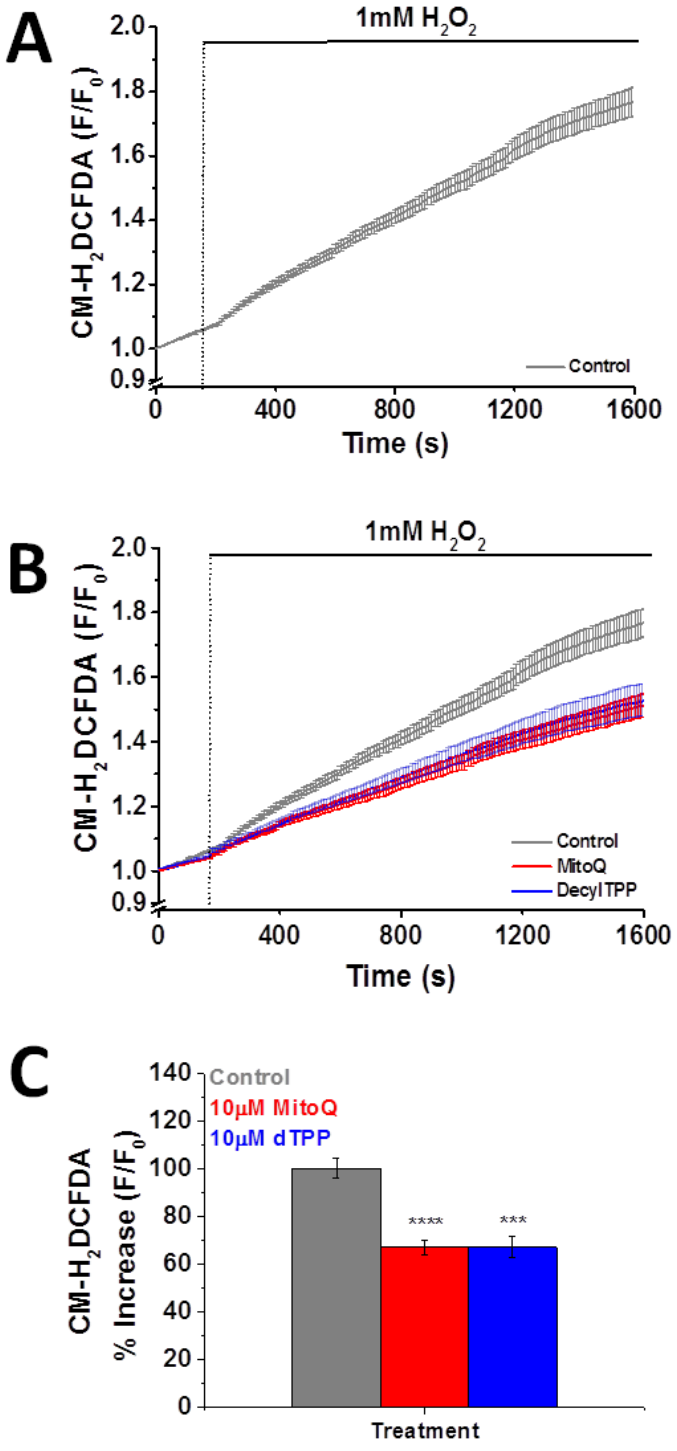

Figure 3.4. 1mM H_2O_2-induced ROS increases are diminished by 10µM MitoQ and 10µM dTPP (A) NaHEPES (Control), **(B)** MitoQ (10µM) and dTPP (10µM) **(C)** Data are expressed as a percent increase of the mean fluorescence intensity during treatment. The data are averages of >80 cells from at least 3 animals and have been normalised to the initial fluorescence reading t=0 expressed as F/F_0 . All data shown are mean ±SEM. *** p<0.001 and **** p<0.0001 vs untreated control.

Concentration-Dependent Effects of MitoQ on Mitochondrial Membrane Potential

Pancreatic acinar cells were loaded with TMRM (30 minutes), a dye that relies on the mitochondrial membrane charge gradient to accumulate in the mitochondria. As the membrane becomes depolarised and this charge gradient diminished, the TMRM dye is lost from the mitochondria resulting in a decrease in fluorescence (Ehrenberg et al. 1988; Scaduto Jr et al. 1999; Lemasters et al. 2007). TMRM thus provides a key tool for observing depolarisation, partial or complete in pancreatic acini.

A baseline of TMRM fluorescence was established prior to a 10 minute treatment with MitoQ and dTPP (1µM). Further experiments included a 30 minutes perfusion of cells with MitoQ (1µM) (Figure 3.5). Protonophore carbonyl cyanide m-chlorophenylhydrazone (CCCP) was then applied at 10µM. CCCP uncoupled the proton gradient established during normal electron transport chain activity from ATP production, dissipating the mitochondrial membrane potential (Hirose et al. 1974; Burkhardt et al. 1989; Park et al. 1997). Neither compounds induced depolarisation of the mitochondria in comparison to cells perfused with NaHEPES physiological saline. Applying MitoQ and dTPP at 10µM (Figure 3.6) induced partial depolarisation detectable by differences in TMRM fluorescence between the control and MitoQ/dTPP treated cells.

Figure 3.5

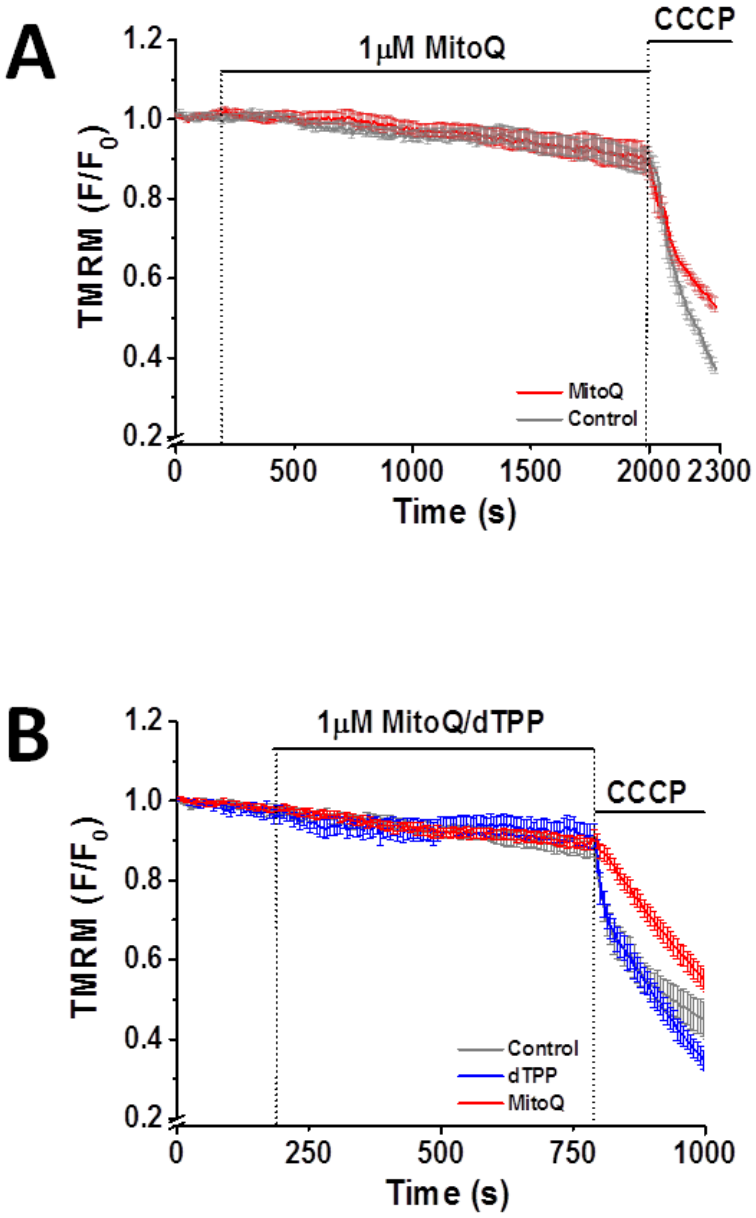

Figure 3.5. MitoQ and DecylTPP had no effect on ΔΨm. (A) NaHEPES (Control) and MitoQ (1μM) 30 minute treatment, **(B)** NaHEPES, MitoQ (1μM) and dTPP (1μM) 10 minute treatment. No significant changes in ΔΨm are seen with either 1μM MitoQ or 1μM dTPP. Traces are averages of >17 cells from at least 3 animals. Data has been normalised to the initial fluorescence reading t=0 expressed as F/F_0. All data shown are mean ±SEM.

Figure 3.6

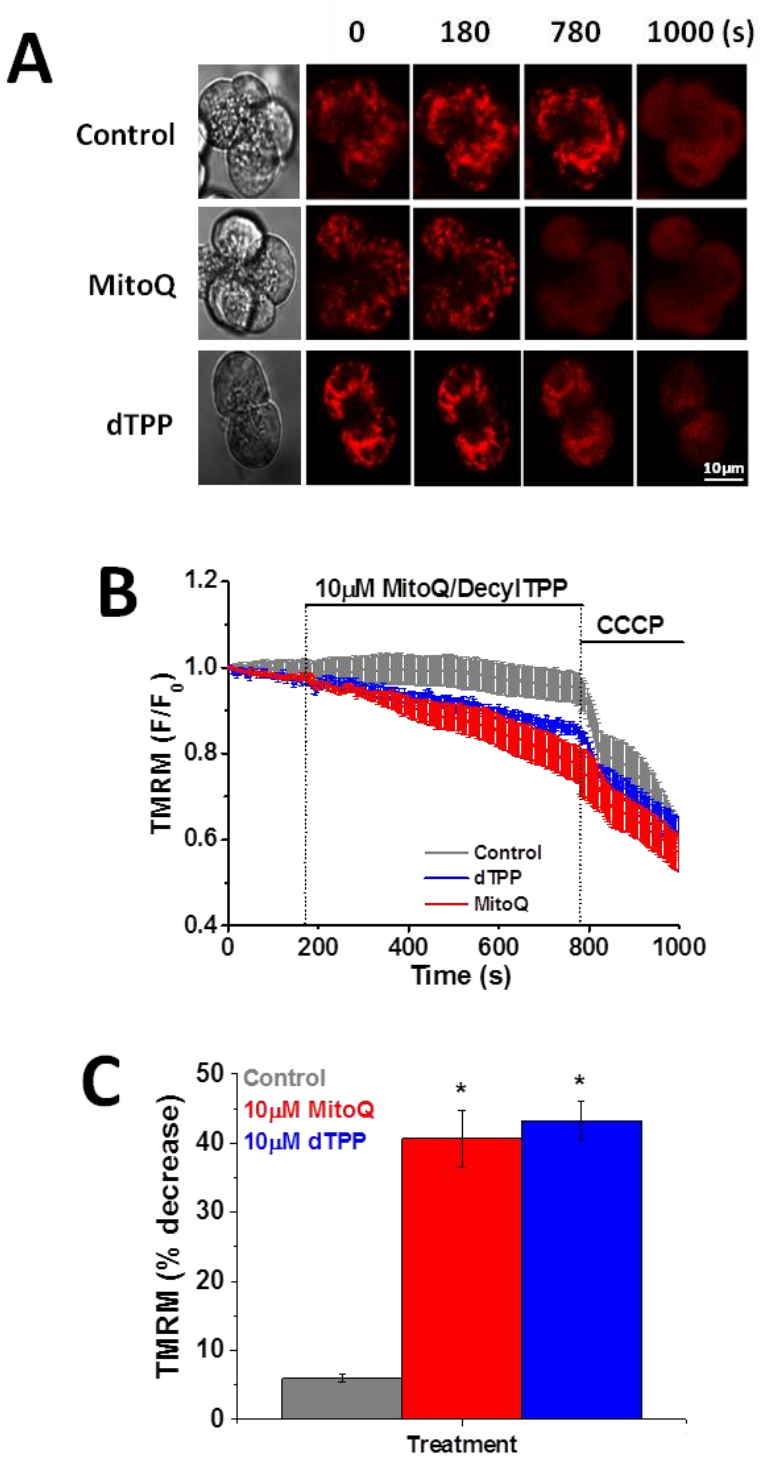

Figure 3.6. 10µM MitoQ and 10µM dTPP caused partial ΔΨm depolarisation. ΔΨm was measured for 10 minutes. **(A)** Time point images for each treatment group (scale bar 10µm), **(B)** NaHEPES (Control), MitoQ (10µM) and dTPP (10µM). **(C)** Percentage of fluorescence intensity decrease of each treatment group from the baseline compared to the control. Traces are averages of >16 cells from at least 3 animals. Data has been normalised to the initial fluorescence reading t=0 expressed as F/F_0. All data shown are mean ±SEM. * $p<0.05$ vs untreated control.

MitoQ-Induced Changes to the Bioenergetics and Redox Status of Pancreatic Acinar Cells

Measuring NAD(P)H autofluorescence enabled the indication of changes in the bioenergetics and redox status of pancreatic acinar cells, via increases or decreases in NAD(P)H autofluorescence. This enabled sensitive measurements in cells not loaded with dye based indicators. The isolated cells were treated on the microscope stage continuously for 10 minutes with MitoQ/dTPP (1µM) prior to the addition of CCCP (10µM). 1µM MitoQ (74% of cells) and 1µM dTPP, (71% of cells) induced a transient increase in levels of NAD(P)H. This was followed by a decrease in NAD(P)H autofluorescence in comparison the NaHEPES control responses (Figure 3.7). Measuring NAD(P)H levels over a longer time point of 30 minutes showed progressive decreases with 1µM MitoQ treatment (Figure 3.8). Imaging both NAD(P)H and FAD^+ simultaneously provides a measure of cellular metabolism using the ratio of oxidation-reduction (redox) NAD(P)H/FAD^+ (Chance et al. 1979; Ostrander et al. 2010). NAD(P)H and FAD^+ autofluorescence were simultaneously measured during continuous perfusion with MitoQ or dTPP (1µM) for 30 minutes (Figure 3.9). MitoQ induced mirrored decreases in NAD(P)H and increases in FAD^+ whereas dTPP did not (in comparison to the control).

Figure 3.7

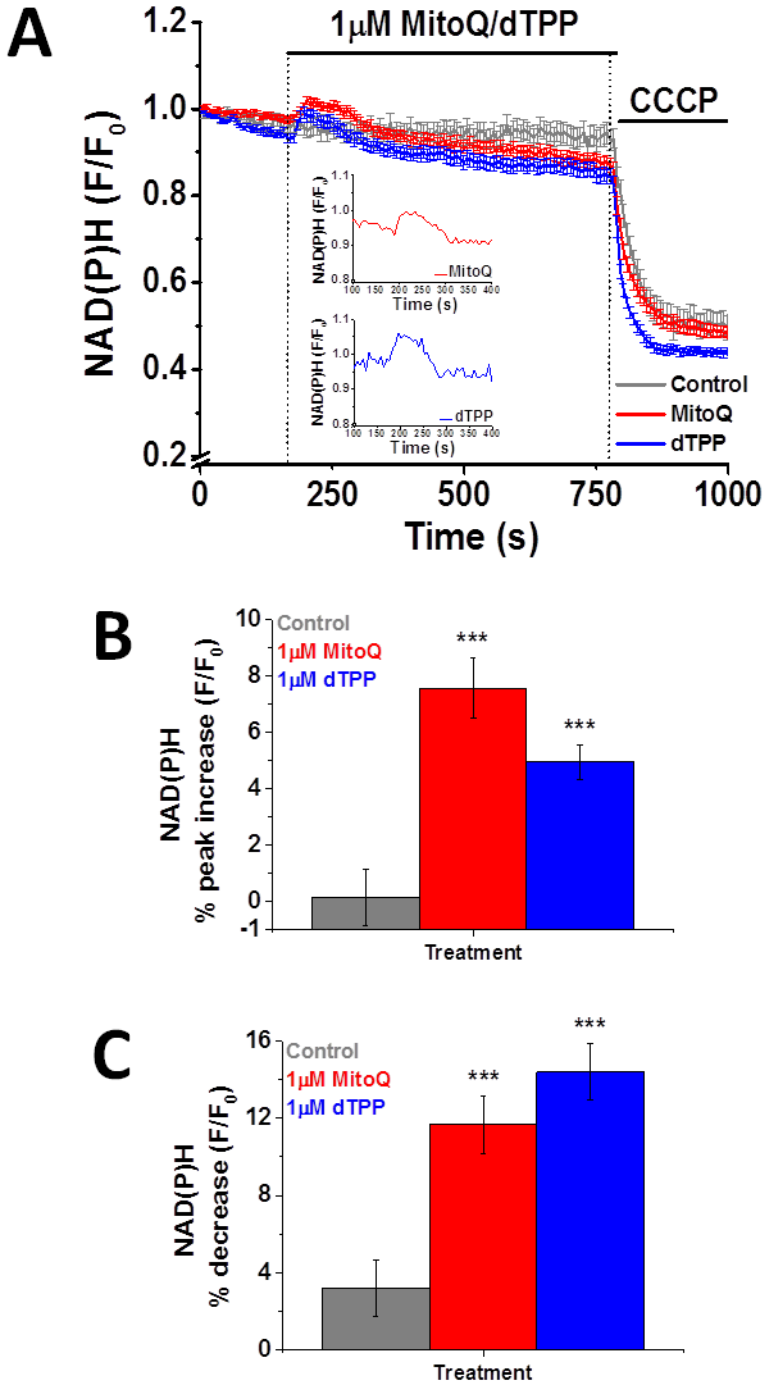

Figure 3.7. MitoQ and dTPP caused transient increases in NADH(P)H levels. NAD(P)H autofluorescence was measured for a 3 minute baseline and 10 minute perfusion with either NaHEPES (Control), MitoQ (1μM) or dTPP (1μM). Traces are averages of >18 cells from at least 3 animals. Data have been normalised to the initial fluorescence reading t=0 expressed as F/F_0 . All data shown are mean ±SEM. **(A)** All treatments, **(B)** Percent increase in NAD(P)H autofluorescence intensity from the baseline to the maximum fluorescence value of the peak. **(C)** Percent decrease in NAD(P)H autofluorescence. *** p<0.001.

Figure 3.8

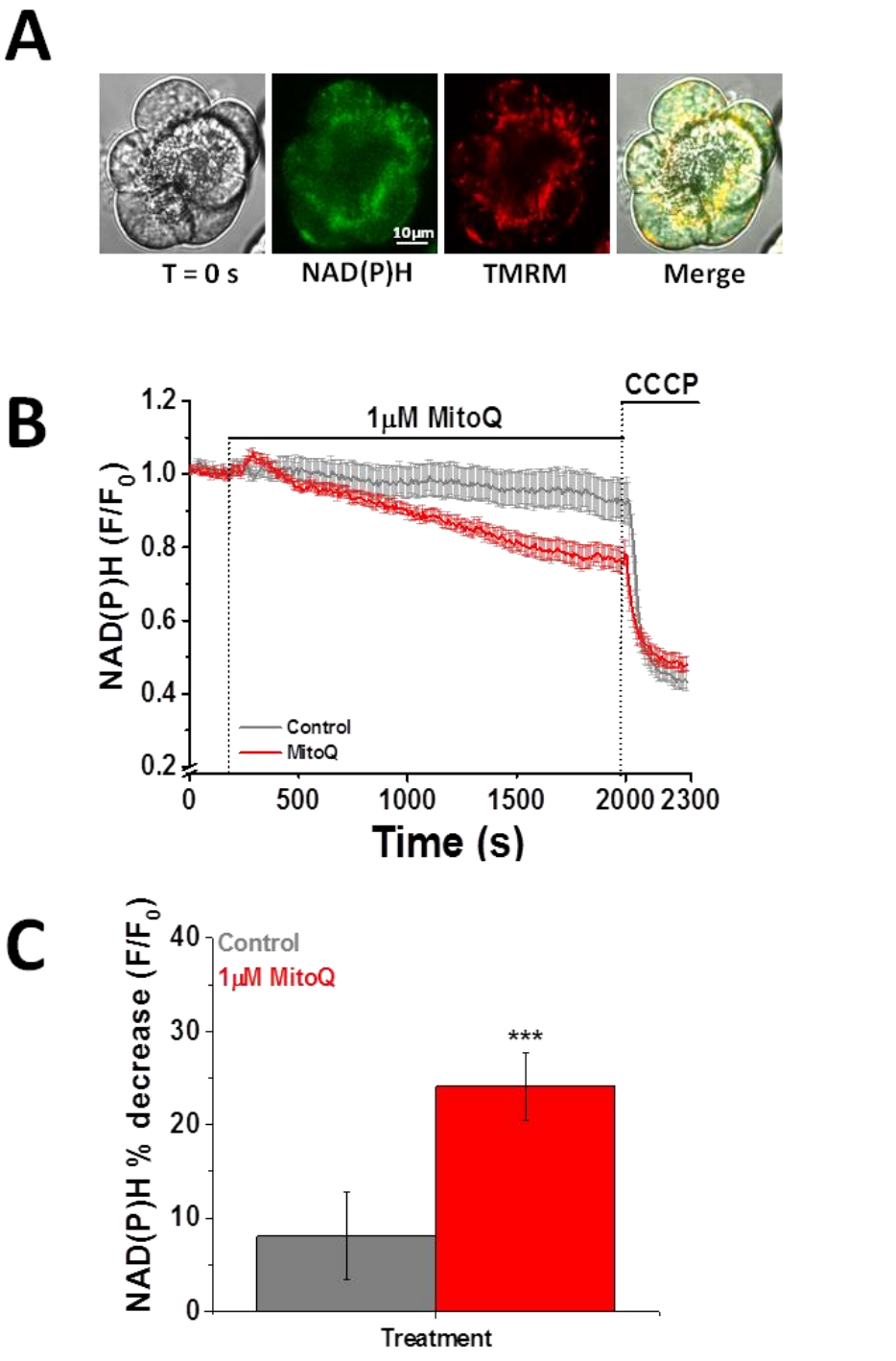

Figure 3.8. MitoQ caused progressive decreases in NADH(P)H levels. NAD(P)H autofluorescence was measured as described previously and pancreatic acinar cells treated with 1µM MitoQ/NaHEPES control for 30 minutes. Traces are averages of >17 cells from at least 3 animals. Data have been normalised to the initial fluorescence reading t=0 expressed as F/F_0 . All data shown are mean ±SEM. **(A)** Representative images of typical NAD(P)H and TMRM fluorescence at t=0 s (scale bar 10µM). **(B)** Control and 1µM MitoQ treatment, **C)** Data presented as a percent decrease in fluorescence intensity during the treatment. *** p<0.001.

Figure 3.9

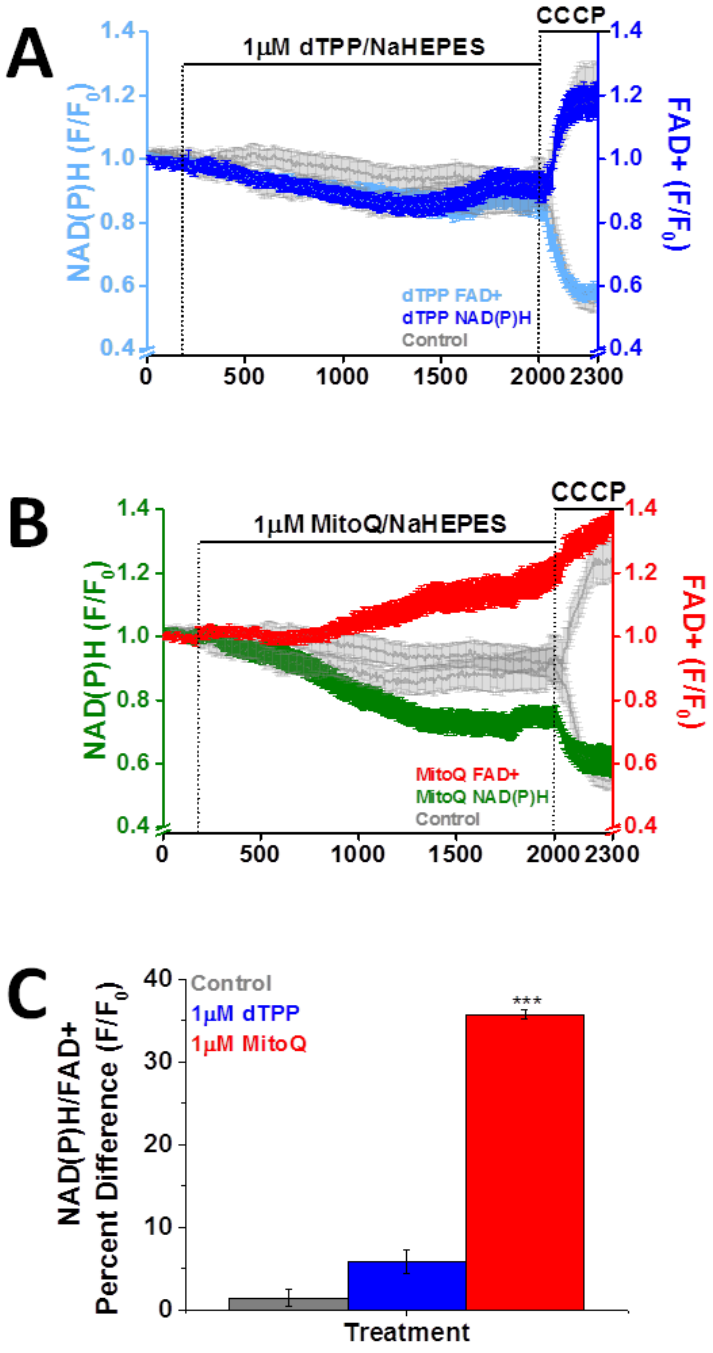

Figure 3.9. MitoQ-induced changes to the redox ratio. NAD(P)H and FAD^+ autofluorescence were measured simultaneously in acinar cells. Traces are averages of >19 cells from at least 3 animals. Data have been normalised to the initial fluorescence reading t=0 expressed as F/F_0 . All data shown are mean ±SEM. **(A)** NAD(P)H and FAD^+ autofluorescence during treatment with dTPP (1µM), **(B)** NAD(P)H and FAD^+ autofluorescence during treatment with MitoQ (1µM), **(C)** 1µM MitoQ treatment induced a significant change in the redox ratio NAD(P)H/FAD^+. The bar chart is presented as a percentage change from the baseline until the end of treatment with NAD(P)H/FAD^+. *** p<0.001 NaHEPES control vs 1µM MitoQ.

The Effects of MitoQ on Ca^{2+} Levels in Pancreatic Acinar Cells

Pancreatic acinar cell suspensions were loaded with Ca^{2+} indicator Fluo-4 (30 minutes) and treated with 1µM MitoQ (Figure 3.10). High affinity ratiometric Ca^{2+} dye Fura-2 was used (Figure 3.11), which is particularly useful in detecting cytosolic Ca^{2+} changes around the basal level. Both MitoQ and dTPP (1µM) induced a transient increase in $[Ca^{2+}]_c$. This effect was observed in 52.5% of cells treated with MitoQ (1µM) and 26.5% of cells treated with dTPP (1µM). A continuous increase in Ca^{2+} was observed in 34.9% of dTPP (1µM) treated cells. The small transient increase had no effect on the CCK hyperstimulation $[Ca^{2+}]_c$ response.

Mitochondrial Ca^{2+} measurements were measured using Rhod-2 in response to MitoQ/dTPP (1µM) treatment applied (Figure 3.12). No changes were detected. Mitochondrial Ca^{2+} concentration changes in response to 10nM CCK were also unaffected by MitoQ/dTPP treatment. MagFluo4 was originally designed for detection and measurement of magnesium (Mg^{2+}) dynamics (Paredes et al. 2008) However, as intracellular Mg^{2+} concentrations remain relatively constant, at around 1mM, MagFluo4 can be effectively applied as a low affinity Ca^{2+} indicator (Kd for Ca^{2+} of 22 µM) to measure ER levels of Ca^{2+}. Preliminary observations showed that MitoQ/dTPP (1µM) had negligible effects on ER Ca^{2+} release in response to 10nM CCK (Figure 3.13).

Figure 3.10

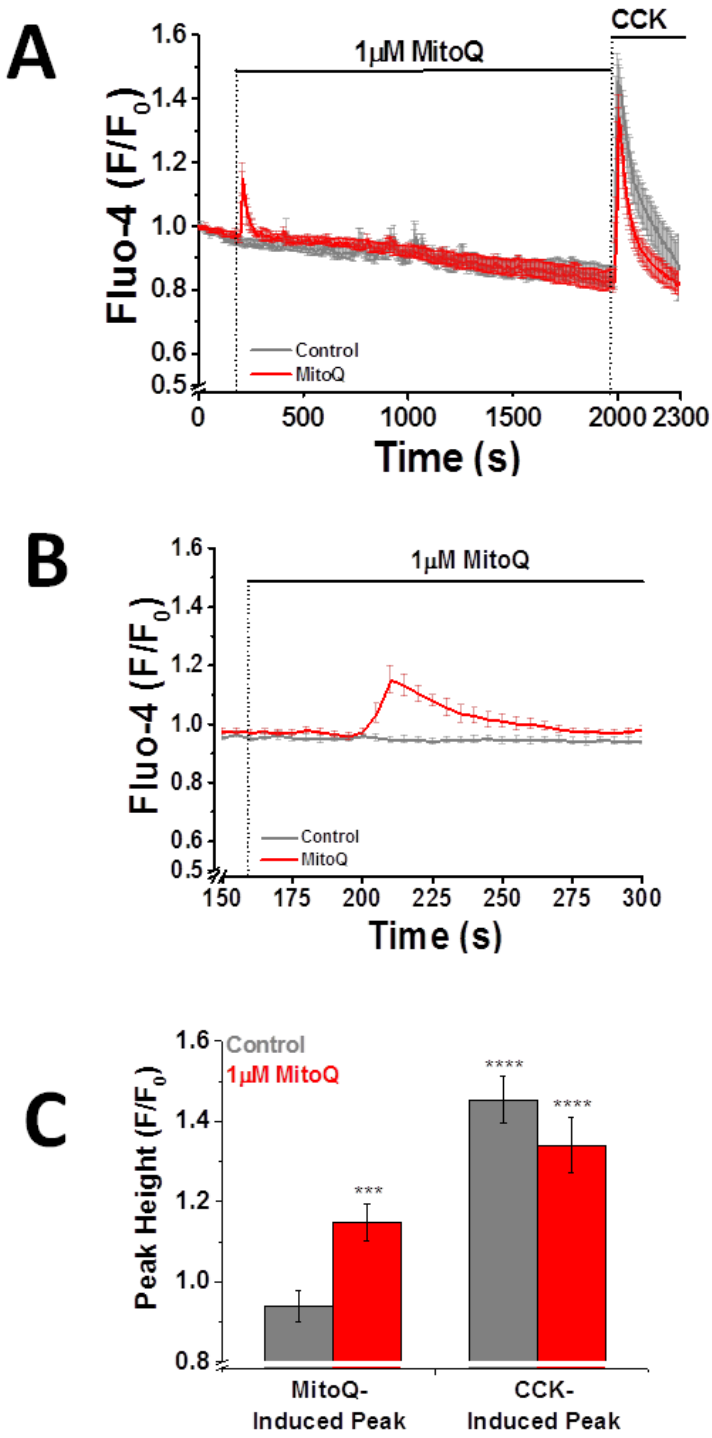

Figure 3.10. MitoQ-induced transient increase in cytosolic Ca^{2+} measured by Fluo-4. Cytosolic Ca^{2+} was measured with Fluo-4. **(A)** NaHEPES (Control) and MitoQ (1µM) treatment **(B)** Focussed view of MitoQ- (1µM) induced transient cytosolic Ca^{2+} increase **(C)** MitoQ- and CCK-induced cytosolic Ca^{2+} increases. Traces are averages of >22 cells from at least 3 animals. Data have been normalised to the initial fluorescence reading t=0 expressed as F/F_0 . All data shown are mean ±SEM. 52% of cells demonstrated this phenomena in the presence of 1µM MitoQ. *** p<0.001 and **** p<0.0001.

Figure 3.11

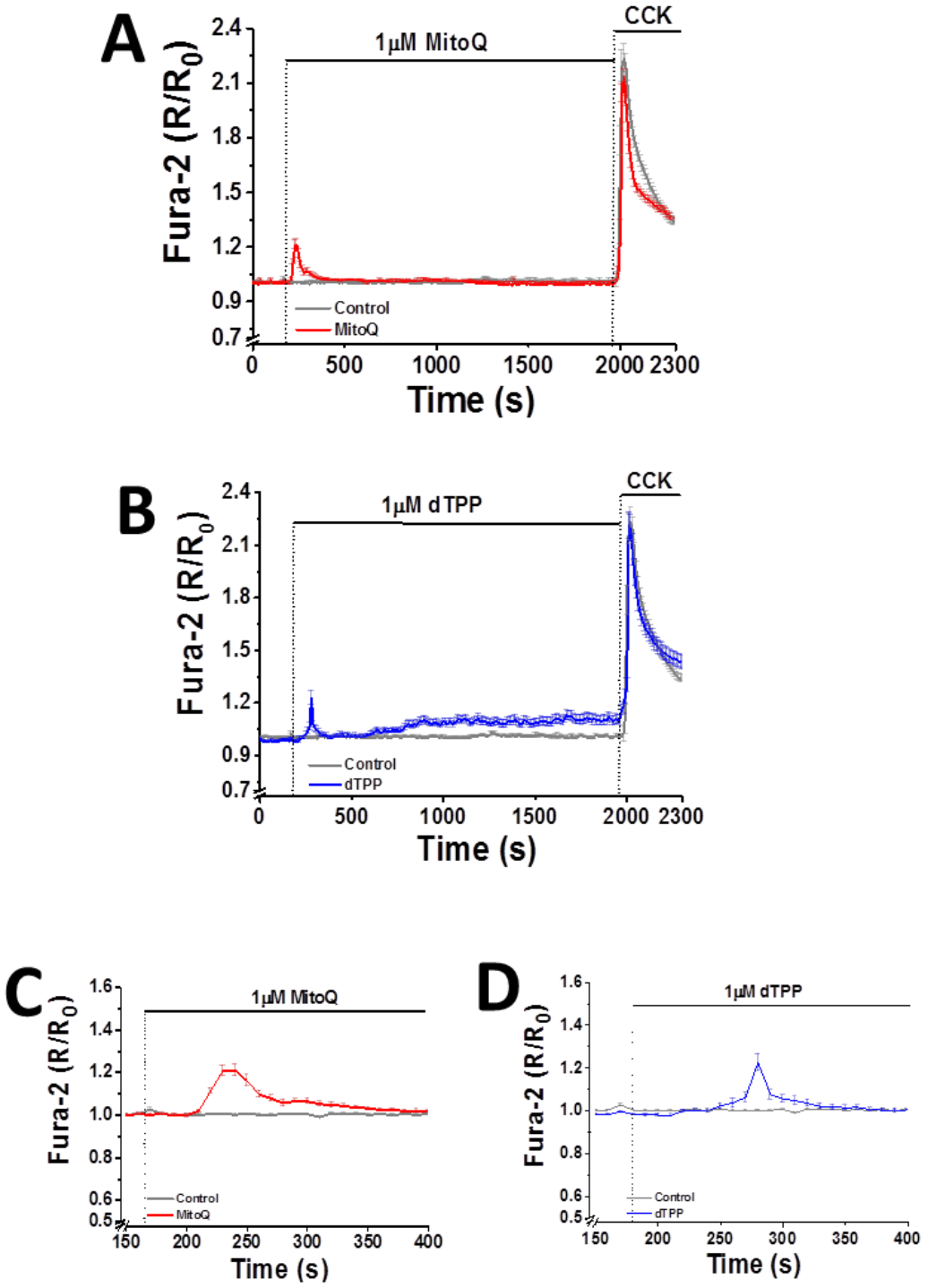

Figure 3.11. The effects of MitoQ and dTPP on cytosolic Ca^{2+} levels measured by Fura-2. (A) MitoQ (1μM) and NaHEPES (Control) and **(B)** dTPP (1μM) and NaHEPES (Control) **(C)** MitoQ- (1μM) and **(D)** dTPP- (1μM) induced transient cytosolic Ca^{2+} increase . The percentage peak increase with both MitoQ (1μM) and dTPP (1μM) treatment was significantly different ($p<0.0001$) to the control treated traces (from mirrored points). The progressive increase in cytosolic Ca^{2+} with dTPP treatment also reached significance ($p<0.0001$). Traces are averages of >165 cells from at least 3 animals. Data have been normalised to the initial ratio (R0). All data shown are mean ±SEM.

Figure 3.12

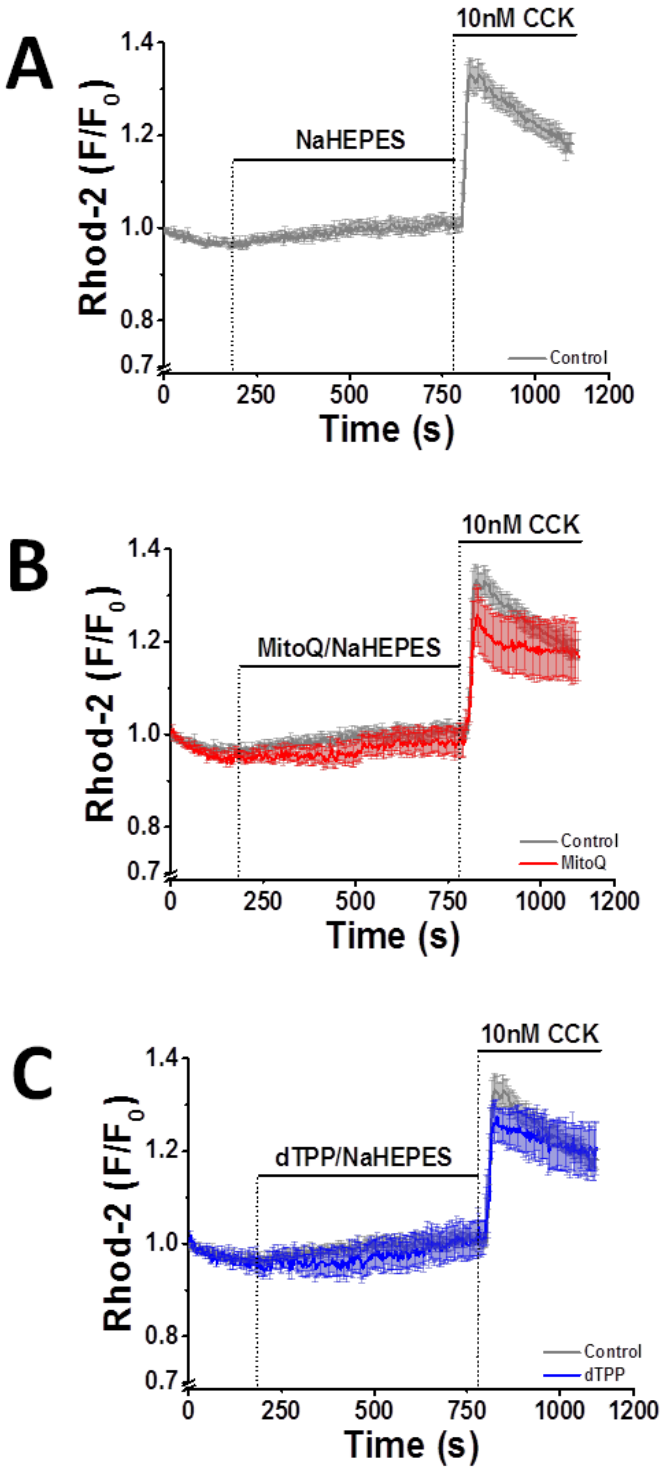

Figure 3.12. Lack of effect by MitoQ and dTPP on mitochondrial levels of Ca^{2+}. Mitochondrial Ca^{2+} was measured using Rhod-2. Pancreatic acinar cells were treated for 10 minutes with either NaHEPES (control), MitoQ (1µM) or dTPP (1µM) prior to treatment with CCK (10nM) for a period of 5 minutes. **(A)** NaHEPES (Control), **(B)** MitoQ (1µM) in comparison to the control treated cells and **(B)** dTPP (1µM) vs control cells. Data shown are mean ±SEM. No significant changes are observed. Traces are averages of >17 cells and 3 animals. Data have been normalised to the initial fluorescence reading t=0 expressed as F/F_0.

Figure 3.13

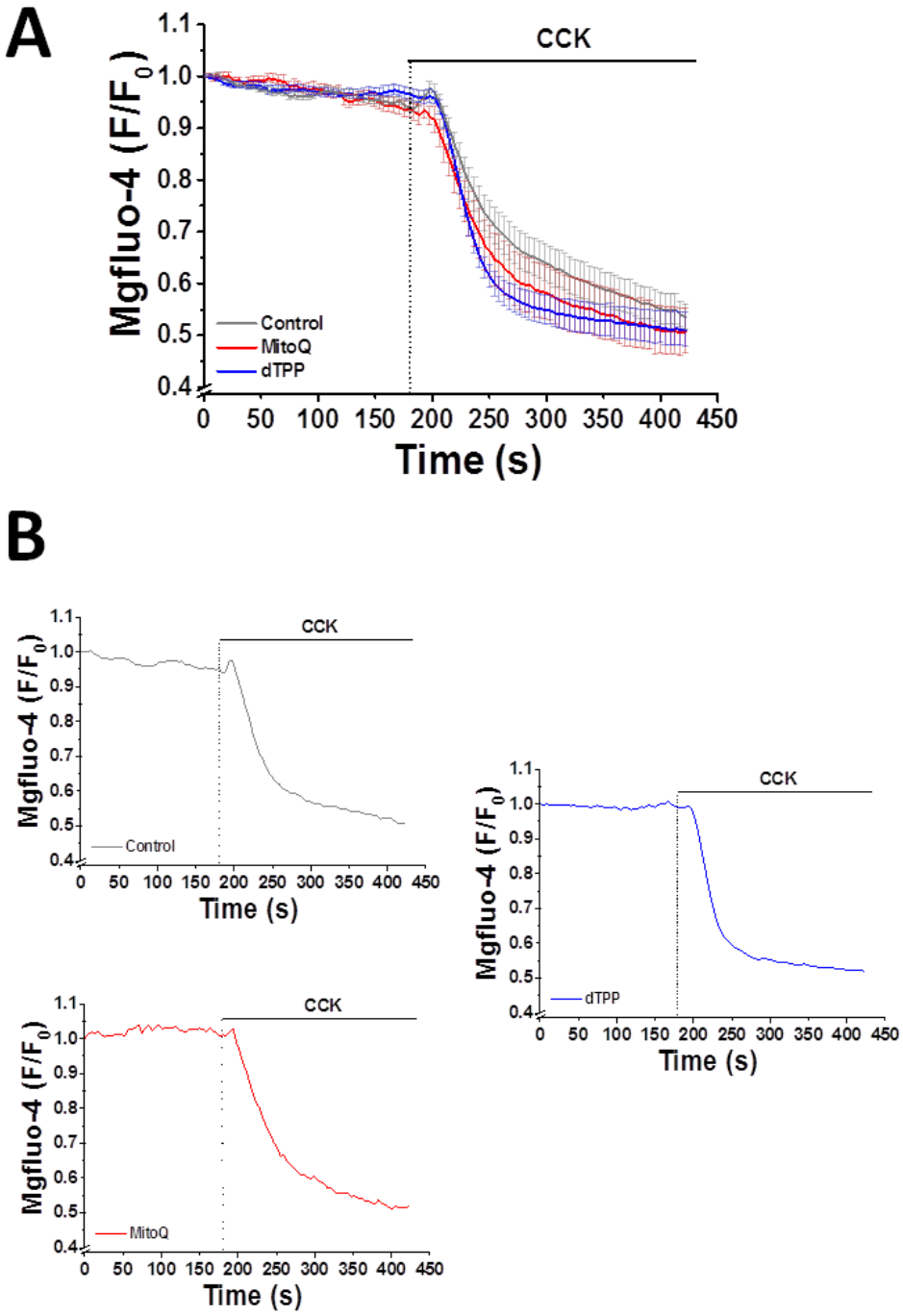

Figure 3.13. MitoQ and dTPP did not alter CCK-induced ER Ca^{2+} responses. ER Ca^{2+} was measured using MagFluo4, treated for 30 minutes with either NaHEPES (control), MitoQ (1µM) or dTPP (1µM) prior to loading onto the microscope stage for imaging. A 3 minute baseline was established prior to treatment with CCK (10nM) for a period of 4 minutes. **(A)** NaHEPES (Control), MitoQ (1µM) and dTPP (1µM). Data shown are mean ±SEM. **(B)** Example individual traces for each treatment group. No significant changes are observed. Traces are averages of 13 cells (control), 7 cells (MitoQ), 8 cells (dTPP) from 1 animal. Data have been normalised to the initial fluorescence reading t=0 expressed as F/F_0.

The Effect of MitoQ and dTPP on Pancreatic Acinar Cell Apoptosis and Necrosis

The balance between necrosis and apoptosis in acute pancreatitis may prove critical to prognosis of the disease. To determine pancreatic acinar cell fate with MitoQ, dTPP and TPP^+ treatment, cell suspensions were loaded with CellEvent® Caspase-3/7 Green reagent as an indicator for apoptosis (Figure 3.14) or Propidium Iodide (PI) as an indicator for cellular necrosis (Figure 3.15). Treatment with 0.2µM, 0.5µM and 1µM MitoQ, dTPP and additional control TPP^+ were applied and measurements recorded over a 13 hour period. MitoQ, dTPP and TPP^+ induced concentration-dependent increases in both cellular apoptosis and necrosis.

Figure 3.14

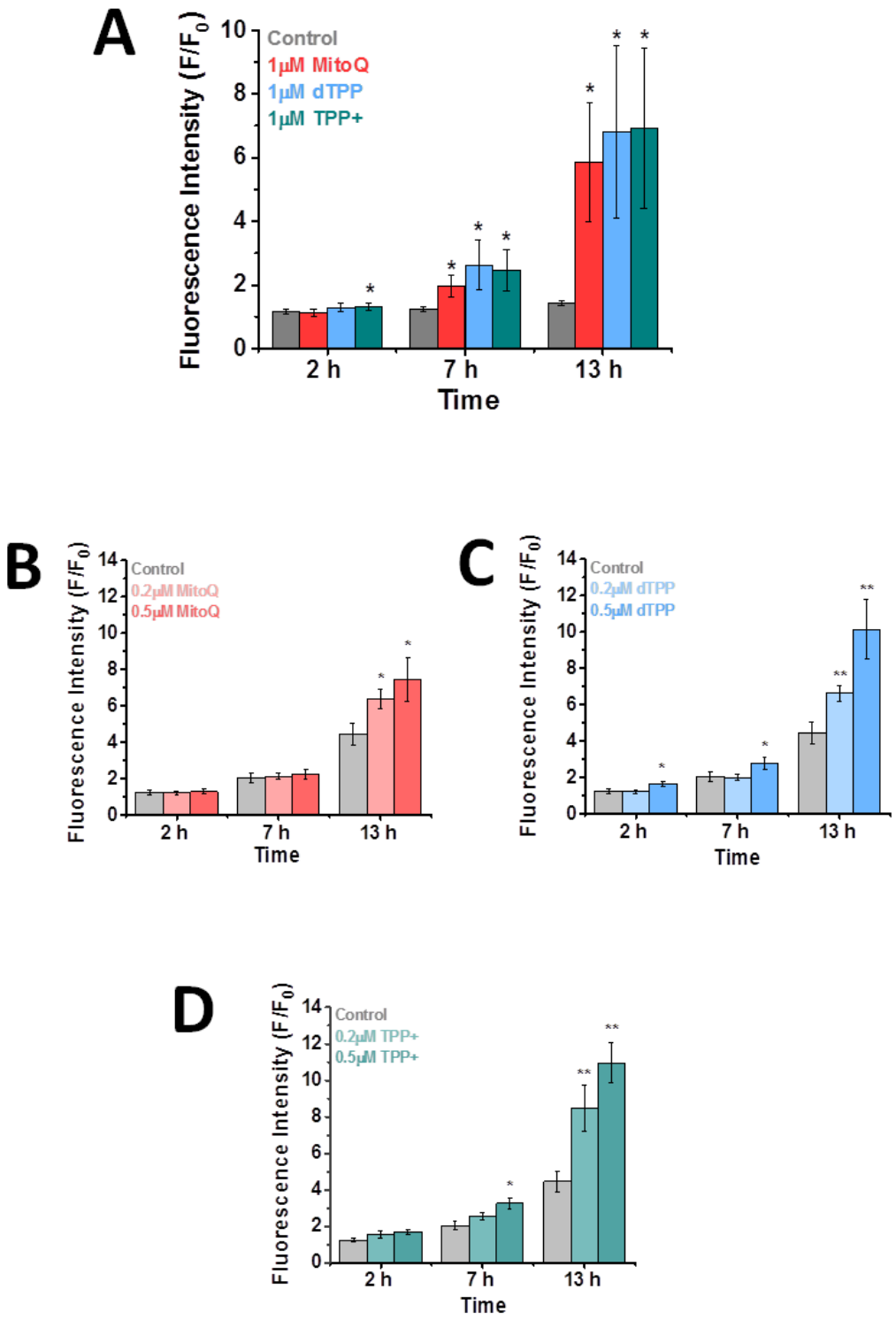

Figure 3.14. MitoQ-, dTPP- and TPP$^+$-induced cellular apoptosis. CellEvent® Caspase-3/7 Green reagent loaded cells were treated with 0.2, 0.5 or 1μM MitoQ/dTPP/TPP$^+$. Results are normalised to the initial fluorescence reading t=0 expressed as F/F_0. **(A)** 1μM MitoQ, dTPP and TPP$^+$, **(B)** MitoQ (0.2, 0.5, 1μM), **(C)** dTPP (0.2, 0.5, 1μM) and **(D)** TPP$^+$ (0.2, 0.5, 1μM). Traces are averages of >6 animals and 12 technical replica's.. All data shown are mean ±SEM. * $p< 0.05$, ** $p<0.01$.

Figure 3.15

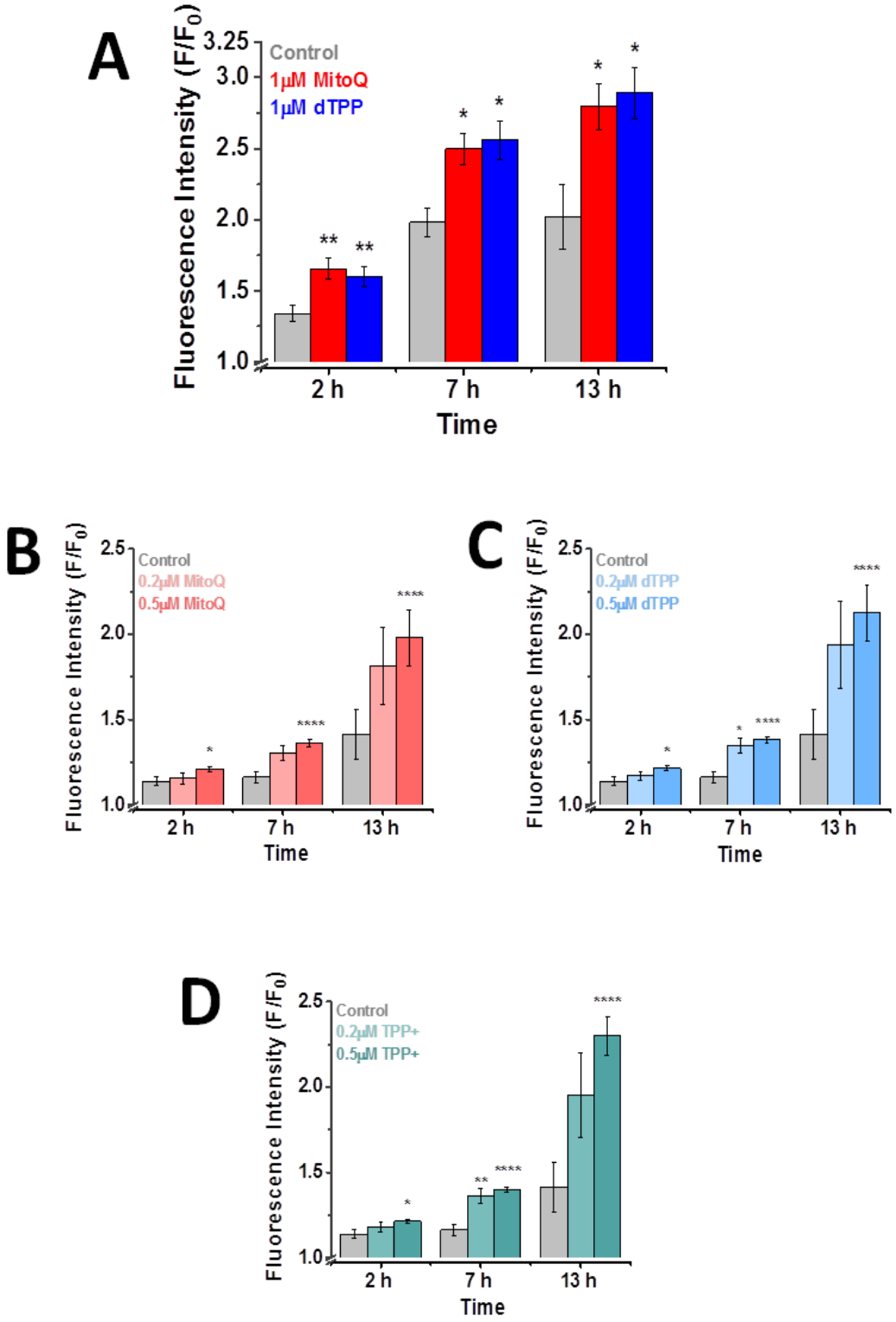

Figure 3.15. MitoQ-, dTPP- and TPP$^+$-induced cellular necrosis. Propidium Iodide loaded cells were treated with 0.2, 0.5 or 1μM MitoQ/dTPP/TPP$^+$. Results are presented been normalised to the initial fluorescence reading t=0 expressed as F/F_0. **(A)** 1μM MitoQ, dTPP and TPP$^+$, **(B)** MitoQ (0.2, 0.5, 1μM), **(C)** dTPP (0.2, 0.5, 1μM) and **(D)** TPP$^+$ (0.2, 0.5, 1μM). Traces are averages of >6 animals and 12 technical replica's. All data shown are mean ±SEM. * p< 0.05, ** p<0.01, **** p< 0.0001.

Discussion

In this section, the effects of mitochondria-targeted antioxidant MitoQ and non-antioxidant moiety controls dTPP and TPP^+ have been evaluated in pancreatic acinar cells. These investigations were to complement *in vivo* studies performed in a hyperstimulatory and bile acid model of AP, which highlighted mixed effects of MitoQ and dTPP. These investigations aimed to shed light as to why previous clinical evaluations of MitoQ in Parkinson's Disease and Hepatitis C patients also lacked success (Gane et al. 2010; Snow et al. 2010).

Cellular ROS

An imbalance of reactive oxygen species (ROS) production and antioxidant status leads to oxidative stress and has been associated with tissue injury and disease processes, including the pathogenesis of AP (Dziurkowska-Marek et al. 2004; Leung et al. 2009; Booth et al. 2011; Hackert et al. 2011). The generation of ROS in pancreatic acinar cells has been shown to inhibit the ATPase pump PMCA, suggesting a role for oxidative stress in modulating Ca^{2+} overload, a major driver of necrosis (Bruce et al. 2007; Baggaley et al. 2008). Many preclinical and clinical investigations have demonstrated increased free radical activities, levels of superoxide anions, hydrogen peroxide, and hydroxyl free radicals in affected tissues (Guyan et al. 1990; Szuster-Ciesielska et al. 2001). Elevated levels of lipid peroxides in blood, plasma and tissue have been shown alongside diminished antioxidant

defences. Depletion of antioxidants such as glutathione (Rahman et al. 2004), Vitamins A and E and Carotenoid (Curran et al. 2000) have been associated with AP (De Waele et al. 1992; Scott et al. 1993). Yet restoring antioxidant levels in the clinical setting has provided conflicting results (Virlos et al. 2003; Siriwardena et al. 2007; Armstrong et al. 2013).

Many clinical attempts to regulate oxidative stress have encountered a reduction in biomarkers of oxidative stress with little or no therapeutic benefit. A meta-analysis indicated that antioxidant therapies such as β-carotene, vitamin A and vitamin E do not improve the outcome of a number of diseases and may actually be detrimental, causing an increase in mortality (Bjelakovic et al. 2007). Although there has been a lack of success of antioxidants in the clinic, there is still evidence for a pivotal role of ROS in the development of AP, amongst many other oxidative stress-related diseases such as hypertension, atherosclerosis, diabetes and kidney disease. Therefore, targeted antioxidants were developed, including MitoQ, MitoE and MitoSOD (Smith et al. 2008).

Most small molecule antioxidants are only up-taken into the mitochondria in small amounts and are distributed around the body. MitoQ is targeted to the mitochondria by conjugation to a TPP moiety and can be actively recycled by ETC complex II to the active antioxidant form within the mitochondria (James et al. 2005; Smith et al. 2008). MitoQ is an effective antioxidant against lipid peroxidation, peroxynitrite and superoxide. In pancreatic acinar cells, MitoQ can effectively inhibit ROS increases and Ca^{2+} oscillations induced by CCK (10pM) in pancreatic acinar cells

(Camello-Almaraz et al. 2006). On the other hand, MitoQ and other ubiquinol based antioxidants have demonstrated the ability to act also as a prooxidant, enhancing superoxide production via redox cycling and therefore H_2O_2 through dismutation (Boveris et al. 1976; James et al. 2004; Doughan et al. 2007; Plecitá-Hlavatá et al. 2009). MitoQ can also inhibit the ETC in a manner dependent on the targeting component TPP^+ and acyl chain (Trnka et al. 2015). MitoQ (1-10µM) demonstrated no detectable prooxidant potential in CM-H_2DCFDA loaded pancreatic acinar cells. CM-H_2DCFDA is a general oxidative stress indicator predominantly effective at detecting hydrogen peroxide, hydroxyl radicals, nitrogen dioxide and carbonate radicals (Wojtala et al. 2014). Levels of oxidant production induced by MitoQ in pancreatic acinar cells may be too diminutive to detect using this technique. It is possible that applying a more specific probe (optimised with spectral analysis) such as DHE (Dihydroethidium) or MitoSOX (DHE plus TPP^+) or electron spin resonance (ESR) spectroscopy in future work may have the potential to highlight more specific increases in superoxide production seen in other cell types (Bindokas et al. 1996; Li et al. 2003; Rivera et al. 2005). To establish if any superoxide production by MitoQ was adequate to cause mitochondrial damage, the activity of TCA dehydrogenases such as aconitase could be assessed.

MitoQ has demonstrated the ability to block numerous redox signalling pathways induced by extracellular H_2O_2, but the mechanisms are not defined (Echtay et al. 2002; Saretzki et al. 2003; Schäfer et al. 2003; Chen et al. 2004; Dhanasekaran et al. 2004; Ross et al. 2005). MitoQ does not react with alkyl peroxides or H_2O_2 directly, although successfully inhibits lipid peroxidation (Kelso et

al. 2001; Asin-Cayuela et al. 2004; James et al. 2005). This would indicate that the effectiveness of MitoQ is predominately downstream of H_2O_2, acting on $OH^{\bullet-}$ formed from iron catalysed Fenton reaction and to inhibit the peroxidation chain reaction rather than directly upon H_2O_2 (Sutton et al. 1984; Braughler et al. 1986; Winterbourn 1987).

The capabilities of MitoQ to inhibit high levels of extracellular H_2O_2- (1mM) induced ROS increases were assessed, administering MitoQ as a pre-treatment. There are a variety of parameters, such as the energised state of the mitochondria (Kelso et al. 2001), which affect the rate of MitoQ accumulation into the mitochondria. Pre-treatment with MitoQ may improve the effectiveness and comparing pre-treatment to treatment provided a key observational tool and comparison to clinical failures encountered with non-targeted antioxidants (Demols et al. 2000). MitoQ (1µM) proved to be an effective antioxidant in pancreatic acinar cells, providing protection against 1mM H_2O_2-induced ROS increases compared to the non-antioxidant moiety dTPP control. Reports have shown that excessive accumulation of lipophilic cations in the mitochondria are toxic due to disruption to ATP synthesis (Smith et al. 2003) membrane integrity and respiration (Murphy 2008). To assess the cellular effects of excessive accumulation in pancreatic acinar cells on ROS levels, a ten-fold concentration of each compound (10µM) was applied to isolated pancreatic acinar cells prior to H_2O_2 treatment (1mM). MitoQ and dTPP (10µM) both reduced 1mM H_2O_2-induced ROS increases, indicating that this reduction is not dependent on the antioxidant moiety but the TPP^+ component and/or acyl chain.

Mitochondrial Membrane Potential

Upon comparative observation of 1µM and 10µM MitoQ/dTPP effects on 1mM H_2O_2-induced ROS increases, it was imperative to assess the effects of both TPP^+ based derivatives on the acinar cell mitochondrial proton gradient, essential for ATP synthesis. Both compounds are dependent on the positively charged TPP^+ cation for their accumulation. A 10-fold increase in cation concentration within the mitochondria is believed to occur for every 61.5 mV increase in membrane potential (Rottenberg 1979). It has been shown that the TPP^+ moiety of MitoQ and dTPP can cause mild uncoupling of the mitochondria in cultured mesangial cells and transgenic *Caenorhabditis elegans* (Reily et al. 2013; Ng et al. 2014) and disruption to respiration and ATP synthesis (Murphy 2008). MitoQ has also been demonstrated to have concentration-dependent effects on induction of proton leak in bovine aortic endothelial (BAE) cells, indicatory of respiratory uncoupling (Fink et al. 2012). In PACs significant mitochondrial depolarisation with 1µM MitoQ was not seen in the period at which it blocked Ca^{2+} oscillations (2–5 min) (Camello-Almaraz et al. 2006). Therefore, we evaluated the potential effects in pancreatic acinar cells over a longer treatment and/or with excessive accumulation at 10µM. MitoQ/dTPP (1µM) treatment did not induce depolarisation of the mitochondria in TMRM loaded cells over 10 minutes, in concurrence with Camello-Almaraz et al. (2006), nor MitoQ (1µM) over a 30 minute period. MitoQ and dTPP (10µM) treatment highlighted the published uncoupling properties of the cation TPP^+ (Reily et al. 2013), at higher concentrations, demonstrated by partial depolarisation of the mitochondria.

Mitochondrial Bioenergetics and Redox Status

Increases and decreases of NAD(P)H levels enabled assessment of changes to acinar cell bioenergetics and redox status induced by MitoQ and dTPP (1µM). Changes in NAD(P)H levels are evident in response to a variety of AP precipitants detailed below. The predominant mode of regulating mitochondrial metabolism is dependent on Ca^{2+} (Duchen 2000; Rizzuto et al. 2000). The mitochondria are equipped with the ability to decode Ca^{2+} signals and facilitate Ca^{2+}-induced upregulation of NADH production and ATP synthesis, in response to an increase in energy requirements (McCormack et al. 1990; Hajnóczky et al. 1995; Robb-Gaspers et al. 1998; Jouaville et al. 1999). An increase in cytosolic Ca^{2+} leads to Ca^{2+} uptake via the MCU driven by the large ΔΨm (Rizzuto et al. 2000; Kirichok et al. 2004; Patron et al. 2013). Increased mitochondrial Ca^{2+} levels can elevate proton motive force through stimulation of the ETC, and critically, increase the activity of mitochondrial dehydrogenases. These include pyruvate dehydrogenase, oxoglutarate dehydrogenase, glycerol phosphate dehydrogenase and isocitrate dehydrogenase, and lead to increased NADH and $FADH_2$ production. Increased levels of reduced NADH and $FADH_2$ fuel the ETC to produce more ATP and match ATP production to cellular requirement. Ca^{2+} activation of NAD-isocitrate dehydrogenase occurs through a Ca^{2+}-induced reduction of Km to substrate threo-Ds-isocitrate and in a manner sensitive to the ATP/ADP ratio and Ca^{2+} concentration (Denton et al. 1978; Rutter et al. 1988; Rutter et al. 1989). NADH is the most predominant supplier of reducing equivalents to the ETC, and NADH, not oxidised NAD^+, fluoresces under UV light, enabling confocal imaging and a valuable indicator

of mitochondrial respiration (Hajnóczky et al. 1995; Mojet M.H. 2000; Voronina et al. 2002). This technique has been used in pancreatic acinar cells to demonstrate the relationship between elevated $[Ca^{2+}]_c$ and $[Ca^{2+}]_m$, leading to an upregulation of NADH levels (Voronina et al. 2002; Bruce et al. 2004). Ca^{2+} transients in pancreatic acinar cells are of varying amplitude and these are reflected in highly variable NADH responses. The comparison of mitochondrial, nuclear and whole cell NADH responses indicated that mitochondrial changes in NADH levels determine whole-cell NADH responses. Influx of Ca^{2+} into the mitochondria, results in changes to the mitochondrial potential, which can be compensated by increased H^+ extrusion due to ETC stimulation (Raraty et al. 2000). After the initial increase in levels of NADH, a small decrease can be observed due to prolonged upregulation of the ETC during longer lasting Ca^{2+} transients (Robb-Gaspers et al. 1998; Voronina et al. 2002).

Further studies investigating NADH responses include pancreatic acinar cell treatment with fatty acid POA and fatty acid ethyl ester POAEE, which caused a progressive decrease in NAD(P)H, accompanied by depletion of ATP due to impaired respiration and uncoupling of oxidative phosphorylation (Criddle et al. 2006). The depletion of ATP led to combined SERCA and PMCA pump failure. The alcohol metabolites caused depletion of the ER Ca^{2+} store in a similar time course to NAD(P)H depletion. The metabolites also elicited maximal loss of $\Delta\Psi m$, an effect abolished in cells loaded with Ca^{2+} chelator BAPTA. The effects on NADH were accentuated with fatty acid POA in comparison to ethyl ester POAEE responses, in line with the dependency of the FAEEs on their FA release. The $NADH/NAD^+$ ratio

has been highlighted to be important in the regulation of TCA cycle α-KGDH production of H_2O_2 (Tretter et al. 2000; Tretter et al. 2004; Doughan et al. 2007). Redox cycling menadione, uses NAD(P)H as an electron donor to induce a progressive generation of ROS alongside a decrease of NAD(P)H (Criddle et al. 2006). Under physiological conditions XOD is found as a dehydrogenase (XOH) and transfers hydrogen from xanthine to NAD, generating NADH. Alcohol consumption promotes the pro-oxidant enzyme xanthine oxidase (XO) form, leading to generation of superoxide and H_2O_2. XOD is a primary ROS source in the pancreas, which causes injury (Closa et al. 1994; Folch et al. 1998). Acetaldehyde is also a XOD substrate which results in the production of ROS also contributing to injury (Fridovich 1989). Initially, alcohol is converted by alcohol dehydrogenase (ADH) and to acetate by aldehyde dehydrogenase (ALDH), each reaction which produces a molecule of NADH, enhancing mitochondrial respiratory chain activity (Wilson et al. 2003).

The presence of a transient increase in NAD(P)H levels followed by a progressive decrease with both compounds, indicated dual effects of the targeting component, not the antioxidant component. The transient increase could be an inhibition of the ETC leading to a decreased cycling of NADH to NAD^+ by complex I of the ETC. The transient effect is likely to be only observed during the accumulation of MitoQ/dTPP into the mitochondria until an equilibration is reached. Alternatively, the increase could be a transient elevation of NADH by the TCA

through a Ca^{2+}-dependent mechanism due to non-specific effects of MitoQ and dTPP.

ETC inhibition is supported by work done in mesangial cells, showing an inhibitory effect of all TPP^{+} derivatives on basal respiration and mild uncoupling of the mitochondrial membrane (Reily et al. 2013). More recently in C2C12 myoblasts and rat skeletal muscle homogenate, results demonstrated inhibition of all four respiratory chain complexes in particular complexes I and III alongside proton leak and loss of mitochondrial membrane potential (Trnka et al. 2015). In bovine aortic endothelial (BAE) cells MitoQ induced concentration-dependent mild increases in cellular respiration, reduced ATP turnover, respiratory uncoupling and elevated basal rate of acidification which suggested enhanced glycolysis (Fink et al. 2012). These findings and those in mesangial cells by (Reily et al. 2013) were supported by preliminary results obtained with the Seahorse XF24 Extracellular Flux Analyser (results not shown), however they need further investigation.

Up-regulation of NADH production (Voronina et al. 2002) has been demonstrated in several cell types, including pancreatic acinar cells, to be due to an increases in $[Ca^{2+}]_c$. This resulted in a mitochondrial Ca^{2+} rise followed by an increase in the activity of mitochondrial dehydrogenases and other ATP production mechanisms (McCormack et al. 1990; Hajnóczky et al. 1995; Robb-Gaspers et al. 1998; Jouaville et al. 1999; Glancy et al. 2012). MitoQ and dTPP induced a small rise

in cytosolic Ca^{2+} levels; however, this was not reflected by an increase in mitochondrial Ca^{2+}. This may also be due to a lack of sensitivity of the probe applied, Rhod-2, to very small changes. ETC Complex I inhibitory effects provide the most likely explanation based on the accumulated evidence. However, further work would need to be performed to assess mitochondrial Ca^{2+} concentration changes with a more sensitive technique such as patch clamp or specific probe detailed later. The transient increase in NAD(P)H could be compared to established ETC complex inhibitors such as complex I inhibitor rotenone. Rotenone inhibition of complex I has also been reported to induce apoptosis, which is in line with our cell death results with MitoQ/dTPP/TPP^+ (Li et al. 2003).

The transient increase in NAD(P)H levels induced by MitoQ and dTPP (1µM) was followed by a decrease, in comparison the NaHEPES control responses. The progressive decrease in levels of NAD(P)H with both MitoQ and dTPP treatment indicated a loss of cellular energy metabolism. This is in line with MitoQ-induced depletion of ATP levels in articular cartilage (Martin et al. 2012). Experiments could investigate the effects of MitoQ/dTPP on ATP levels indirectly using fluorescent indicator magnesium green. The decrease of NAD(P)H may be due to the mild uncoupling effect of the targeting component or non-specific effects of the TPP^+ group on cellular bioenergetics (Ross et al. 2005; Fink et al. 2012). Measuring NAD(P)H levels over a longer time period demonstrated that the decreases seen with 1µM MitoQ were progressive. Previous results have shown some similar effects of MitoQ and dTPP (1µM) treatments such as on NAD(P)H levels and $\Delta\Psi m$.

However *in vivo* there were apparent differences (Huang et al. 2015). These findings were mirrored by *in vitro* work showing MitoQ-induced progressive increases in levels of FAD^+ autofluorescence, which were mirrored to the progressive NAD(P)H decrease. On the other hand treatment with 1μM dTPP did not cause changes to FAD^+ fluorescence from the control. This would suggest that this effect is contributed to the antioxidant moiety of MitoQ, which is reduced predominantly by ETC complex II. It is possible that the recycling of MitoQ back into the quinone form by complex II, leads to enhanced $FADH_2$ consumption, reflected in a progressive elevation of oxidised FAD^+ levels.

Ca^{2+} Signalling

In the exocrine pancreas, the mitochondria play a critical role in limiting and managing the apical to the basolateral propagation of $[Ca^{2+}]_c$ waves and plasma membrane Ca^{2+} influx (Tinel et al. 1999). The inhibitory effects of MitoQ on the ETC, which have been demonstrated in other cell types, could lead to disruption of this delicate management of Ca^{2+} homeostasis (Leo et al. 2008; Reily et al. 2013). MitoQ can significantly increase mitochondria Ca^{2+} concentration in HeLa cells and inhibit Ca^{2+} oscillations and ROS increases stimulated by CCK (10pM) in pancreatic acinar cells (Camello-Almaraz et al. 2006; Leo et al. 2008). The study in HeLa cells demonstrated that MitoQ and MitoE (Vitamin E conjugated to TPP^+) increased mitochondria Ca^{2+} levels due to the TPP^+ component inhibitory effects on the Na^+ (or H^+)/Ca^{2+} exchanger. This led to increased intra-mitochondrial Ca^{2+} levels which

were greater with the targeting component TPP^+ than MitoQ (Reily et al. 2013), therefore impairing mitochondrial management of Ca^{2+} signals. The efflux of mitochondrial Ca^{2+} in pancreatic acinar cells occurs via the Na^+/Ca^{2+} exchanger NCLX (Palty et al. 2010; Nita et al. 2015).

The effects of MitoQ and dTPP on both basal and CCK induced cytosolic Ca^{2+} changes were evaluated. Assessment of 1µM MitoQ and 1µM dTPP on basal cytosolic Ca^{2+} had not been previously carried out in pancreatic acinar cells. Results with both Ca^{2+} indicator Fluo-4 and high affinity ratiometric Ca^{2+} dye Fura-2, showed a small transient increase in cytosolic Ca^{2+} with 1µM MitoQ treatment. This effect was also observed with dTPP (1µM) treatment. The frequency of this effect differed between the two compounds and was observed in 52.5% of cells treated with MitoQ (1µM) compared to 26.5% in dTPP (1µM) treated cells. This may indicate non-specific effects of both the TPP^+ component and the antioxidant moiety of MitoQ. Non-specific effects of dTPP on basal cytosolic Ca^{2+} were also observed with a prolonged increase in Ca^{2+} in 34.9% of dTPP (1µM) treated cells. To assess the origin of the small transient increase in $[Ca^{2+}]_c$ observed during MitoQ/dTPP treatment, experiments could apply Ca^{2+}-free NaHEPES in the extracellular media, which would establish or rule out a possible extracellular Ca^{2+} source. Pre-incubating cells with Ca^{2+} chelator 1, 2-bis(2-aminophenoxy)ethane-N,N,N',N'-tetraacetic acid tetrakis(acetoxymethyl ester) (BAPTA-AM) would establish if the transient increase in NAD(P)H is Ca^{2+}-dependent.

Animals infused with high doses of CCK, exhibit pancreatic oedema and acinar cell injury, which closely mimics AP in humans. While MitoQ can inhibit physiological CCK-induced Ca^{2+} responses (Camello-Almaraz et al. 2006; Davidson et al. 2012), there were no alterations to the cytosolic Ca^{2+} increases induced by hyperstimulatory CCK levels in Fluo-4 or Fura-2 loaded cells. The effects of MitoQ and dTPP were evaluated on mitochondrial or endoplasmic reticulum induced CCK hyperstimulation responses. Fluorescent indicators Rhod-2 AM and Mag-Fluo-4 were employed. Rhod-2 AM, due to its positive charged nature in the AM form is principally trapped in the mitochondria and enabling the assessment of mitochondrial Ca^{2+} changes (Duchen 1999; Park et al. 2001). The ER is the main Ca^{2+} storage organelle and mitochondrial Ca^{2+} supplier. Ca^{2+} levels can be monitored in Mag-Fluo-4 loaded cells (Park et al. 2000; Park et al. 2001; Petersen et al. 2001; Myoung et al. 2002). No effect on CCK-induced changes to mitochondrial or ER Ca^{2+} was observed. Future experiments could assess the treatment effects of MitoQ and dTPP on ER Ca^{2+}. Rhod-2 may not provide adequate sensitivity for measuring small fluctuations in mitochondrial Ca^{2+} therefore patch clamp technique could measure any increases. Alternatively construction of a target Ca^{2+} sensor such as GCaMPs TOM-GCaMP6 to monitor specific mitochondrial Ca^{2+} signalling could be applied (Zhou et al. 1998; Kirichok et al. 2004; Williams et al. 2013).

Apoptosis and Necrosis

The balance between necrosis and apoptosis in acute pancreatitis can be critical to the disease outcome (Kloppel et al. 1993; Criddle et al. 2007). Induction of apoptosis via a regulated cascade of signalling events results in a more efficient removal of dead cell debris from a tissue. However, the promotion of inflammation with necrosis makes this clearance problematic (Melino et al. 2005). MitoQ and dTPP have demonstrated induction of both apoptosis and necrosis at the 1µM concentration (Huang et al. 2015). Further experiments incorporating TPP^+ showed that apoptosis and necrosis were induced by all the TPP^+ derivatives (MitoQ, dTPP and TPP^+) in a concentration-dependent manner (0.2µM-1µM). The induction of apoptosis with MitoQ and dTPP are in accordance with a study demonstrating the increased levels of endothelial cell apoptosis with MitoQ (1-5µM) treatment (Doughan et al. 2007). It has also been reported that MitoQ can also induce an alternative mechanism of cell death, autophagy, in breast cancer cell lines (MDA-MB-231) which can promote cell survival in response to stress (Mehrpour et al. 2010). Autophagy is a mechanism, which is impaired in acute pancreatitis (Gukovskaya et al. 2012; Gukovsky et al. 2012). however, the collective *in vitro* and *in vivo* results with MitoQ treatment do not support a protective role in this cell type or in AP.

Conclusions

The findings of this section demonstrate the adverse effects of MitoQ and TPP^+ derivatives on pancreatic acinar cells. These results are in line with adverse effects encountered in alternative cell types (Reily et al. 2013; Trnka et al. 2015). The results obtained in pancreatic acinar cells do not support the use of MitoQ in alleviating the severity of AP.

Chapter 4

Protective Capabilities of Mitoquinone against Toxin-Induced Effects on Pancreatic Acinar Cells

Having assessed the effects of MitoQ on basal and H_2O_2-induced ROS elevations, intracellular Ca^{2+}, $\Delta\Psi m$, NAD(P)H/FAD^+ and cell death; the *in vitro* effects of MitoQ in response to AP precipitants CCK, TLCS and FAEEs were evaluated.

Bile Acid-Induced Toxic Effects:

Lack of Protection with MitoQ Pre-treatment

$[ROS]_I$ was measured in PACs loaded with 10µM of the chloromethyl derivative CM-H_2DCFDA and treated with 500µM TLCS, 1mM and 10mM H_2O_2. Both TLCS and H_2O_2 caused progressive increases in levels of ROS, measured by increases in CM-H_2DCFDA fluorescence (Figure 4.1). 30 minutes pre-treatment with MitoQ (1µM) has previously demonstrated successful reduction of H_2O_2 induced ROS increases, however MitoQ did not inhibit TLCS-induced ROS increases in comparison to the NaHEPES and dTPP (1µM) controls (Figure 4.2).

Mitochondrial membrane potential was measured in TMRM loaded cells and basal fluorescence was measured for a 3 minutes time interval prior to the addition of 500µM TLCS (or NaHEPES for the control) for 10 minutes. 10µM CCCP was applied for 5 minutes to uncouple the mitochondrial membrane completely and therefore disperse the TMRM dye. TLCS caused progressive membrane depolarisation (Figure 4.3A). NAD(P)H levels were also monitored during treatment

with TLCS and induced a transient increase in NAD(P)H followed by a progressive decline (Figure 4.3B).

Pancreatic acinar cell suspensions were pre-treated as previously described with MitoQ (1µM), dTPP (1µM) or alternatively maintained in NaHEPES for 30 minutes. Basal fluorescence was measured for a 3 minutes time interval prior to the addition of 500µM TLCS (or NaHEPES for the control) for 10 minutes. MitoQ (1µM) did not protect against the TLCS-induced partial membrane depolarisation (Figure 4.4).

As an indicator of cellular apoptosis, CellEvent® Caspase-3/7 Green reagent was loaded into isolated PACs and treated with either NaHEPES or 500µM TLCS. TLCS did not induce apoptosis in comparison to the NaHEPES control (Figure 4.5). Propidium Iodide (PI) was loaded into isolated PACs to monitor cellular necrosis. 500µM TLCS caused rapid and substantial increases in cellular necrosis in comparison to the physiological saline control (NaHEPES) as indicated by the PI fluorescence readings obtained (Figure 4.6).

Measurements of CellEvent® Caspase-3/7 Green reagent fluorescence obtained with TLCS treatment are elevated with 1µM MitoQ and dTPP pre-treatment, however apoptosis was not induced beyond the level generated with

the control treated cells (Figure 4.7). MitoQ (1µM) provided no overall protection against TLCS induced necrosis, although a protective capacity was demonstrated at the 1 h time point not demonstrated by the dTPP control (Figure 4.8). The lack of overall protective capability of MitoQ against TLCS-induced necrosis, is consistent with the end point (30 minutes) experiments performed by Booth et al. (2011). Preliminary data showed that an increased pre-treatment concentration of MitoQ (5µM) abolished the protective effects seen with 1µM at 1 h treatment with 500µM TLCS (Figure 4.9).

Figure 4.1

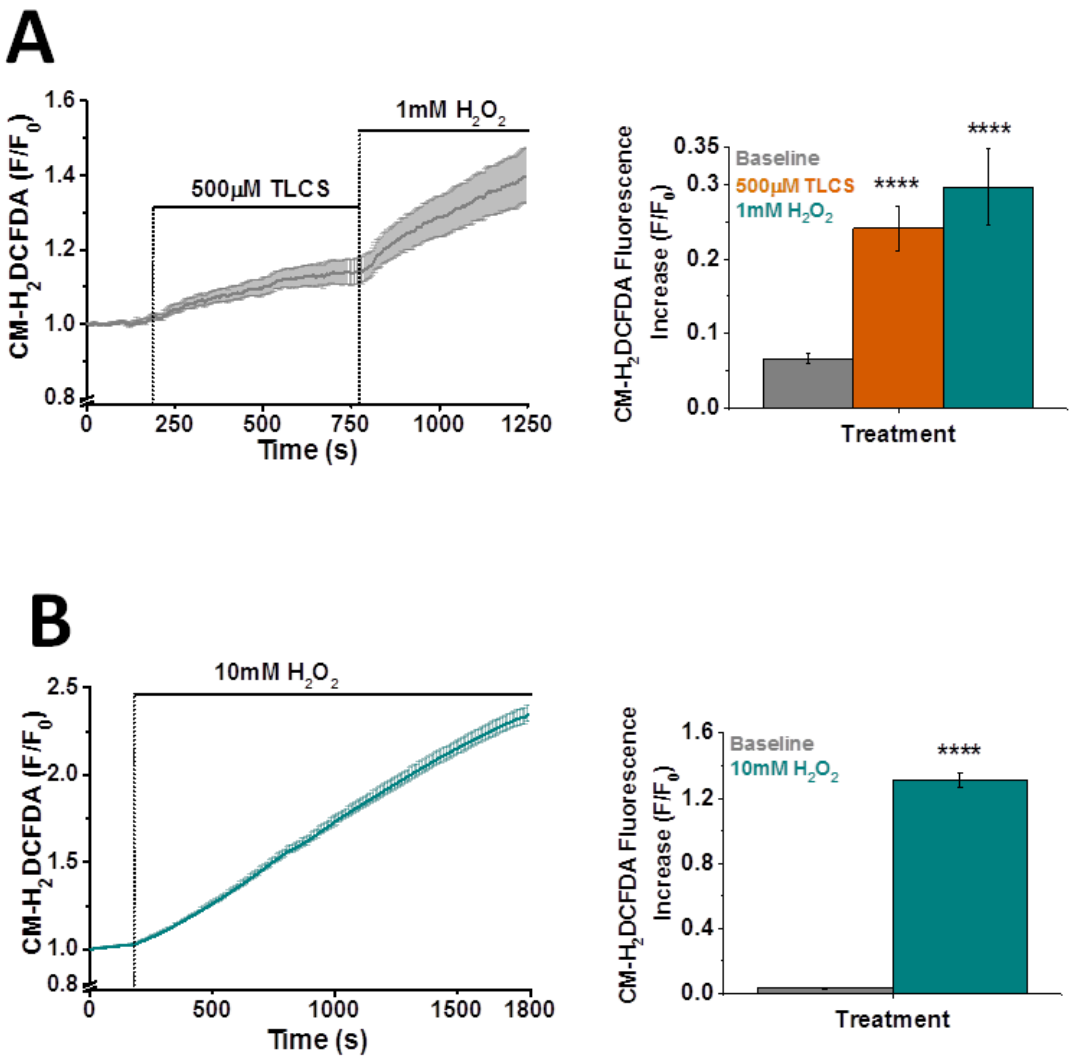

Figure 4.1. TLCS and H_2O_2-induced progressive increases in ROS levels. CM-H_2DCFDA loaded cells were treated with **(A)** 500µM TLCS followed by 1mM H_2O_2 line and bar chart presentation of CM-H_2DCFDA fluorescence increase during treatment. **(B)** 10mM H_2O_2 line and bar chart presentation of CM-H_2DCFDA fluorescence increase during treatment. A - Traces are averages of 26 cells and >5 animals and B - 198 cells from 4 animals. Data have been normalised to the initial fluorescence reading t=0 expressed as F/F_0. All data shown are mean ±SEM.

Figure 4.2

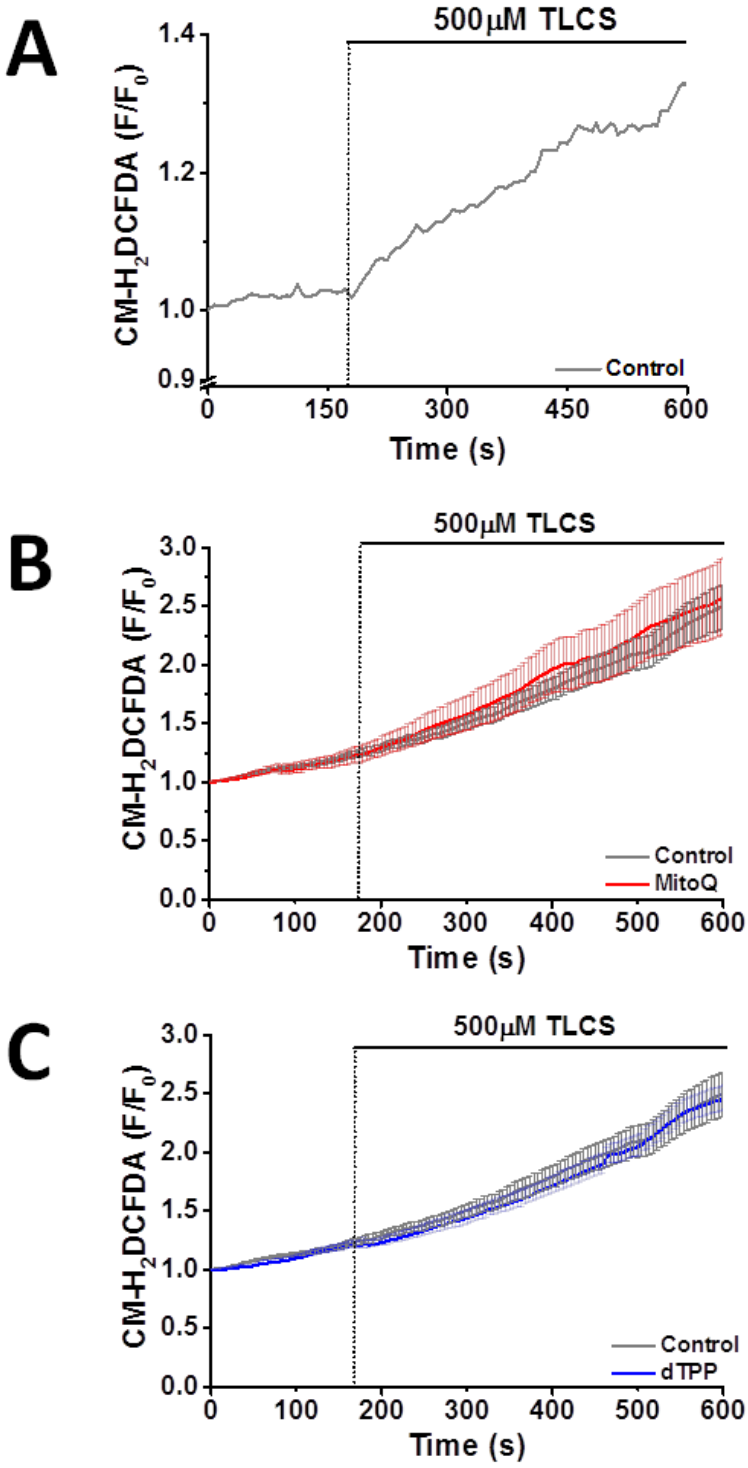

Figure 4.2. 1µM MitoQ did not diminish TLCS-induced $[ROS]_i$ increases measured by CM-H_2DCFDA. Pancreatic acinar cells were pre-treated with either NaHEPES, 1µM MitoQ or 1µM dTPP prior to treatment with 500µM TLCS. **(A)** Example trace of 500µM-induced TLCS ROS increases, **(B)** TLCS-induced ROS increases were not reduced with 1µM MitoQ pre-treatment, **(C)** dTPP pre-treated cells vs control. Traces are averages of >15 cells from >3 animals. Data have been normalised to the initial fluorescence reading t=0 expressed as F/F_0. All data shown are mean ±SEM.

Figure 4.3

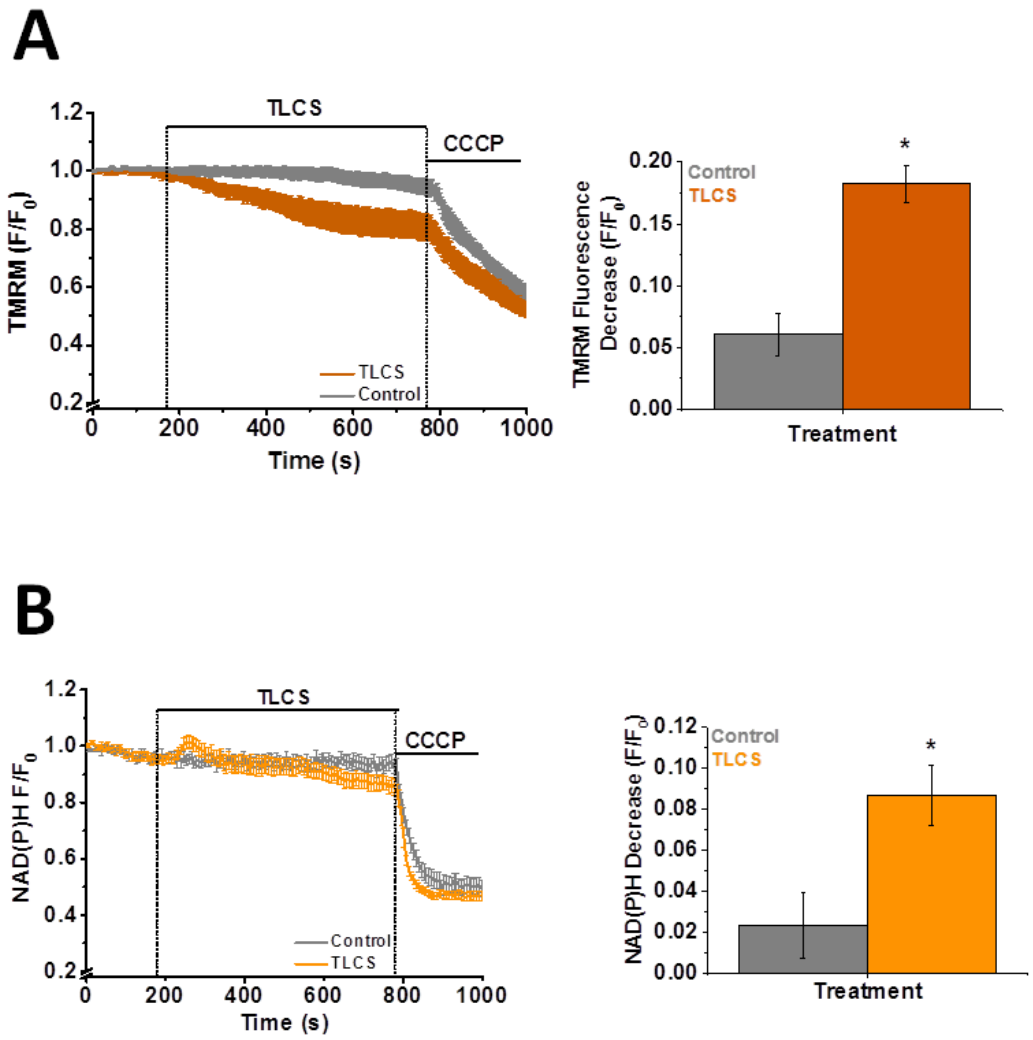

Figure 4.3. The effect of TLCS on ΔΨm and NAD(P)H. TMRM loaded cells were treated with 500µM TLCS for a 10 minute period prior to treatment with uncoupler CCCP (10µM) **(A)** TLCS caused progressive membrane depolarisation and **(B)** transient increases in NAD(P)H followed by a progressive decrease. Traces are averages of at least 15 cells and >3 animals. Data has been normalised to the initial fluorescence reading t=0 expressed as F/F_0. All data shown are mean ±SEM. * $p<0.05$.

Figure 4.4

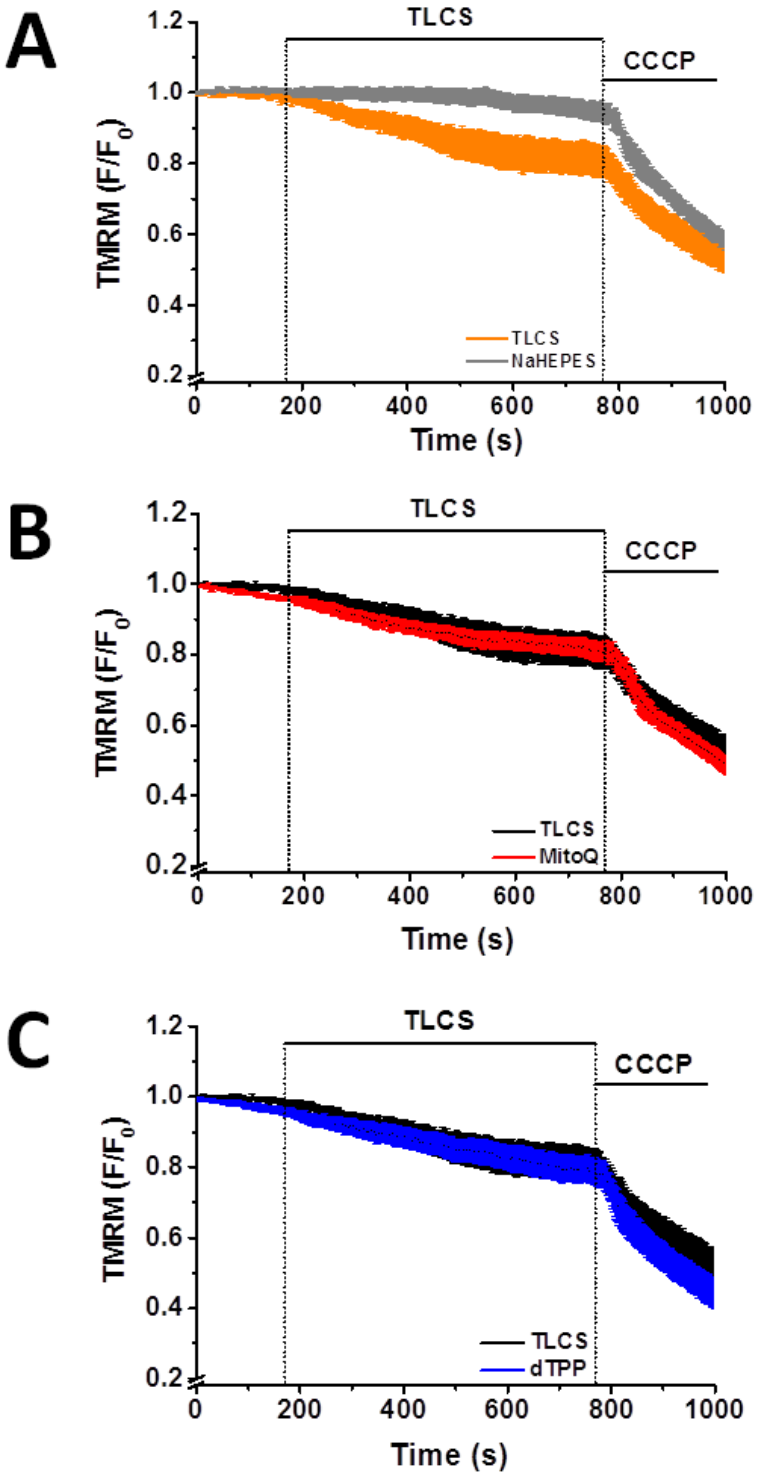

Figure 4.4. 1µM MitoQ does not protect against TLCS-induced loss of ΔΨm. TMRM loaded cells were pre-treated as previously described. **(A)** Control cells with and without 500µM TLCS treatment, **(B)** MitoQ (1µM) or **(C)** dTPP (1µM). No significant improvement was seen with treating cells with 1µM MitoQ. Traces are averages of at least 15 cells and >3 animals. Data has been normalised to the initial fluorescence reading t=0 expressed as F/F_0. All data shown are mean ±SEM.

Figure 4.5

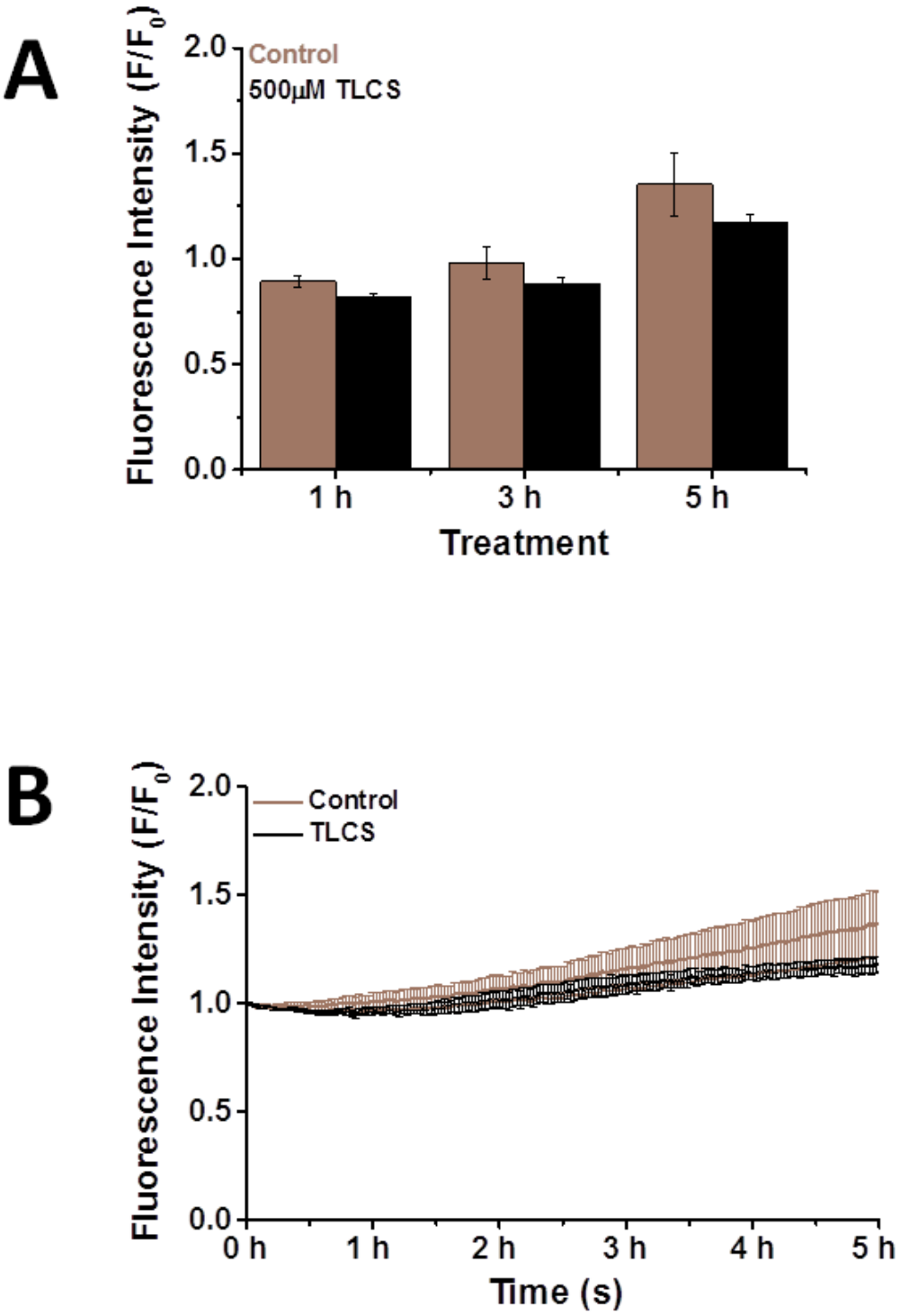

Figure 4.5. Lack of effect of TLCS on pancreatic acinar cell apoptosis. CellEvent® Caspase-3/7 Green reagent loaded cells were treated with NaHEPES or 500µM. The data has been normalised to the initial fluorescence reading t=0 expressed as F/F_0. **(A)** Bar chart representative of time points **(B)** Line graph presentation of data. Traces are averages of >5 animals. All data shown are mean ±SEM. The increase in fluorescence with TLCS is not significantly different from the control.

Figure 4.6

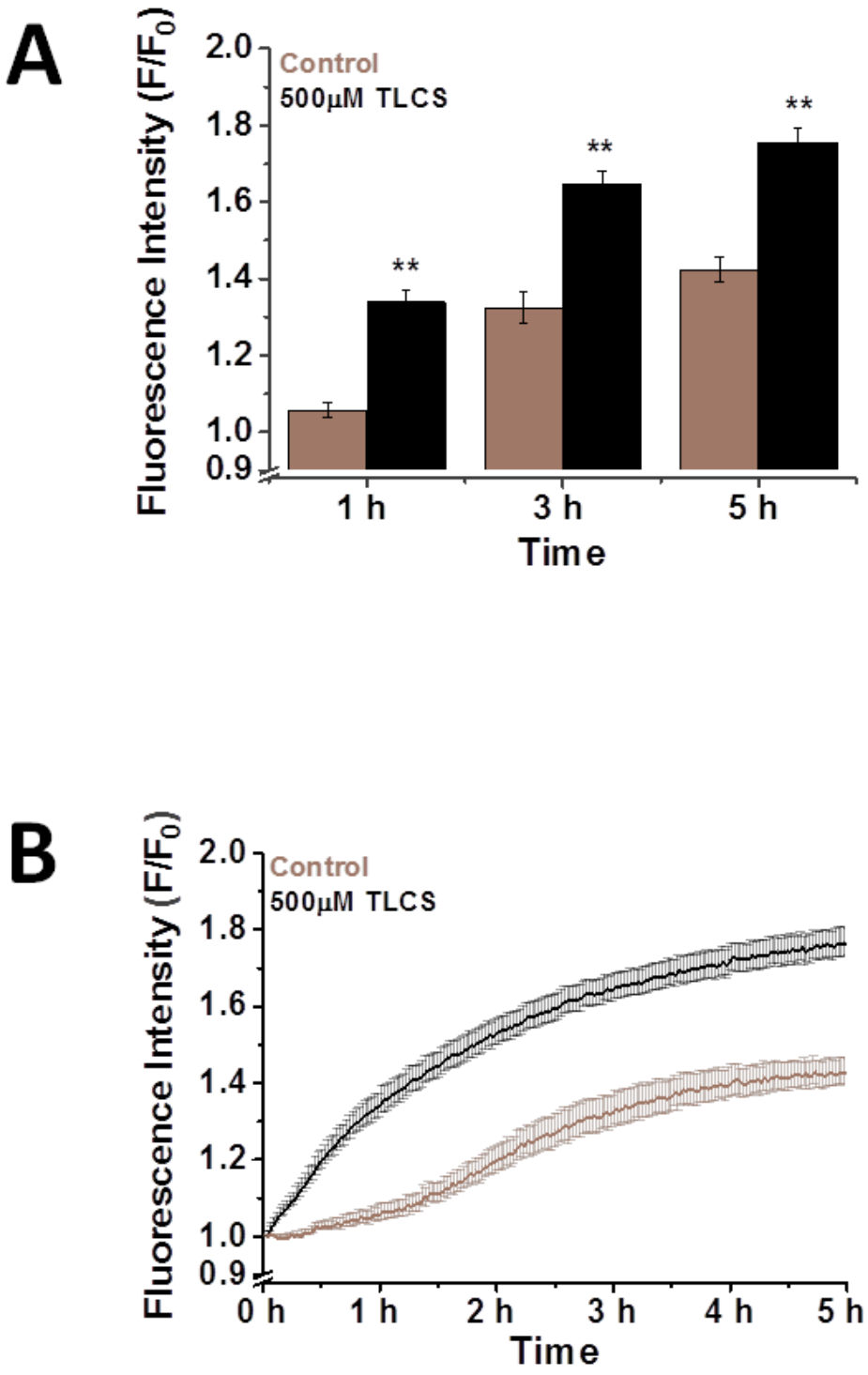

Figure 4.6. TLCS-induced necrosis of pancreatic acinar cells. Propidium Iodide (PI) loaded cells were treated with either NaHEPES or 500µM TLCS. A large increase in cellular necrosis was observed. Data has been normalised to the initial fluorescence reading t=0 expressed as F/F_0. **(A)** Bar chart representative of time points **(B)** Line graph presentation of data. Traces are averages of >5 animals. All data shown are mean ±SEM. ** $p<0.01$.

Figure 4.7

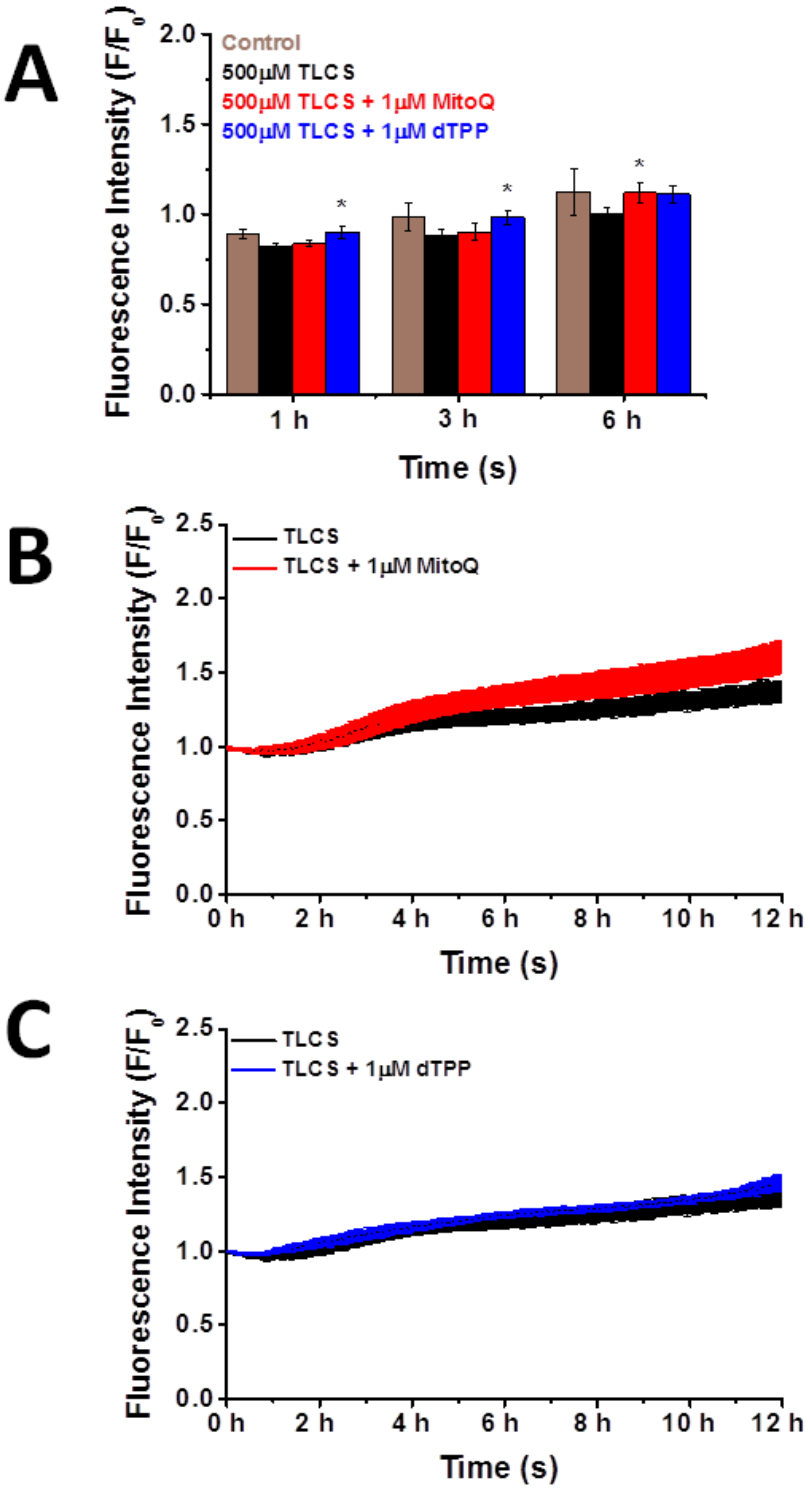

Figure 4.7. Effects of MitoQ and dTPP on TLCS-induced apoptosis. CellEvent® Caspase-3/7 Green reagent loaded cells were treated with 500µM TLCS. Data have been normalised to the initial fluorescence reading t=0 expressed as F/F_0. **(A)** Bar chart representative of time points **(B)** Line graph presentation of TLCS treated cells with and without 1µM MitoQ pre-treatment **(C)** Line graph presentation of TLCS treated cells with and without 1µM dTPP pre-treatment. Traces are averages of >5 animals. All data shown are mean ±SEM. * = $p<0.05$.

Figure 4.8

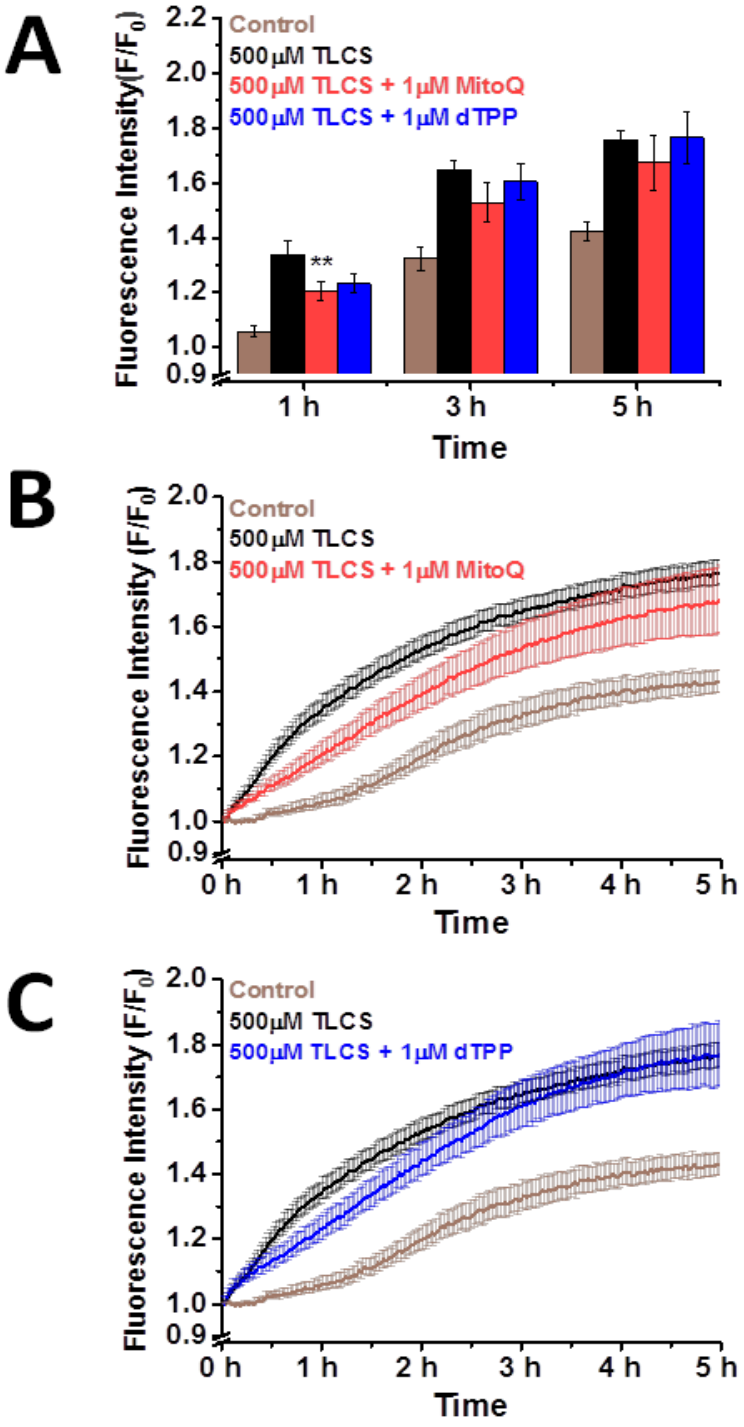

Figure 4.8. Effects of MitoQ and dTPP on TLCS-induced cellular necrosis. PI loaded cells were pre-treated with 1µM MitoQ, 1µM dTPP or NaHEPES (control) for 30 minutes prior to the addition of 500µM TLCS. Data has been normalised to the initial fluorescence reading t=0 expressed as F/F_0. **(A)** Bar chart display of time points 1 h, 3 h and 5 h **(B)** Line graph presentation showing the effect of 1µM MitoQ pre-treatment on TLCS induced cell necrosis **(C)** The effect of 1µM dTPP pre-treatment on TLCS induced cell necrosis. Traces are averages of >5 animals. All data shown are mean ±SEM. * = $p<0.05$

Figure 4.9

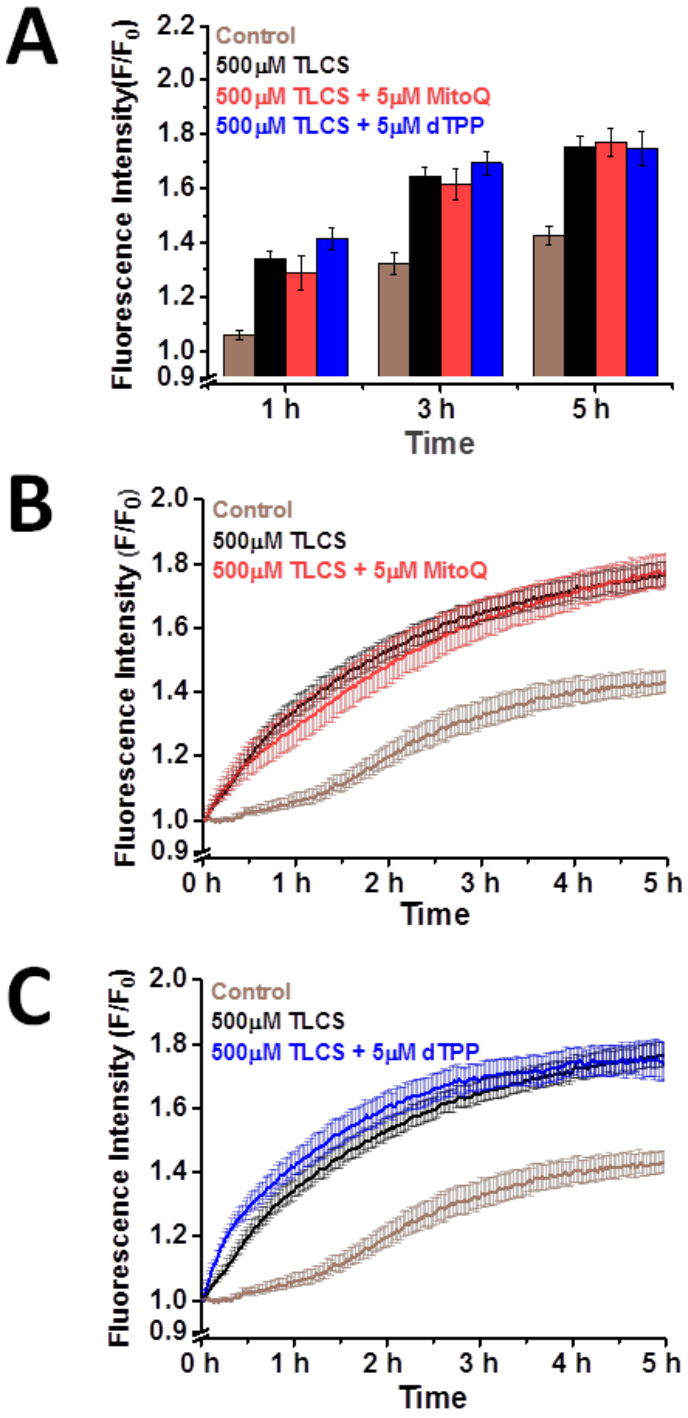

Figure 4.9. Effects of 5µM MitoQ on TLCS-induced cell necrosis. Propidium Iodide (PI) loaded cells were pre-treated with 5µM MitoQ or 5µM dTPP for 30 minutes prior to the addition of 500µM TLCS. Control cells were in the presence of NaHEPES alone. Data has been normalised to the initial fluorescence reading t=0 expressed as F/F_0. **(A)** Bar chart representative of time points 1 h, 3 h and 5 h **(B)** Line graph presentation showing the effect of 5µM MitoQ pre-treatment on TLCS induced cell necrosis **(C)** The effect of 5µM dTPP pre-treatment on TLCS induced cell necrosis. Traces are averages of 2 animals and 6 technical replica's. All data shown are mean ±SEM.

CCK Hyperstimulation-Induced Toxic Effects: Lack of Protection with MitoQ Pre-treatment

Mitochondrial membrane potential was measured in cells loaded with the dye TMRM and pre-treated with MitoQ (1µM), dTPP (1µM), or physiological saline for 30 minutes. Fluorescence measurements in response to 10nM CCK treatment were obtained for 10 minutes. Results showed a progressive decline in TMRM fluorescence indicative of loss of membrane potential. The depolarisation seen with CCK hyperstimulation is partial, as with TLCS treatment and complete depolarisation induced by the uncoupling action of CCCP. MitoQ (1µM) did not protect against CCK-induced loss of membrane potential and dTPP (1µM) exacerbated the effects (Figure 4.10). CCK stimulation produced an increase in NAD(P)H levels measured by monitoring levels of NAD(P)H autofluorescence in isolated PACs. Pre-treatment with MitoQ and dTPP (1µM) abolished this affect and induced a decline in NAD(P)H levels (Figure 4.11).

Typical physiological CCK (10pM) induced $[Ca^{2+}]_c$ responses are of an oscillatory manner and hyperstimulatory CCK (10nM) responses a single large increase and following plateau (Figure 4.12). MitoQ, dTPP, dUb and TPP^+ at 1µM did not affect CCK hyperstimulation responses (Figure 4.13). CCK hyperstimulation (10nM) induced progressive and substantial increases in apoptosis, indicated by increases in CellEvent® Caspase-3/7 Green reagent fluorescence intensity and necrosis in PI loaded isolated PACs. These results were in comparison to a NaHEPES

control group (Figure 4.14 and 4.15). MitoQ demonstrated no protection against CCK-induced apoptosis or necrosis and exacerbated CCK-induced necrosis alongside dTPP at 1µM (Figures 4.16-4.19). CCK and TLCS induced differing levels of necrosis and apoptosis. CCK induced both apoptosis and necrosis of which the latter was a biphasic trend. Comparatively TLCS induced negligible apoptosis and predominantly necrosis (Figure 4.20).

Figure 4.10

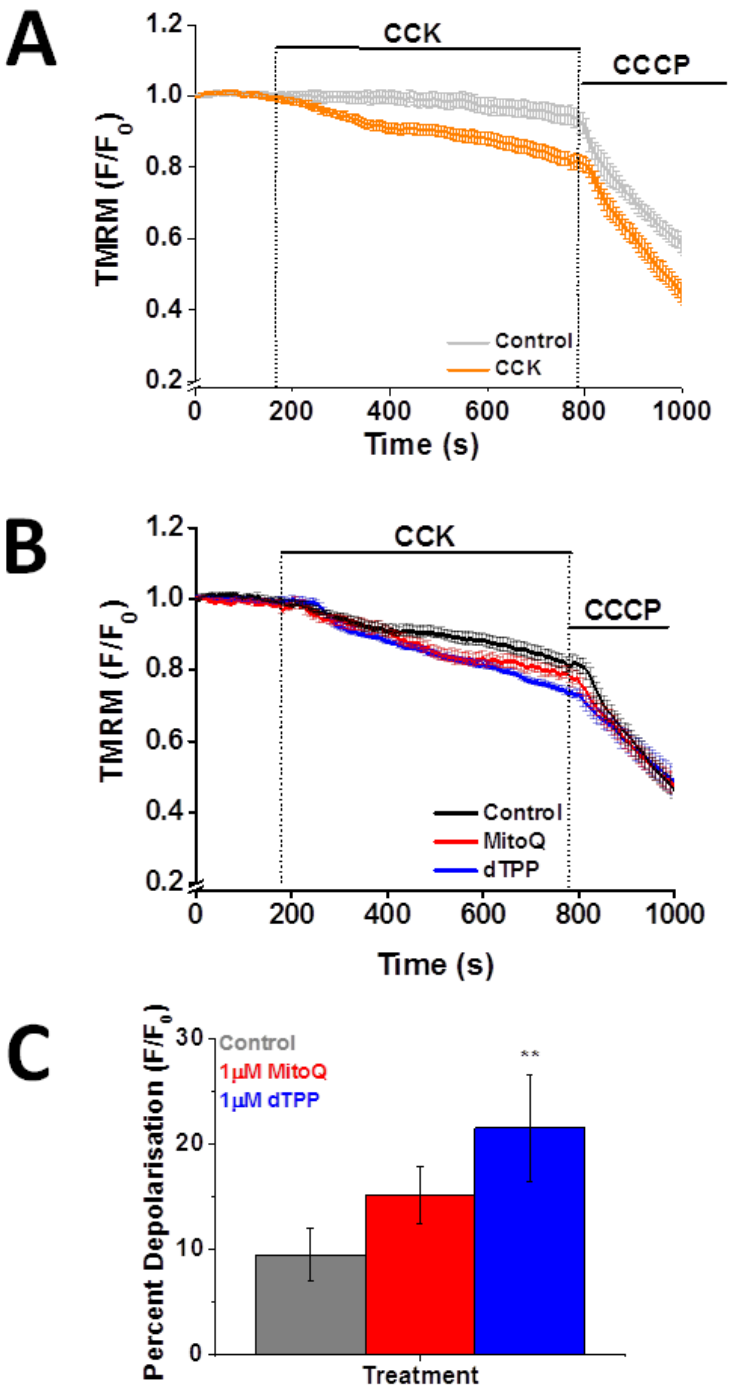

Figure 4.10. 1µM MitoQ did not protect against CCK-induced loss of ΔΨm. ΔΨm was measured in cells loaded with TMRM dye. Pancreatic acinar cell suspensions were pre-treated as previously described. **(A)** Control cells with and without 10nM CCK treatment, **(B)** MitoQ and dTPP (1µM) pre-treatment effects and **(C)** percent depolarisation with each treatment. Traces are averages of at least 15 cells and >3 animals. Data has been normalised to the initial fluorescence reading t=0 expressed as F/F_0. All data shown are mean ±SEM. dTPP significantly exacerbated CCK induced partial membrane depolarisation ** $p<0.01$.

Figure 4.11

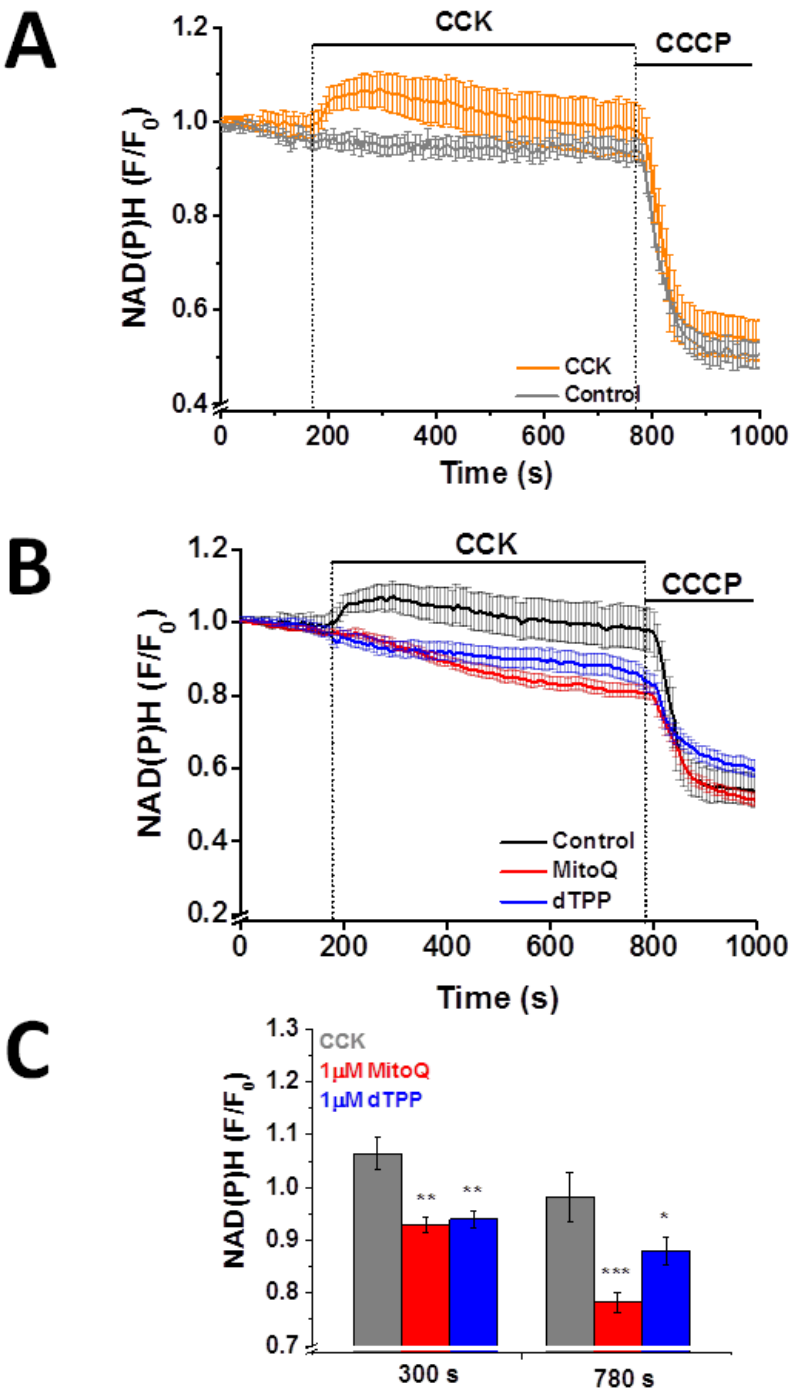

Figure 4.11. 1µM MitoQ and 1µM dTPP abolished CCK-induced NAD(P)H responses. Pancreatic acinar cell suspensions were pre-treated as previously described and NAD(P)H autofluorescence was measured for a 3 minute baseline before a 10 minute treatment with 10nM CCK. **(A)** Control cells with and without 10nM CCK treatment, **(B)** MitoQ and dTPP (1µM) pre-treatment vs control **(C)** MitoQ and dTPP pre-treatment effects at 300 s and 780 s. Traces are averages of at least 26 cells and >3 animals. Data has been normalised to the initial fluorescence reading t=0 expressed as F/F_0. All data shown are mean ±SEM. * $p<0.05$, ** $p<0.01$, *** $p<0.001$.

Figure 4.12

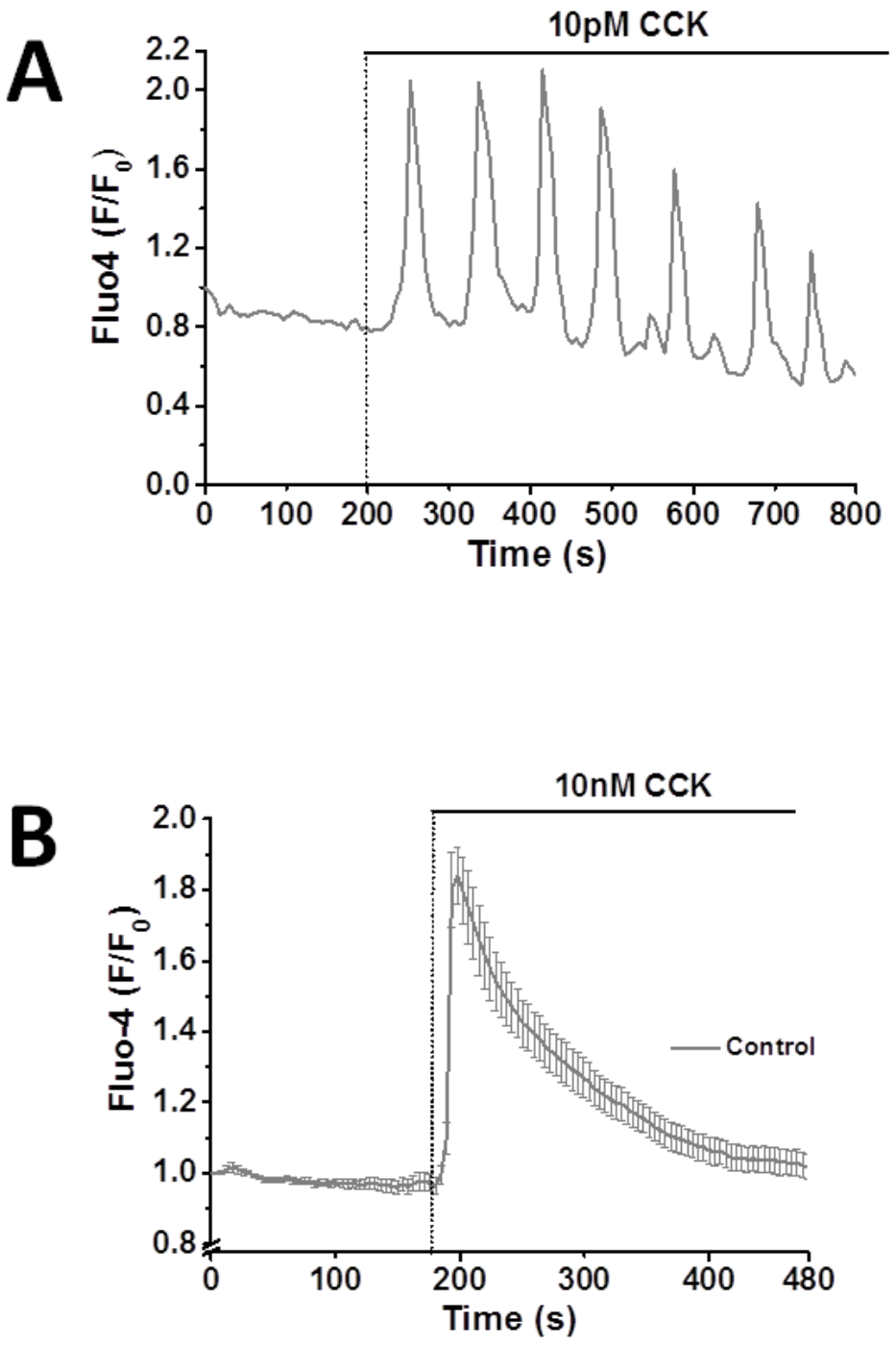

5

Figure 4.12. CCK-induced $[Ca^{2+}]_c$ responses. Cytosolic Ca^{2+} was measured with Fluo-4. Basal measurements (NaHEPES) were taken prior to treatment with physiological levels of CCK (10pM) or hyperstimulation concentrations (10nM). **(A)** 10pM CCK induced $[Ca^{2+}]_c$ oscillations (example trace) and **(B)** 10nM CCK induced large transient increase in $[Ca^{2+}]_c$. Traces are averages of >18 cells from at least 3 animals. Data has been normalised to the initial fluorescence reading t=0 expressed as F/F_0. Data shown are mean ±SEM.

Figure 4.13

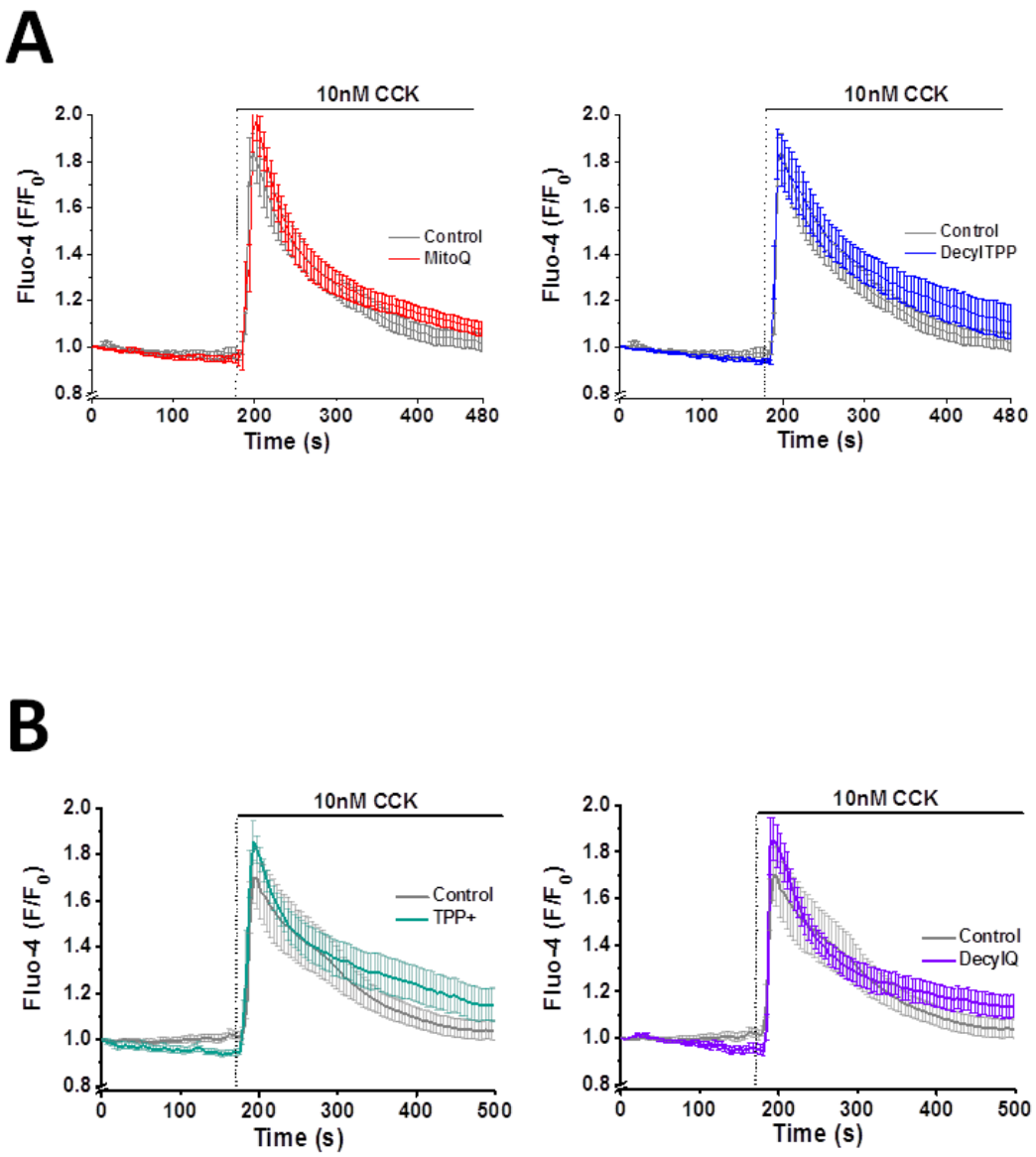

Figure 4.13. 1µM MitoQ/dTPP/dUb/TPP+ did not affect CCK hyperstimulation-induced $[Ca^{2+}]_c$ increases. Cytosolic Ca^{2+} was measured with Fluo-4. Pancreatic acinar cells were pre-treated with either 1µM MitoQ, 1µM dTPP, 1µM dUb, 1µM TPP^+ or NaHEPES (control). Basal measurements (NaHEPES) were taken for 3 minutes followed by a further 5 minutes perfusion with 10nM CCK . **(A)** The Effect of MitoQ (1µM) and dTPP (1µM) on CCK induced cytosolic Ca^{2+} responses **(B)** The Effect of dUb (1µM) and TPP^+ (1µM) on CCK induced cytosolic Ca^{2+} responses Traces are averages of >18 cells from at least 3 animals. Data has been normalised to the initial fluorescence reading t=0 expressed as F/F_0. All data shown are mean ±SEM.

Figure 4.14

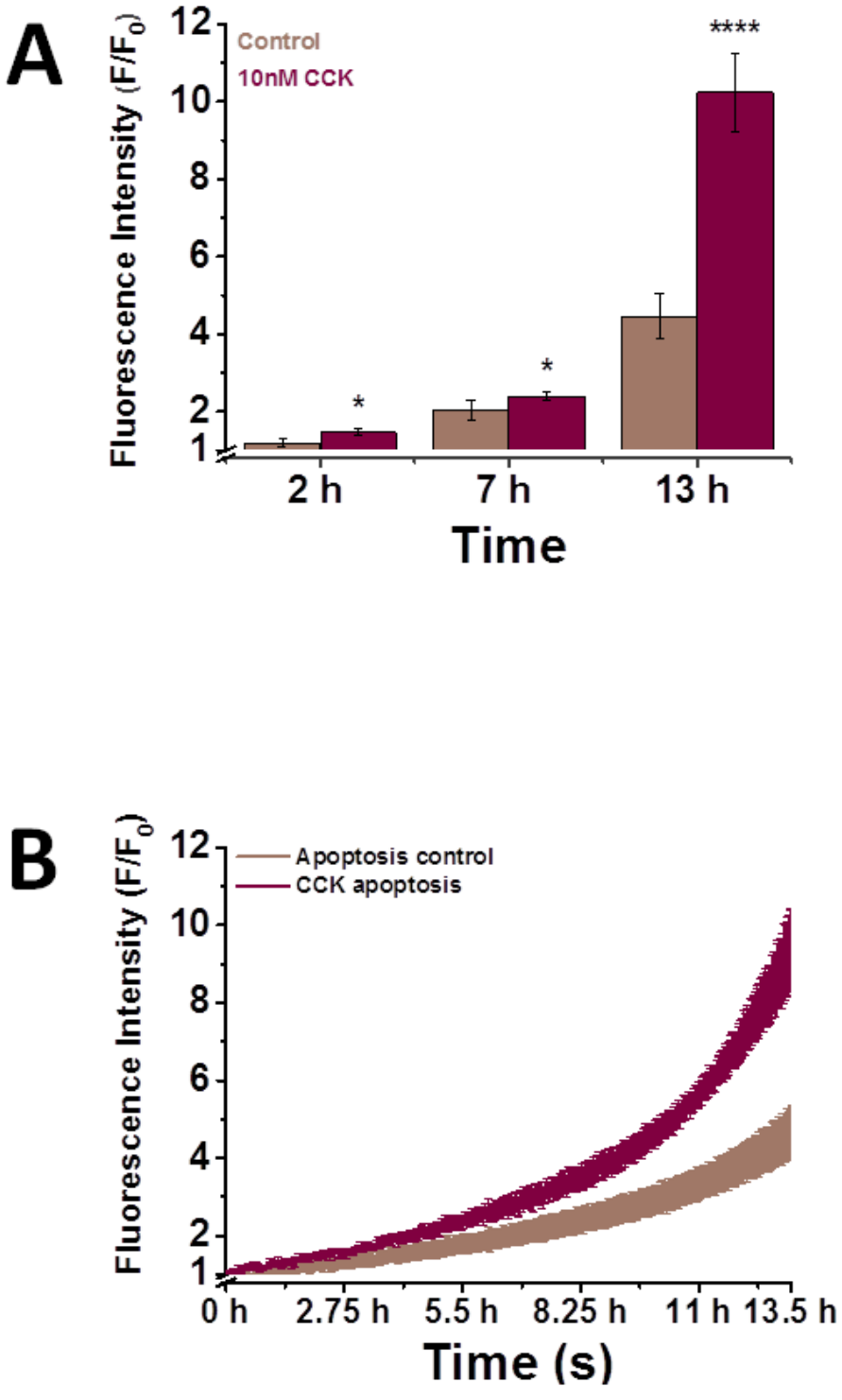

Figure 4.14. CCK-induced apoptosis. CellEvent® Caspase-3/7 Green reagent loaded cells were treated with either NaHEPES or 10nM CCK. The data has been normalised to the initial fluorescence reading t=0 expressed as F/F_0. **(A)** Bar chart representative of time points **(B)** Line graph presentation of data. Traces are averages of >6 animals. All data shown are mean ±SEM. * $p<0.05$, **** $p<0.0001$.

Figure 4.15

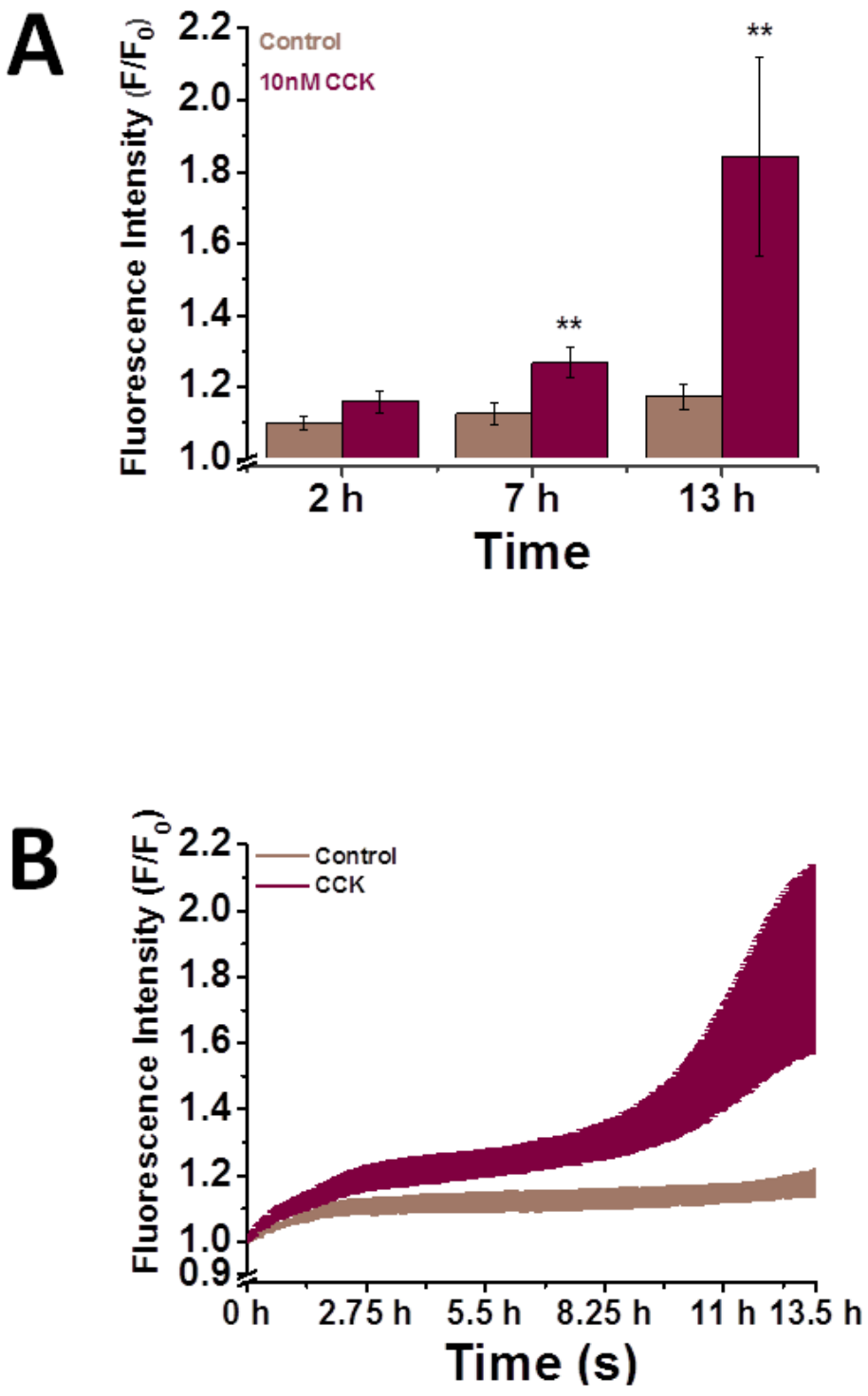

Figure 4.15. CCK-induced necrosis. Propidium Iodide (PI) loaded cells were treated with NaHEPES or 10nM CCK. The data has been normalised to the initial fluorescence reading t=0 expressed as F/F_0. **(A)** Bar chart representative of time points **(B)** Line graph presentation of data. Traces are averages of >6 animals. All data shown are mean ±SEM. ** $p<0.01$.

Figure 4.16

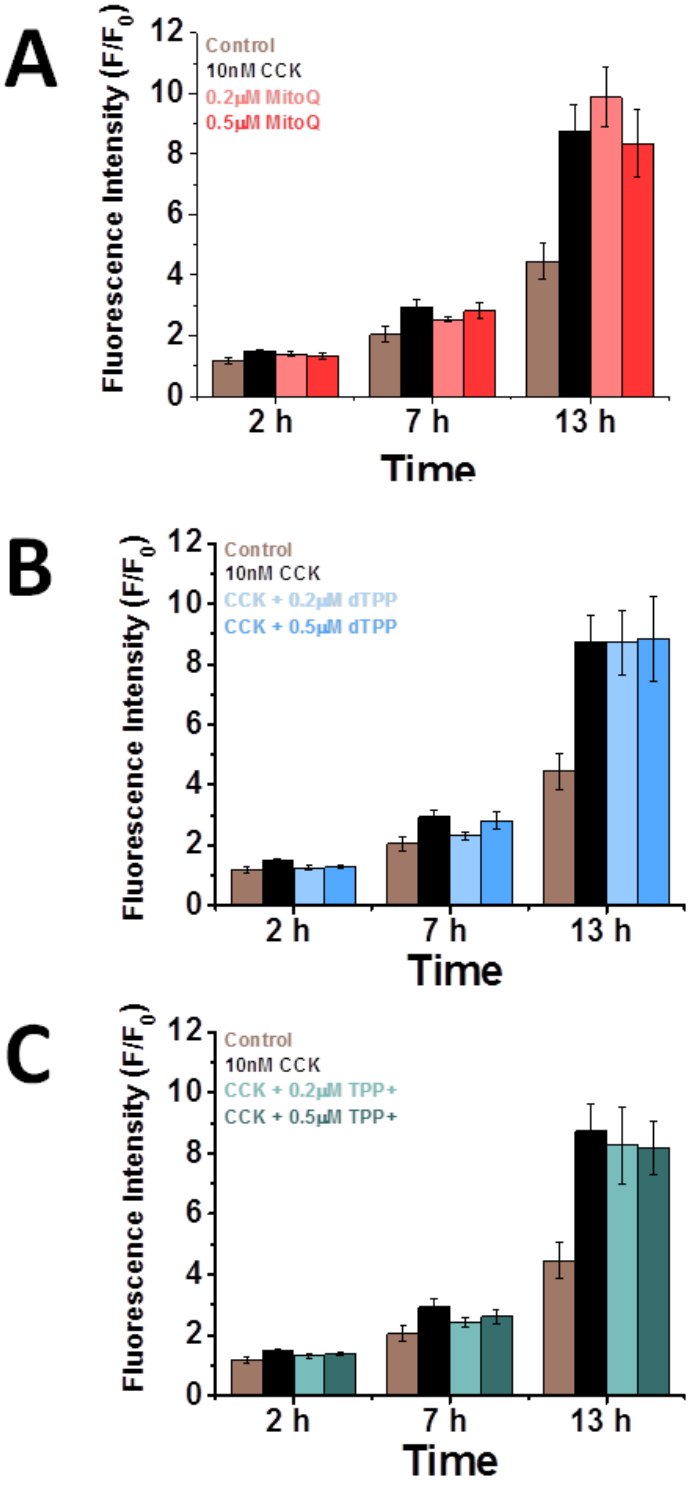

Figure 4.16. MitoQ (0.2μM and 0.5μM) did not protect against CCK-induced apoptosis. CellEvent® Caspase-3/7 Green reagent loaded cells were pre-treated for 30 minutes with either **(A)** 0.2μM and 0.5μM MitoQ, **(B)** 0.2μM and 0.5μM dTPP, **(c)** 0.2μM and 0.5μM TPP^+ before administration of 10nM CCK to each CCK treatment group. The data has been normalised to the initial fluorescence reading t=0 expressed as F/F_0. The data is presented as bar chart time points. Traces are averages of >6 animals. All data shown are mean ±SEM.

Figure 4.17

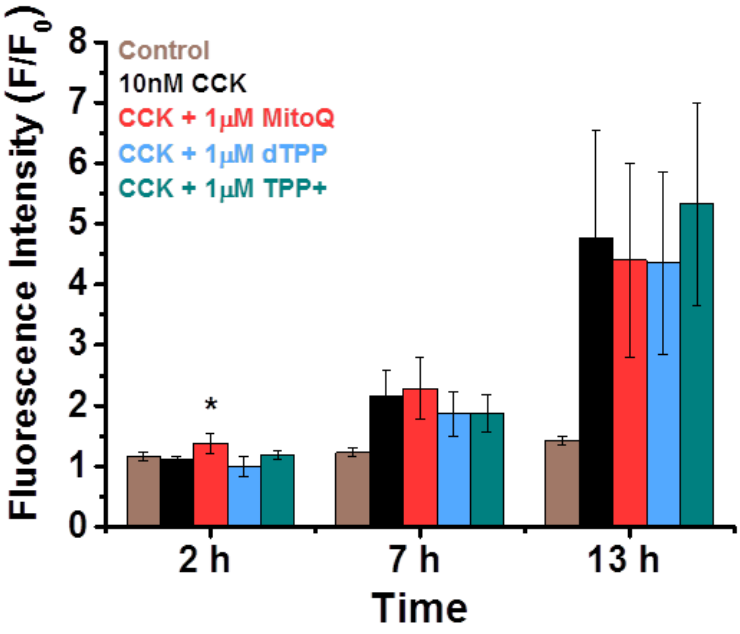

Figure 4.17. 1μM MitoQ did not protect against CCK-induced apoptosis. CellEvent® Caspase-3/7 Green reagent loaded cells were pre-treated for 30 minutes with either 1μM MitoQ, 1μM dTPP, 1μM TPP^+ before administration of 10nM CCK to each CCK treatment group. The data has been normalised to the initial fluorescence reading t=0 expressed as F/F_0. The data is presented as bar chart time points. Traces are averages of >5 animals. All data shown are mean ±SEM. 1μM MitoQ exacerbated CCK induced cellular apoptosis at the 2 hour time point (*$p<0.05$).

Figure 4.18

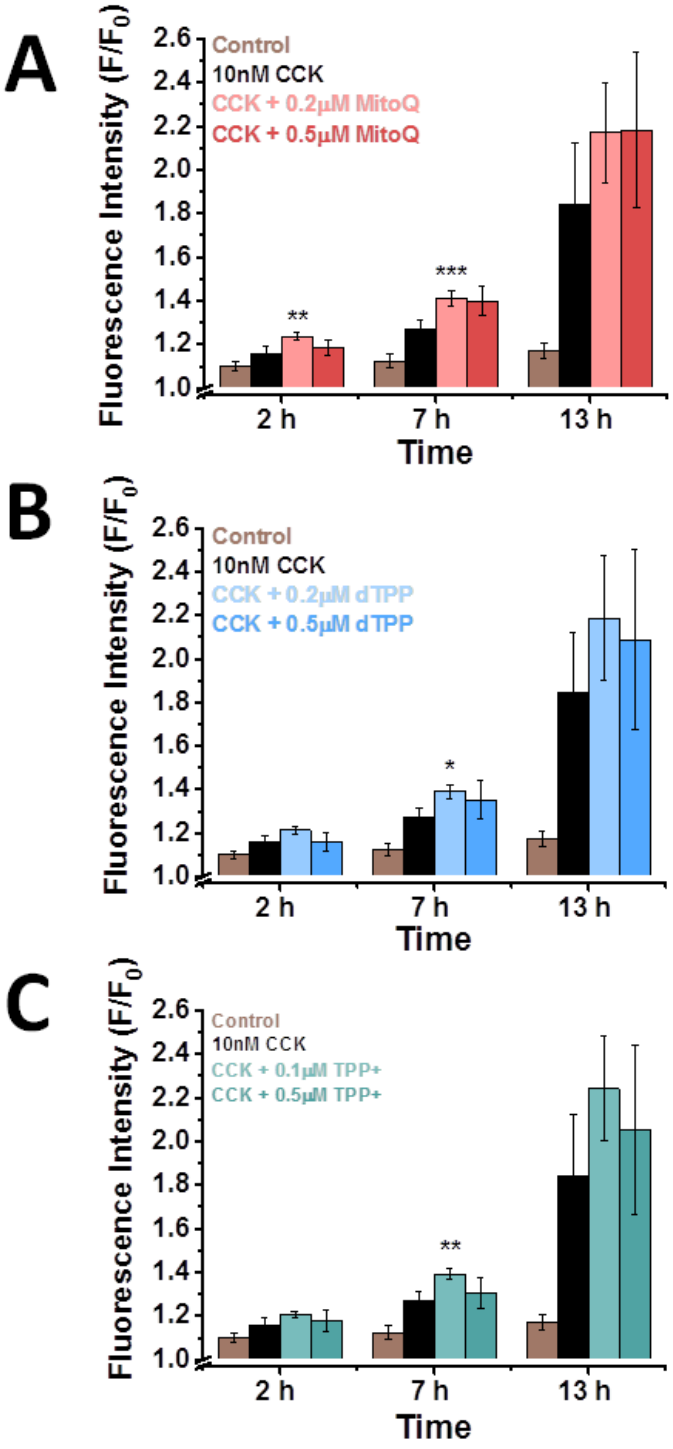

Figure 4.18. MitoQ (0.2 and 0.5µM) did not protect against CCK-induced necrosis. PI loaded cells were pre-treated for 30 minutes with either **(A)** 1µM MitoQ, **(B)** 1µM dTPP, **(c)** 1µM TPP^+ before administration of 10nM CCK. The data has been normalised to the initial fluorescence reading t=0 expressed as F/F_0. The data is presented as bar chart time points. Traces are averages of >6 animals. All data shown are mean ±SEM. 0.2µM MitoQ exacerbated CCK induced necrosis at 2 h and 7 h time points and both 0.2µM dTPP and TPP^+ at 7 h. * $p<0.05$, ** $p<0.01$, *** $p<0.001$.

Figure 4.19

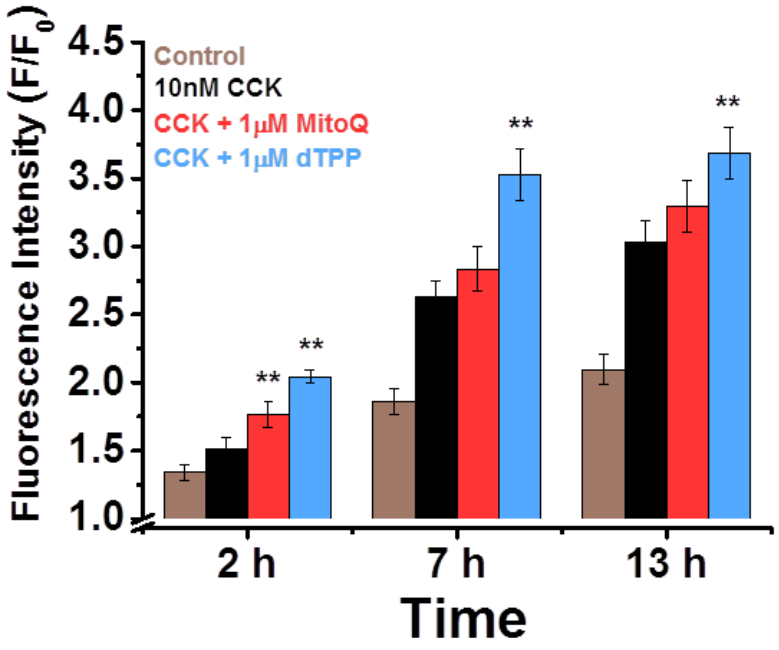

Figure 4.19. Lack of protection by MitoQ against CCK-induced necrosis. PI loaded cells were pre-treated for 30 minutes with either 1μM MitoQ, 1μM dTPP before administration of 10nM CCK to each CCK treatment group. The data has been normalised to the initial fluorescence reading t=0 expressed as F/F_0. The data is presented as bar chart time points and are averages of >12 animals. All data shown are mean ±SEM ** $p<0.01$.

Figure 4.20

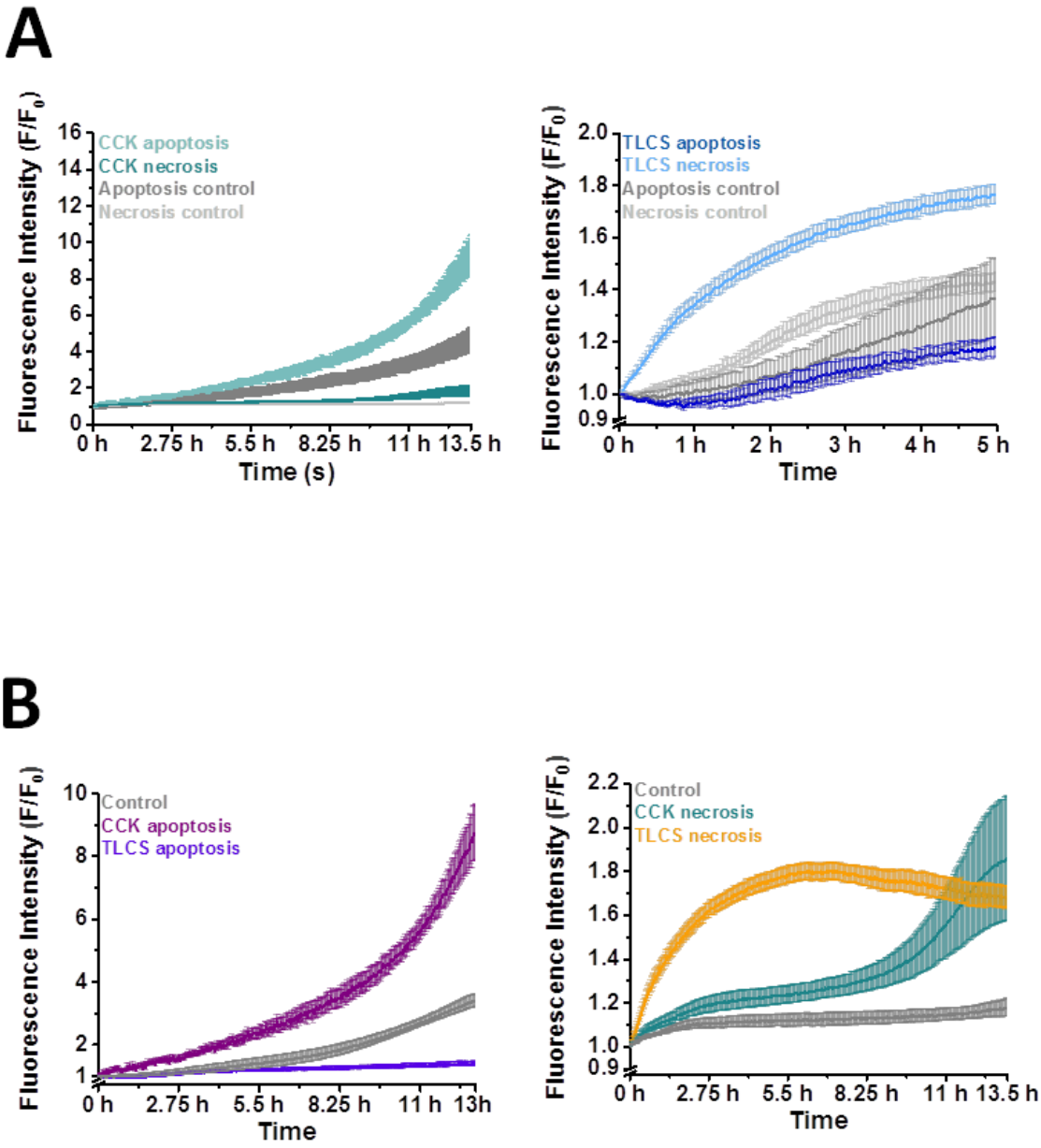

Figure 4.20. CCK and TLCS-induced apoptosis and necrosis. Comparison of levels of apoptosis and necrosis with **(A)** 10nM CCK and 500µM TLCS and **(B)** CCK versus TLCS apoptosis and necrosis. The data has been normalised to the initial fluorescence reading t=0 expressed as F/F_0. Traces are averages of >6 animals. All data shown are mean ±SEM.

Pancreatic Acinar Cell Apoptosis and Necrosis: The Effects of POAEE, Ethanol and MitoQ Pre-treatment

For the following cellular apoptosis and necrosis plate reader experiments, POAEE was solubilised in 85mM or 850mM ethanol with 280mM polyethylene glycol (PEG). CellEvent® Caspase-3/7 Green reagent loaded cells were again used to indicate levels of cellular apoptosis and PI for necrosis in isolated PACs. 85mM and 850mM EtOH demonstrated dose dependent effects on the induction of both apoptosis and necrosis (Figure 4.21 and 4.22). 100µM POAEE induced substantial apoptosis and necrosis in comparison to the NaHEPES control (Figure 4.23 and 4.24). Isolated PACs were pre-treated with MitoQ (0.2µM and 1µM) and treated with POAEE. MitoQ demonstrated concentration-dependent inhibition of POAEE-induced cellular apoptosis (Figure 4.25 and 4.26) and had no effect on levels of POAEE-induced necrosis (Figure 4.27-28). In cells treated with 850mM Ethanol, MitoQ (0.2µM and 1µM) demonstrated concentration-dependent inhibition of EtOH-induced apoptosis but not necrosis (Figure 4.29-31).

Figure 4.21

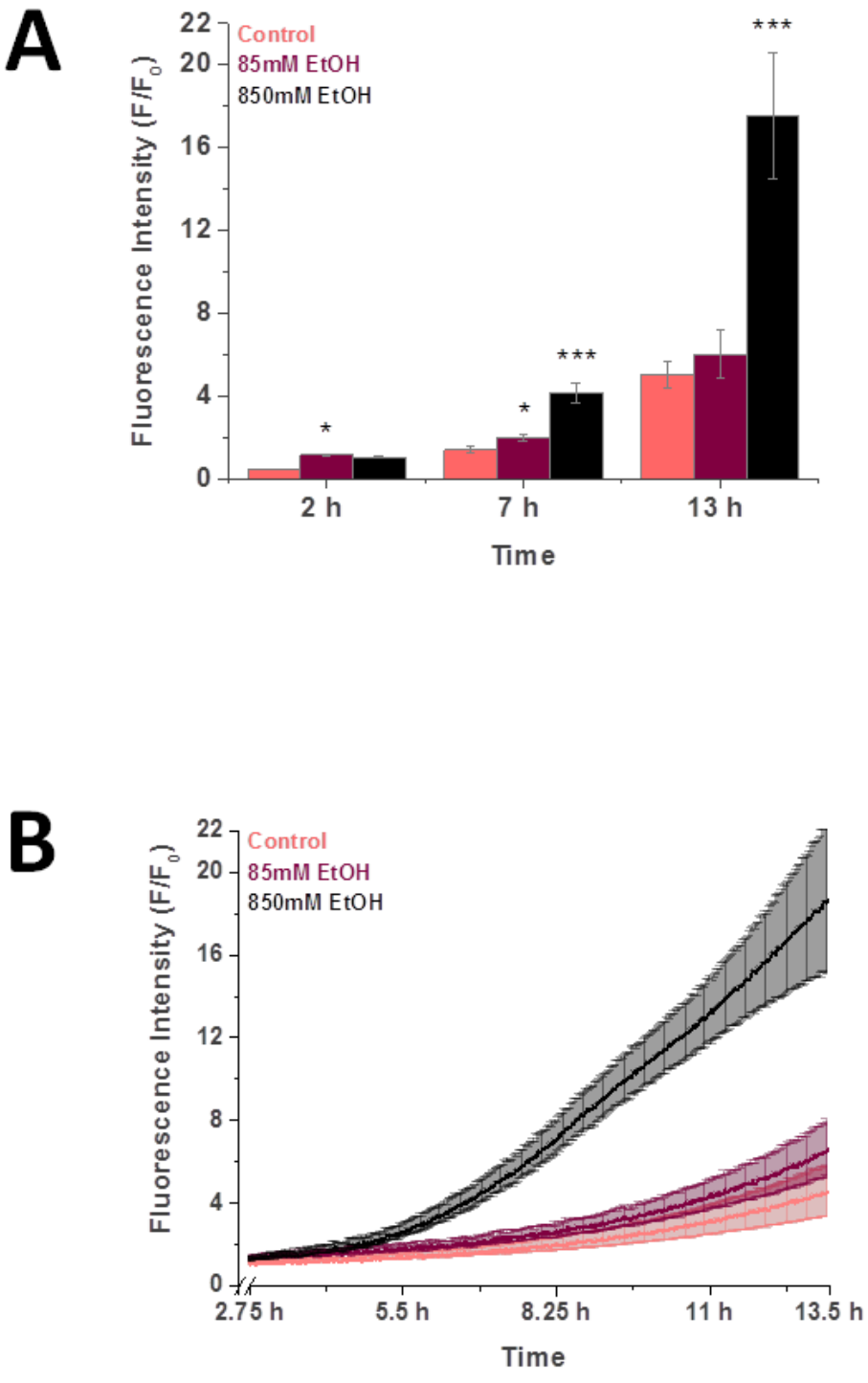

Figure 4.21. The effects of ethanol on apoptosis. CellEvent® Caspase-3/7 Green reagent loaded cells were treated with 85mM ethanol or 850mM ethanol. The data has been normalised to the initial fluorescence reading t=0 expressed as F/F_0. **(A)** Bar chart representative of time points **(B)** Line graph presentation of data. Traces are averages of >9 animals. All data shown are mean ±SEM. * $p<0.05$, *** $p<0.001$.

Figure 4.22

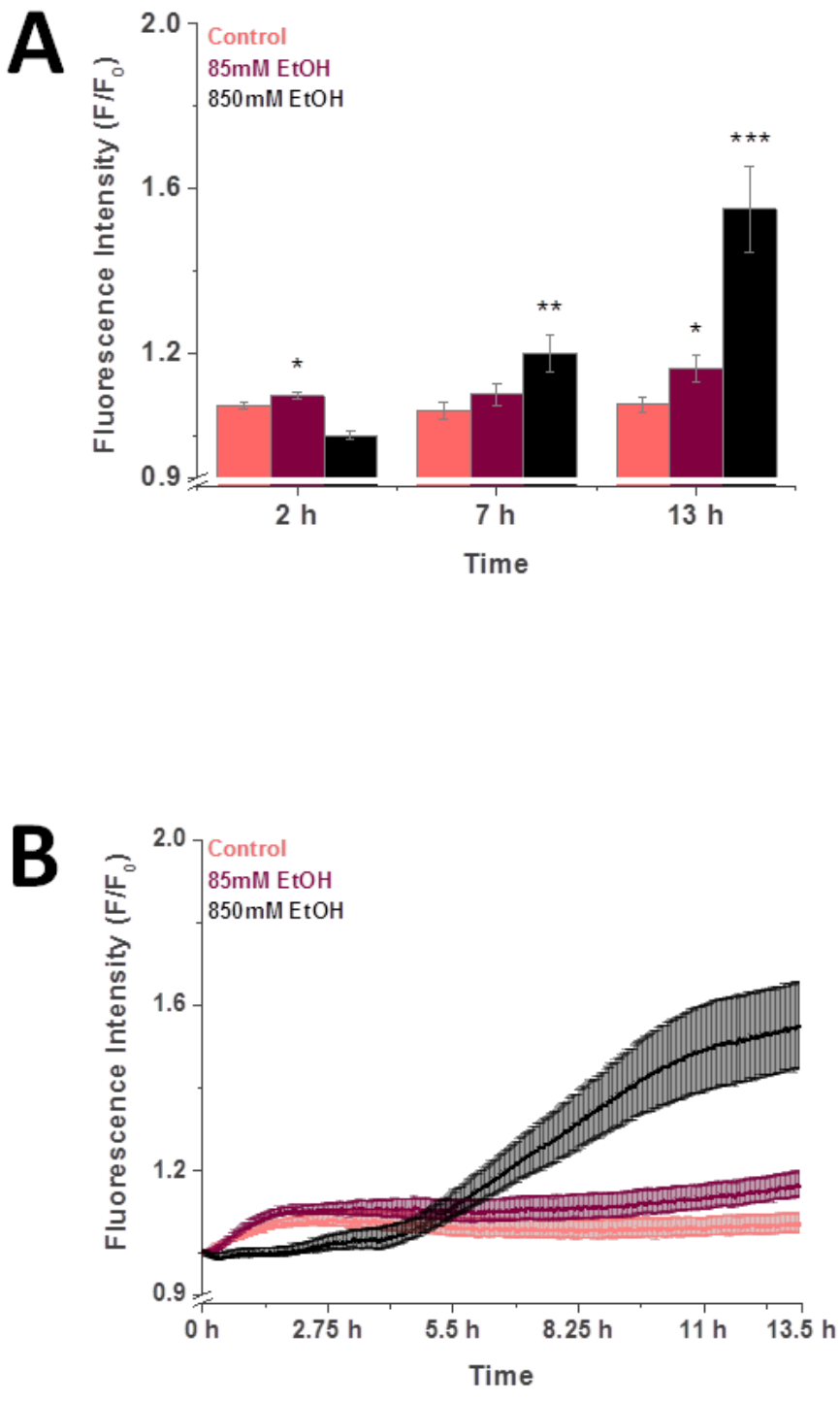

Figure 4.22. The effects of ethanol on necrosis. PI loaded cells were treated with 85mM ethanol or 850mM ethanol. The data has been normalised to the initial fluorescence reading t=0 expressed as F/F_0. **(A)** Bar chart representative of time points **(B)** Line graph presentation of data. Traces are averages of >9 animals. All data shown are mean ±SEM. * $p<0.05$, ** $p<0.01$ and *** $p<0.001$.

Figure 4.23

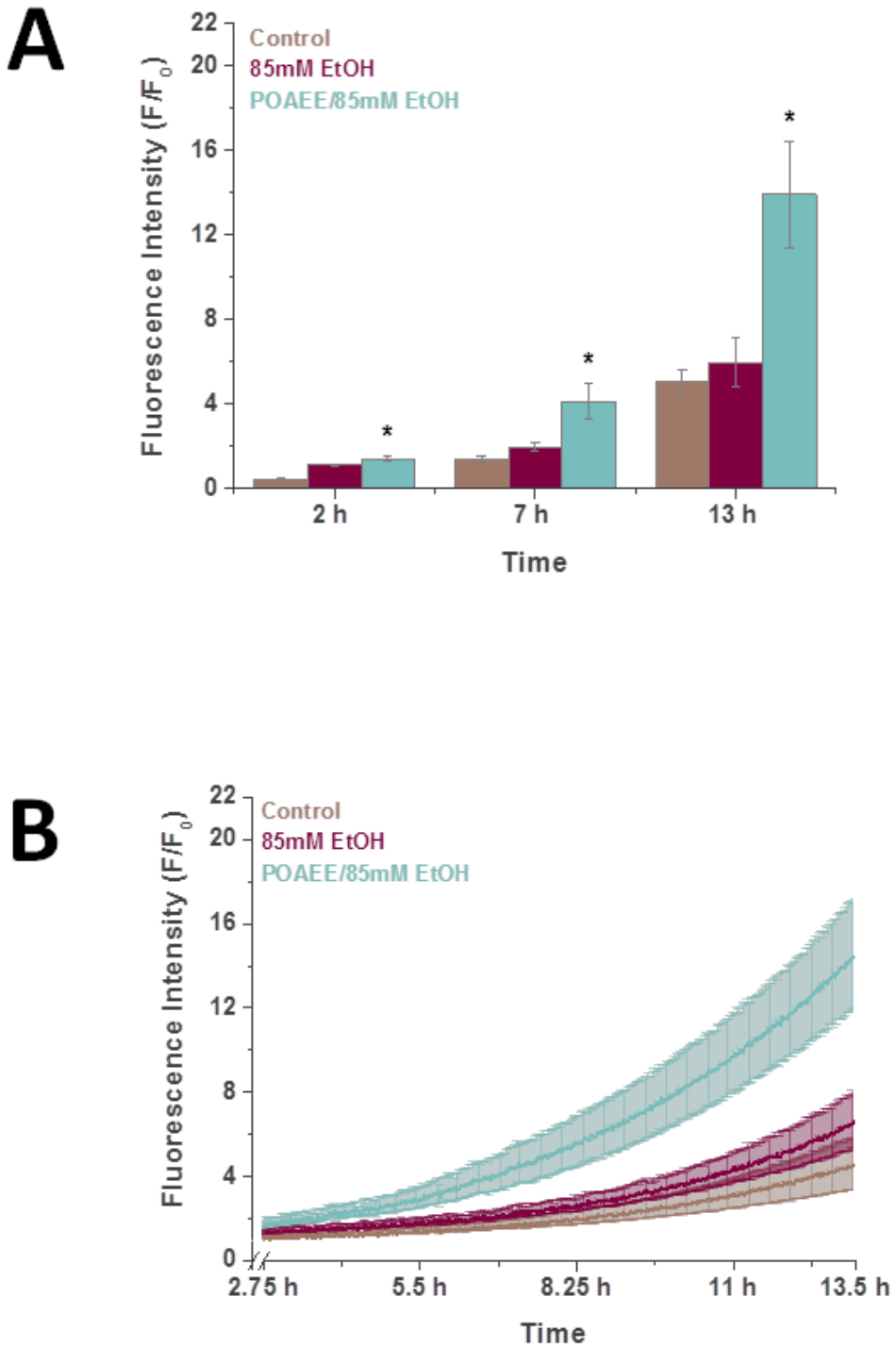

Figure 4.23. POAEE-induced apoptosis. Caspase-3/7 reagent loaded cells were treated with 100µM POAEE solubilised in 85mM ethanol. The data has been normalised to the initial fluorescence reading t=0 expressed as F/F_0. **(A)** Bar chart representative of time points, **(B)** Line graph presentation of 100µM POAEE induced apoptosis with 85mM EtOH and EtOH alone. Traces are averages of >9 animals. All data shown are mean ±SEM. * $p<0.05$.

Figure 4.24

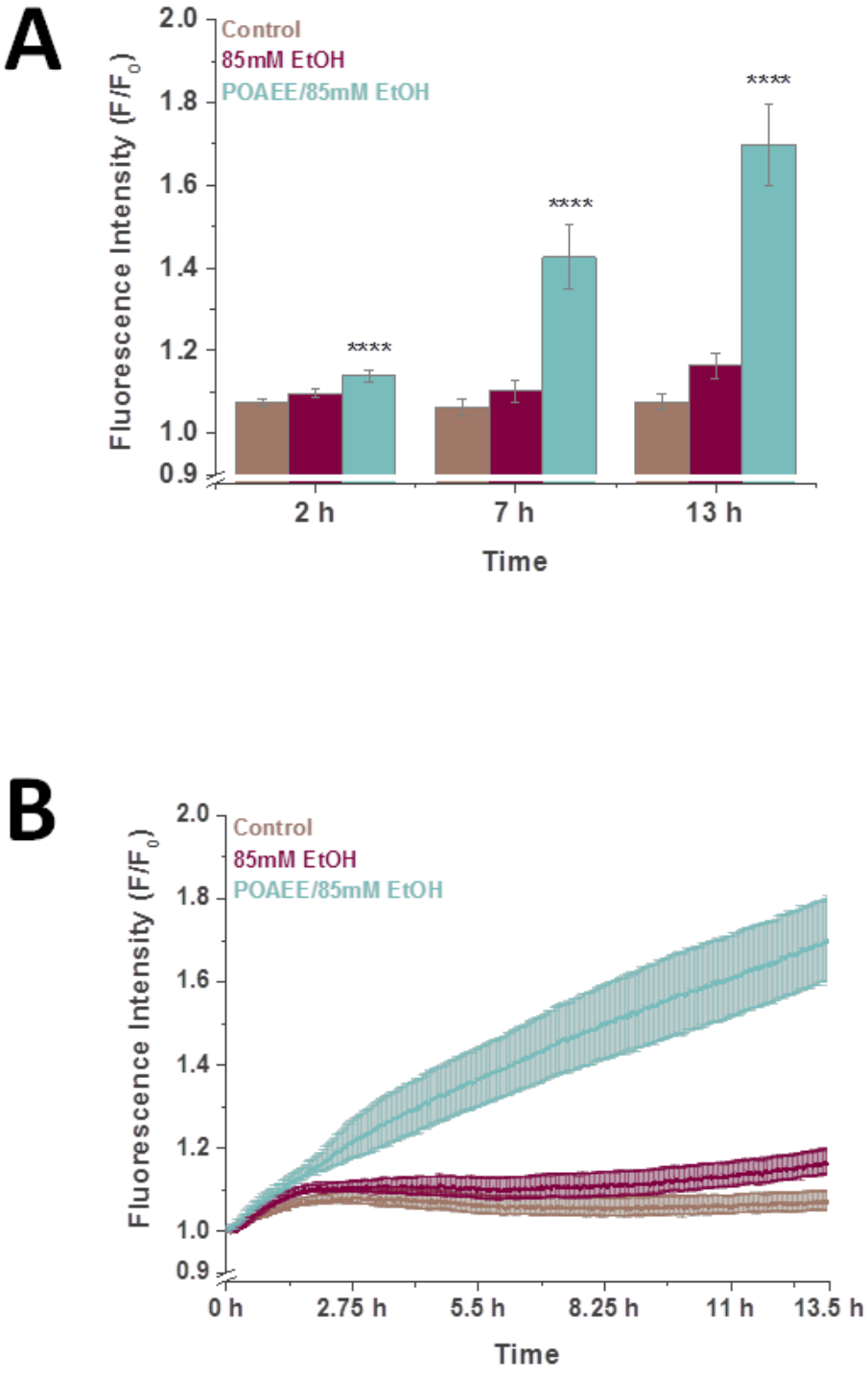

Figure 4.24. POAEE-induced necrosis. PI loaded cells were treated with 100µM POAEE solubilised in 85mM ethanol. The data has been normalised to the initial fluorescence reading t=0 expressed as F/F_0. **(A)** Bar chart representative of time points, **(B)** Line graph presentation of 100µM POAEE induced apoptosis with 85mM EtOH and EtOH alone. Traces are averages of >9 animals. All data shown are mean ±SEM. **** p<0.0001.

Figure 4.25

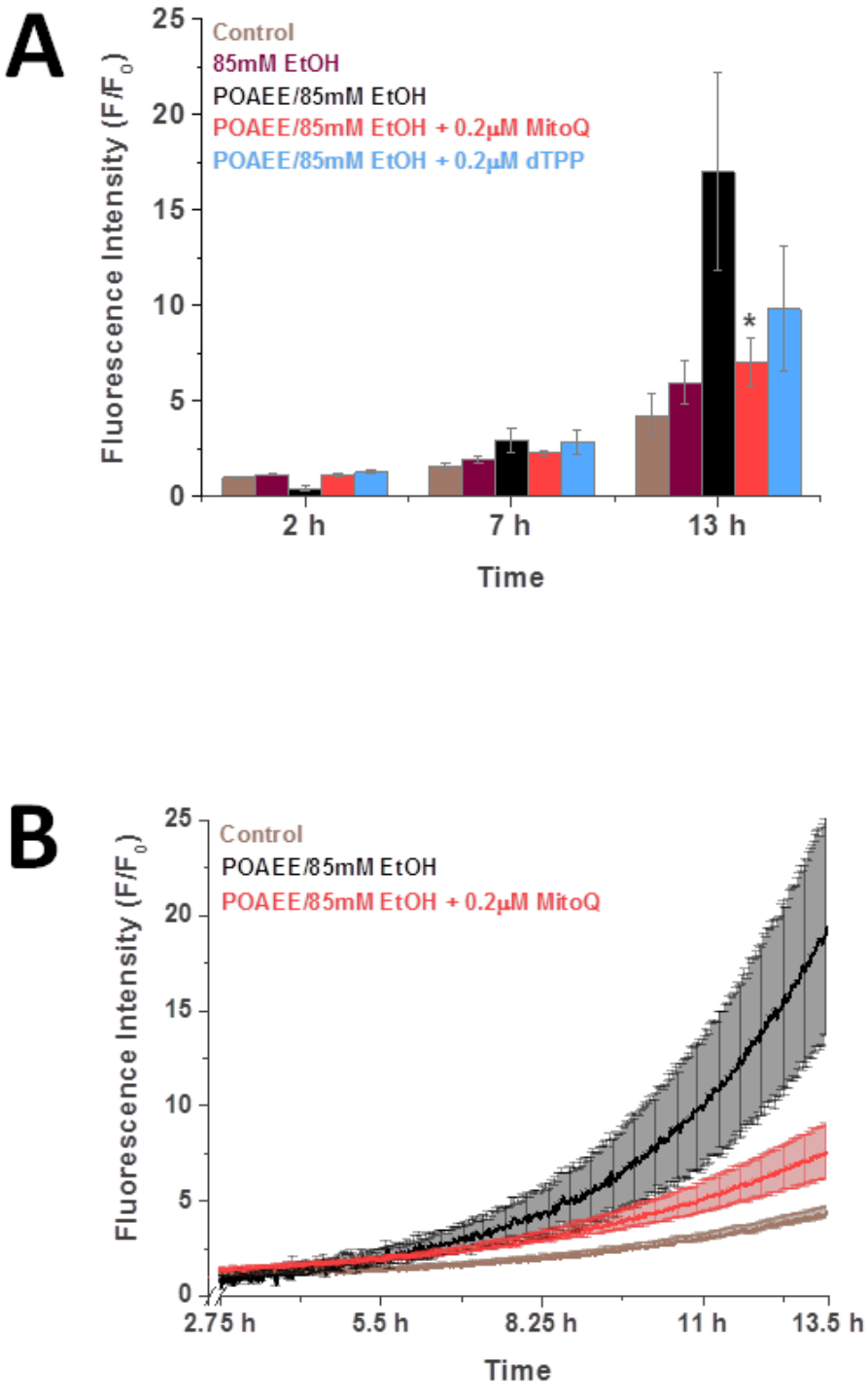

Figure 4.25. MitoQ concentration-dependent inhibition of 100 µM POAEE/85mM ethanol-induced apoptosis. Caspase-3/7 reagent loaded cells were pre-treated for 30 minutes with either 0.2µM MitoQ or 0.2µM dTPP prior to treatment with 100µM POAEE/85mM ethanol. The data has been normalised to the initial fluorescence reading t=0 expressed as F/F_0. **(A)** Bar graph presentation of 100µM POAEE/85mM EtOH with 1µM MitoQ and 1µM dTPP, **(B)** Line graph presentation of 100µM POAEE/85mM EtOH with 1µM MitoQ. Traces are averages of >9 animals. All data shown are mean ±SEM. * $p<0.05$.

Figure 4.26

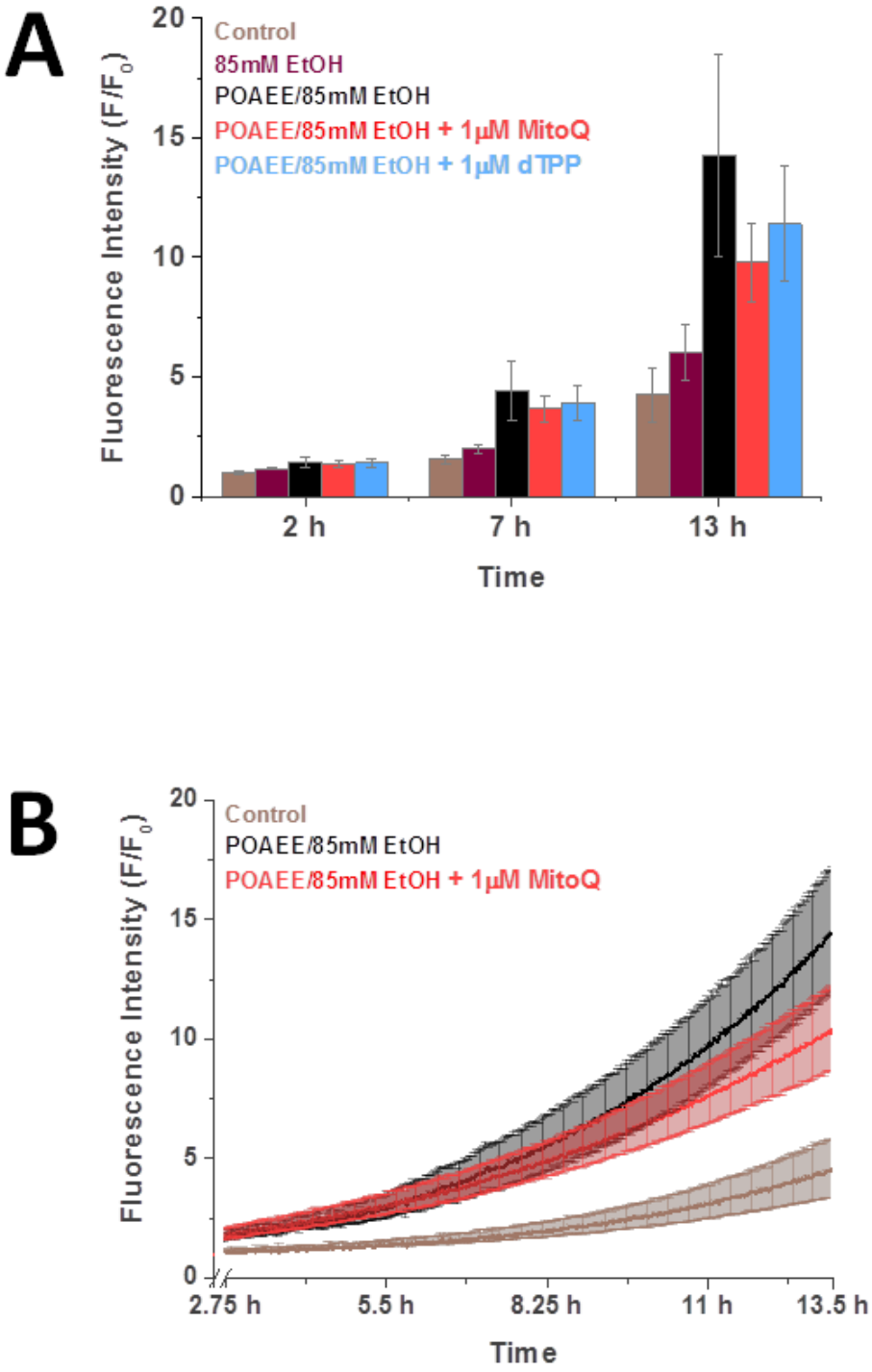

Figure 4.26. MitoQ (1µM) had no effect on 100 µM POAEE/85mM ethanol-induced apoptosis. Caspase-3/7 reagent loaded cells were pre-treated for 30 minutes with either 1µM MitoQ or 1µM dTPP prior to treatment with 100µM POAEE/85mM ethanol. The data has been normalised to the initial fluorescence reading t=0 expressed as F/F_0. **(A)** Bar graph presentation of 100µM POAEE/85mM EtOH with 1µM MitoQ and 1µM dTPP, **(B)** Line graph presentation of 100µM POAEE/85mM EtOH with 1µM MitoQ. Traces are averages of >9 animals. All data shown are mean ±SEM.

Figure 4.27

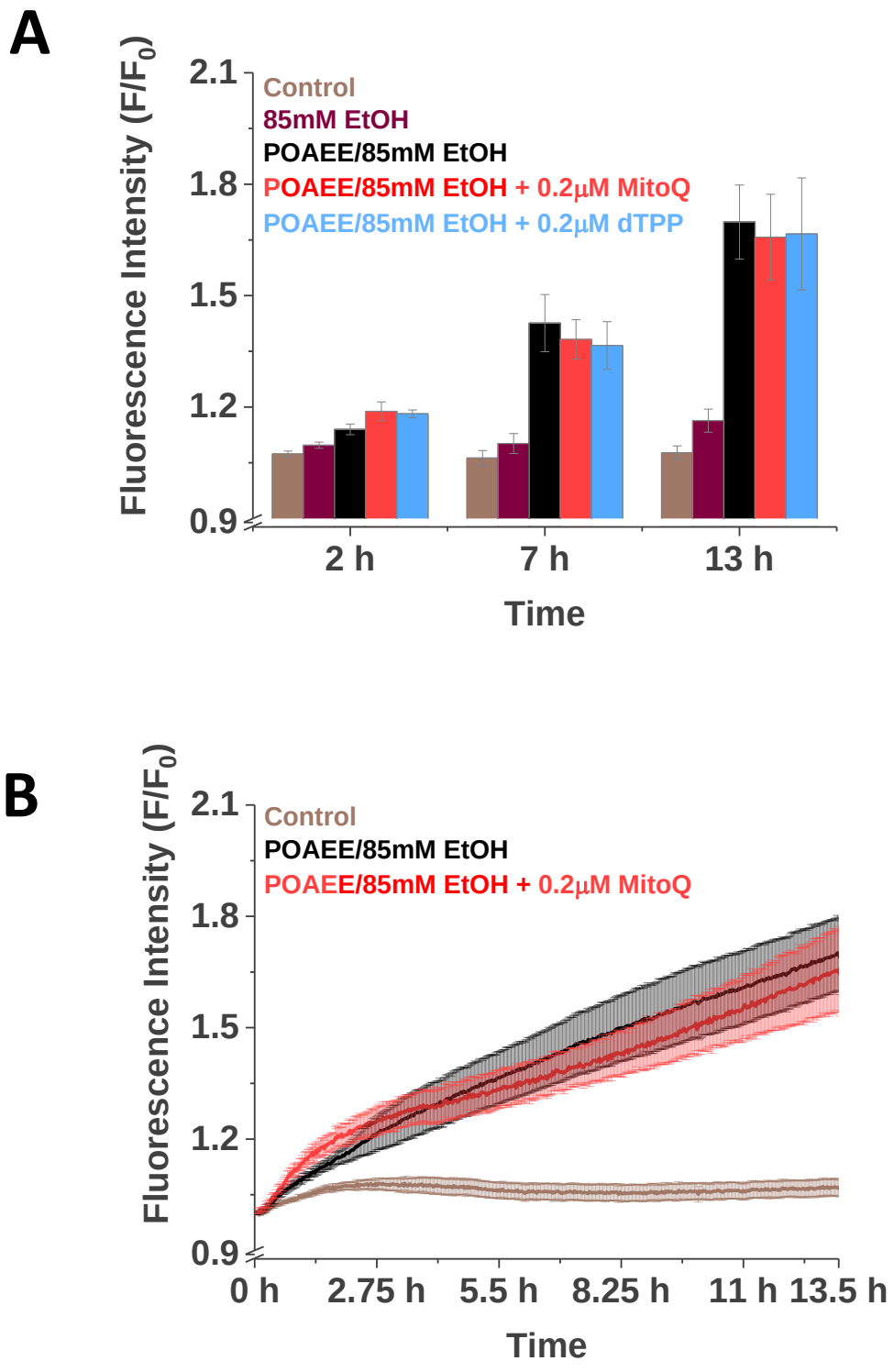

Figure 4.27. MitoQ (0.2μM) did not protect against 100 μM POAEE/85mM ethanol-induced apoptosis. PI loaded cells were pre-treated for 30 minutes with 0.2μM or 1μM MitoQ prior to treatment with 100μM POAEE/85mM ethanol. The data has been normalised to the initial fluorescence reading t=0 expressed as F/F_0. **(A)** 0.2μM MitoQ bar graph presentation and **(B)** 0.2μM MitoQ line graph presentation. Traces are averages of >9 animals. All data shown are mean ±SEM.

Figure 4.28

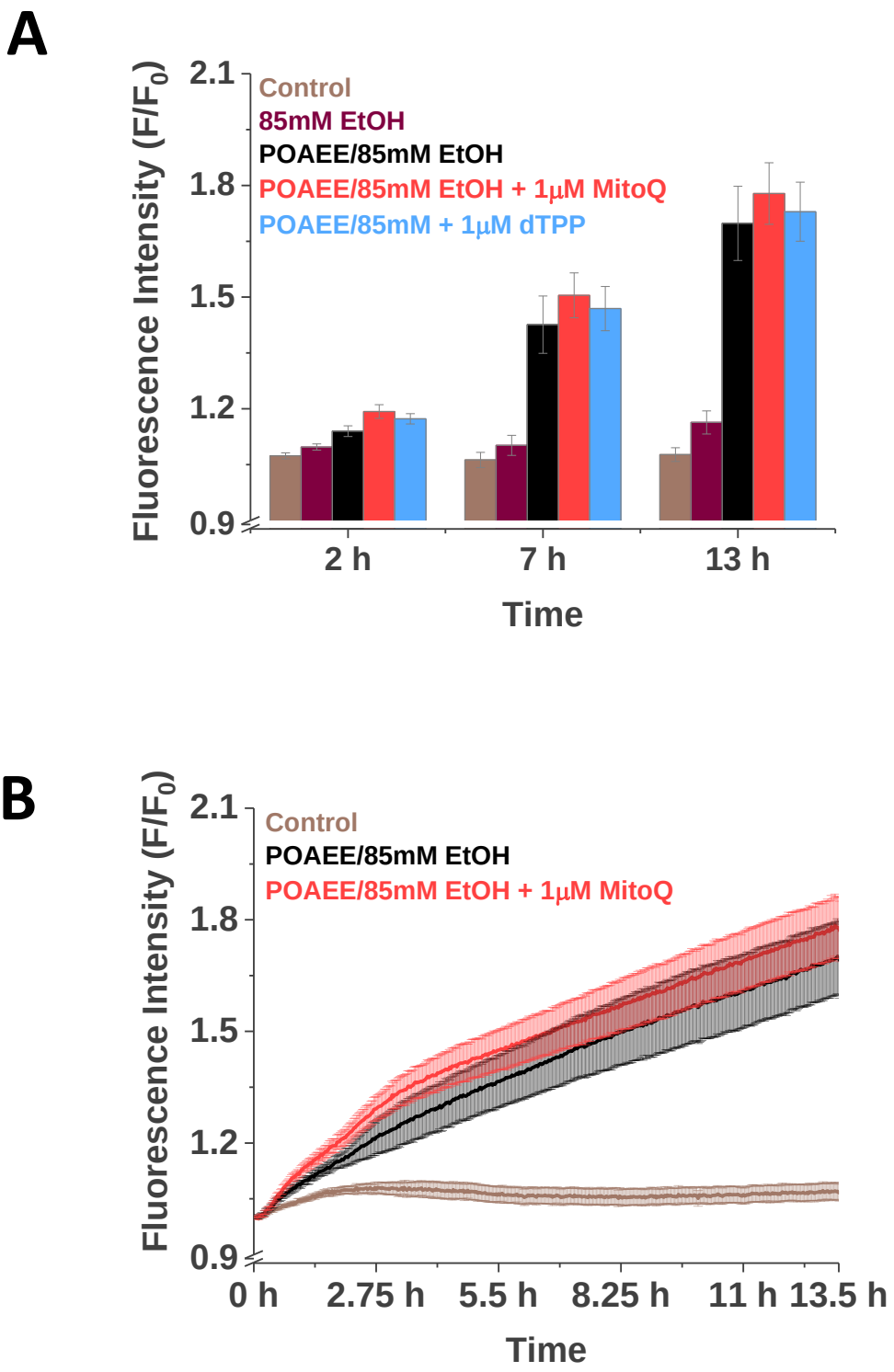

Figure 4.28. MitoQ (1µM) did not protect against 100 µM POAEE/85mM ethanol-induced necrosis. PI loaded cells were pre-treated for 30 minutes with 1µM MitoQ prior to treatment with 100µM POAEE/85mM ethanol. The data has been normalised to the initial fluorescence reading t=0 expressed as F/F_0. **(A)** bar chart and **(B)** line graph presentation. Traces are averages of >9 animals. All data shown are mean ±SEM.

Figure 4.29

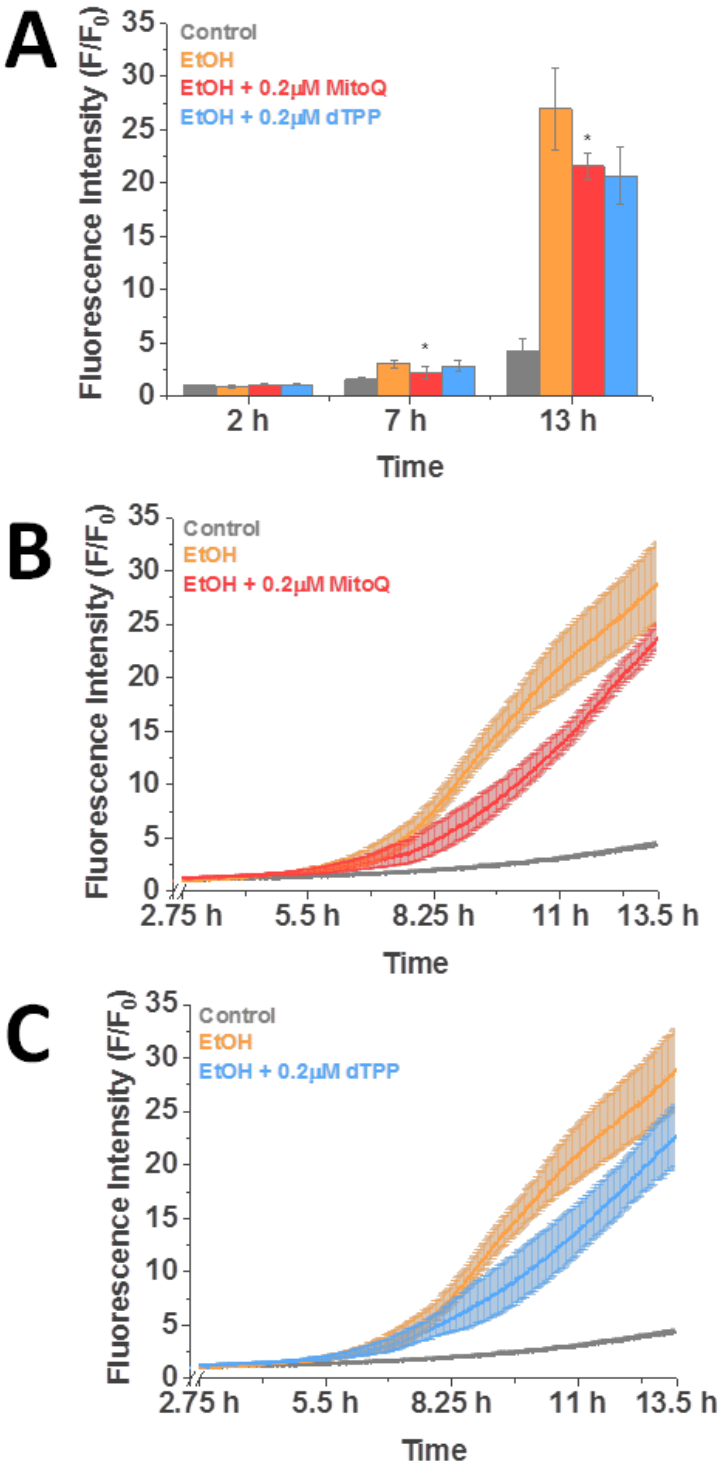

Figure 4.29. MitoQ concentration-dependent inhibition of EtOH-induced apoptosis. Caspase-3/7 reagent loaded cells were pre-treated for 30 minutes with either 0.2µM MitoQ or 0.2µM dTPP prior to treatment with 850mM ethanol. The data has been normalised to the initial fluorescence reading t=0 expressed as F/F_0. **(A)** Bar graph presentation of 850mM EtOH with 1µM MitoQ and 1µM dTPP, **(B)** Line graph presentation of 850mM EtOH with 1µM MitoQ ad **(C)** 1µM dTPP. Traces are averages of >9 animals. All data shown are mean ±SEM. * $p<0.05$.

Figure 4.30

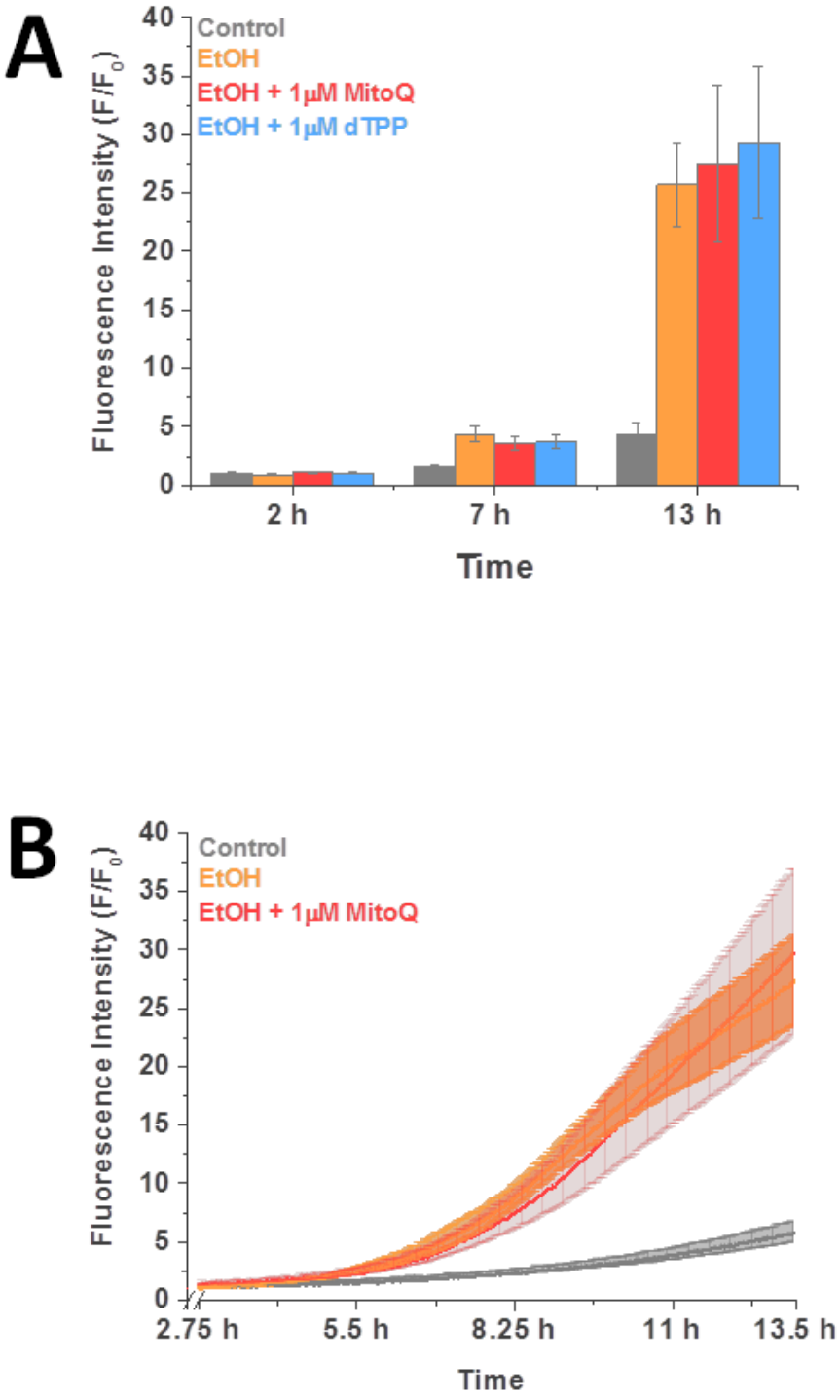

Figure 4.30. MitoQ (1µM) had no effect on EtOH-induced apoptosis. Caspase-3/7 reagent loaded cells were pre-treated for 30 minutes with either 1µM MitoQ or 1µM dTPP prior to treatment with 850mM ethanol. The data has been normalised to the initial fluorescence reading t=0 expressed as F/F_0. **(A)** Bar graph presentation of 850mM EtOH with 1µM MitoQ and 1µM dTPP, **(B)** Line graph presentation of 850mM EtOH with 1µM MitoQ. Traces are averages of >9 animals. All data shown are mean ±SEM.

Figure 4.31

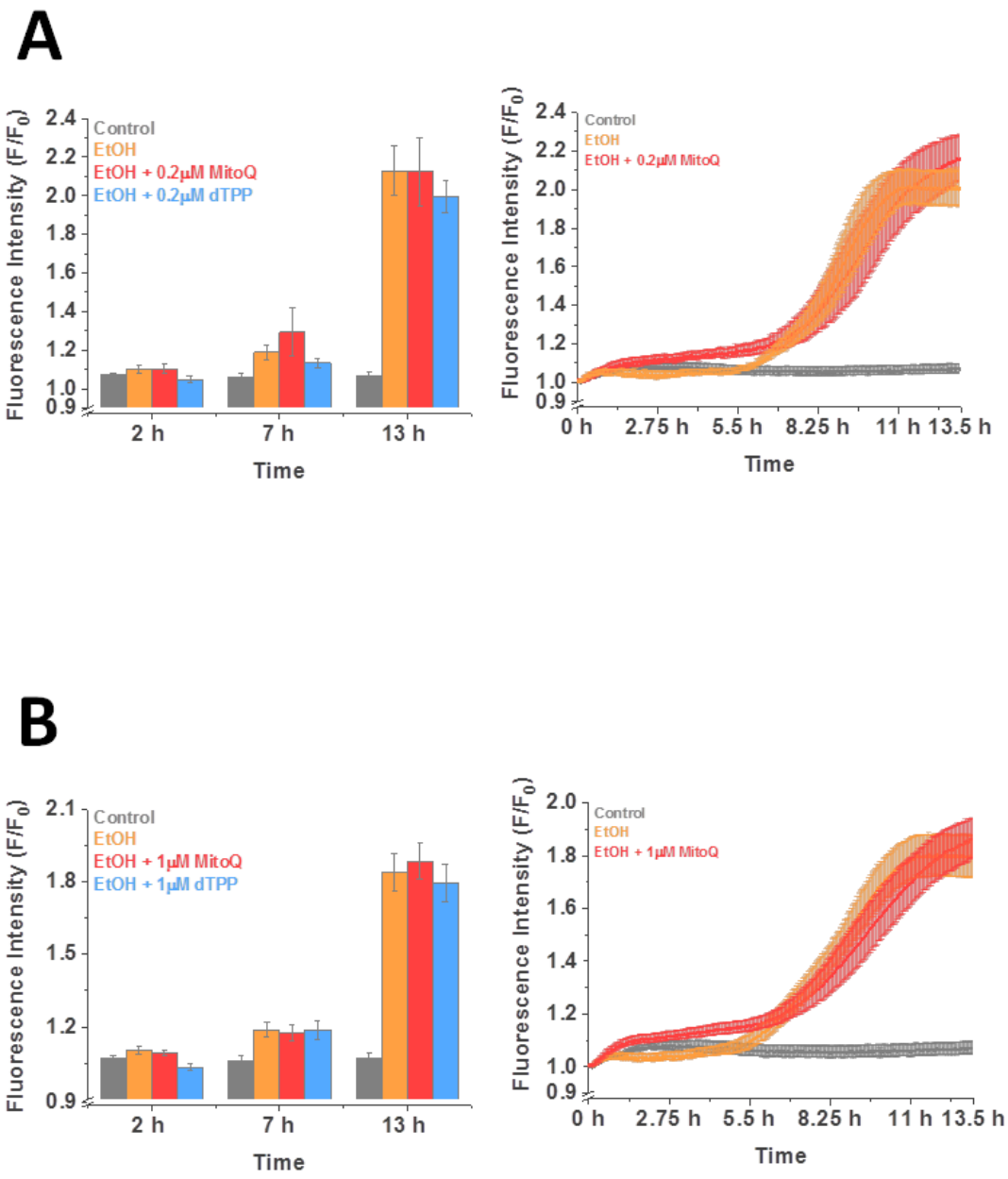

Figure 4.31. MitoQ did not protect against 850mM ethanol-induced necrosis. PI loaded cells were pre-treated for 30 minutes with 0.2µM or 1µM MitoQ prior to treatment with 850mM ethanol. The data has been normalised to the initial fluorescence reading t=0 expressed as F/F_0. **(A)** 0.2µM MitoQ bar and line graph presentation **(B)** 1µM MitoQ bar and line graph presentation. Traces are averages of >9 animals. All data shown are mean ±SEM.

Discussion

Our study has evaluated, *in vitro,* the protective capabilities of MitoQ against CCK- and TLCS-induced toxic effects to compliment work performed with *in vivo* models of experimental AP (Huang et al. 2015). Additionally, non-oxidative ethanol metabolite POAEE and ethanol were included. Previous preclinical evaluations of antioxidants in AP models have produced mixed results, with unsuccessful translation to the clinic thus far (Virlos et al. 2003; Bjelakovic et al. 2007; Siriwardena et al. 2007; Bansal et al. 2011). The effects of targeted antioxidants, such as MitoQ, have not been investigated in hyperstimulation, bile acid and non-oxidative metabolite models of AP *in vitro* and *in vivo*.

Bile Acid-Induced Toxic Effects

Previously our group has shown that in isolated PACs, 200µM TLCS induced small Ca^{2+} elevations of an oscillatory nature in the perigranular mitochondrial region (Petersen and Tepikin, 2008) and 500µM TLCS induced sustained elevations of $[Ca^{2+}]_C$ and $[Ca^{2+}]_M$ alongside a decline in NAD(P)H and ATP levels (Voronina et al. 2004; Voronina et al. 2010). MitoQ inhibited TLCS- (200µM) induced apoptosis in end point experiments (30 minutes), which could indicate a protective role for ROS in these cells (Booth et al. 2011). TLCS (200µM) did not elicit detectable ROS increases until a dose of 500µM in DCFDA loaded cells or with inhibition of NQO1. These ROS elevations were abolished in cells pre-treated with L-BAPTA and $0Ca^{2+}$ in

the extracellular media, which indicated Ca^{2+}-dependent ROS increases. It is likely that there are ROS increases with 200µM TLCS, which are not detected by H_2DCFDA due to a lack of sensitivity to mild oxidative stress. MitoQ demonstrated improved effectiveness against 200µM TLC-induced apoptosis, indicating a role of ROS in the TLCS-induced apoptosis. Application of 500µM TLCS in our experiments predominantly resulted in a necrotic mechanism of cell death in isolated PACs which supports the study by Booth et al. (2011). Antioxidant pre-treatment with MitoQ (1µM) did not protect against TLCS- (500µM) induced apoptosis over long time course experiments (13 hours). This contradicts data published by Booth et al. (2011) demonstrating concentration-dependent induction of apoptosis with TLCS (200 and 500µM) and the ability of MitoQ (1µM) to inhibit 200µM TLCS-induced effects in end point experiments (30 minutes). The confocal method employed by Booth et al. (2011) has a higher level of sensitivity, enabling single cell observations in contrast to a population, as analysed using the plate reader method. The lower concentration of 200µM TLCS applied by the authors induced proportionally less total cell death than with 500µM treatment (38% to 63.9%). While 500µM TLCS caused a near negligible increase in apoptosis in comparison to 200µM (2%), the percentage of cells which underwent necrosis increased by 23.9%. The improved sensitivity of the method in short time point experiments enabled the demonstration of early inhibition of apoptosis by MitoQ; an inhibition which the plate reader experiments demonstrate is not present in longer term experiments.

MitoQ (1µM) showed mild inhibition of TLCS induced necrosis at the 1 h time point, an effect which was abolished when pre-treating at higher concentrations of 5µM MitoQ. MitoQ (1µM) also did not protect against other TLCS-induced effects such as induction of ROS production and membrane depolarisation. The lack of protection provided *in vitro* is mirrored in our *in vivo* study with murine biliary experimental model of AP, TLCS-AP (Huang et al. 2015). Results obtained *in vitro* were again complex, with TLCS-AP not alleviated by treatment with the mitochondria-targeted antioxidant.

Although no studies have directly measured oxidative stress in mouse TLCS-AP, elevated markers have been demonstrated in the pancreas and erythrocytes following pancreatic ductal taurocholate administration in rats (Telek et al. 1999; Rau et al. 2000; Yasar et al. 2002). The study of Rau and colleagues (Rau et al. 2000) indicated that whilst ROS might be mediators of tissue damage, their extracellular generation alone did not induce typical biochemical and morphological changes indicative of AP. A lack of a protective effect of MitoQ in the current TLCS-AP model would support this view. In contrast, non-targeted antioxidant NAC, prevented TLCS- and menadione-induced ROS increases in PACs (Criddle et al. 2006; Booth et al. 2011). NAC pre-treatment also reduced tissue necrosis, leukocyte infiltration, oedema, and haemorrhage in taurocholate-induced AP (Yagci et al. 2004). MitoQ has demonstrated several adverse effects, such as inhibitory effects on the ETC and mitochondrial membrane uncoupling (James et al. 2005; Plecitá-Hlavatá et al. 2009; Fink et al. 2012; Reily et al. 2013). Further reported adverse effects include the

capacity to increase glucose oxidation and reduce fat oxidation at doses that did not alter membrane potential (Fink et al. 2009), as well as enhanced NF-B activation and up-regulation of ICAM-1 expression (Mukherjee et al. 2007). MitoQ also showed redox-cycling properties similar to menadione at the level of complex I and caused superoxide production (Doughan et al. 2007).

Nevertheless, MitoQ has shown some effectiveness as an antioxidant in a number of studies, particularly against H_2O_2-induced ROS increases and apoptosis (Saretzki et al. 2003; Dhanasekaran et al. 2004; Ghosh et al. 2010; Chacko et al. 2011; Ng et al. 2014). Although not detected by CM-H_2DCFDA in our studies, MitoQ has demonstrated prooxidant capabilities in alternative cells types (O'Malley et al. 2006; Plecitá-Hlavatá et al. 2009), counteracting the beneficial antioxidant effects. Evidence from our studies and published literature indicate that the beneficial antioxidant capacity of MitoQ is effectively nullified by the adverse effects of the targeting component, such as mild uncoupling and ETC inhibition (James et al. 2005; Plecitá-Hlavatá et al. 2009; Fink et al. 2012; Reily et al. 2013; Trnka et al. 2015). The inhibitory mechanisms of MitoQ on the ETC as demonstrated in alternative cell types have yet to be investigated in PACs and could be assessed in comparison to known ETC complex inhibitors such as complex I inhibitor rotenone.

CCK Hyperstimulation-Induced Toxic Effects

A pivotal study demonstrated that the application of 1µM MitoQ during ongoing $[Ca^{2+}]_i$ oscillations evoked by physiological concentrations of CCK, resulted in a clear inhibition. The inhibition of Ca^{2+} oscillations was demonstrated alongside a reduction of CCK-induced ROS increases (Camello-Almaraz et al. 2006). Non-targeted antioxidants ubiquinone and SOD mimic MnTBAP also inhibited 10pM CCK-induced $[Ca^{2+}]_i$ oscillations, supporting a ROS-dependent Ca^{2+} mobilisation. Although MitoQ had the capacity to inhibit $[Ca^{2+}]_i$ oscillations in the study by Camello-Almaraz et al. (2006), there was no effect on the maximal $[Ca^{2+}]_i$ response to CCK hyperstimulation. In contrast, MitoQ pre-treated cells exhibited a complete inhibition of CCK-induced NAD(P)H increases, which has been previously attributed to increases in cytosolic and mitochondrial Ca^{2+} (Hajnoczky et al. 1995; Voronina et al. 2010). This removal of the NAD(P)H increases is also seen in cells with dTPP control treatment. Therefore it is likely that the targeting component of both compounds is interfering with CCK induced NAD(P)H responses in the mitochondria, independent of antioxidant decreases in ROS. The targeting component of MitoQ could be having non-specific effects on mitochondrial Ca^{2+} uptake and therefore abolishing NAD(P)H increases. Another theory would be that the mild uncoupling properties of the targeting component subsequently upregulate NAD(P)H consumption to fuel the ETC and maintain the $\Delta\Psi m$. This could effectively nullify upregulation of NAD(P)H production by the TCA.

In HeLa cells the TPP^+ moiety has demonstrated inhibitory effects on the mitochondrial Na^+/Ca^{2+} exchanger, which resulted in accumulation of Ca^{2+} within the mitochondria following IP_3 receptor mediated Ca^{2+} release into the cytosol (Leo et al. 2008). Our preliminary results with Rhod-2 do not support a mitochondrial accumulation of Ca^{2+}, although this could be a lack of sensitivity of Rhod-2 to very small increases. The inhibition of NAD(P)H increases was not reflected in any detectable prevention of CCK-induced mitochondrial membrane depolarisation.

CCK at physiological and hyperstimulatory concentrations has opposite effects to TLCS on ATP levels. CCK can induce accelerated mitochondrial ATP production and consumption, in comparison to ATP depletion induced by TLCS (Voronina et al. 2010). It was anticipated that MitoQ might inhibit CCK-induced apoptosis due to a demonstrated inhibition of CCK-induced ROS production, a known apoptosis inducer (Camello-Almaraz et al. 2006; Booth et al. 2011). However, MitoQ and dTPP (and TPP^+ in certain experiments) had little effect on apoptosis and worsened CCK-induced necrosis. More specifically, at the 2 h time point MitoQ exacerbated CCK-induced apoptosis but not at the later time points presented (7 h and 13 h). MitoQ also no longer exacerbates CCK-induced necrosis at 13 h in comparison to the CCK treated group. The large confidence interval at 13 h suggests a large population variance, which may give an imprecise effect size at this time point. The presence of exacerbated necrosis with MitoQ, dTPP and TPP^+ would indicate a TPP^+ derivative-induced mechanism via mild uncoupling, decrease in CCK

induced NAD(P)H and ATP production necessary for apoptosis (Nicotera et al. 1998; Gukovskaya et al. 2004; Criddle et al. 2007).

The complimentary *in vivo* work (Huang et al. 2015), supported our CCK and TLCS cell death observations. The milder pathology induced by caerulein in the CER-AP model is reflected by a substantial induction of both apoptosis and necrosis *in vitro*. In contrast, TLCS-AP elicits a severe pathology and predominantly necrotic path of cell death in the absence of substantial apoptosis, as a protective mechanism. *In vivo* investigations indicated some protective actions of MitoQ evident in the CER-AP model, although effects were variable and shared by the non-antioxidant moiety control dTPP. MitoQ partially protected against the severity of CER-AP as assessed by pancreatic histopathology, but without a significant reduction of pancreatic necrosis or apoptosis. No reduction of serum amylase or pancreatic trypsin was evident, whilst MitoQ concurrently elevated systemic injury markers such as lung MPO activity and serum IL-6. In addition, dTPP significantly improved overall and individual pancreatic histopathology scores, decreased pancreatic trypsin, and reduced pancreatic MPO activity. Currently the explanation for any beneficial effect of dTPP is unclear, but some deleterious effects of MitoQ may have resulted from the antioxidant activity.

POAEE and Ethanol Effects on Pancreatic Acinar Cell Death

PACs provide the main source of ethanol metabolism in the pancreas via both the oxidative metabolic pathway, involving alcohol dehydrogenase (ADH), and non-oxidative pathways. Non-oxidative metabolism leads to the production of diverse FAEEs, such as POAEE, from the reaction of alcohol with fatty acids. FAEEs including POAEE can be detected in patient serum levels following ethanol ingestion (Bjelakovic et al. 2007) and are produced by FAEE synthases, diverse enzymes under characterisation, including carboxylester lipase (CEL) and triglyceride lipase (Wilson et al. 2003).

FAEEs have been implicated in acute pancreatitis alongside mitochondrial dysfunction, Ca^{2+}-dependent mitochondrial inhibition leading to loss of NAD(P)H, decreases in ATP and increased necrosis (Lange et al. 1983; Sztefko et al. 2001; Criddle et al. 2006; Voronina et al. 2010; Ng et al. 2014). Inhibition of FAEE synthase prevents these cytosolic Ca^{2+} increases and associated mitochondrial dysfunction (Huang et al. 2014). While non-oxidative metabolite POAEE-induced a decrease in ATP in PACs, ethanol (200mM) failed to generate measurable changes. TLCS and fatty acid POA also induced these changes whereas CCK did not, a major contributing factor to the more damaging effects of these compounds *in vivo* as well as *in vitro*. It is believed that the CCK-induced increase in ATP production is a protective mechanism against Ca^{2+}-induced loss of energy (Voronina et al. 2004; Voronina et al. 2010). FAEEs have also been reported to elicit premature activation

of proteases and lipases resulting in digestion of cellular structures (Haber et al. 1993) and activation of NF-κB, leading to the expression of a variety of inflammatory mediators (Gukovskaya et al. 2002). Oxidative metabolism of ethanol may also provide minor contributions to the development of AP via oxidative stress, as shown in rat pancreatic tissue (Altomare et al. 1996)

Ethanol (1-50mM) is known to impair CCK induced ROS generation and amylase secretion (González et al. 2006; Fernandez-Sanchez et al. 2009) inhibited by antioxidant cinnamtannin B-1 (Del Castillo-Vaquero et al. 2010). Treatment with 850mM ethanol induced only very small transient elevations in cytosolic Ca^{2+} in comparison to ACh (10µM), whereas POAEE (100µM) elicited substantial Ca^{2+} increases (Criddle et al. 2004). In contrast, 850mM EtOH is substantially greater than the range of blood alcohol levels in intoxicated humans (< or = 100 mmol/L) which induces DNA alterations (Lamarche et al. 2004). The reason for these results is that the toxic effects of alcohol are predominantly caused by non-oxidative metabolites fatty acids and fatty acid ethyl esters. Previously, our group has shown that exogenous application of POAEE caused significant cell death and low level ethanol/POA (10mM/20µM) demonstrated elevated toxicity during inhibition of oxidative ethanol metabolism (Huang et al. 2014). The low level/POA results were mirrored *in vivo* with elevated disease biochemical markers and development of pancreatic necrosis, oedema and neutrophil infiltration. These changes are consistent with those observed post FAEE administration in rats (Werner et al. 1997) or intravenous ethanol under inhibition of oxidative metabolism of ethanol (Werner et al. 2001).

The short term effects of ethanol on intracellular Ca^{2+} appear small (Criddle et al. 2004). Within several hours of ethanol infusion in rats, trypsinogen activation, pancreatic oedema, and pancreatic acinar cell apical vacuolization appear (Werner et al. 2002). These changes are associated with the formation of FAEEs within the pancreas (Werner et al. 2002; Lamarche et al. 2004). The use of ethanol in combination with POAEE has clinical parallels with intoxicated human blood FAEE concentrations, reported up to 50µM mirrored by the concentration of ethanol (Laposata et al. 1986; Werner et al. 1997; Soderberg et al. 2003). Ethanol and POAEE studies indicate that alcohol-induced toxic effects are predominantly FAEE driven. This is of great clinical relevance in an organ with dominantly non-oxidative ethanol metabolism.

Levels of cellular apoptosis and necrosis induced by high dose POAEE (100µM) solubilised in ethanol (85mM) were assessed. MitoQ pre-treatment was evaluated for any protective capabilities. Previous optimisation of our plate reader cell death experiments led to the addition of high molecular weight polyethylene glycol (PEG) alongside ethanol to ensure effective POAEE solubilisation over the long time point experiments. POAEE (100µM) induced a substantial increase in apoptosis and necrosis in comparison to both 85mM EtOH alone and NaHEPES. These results support observations that FAEEs elicit more damaging effects than ethanol alone (Werner et al. 1997; Ammann 2001; Werner et al. 2001; Huang et al. 2014).

MitoQ effectively inhibited POAEE-induced apoptosis at 0.2µM but not 1µM in conjunction with concentration-dependent inhibition of 850mM EtOH-induced apoptosis. MitoQ did not exhibit the same protection against POAEE-induced apoptosis solubilised in 850mM EtOH (results not shown). These results could suggest a considerably greater ROS generation with high dose POAEE/EtOH and subsequent overloaded antioxidant capacity. These results support work produced by Fernandez-Sanchez et al. (2009) with antioxidant cinnamtannin B-1 highlighting a reduction both in 50mM EtOH-induced ROS production, an action that reverted the effect of ethanol on 1nM CCK-8 induced Ca^{2+} mobilization.

Conclusions

In conclusion, MitoQ demonstrated a lack of protective effects against toxin effects and concentration-dependent inhibition of POAEE-induced apoptosis. Inhibition of apoptosis is unlikely to be protective in clinical applications, as further supported by our CCK and TLCS apoptosis/necrosis comparisons.

Chapter 5

The Effects of H_2O_2 on Pancreatic Acinar Cells

In this chapter the comparative cellular effects of submillimolar and millimolar H_2O_2 on PACs and the protective capabilities of MitoQ were evaluated. These results are also briefly compared to the toxin-induced effects of CCK, POAEE and ethanol on levels of ROS and cell death.

The Cellular Effects of H_2O_2 on PACs

NAD(P)H and FAD^+ autofluorescence were measured simultaneously during treatment with micromolar concentrations of H_2O_2 (10µM, 30µM and 300µM H_2O_2). Pancreatic acinar cell suspensions were treated for 5 minutes with each compound prior to uncoupler CCCP. Preliminary data demonstrated concentration-dependent progressive effects on NAD(P)H and FAD^+ levels (Figure 5.1). Experiments investigating the effects of 1µM H_2O_2 demonstrated recovery of NAD(P)H levels in 55% of cells (5/9) during treatment (data not shown). High millimolar H_2O_2 treatment induced large irreversible changes to NAD(P)H and FAD^+ levels. H_2O_2 induced dose dependent effects on NAD(P)H/FAD^+ levels (Figure 5.2). MitoQ (1µM) exacerbated submillimolar H_2O_2 concentration-dependent effects on the NAD(P)H/FAD^+ with the main effects on levels of NAD(P)H. Although MitoQ induced a more rapid change to millimolar H_2O_2 effects, these were not significant beyond 3 minutes treatment with H_2O_2 (Figure 5.3). MitoQ pre-treatment also abolished 10mM H_2O_2-induced decline in NAD(P)H levels. dTPP exhibited non-specific effects different to those demonstrated with MitoQ treatment. These were a decrease in

FAD^+ levels with 10µM and 30µM H_2O_2 and dTTP abolished the uncoupling effect of CCCP (Figure 5.4).

Cell suspensions were loaded with the TMRM dye and treated with submillimolar 50µM and 500µM H_2O_2 for 10 minutes, per treatment, prior to the addition of CCCP. Both concentrations of H_2O_2 caused a progressive loss of ΔΨm exacerbated at the higher concentration of 500µM. A 4.1% decrease in TMRM fluorescence was induced with 50µM and a 12.4% decrease with 500µM compared to a final decrease with CCCP of 20.4% (Figure 5.5). Cytosolic Ca^{2+} was measured in cells loaded with Fluo-4 and the treated for 10 minutes with 50µM H_2O_2, 10 minutes with 500µM H_2O_2 and 5 minutes with uncoupler CCCP (10µM). Both 50µM and 500µM H_2O_2 induced increases in cytosolic Ca^{2+} (Figure 5.6). 50µM H_2O_2 treatment predominantly induced a progressive increase in $[Ca^{2+}]_c$, although 7% percent of cells exhibited a singular Ca^{2+} spike. 500µM H_2O_2 induced a large progressive increase in $[Ca^{2+}]_c$. 50µM and 500µM H_2O_2 induced a concentration-dependent ΔΨm depolarisation mirrored to the $[Ca^{2+}]_c$ elevation. NAD(P)H responses were more sensitive and the comparative decrease in NAD(P)H in response to H_2O_2 was more substantial in comparison to $[Ca^{2+}]_c$ and ΔΨm changes (Figure 5.7).

Figure 5.1

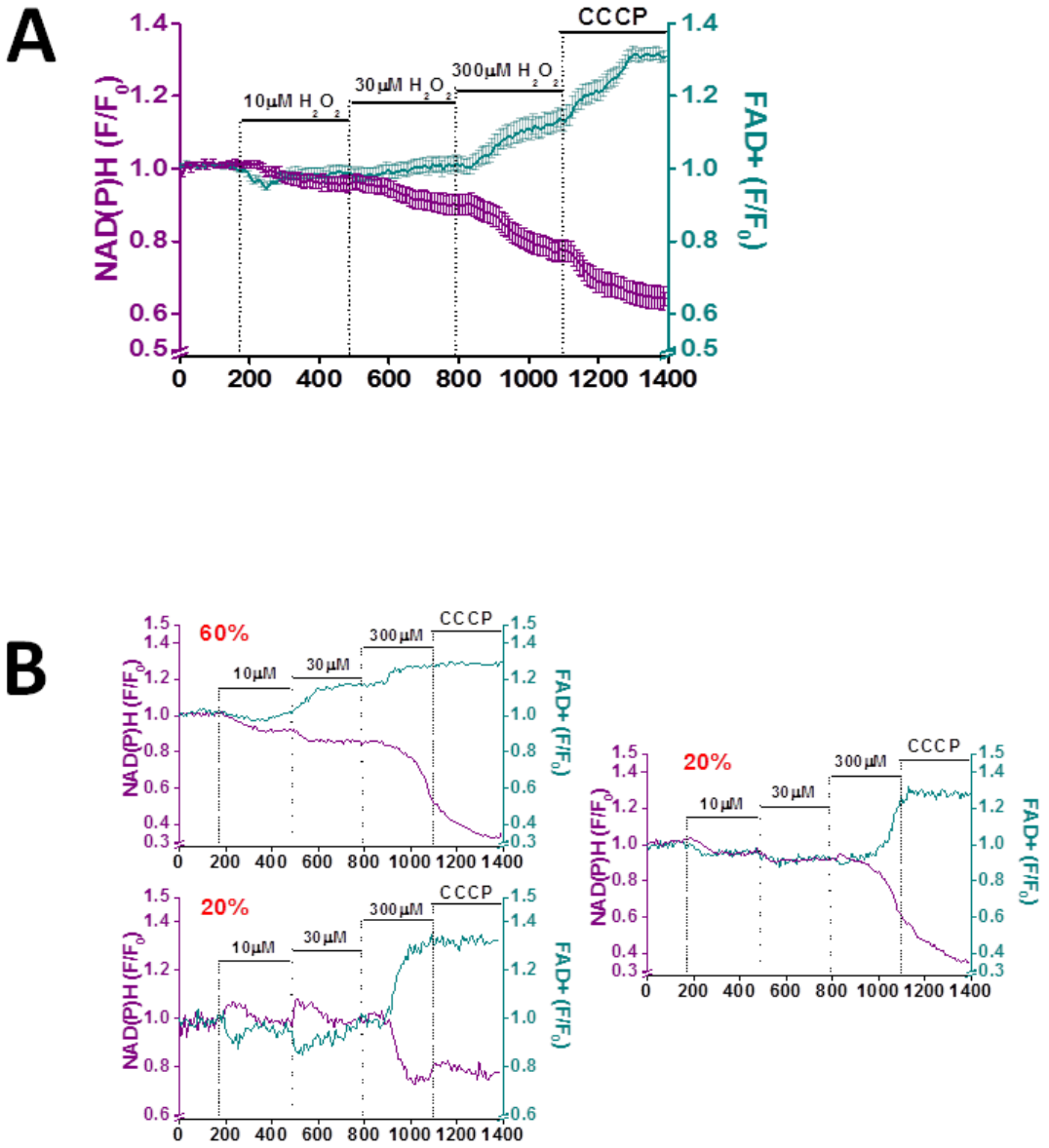

Figure 5.1. Concentration-dependent effects of H_2O_2 on the redox ratio. NAD(P)H and FAD^+ autofluorescence were measured simultaneously. **(A)** Treatment with 10µM, 30µM and 300µM H_2O_2. **(B)** Example traces of submillimolar H_2O_2 effects. Traces are averages of >34 cells from at least 3 animals. Data have been normalised to the initial fluorescence reading t=0 expressed as F/F_0. All data shown are mean ±SEM.

Figure 5.2

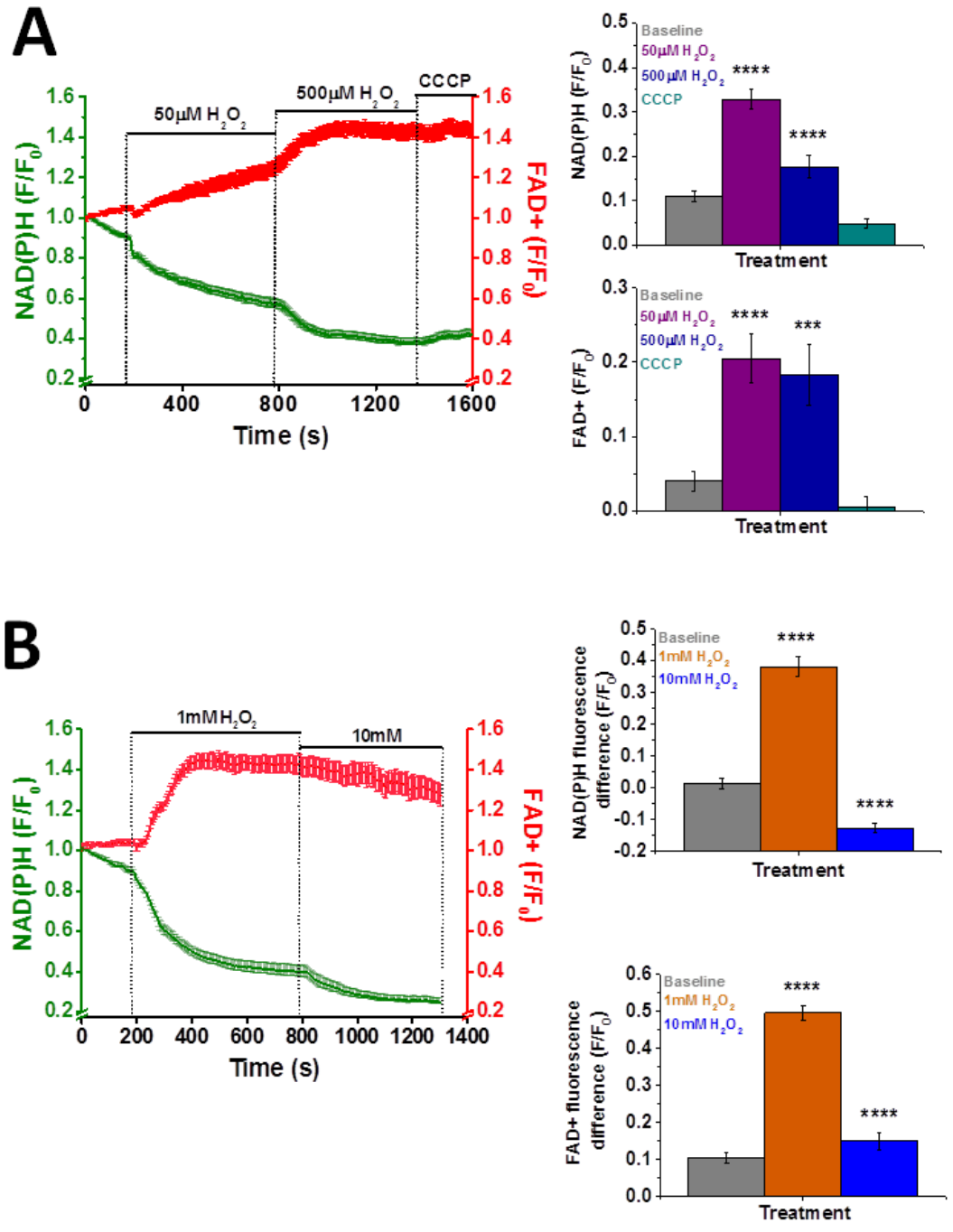

Figure 5.2. Submillimolar and millimolar H_2O_2-induced changes on NAD(P)H and FAD^+ levels. NAD(P)H and FAD^+ autofluorescence was measured simultaneously in acinar cells and treated for 10 minutes with **(A)** 50µM and 500µM H_2O_2 or **(B)** 1mM and 10mM. Line graph presentation of results. NAD(P)H and FAD^+ changes in fluorescence (F/F_0). A - Traces are averages of at least 44 cells and 4 animals. B – Control traces are averages of 34 cells and 2 mice and MitoQ pre-treated traces averages of 9 cells and 1 animal. Data has been normalised to the initial fluorescence reading t=0 expressed as F/F_0 . All data shown are mean ±SEM. *** p<0.001, **** p<0.0001.

Figure 5.3

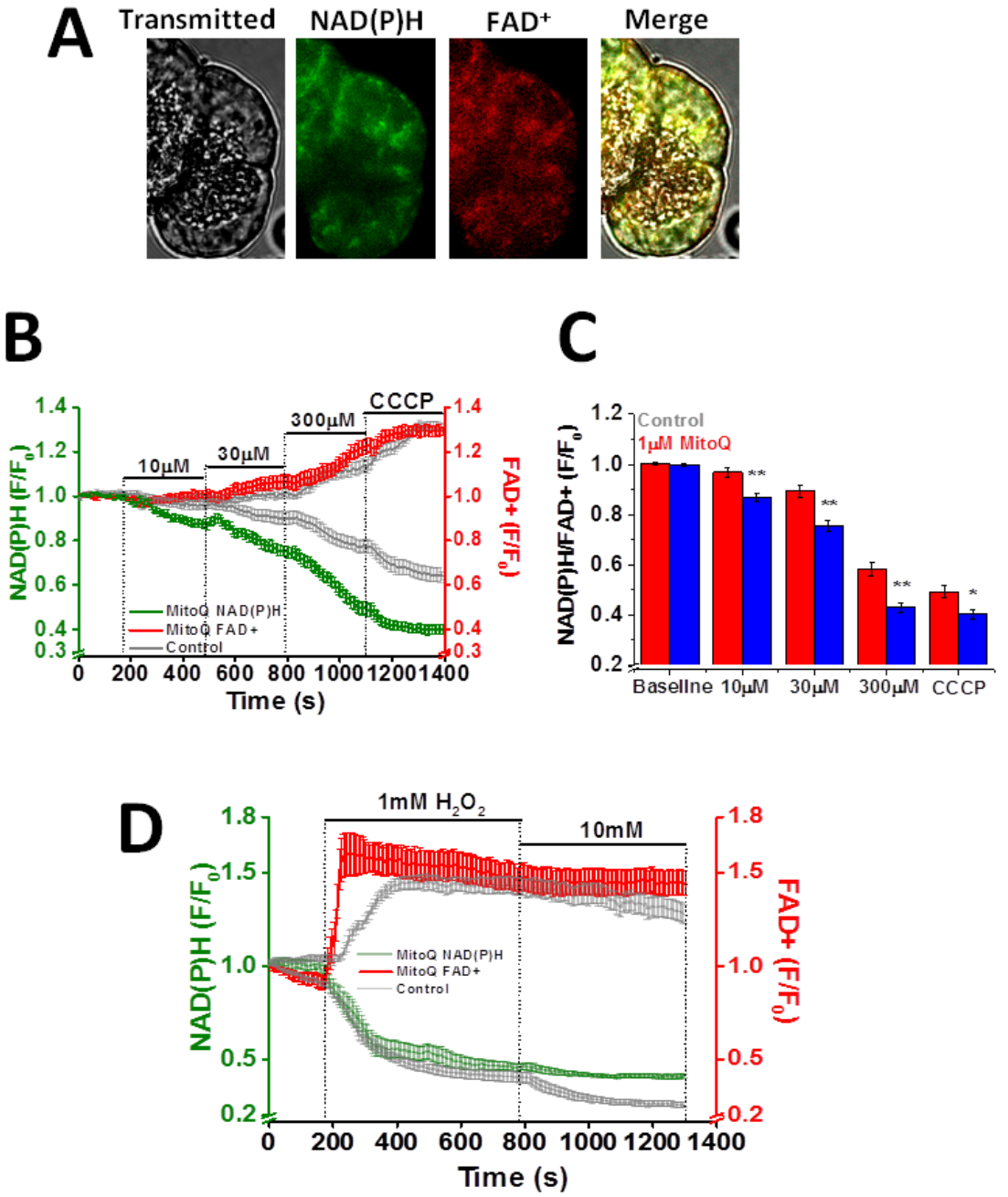

Figure 5.3. MitoQ exacerbates the concentration-dependent effects of H_2O_2 on the redox ratio. NAD(P)H and FAD^+ autofluorescence were measured simultaneously after a 30 minute pre-treatment with MitoQ (1µM) or NaHEPES. **(A)** Treatment with 10µM, 30µM and 300µM H_2O_2 **(B)** Bar chart presentation of NAD(P)H/FAD^+ ratio decreases with each treatment with and without MitoQ pre-treatment, **(C)** Treatment with 1mM and 10mM H_2O_2. Traces are averages of >34 cells from at least 3 animals (A). Control traces are an average of 34 cells from 2 animals and MitoQ pre-treated traces averages of 9 cells and 1 animal (B). Data has been normalised to the initial fluorescence reading t=0 expressed as F/F_0 . All data shown are mean ±SEM. * $p<0.05$, ** $p<0.01$.

Figure 5.4

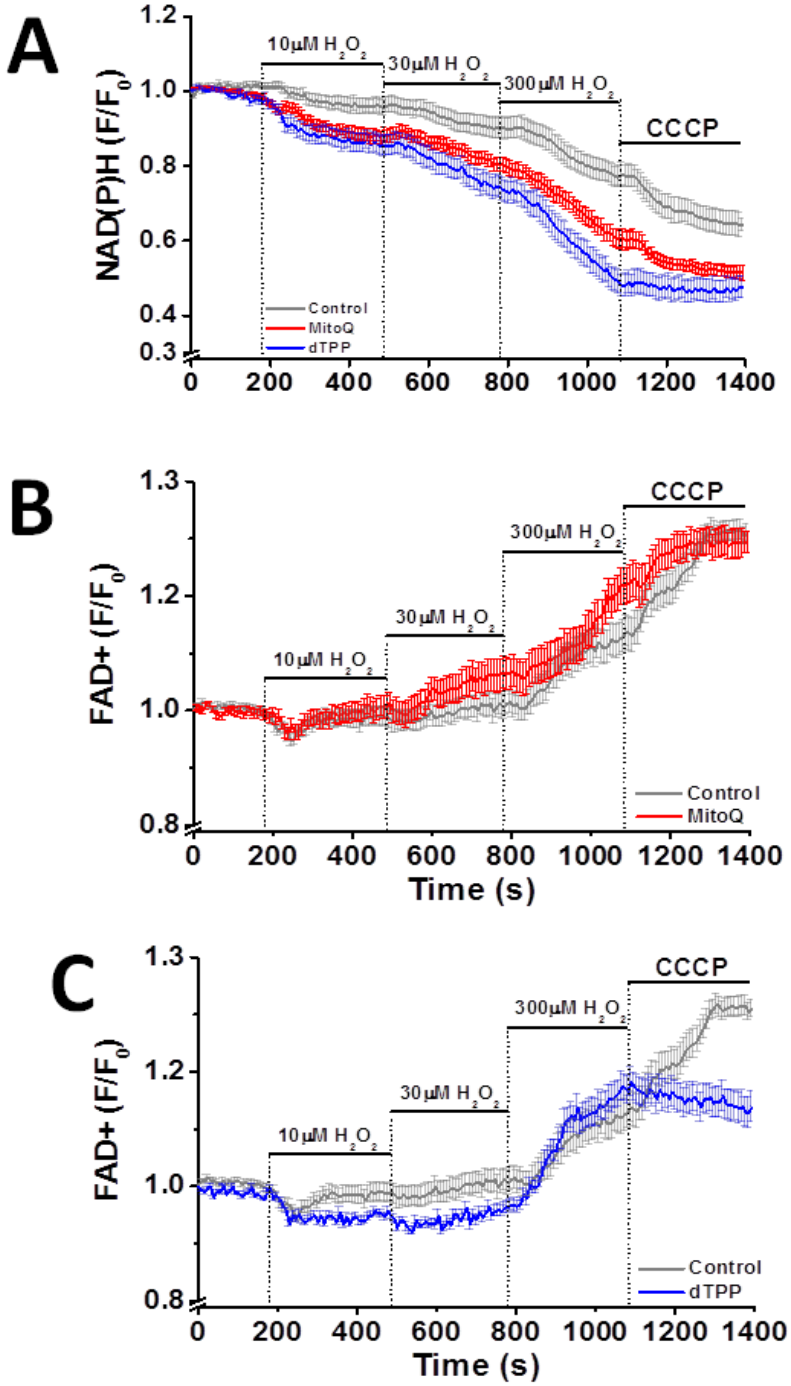

Figure 5.4. MitoQ and dTPP had differing effects on concentration-dependent H_2O_2 induced changes to NAD(P)H and FAD^+. Pancreatic acinar cells were pre-treated with 1µM MitoQ, 1µM dTPP or NaHEPES (control). NAD(P)H and FAD^+ autofluorescence were measured simultaneously **(A)** NAD(P)H with each treatment **(B)** FAD^+ with MitoQ (1µM) pre-treatment, (C) FAD^+ with dTPP (1µM) pre-treatment. Traces are averages of >34 cells from at least 3 animals. Data has been normalised to the initial fluorescence reading t=0 expressed as F/F_0 . All data shown are mean ±SEM.

Figure 5.5

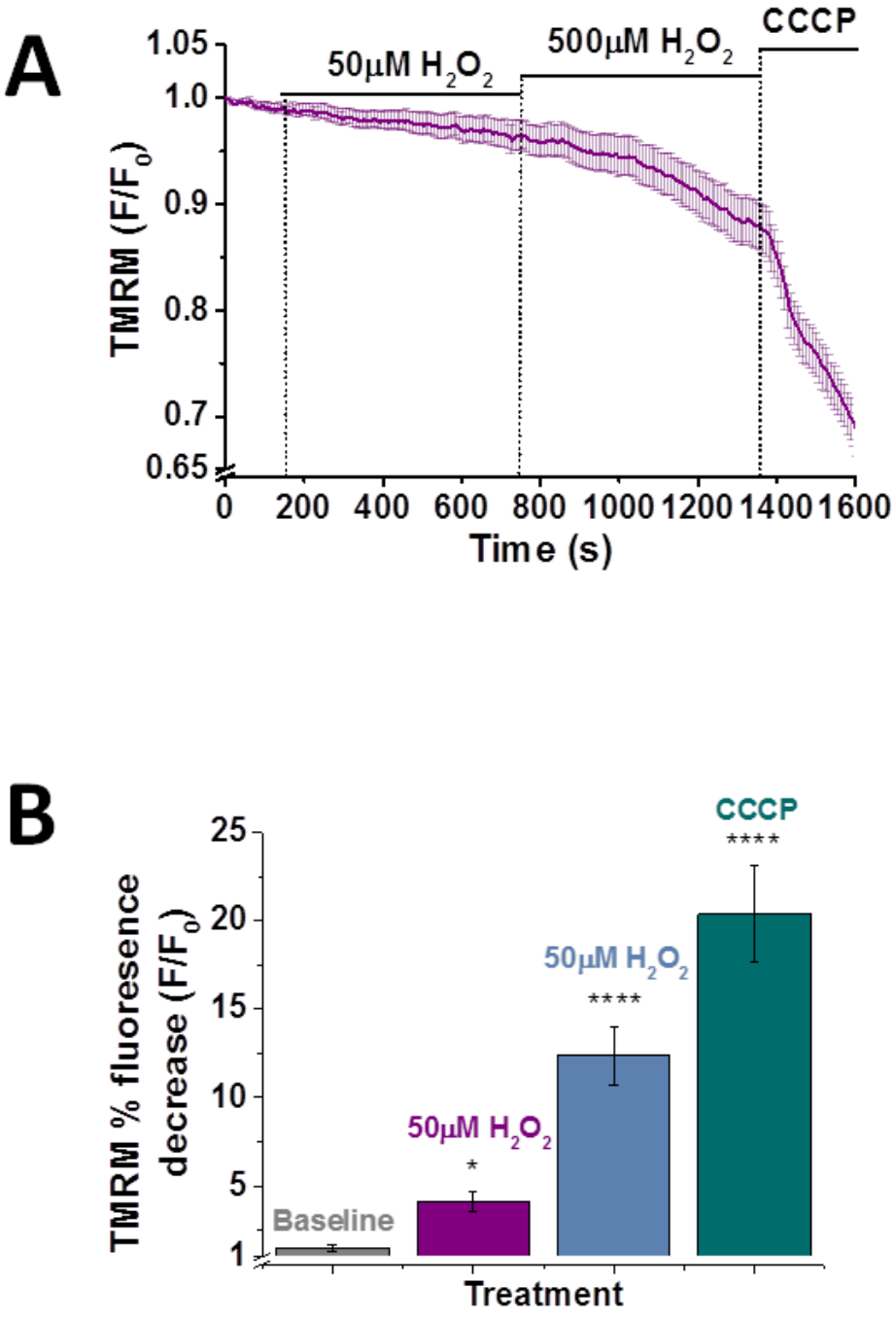

Figure 5.5. Submillimolar H_2O_2-induced loss of ΔΨm. Pancreatic acinar cell suspensions were treated for 10 minutes with 50µM H_2O_2, 10 minutes with 500µM H_2O_2 and 5 minutes with uncoupler CCCP (10µM). **(A)** Line graph presentation of results. **(B)** Bar chart presentation showing the percentage decrease in TMRM fluorescence during each corresponding treatment. Traces are averages of at least 56 cells and >4 animals. Data has been normalised to the initial fluorescence reading t=0 expressed as F/F_0 . All data shown are mean ±SEM and both treatments reach significance * $p < 0.5$, **** $p < 0.0001$.

Figure 5.6

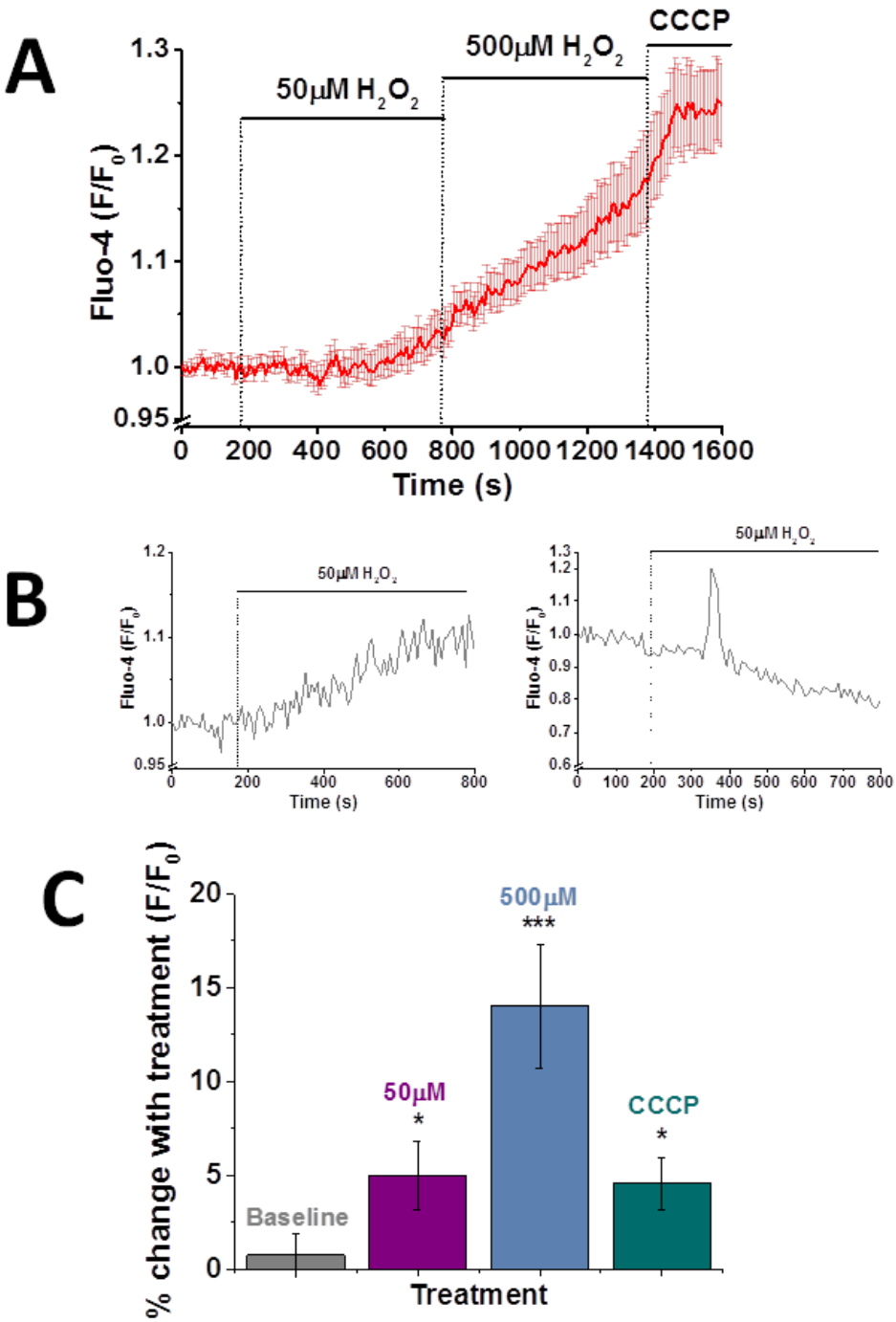

Figure 5.6. Concentration-dependent elevation of $[Ca^{2+}]_c$ induced by submillimolar H_2O_2. Cytosolic Ca^{2+} was measured in cells loaded with Fluo-4. Pancreatic acinar cell suspensions were treated for 10 minutes with 50μM H_2O_2, 10 minutes with 500μM H_2O_2 and 5 minutes with uncoupler CCCP (10μM). **(A)** Line graph presentation of results. **(B)** Example traces with 50μM H_2O_2 treatment. **(C)** Bar chart presentation showing the percentage change in $[Ca^{2+}]_c$ during each treatment. Traces are averages of at least 31 cells and >4 animals. Data has been normalised to the initial fluorescence reading t=0 expressed as F/F_0 . All data shown are mean ±SEM. * = $p < 0.05$, *** = $p < 0.001$.

Figure 5.7

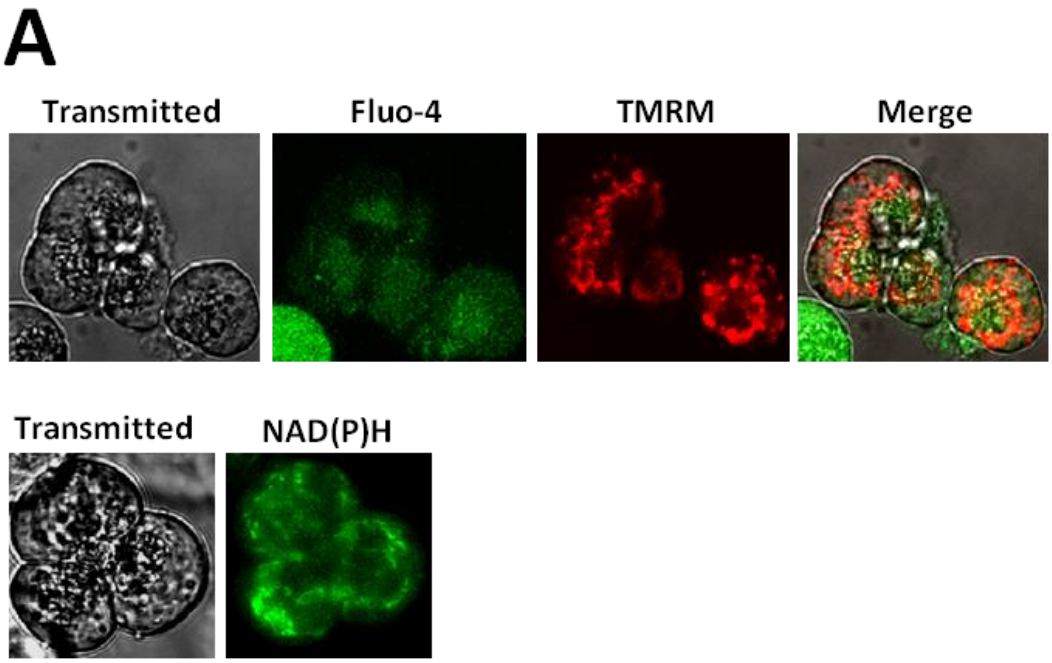

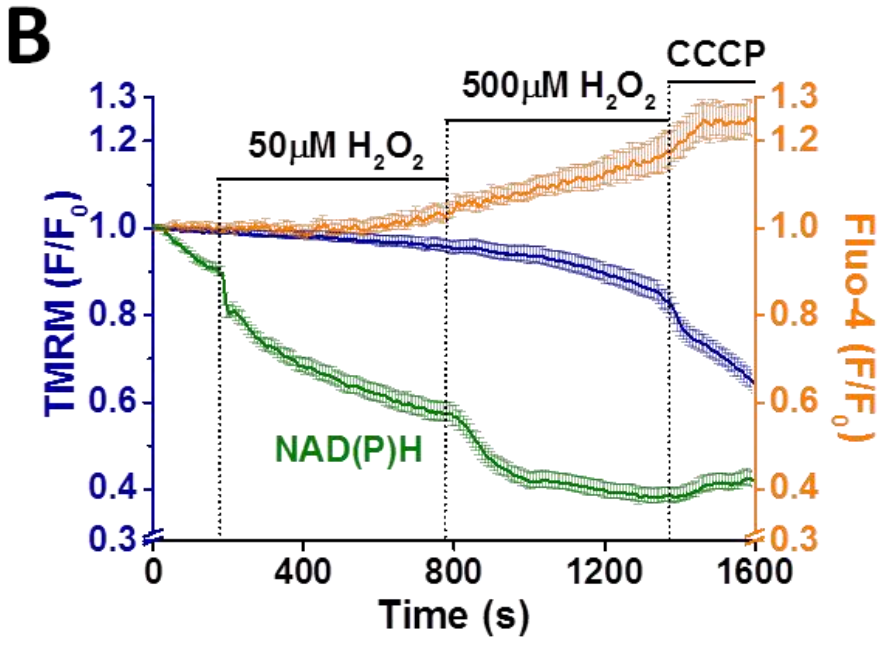

Figure 5.7. Comparative concentration-dependent effects of submillimolar H_2O_2 on ΔΨm, $[Ca^{2+}]_c$ and NAD(P)H. Measurements were taken as described in the previous two figures. **(A)** Example loading of Fluo-4, TMRM and NAD(P)H autofluorescence, **(B)** TMRM, Fluo-4, NAD(P)H results in response to 50µM and 500µM H_2O_2. Traces are averages of at least 31 cells and >4 animals. Data has been normalised to the initial fluorescence reading t=0 expressed as F/F_0 . All data shown are mean ±SEM.

The Cellular Effects of H_2O_2 on CypD KO Mouse PACs

$Ppif^{-/-}$ PACs were isolated and loaded with TMRM to measure mitochondrial membrane potential. 1mM H_2O_2 was perfused via the gravity perfusion system for a 10 minutes period prior to addition of uncoupler CCCP. The ΔΨm depolarisation was progressive in both control C57BL/6 and $Ppif^{-/-}$ cells and no significant differences were seen in the percentage TMRM fluorescence change in $Ppif^{-/-}$ cells (Figure 5.8). NAD(P)H autofluorescence was measured in cells treated for 10 minutes with 1mM H_2O_2 followed by 5 minutes with uncoupler CCCP (10μM). The effects of 1mM H_2O_2 were exacerbated in $Ppif^{-/-}$ cells (Figure 5.9). CM-H_2DCFDA loaded cells treated for 10 minutes with 1mM H_2O_2 demonstrated elevated ROS increases in $Ppif^{-/-}$ cells compared to C57BL/6 control cells (Figure 5.10).

Figure 5.8

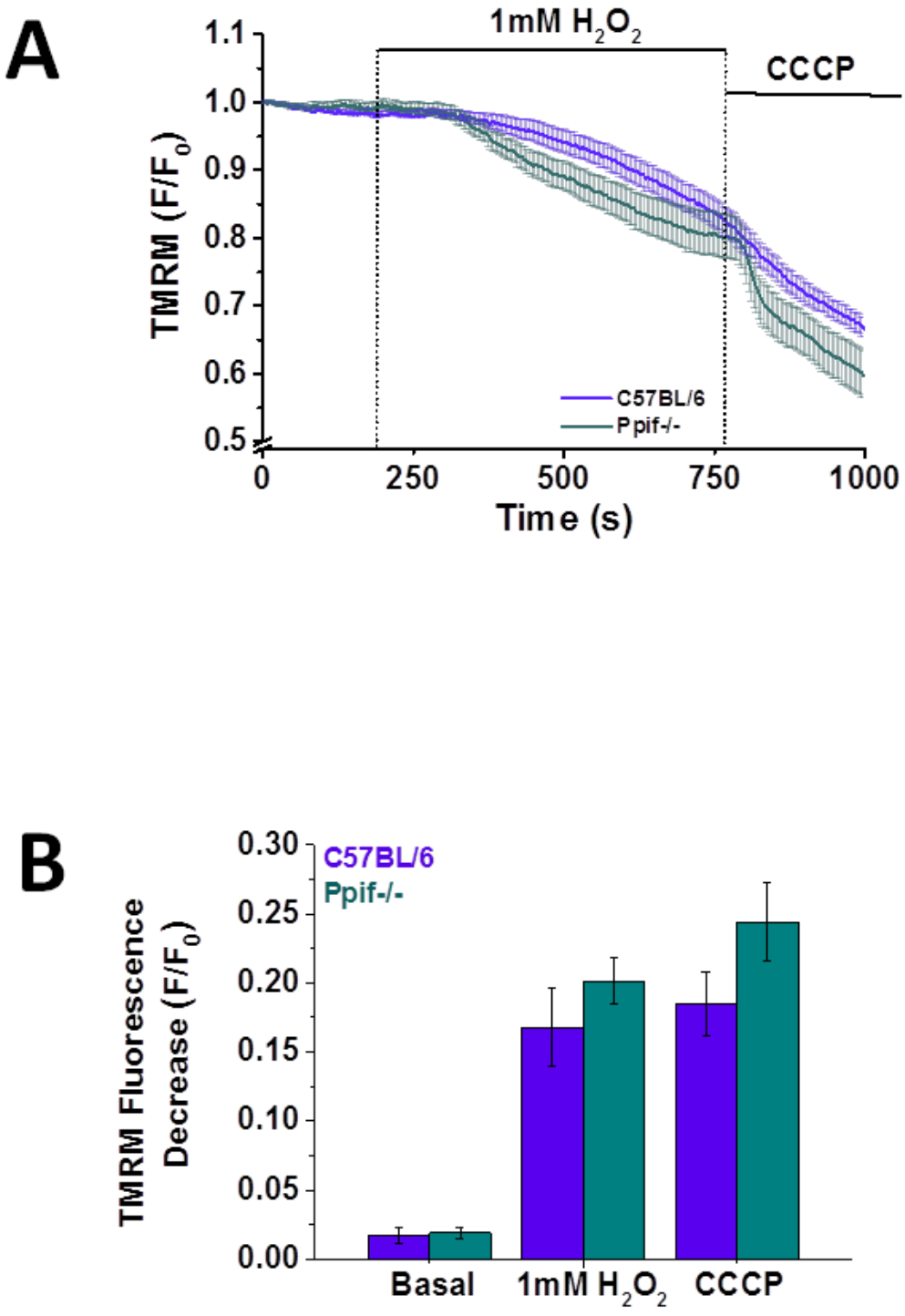

Figure 5.8. Millimolar H_2O_2 effects on ΔΨm are unchanged in Ppif-/- cells. Mitochondrial membrane potential was measured in cells loaded with TMRM dye and treated with 1mM H_2O_2 and uncoupler CCCP (10µM). Traces are averages of at least 67 cells and >4 animals. Data has been normalised to the initial fluorescence reading t=0 expressed as F/F_0 . All data shown are mean ±SEM.

Figure 5.9

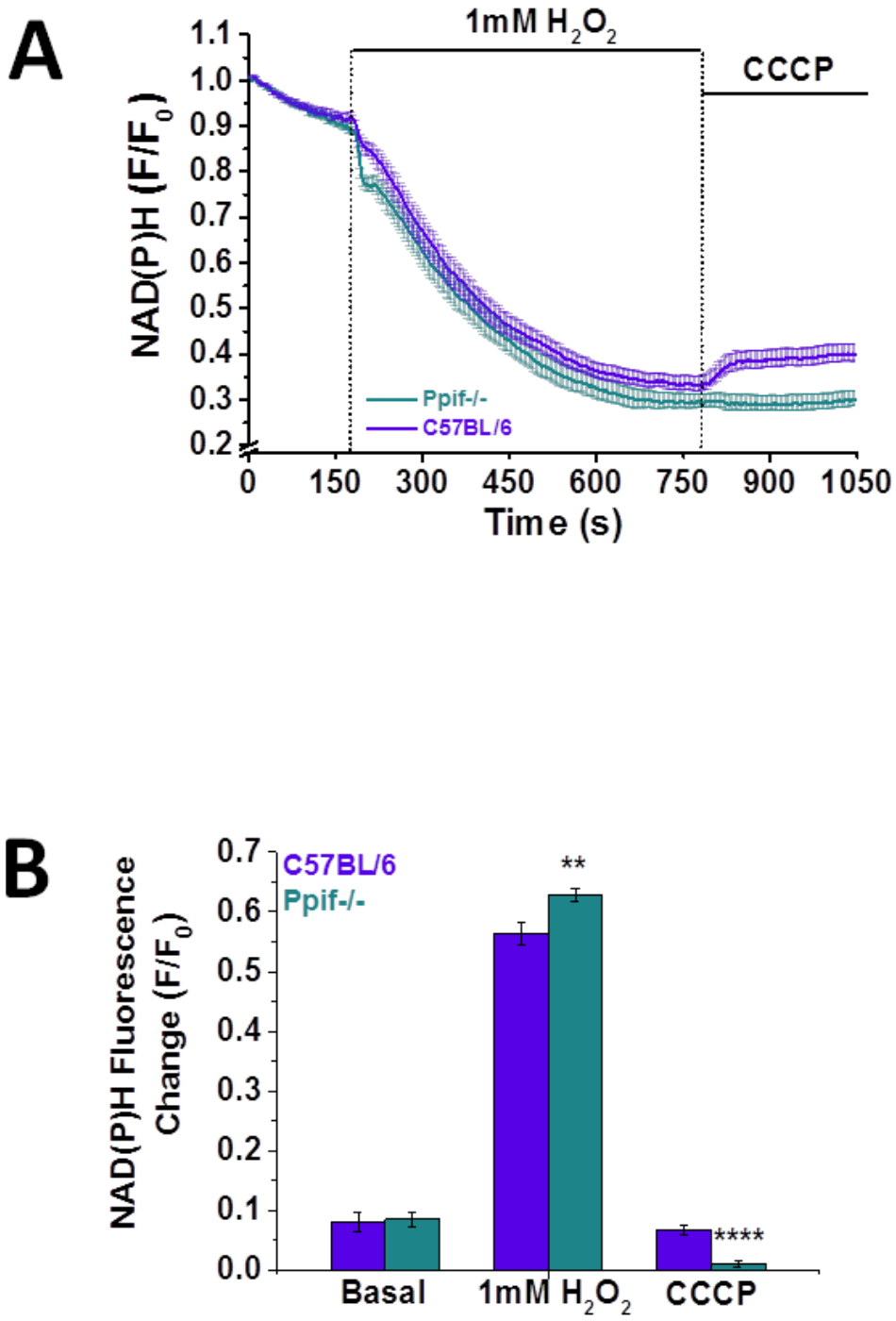

Figure 5.9. Millimolar H_2O_2 effects on NAD(P)H are exacerbated in Ppif-/- cells. NAD(P)H autofluorescence was measured in cells treated for 10 minutes with 1mM H_2O_2 followed by 5 minutes with uncoupler CCCP (10µM). **(A)** Line graph presentation of results. **(B)** Black 6 control results, **(C)** Ppif-/- results. Traces are averages of at least 84 cells and >4 animals. Data has been normalised to the initial fluorescence reading t=0 expressed as F/F_0 . All data shown are mean ±SEM. ** p<0.01, **** p<0.0001.

Figure 5.10

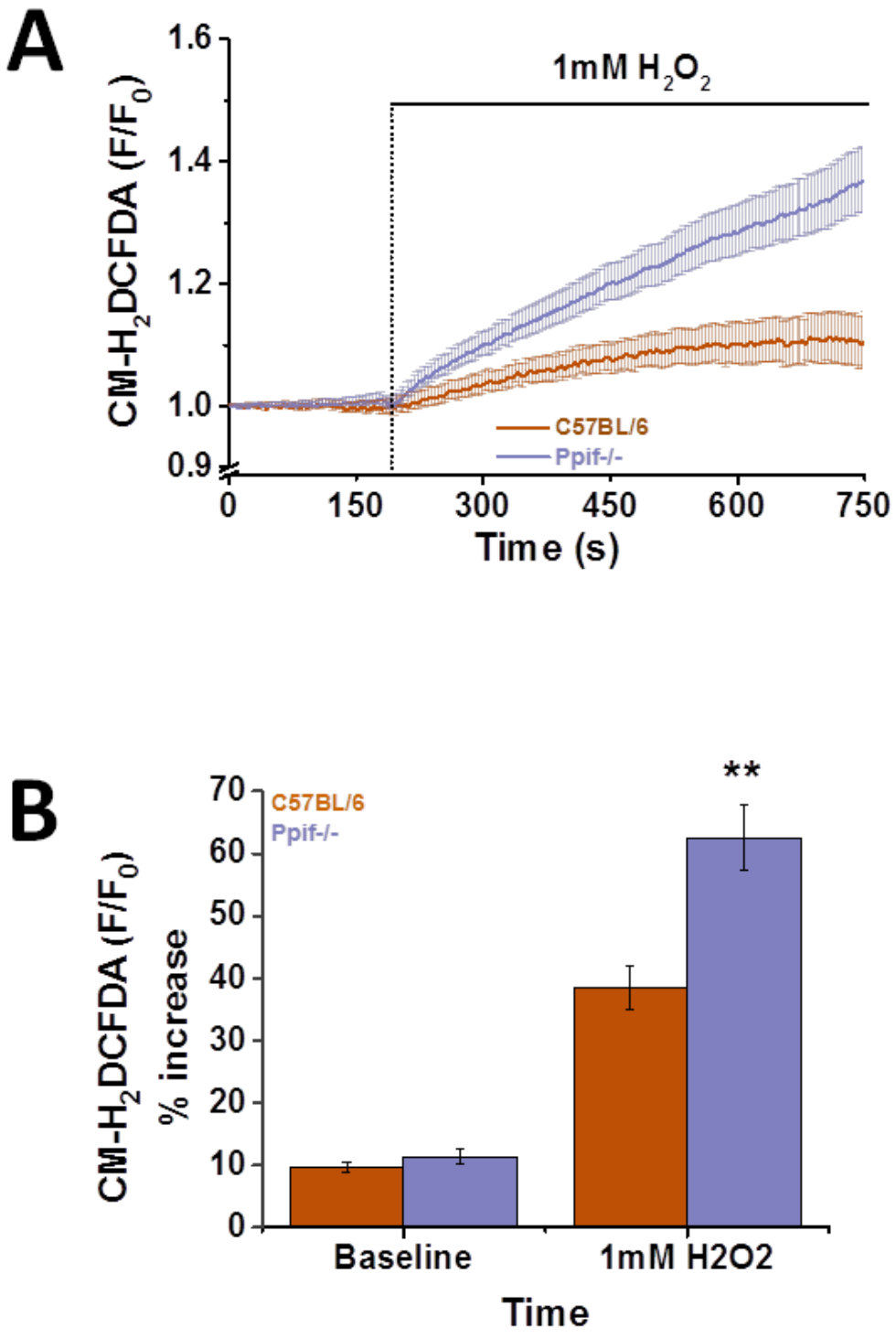

Figure 5.10. Millimolar H_2O_2-induced ROS increases are elevated in Ppif-/- cells . CM-H_2DCFDA loaded cells treated for 10 minutes with 1mM H_2O_2. **(A)** Line graph presentation of results. **(B)** Bar chart results of ROS increases with each treatment. Traces are averages of at least 31 cells and 3 animals. Data has been normalised to the initial fluorescence reading t=0 expressed as F/F_0 . All data shown are mean ±SEM. ** p<0.01.

The Effects of H_2O_2 on Cellular ROS Levels

Cells were loaded with CM-H_2DCFDA for 30 minutes and treated with 1µM, 5µM, 500µM H_2O_2. Fluorescence changes were concentration-dependent and 500µM H_2O_2-induced increases in ROS levels were significantly different from the NaHEPES control at 40 minutes onwards. 1µM and 5µM H_2O_2-induced increases in ROS levels were significant after the 80 minute period (Figure 5.11).

Cells were pre-treated with MitoQ (1µM) either for 10 minutes or 30 minutes. MitoQ inhibited 1mM H_2O_2-induced ROS increases when pre-treated for 30 minutes but not 10 minutes, an inhibition not seen with dTPP and TPP^+ (1µM) control compound treatment (Figure 5.12). Cells pre-treated with MitoQ (0.2, 0.5, 1µM) for a 10 minute period did not inhibit 500µM H_2O_2-induced ROS increases (Figure 5.13A). A 30 minute pre-treatment with MitoQ (0.2, 0.5, 1µM) was concentration-dependent and only inhibited with 0.2µM and 1µM H_2O_2 not 0.1µM MitoQ pre-treatment (Figure 5.13B-D).

After a 40 minute treatment with 10nM CCK, 100µM POAEE and 500µM H_2O_2 there were significant increases in ROS levels in comparison to the NaHEPES control. Later time points of 80 minutes and 120 minutes demonstrated ROS increases only significant with POAEE and 500µM H_2O_2 treatment only (Figure 5.14).

Figure 5.11

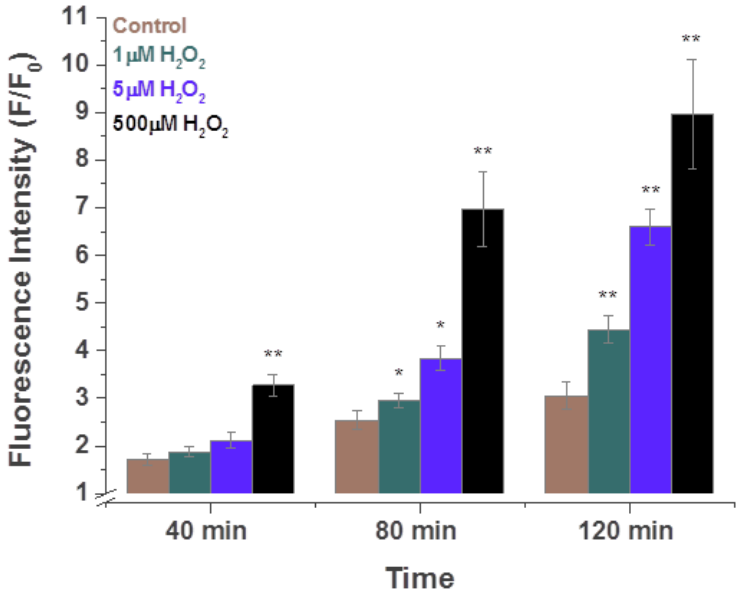

Figure 5.11. Concentration-dependent submillimolar H_2O_2-induced ROS increases. CM-H_2DCFDA loaded cells were treated with increasing concentrations of H_2O_2 (1µM, 5µM, 500µM). Traces are averages of at least 3 animals. Data has been normalised to the initial fluorescence reading t=0 expressed as F/F_0 . All data shown are mean ±SEM.

Figure 5.12

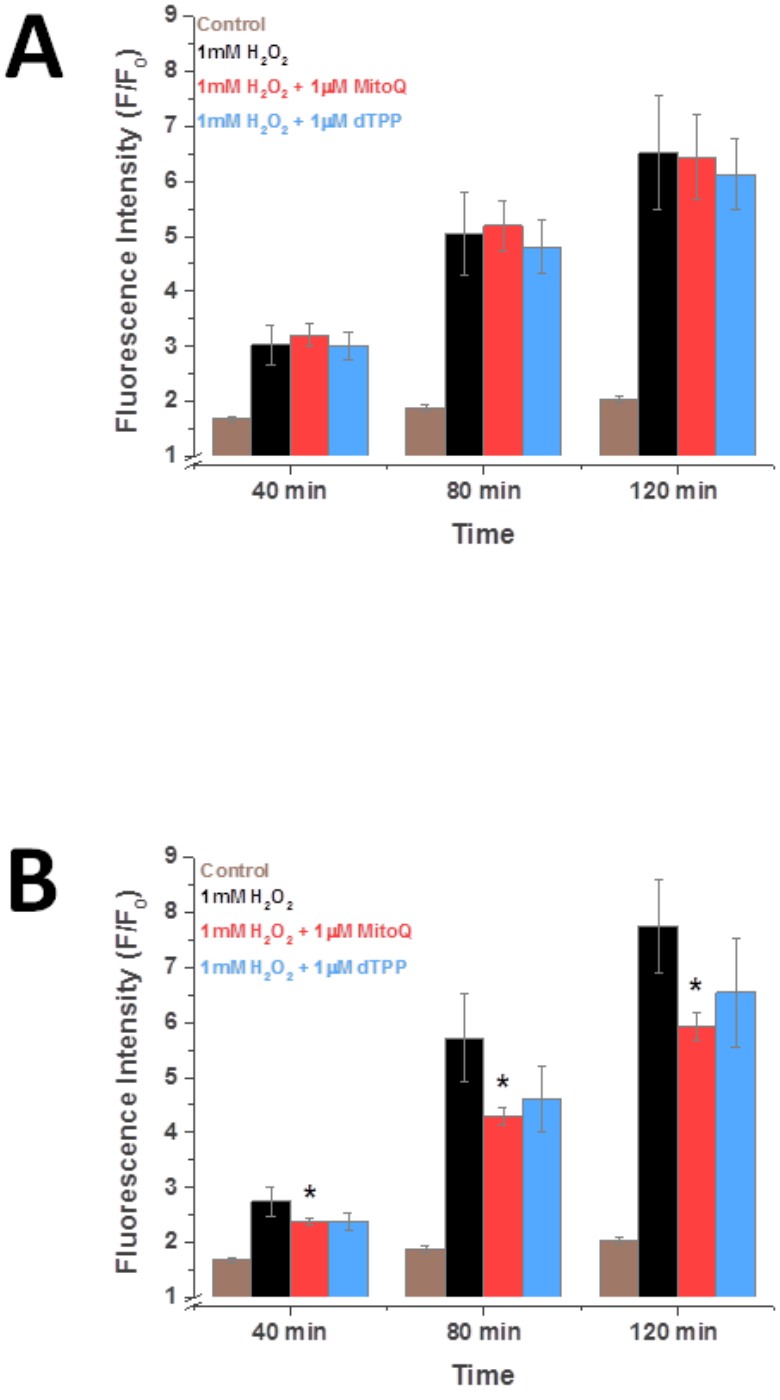

Figure 5.12. Pre-treatment dependent MitoQ inhibition of millimolar H_2O_2-induced ROS increases. CM-H_2DCFDA loaded cells were pre-treated with 1µM MitoQ (and dTPP control) for either 10 minutes or 30 minutes prior to the addition of 1mM H_2O_2. **(A)** 10 minutes pre-treatment with 1µM MitoQ (and dTPP control). **(B)** 30 minutes pre-treatment with 1µM MitoQ (and dTPP control). Traces are averages of at least 3 animals. Data has been normalised to the initial fluorescence reading t=0 expressed as F/F_0 . All data shown are mean ±SEM. * $p<0.05$.

Figure 5.13

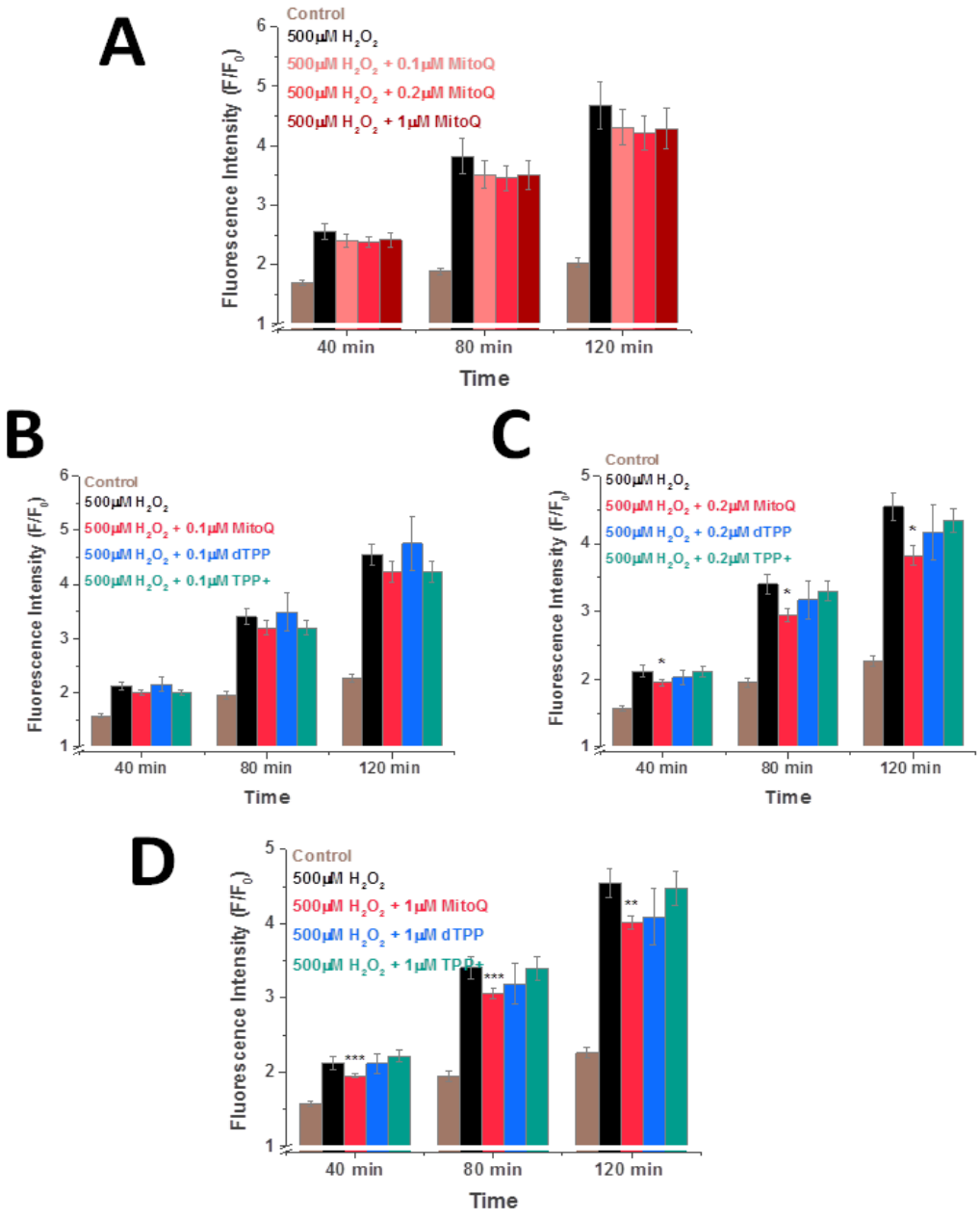

Figure 5.13. Pre-treatment and concentration-dependent MitoQ inhibition of submillimolar H_2O_2-induced ROS increases. CM-H_2DCFDA loaded cells were pre-treated with either 0.1μM, 0.2μM or 1μM MitoQ for either 10minutes or 30 minutes prior to the addition of 500μM H_2O_2 **(A)** 10 minutes pre-treatment with 0.1μM, 0.2μM or 1μM MitoQ. **(B)** 30 minutes pre-treatment with 0.1μM MitoQ, dTPP or TPP^+, **(C)** 30 minutes pre-treatment with 0.2μM MitoQ, dTPP or TPP^+, **(D)** 30 minutes pre-treatment with 1μM MitoQ, dTPP or TPP^+. Traces are averages of at least 3 animals. Data has been normalised to the initial fluorescence reading t=0 expressed as F/F_0 . All data shown are mean ±SEM. * p<0.05, ** p<0.01, *** p<0.001.

Figure 5.14

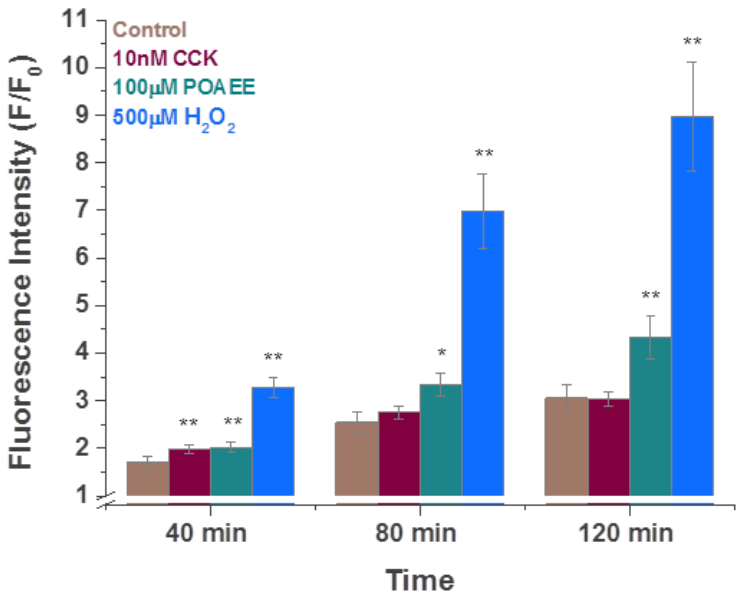

Figure 5.14. H_2O_2, POAEE and CCK induced ROS increases. 500µM H_2O_2, POAEE and 10nM CCK induced ROS increases measured by CM-H_2DCFDA. Traces are averages of at least 3 animals. Data has been normalised to the initial fluorescence reading t=0 expressed as F/F_0. All data shown are mean ±SEM.

The Effect of H_2O_2 on Pancreatic Acinar Cell Apoptosis and Necrosis

Acinar cells were loaded with a Caspase-3/7 Green reagent as an indicator of cellular apoptosis and levels of fluorescence monitored. Treatment (1µM, 5µM and 10µM H_2O_2) or NaHEPES (control) was administered for a 13 hour period and induced concentration-dependent increases in apoptosis. Significant changes were detected with 5µM and 10µM H_2O_2 at 7 hours and additionally with 1µM at 13 hour (Figure 5.15). In PI loaded cells 1µM, 5µM and 10µM H_2O_2 induced cellular necrosis also in a concentration-dependent manner. Significance changes were detected at 7 hours with 10µM and at 13 hours with 5µM and 10µM (Figure 5.16).

500µM and 1mM H_2O_2 predominantly induced a necrotic method of cell death in a concentration-dependent manner. Caspase-3/7 Green reagent loaded cells also showed a rapid increase in cellular apoptosis induced by 500µM and 1mM H_2O_2 within a 3 hour period in comparison to the NaHEPES control (Figure 5.17). The majority of cellular necrosis was also elicited over an initial 3 hour period (Figure 5.18). The proportion of cellular necrosis and apoptosis is dependent on the concentration. The lower concentrations of 1µM, 5µM and 10µM H_2O_2 principally induced an apoptotic mechanism of cell death (Figure 5.19) whereas higher concentrations of 500µM and 1mM H_2O_2 predominantly induced necrotic cell death (Figure 5.20). The comparison is clearly highlighted in figure 5.21.

Figure 5.15

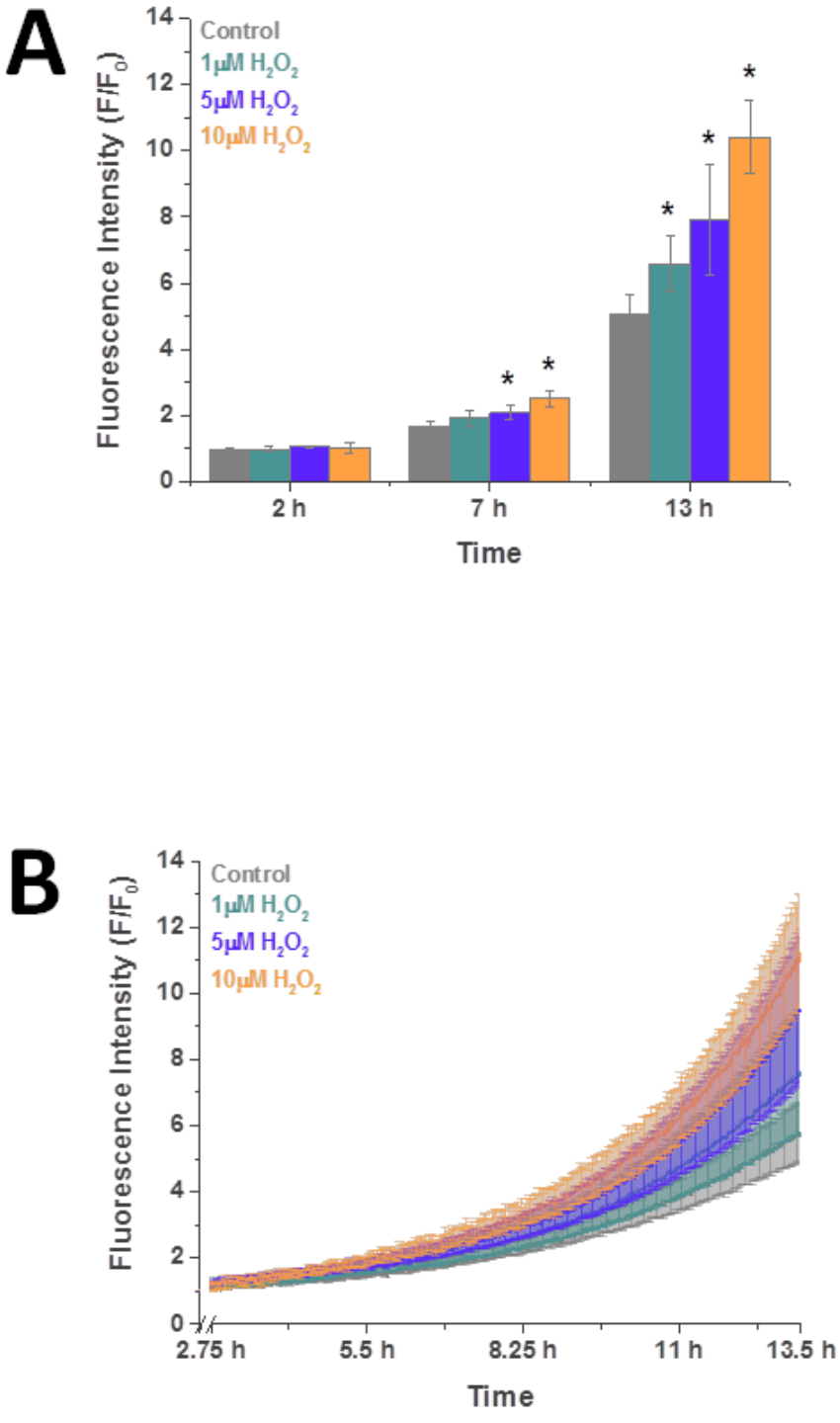

Figure 5.15. Submillimolar H_2O_2-induced apoptosis. CellEvent® Caspase-3/7 Green reagent was loaded into isolated pancreatic acinar cells as an indicator of cellular apoptosis. Treatment (1μM, 5μM and 10μM H_2O_2) or NaHEPES (control) was administered. The data has been normalised to the initial fluorescence reading t=0 expressed as F/F_0. **(A)** Bar chart representative of time points. **(B)** Line graph presentation. Traces are averages of 9 animals. All data shown are mean ±SEM. * $p<0.05$.

Figure 5.16

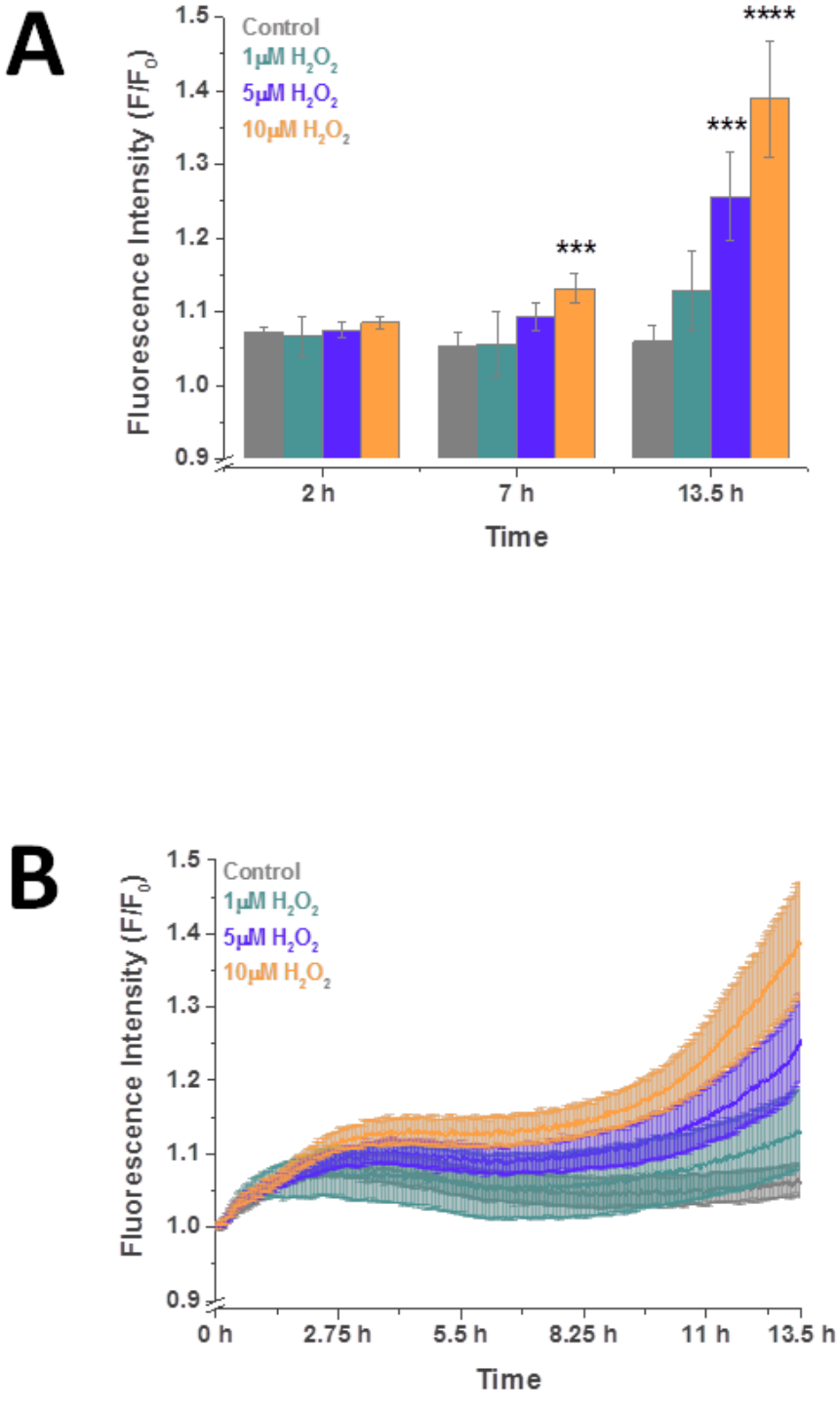

Figure 5.16. Submillimolar H_2O_2-induced necrosis. PI loaded cells were treated 1μM, 5μM and 10μM H_2O_2. The data has been normalised to the initial fluorescence reading t=0 expressed as F/F_0. **(A)** Bar chart representative of time points. **(B)** Line graph presentation. Traces are averages of 9 animals. All data shown are mean ±SEM. *** p<0.001, **** p<0.0001.

Figure 5.17

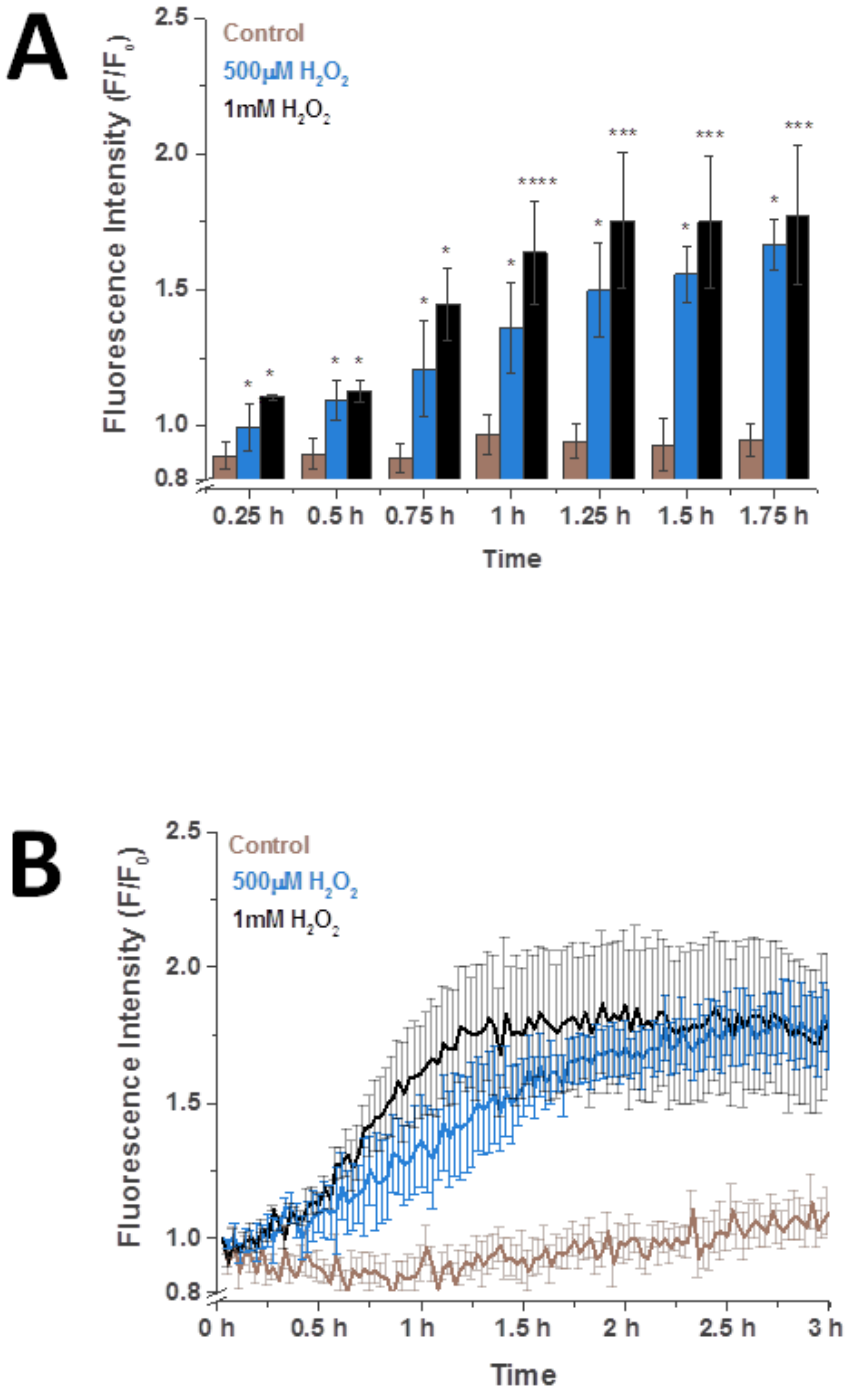

Figure 5.17. Submillimolar and millimolar H_2O_2-induced apoptosis. CellEvent® Caspase-3/7 Green reagent was loaded into isolated pancreatic acinar cells as an indicator of cellular apoptosis. Treatment (500µM, 1mM H_2O_2) or NaHEPES (control) was administered to each designated well in a 96 well plate prior to imaging over a 13 hour period. The data has been normalised to the initial fluorescence reading t=0 expressed as $F/F_{0.}$ **(A)** Bar chart representative of time points **(B)** Line graph presentation. Traces are averages of 9 animals. All data shown are mean ±SEM. * p<0.05, *** p<0.001, **** p<0.0001.

Figure 5.18

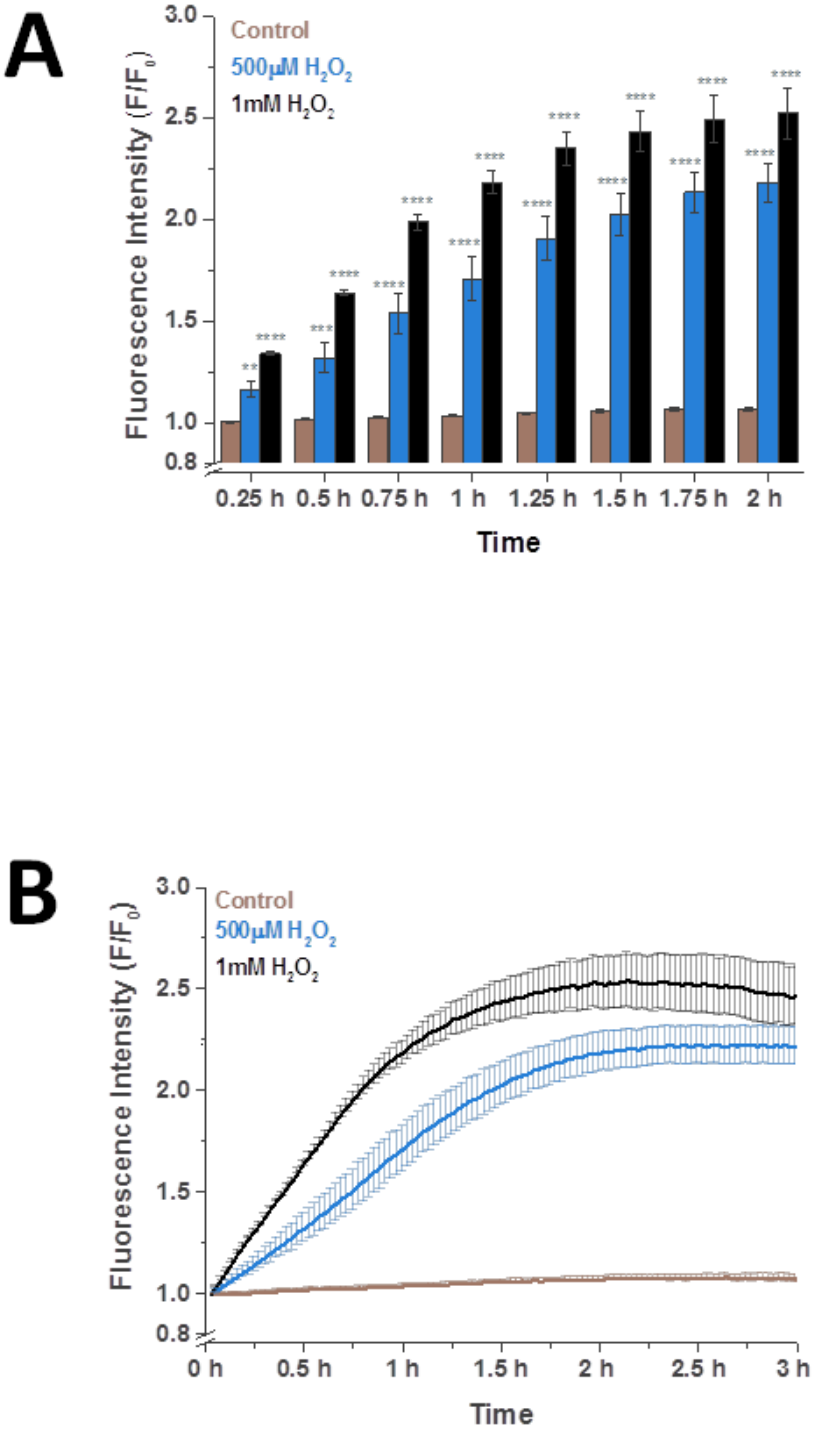

Figure 5.18. Submillimolar and millimolar H_2O_2-induced necrosis. PI loaded cells were treated with either 500µM or 1mM H_2O_2. The data has been normalised to the initial fluorescence reading t=0 expressed as F/F_0. **(A)** Bar chart representative of time points. **(B)** Line graph presentation. Traces are averages of 9 animals. All data shown are mean ±SEM. ** p<0.01, *** p<0.001, **** p<0.0001.

Figure 5.19

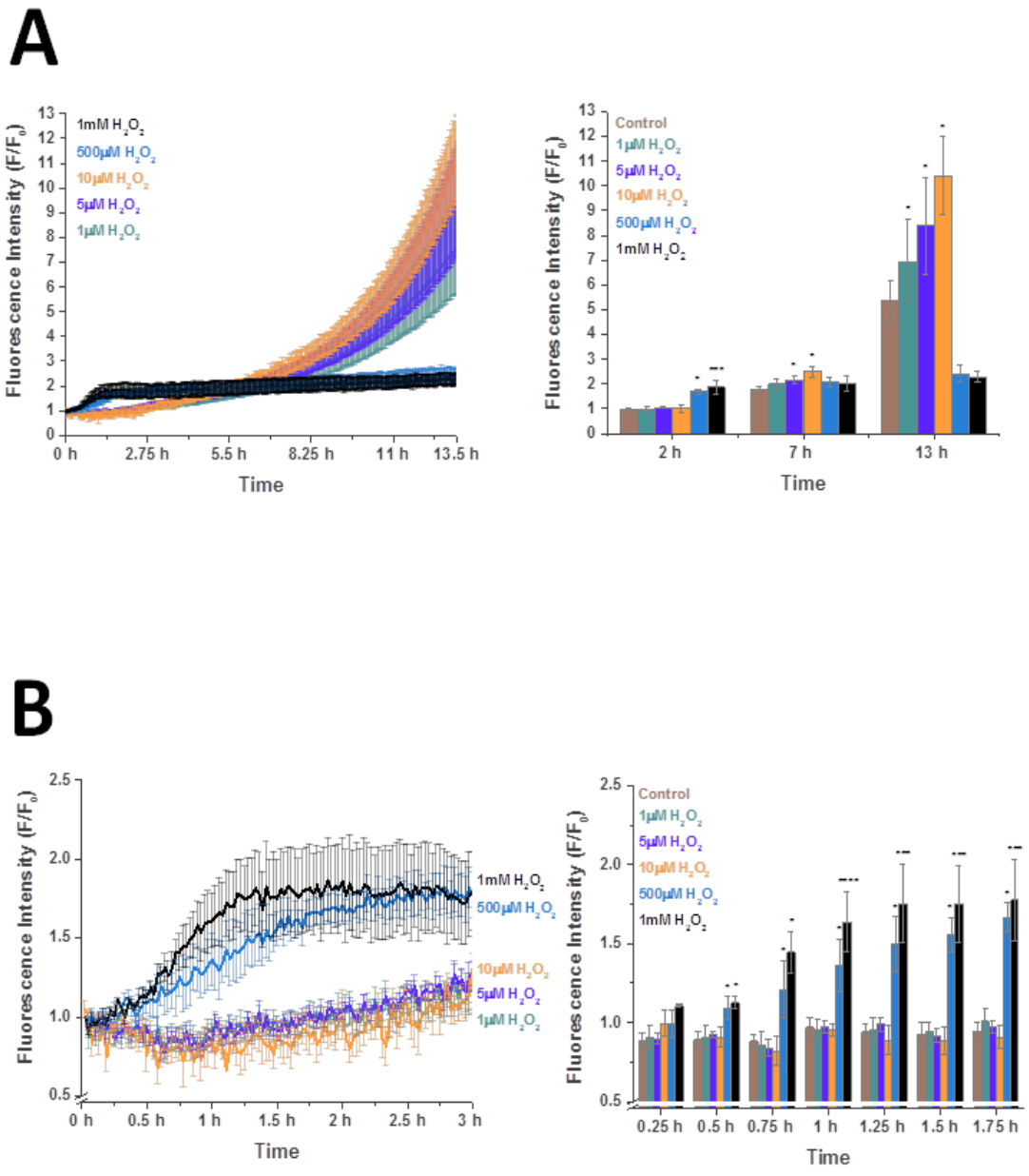

Figure 5.19. Submillimolar and millimolar concentration-dependent induction of apoptosis. CellEvent® Caspase-3/7 Green reagent loaded cells were treated as previously described. The data has been normalised to the initial fluorescence reading t=0 expressed as F/F_0. **(A)** The effects of 1µM, 5µM, 10µM, 500µM and 1mM H_2O_2 on apoptosis presented as a line graph and bar chart from the beginning to end of readings obtained to show maximum cell death with each treatment. **(B)** 0-3 h time points (comparison to maximal cellular apoptosis reached with 500µM and 1mM H_2O_2). Traces are averages of 9 animals. All data shown are mean ±SEM. * p<0.05, *** p<0.001, **** p<0.0001.

Figure 5.20

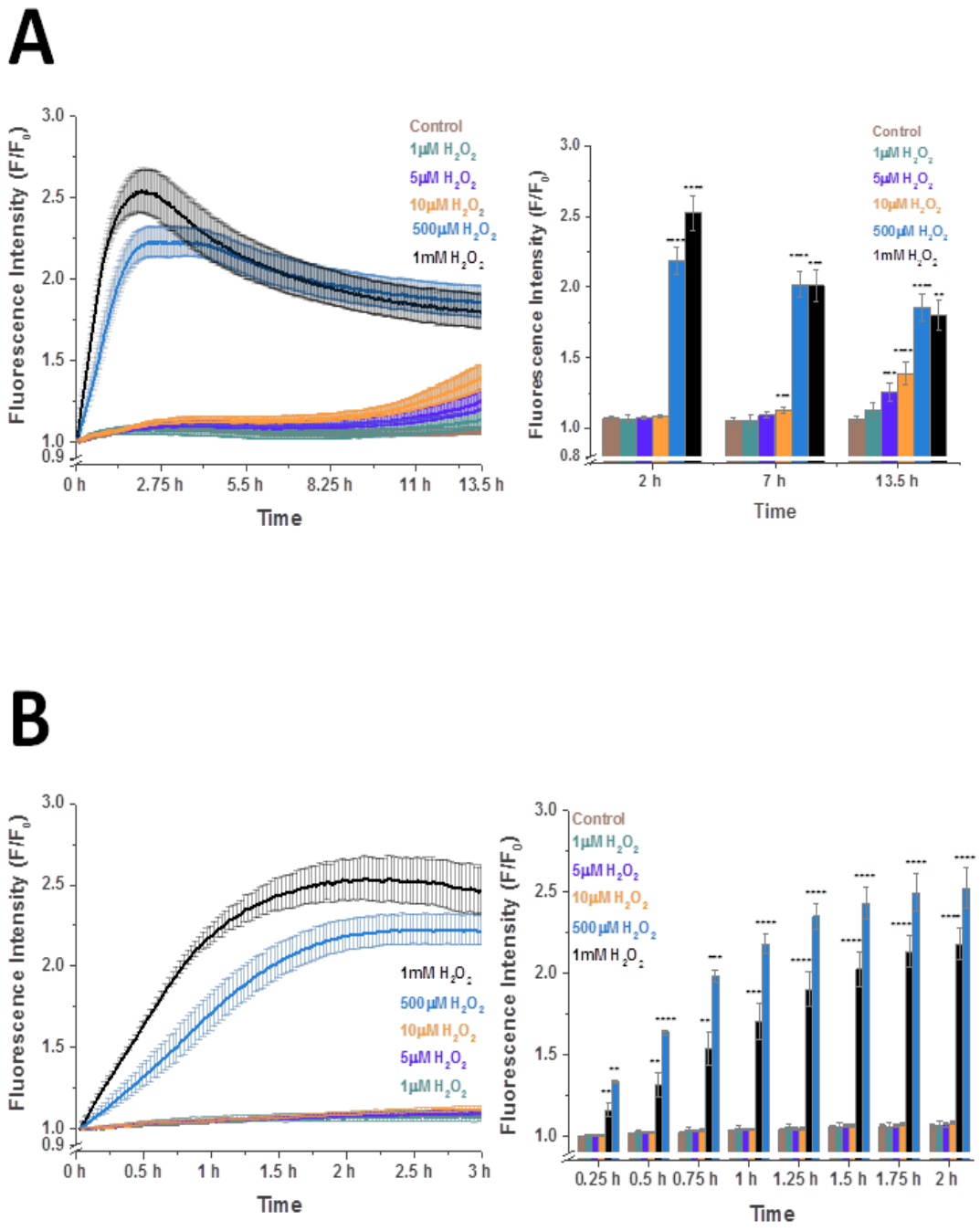

Figure 5.20. Submillimolar and millimolar concentration-dependent induction of necrosis. PI loaded cells were treated as previously described. The data has been normalised to the initial fluorescence reading t=0 expressed as F/F_0. **(A)** The effects of 1μM, 5μM, 10μM, 500μM and 1mM H_2O_2 on necrosis presented as a line graph and bar chart from the beginning to end of readings obtained to show maximum cell death with each treatment. **(B)** 0-3 h time points (comparison of maximal cellular necrosis reached with 500μM and 1mM H_2O_2). Traces are averages of 9 animals. All data shown are mean ±SEM. ** p<0.01, *** p<0.001, **** p<0.0001.

Figure 5.21

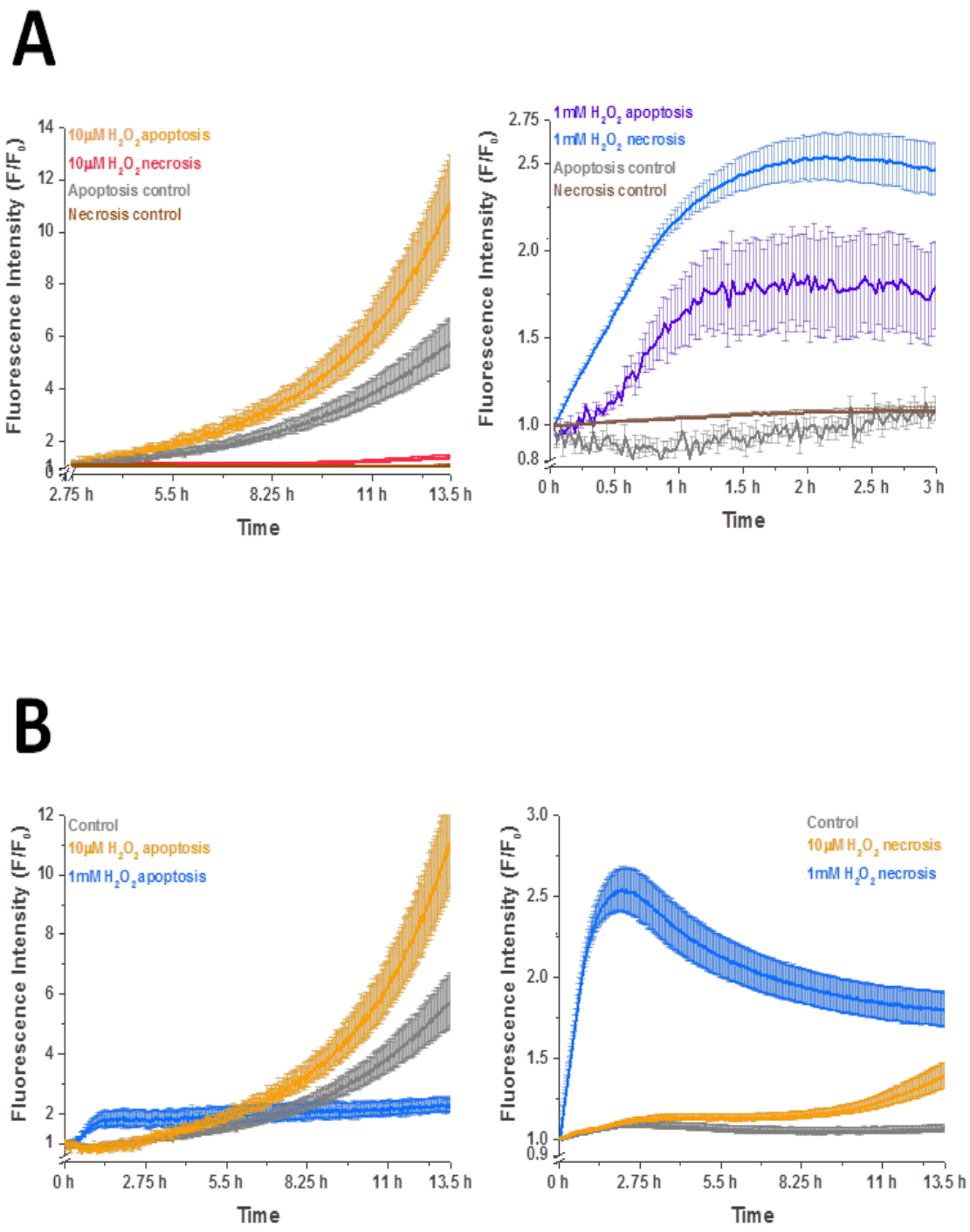

Figure 5.21. Comparative 10μM and 1mM H_2O_2-induced apoptosis and necrosis. (A) Comparative apoptosis and necrosis induced by 10μM H_2O_2 and 1mM H_2O_2. **(B)** Differences in levels of apoptosis and necrosis induced by 10μM H_2O_2 and 1mM H_2O_2. Line graph presentation. Traces are averages of 9 animals. The data has been normalised to the initial fluorescence reading t=0 expressed as F/F_0. All data shown are mean ±SEM. * $p<0.05$.

In Caspase-3/7 Green reagent loaded cells 0.2µM MitoQ pre-treatment exacerbated 500µM H_2O_2-induced pancreatic acinar cell apoptosis at the 1 hour time point and 1µM dTPP at all time points displayed. TPP^+ (1µM) worsened levels of apoptosis at the final 2 hour time point (Figure 5.22). MitoQ, dTPP and TPP^+ had no effect on 1mM H_2O_2-induced apoptosis in Caspase-3/7 Green reagent loaded cells (Figure 5.23). Cells were loaded with PI and pre-treated for 30 minutes with 0.2µM and 1µM MitoQ, dTPP and TPP^+. All TPP derivatives exacerbated 500µM (Figure 5.24) and not 1mM H_2O_2-induced necrosis (Figure 5.25).

Treatment with 1µM, 5µM and 10µM H_2O_2 and 100µM POAEE induced apoptosis detectable in Caspase-3/7 Green reagent loaded cells. At the earlier time point of 2 h only 100µM POAEE induced significant increases in apoptosis (Figure 5.26A). All treatments except 1µM H_2O_2 induced cellular necrosis in PI loaded cells. At 2 hours 100µM POAEE also induced significant increases in necrosis and at 7 hours with 10µM H_2O_2 treatment (Figure 5.26B).

Figure 5.22

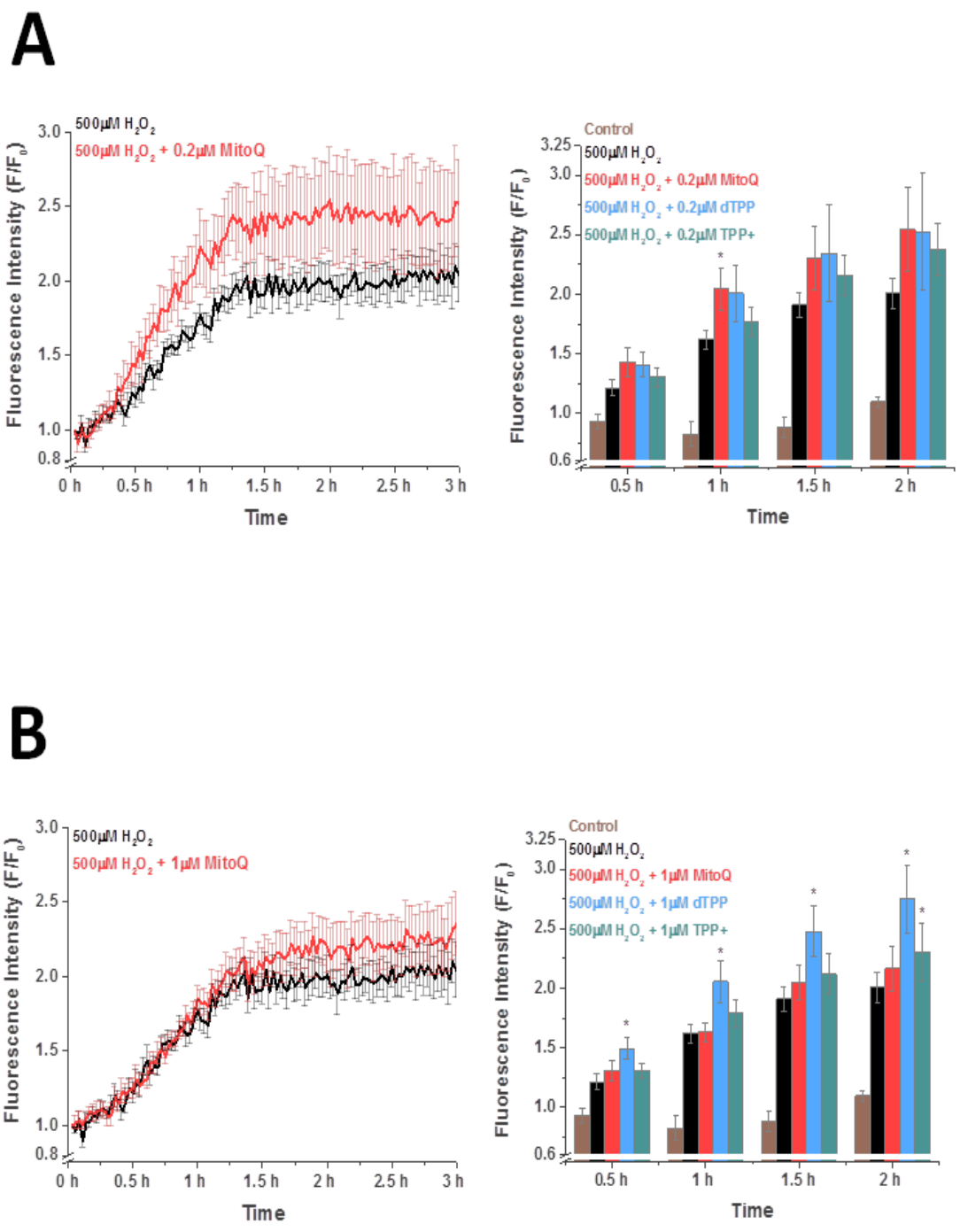

Figure 5.22. MitoQ, dTPP and TPP^+ exacerbated submillimolar H_2O_2-induced apoptosis. CellEvent® Caspase-3/7 Green reagent loaded cells were treated as previously described and pre-treated for 30 minutes with 1μM MitoQ/dTPP/TPP^+. The data has been normalised to the initial fluorescence reading t=0 expressed as F/F_0. **(A)** The effects of 1μM MitoQ (and dTPP/TPP^+) on 500μM H_2O_2 induced apoptosis presented as a line graph and bar chart. **(B)** The effects of 1μM MitoQ (and dTPP/TPP^+) on 500μM H_2O_2 induced apoptosis presented as a line graph and bar chart. Traces are averages of 9 animals. All data shown are mean ±SEM. * $p<0.05$.

Figure 5.23

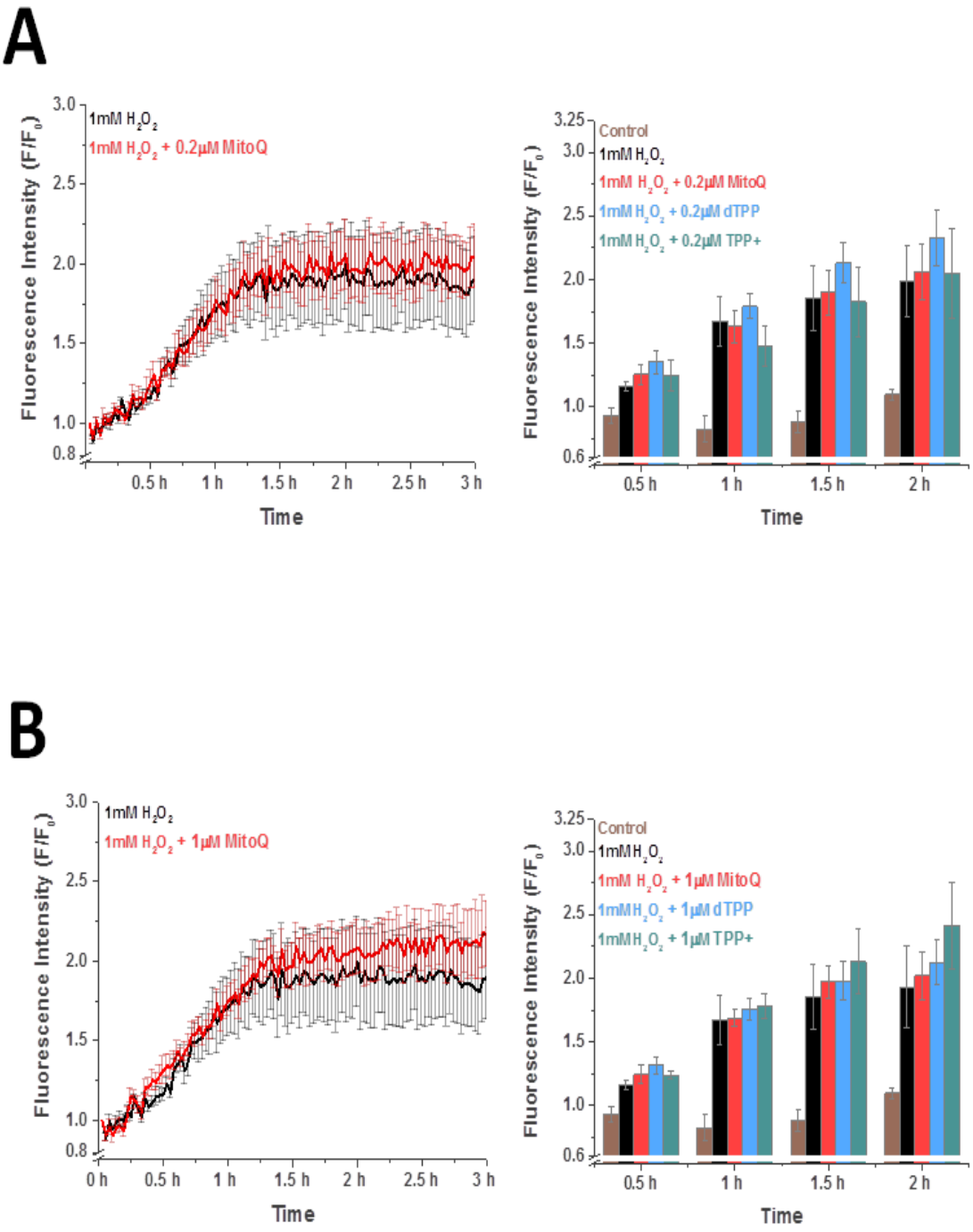

Figure 5.23. MitoQ had no effect on millimolar H_2O_2-induced apoptosis. CellEvent® Caspase-3/7 Green reagent loaded cells were treated as previously described and pre-treated for 30 minutes with 1μM MitoQ/dTPP/TPP$^+$. The data has been normalised to the initial fluorescence reading t=0 expressed as F/F_0. **(A)** The effects of 1μM MitoQ (and dTPP/TPP$^+$) on 1mM H_2O_2-induced apoptosis presented as a line graph and bar chart **(B)** The effects of 1μM MitoQ (and dTPP/TPP$^+$) on 1mM H_2O_2-induced apoptosis presented as a line graph and bar chart. Traces are averages of 9 animals. All data shown are mean ±SEM.

Figure 5.24

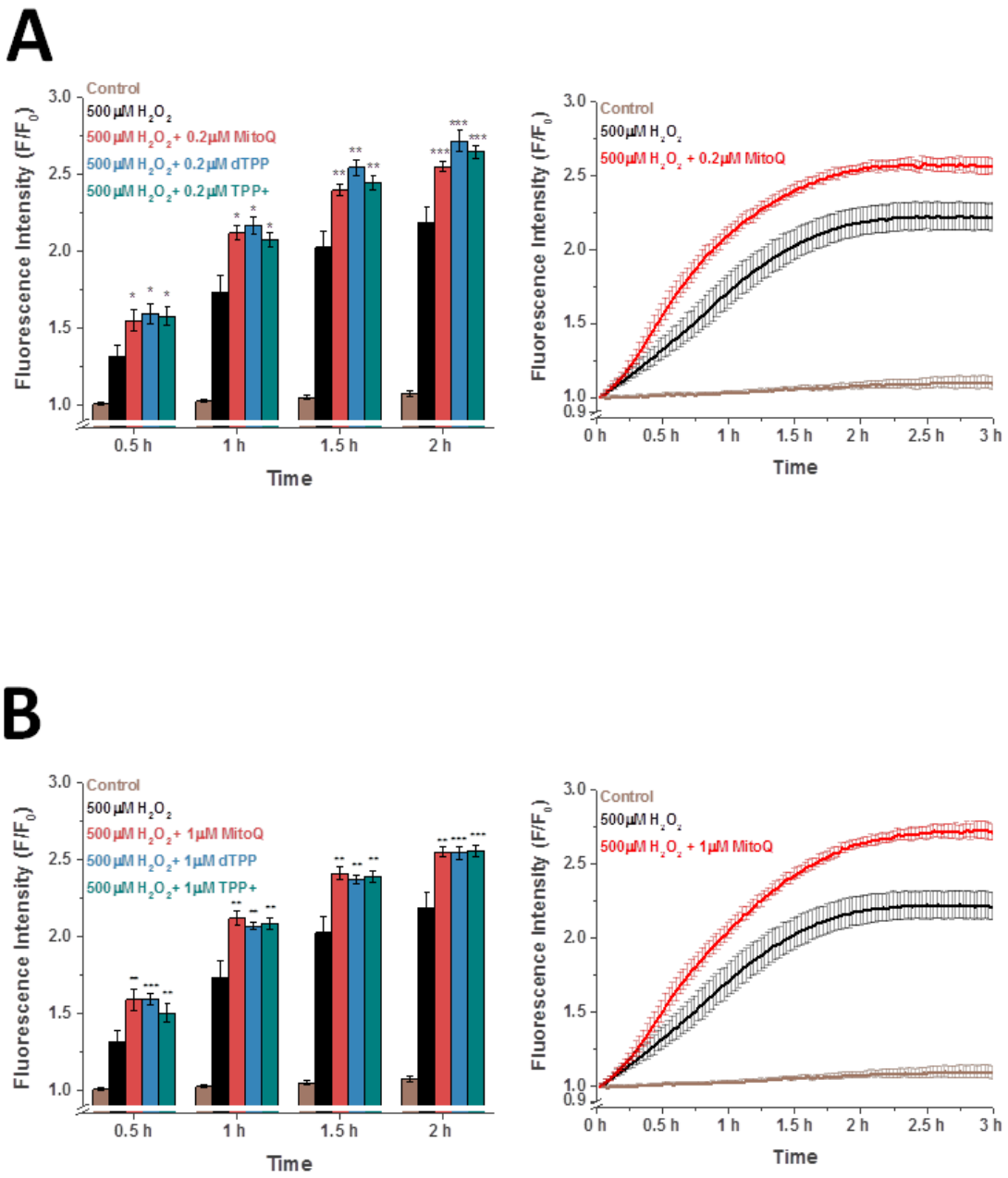

Figure 5.24. MitoQ, dTPP and TPP^+ exacerbated submillimolar H_2O_2-induced necrosis. PI loaded cells were treated as previously described and pre-treated for 30 minutes with 0.2µM and 1µM MitoQ. The data has been normalised to the initial fluorescence reading t=0 expressed as F/F_0. **(A)** 0.2µM MitoQ pre-treatment effects presented as a line graph and bar chart **(B)** 1µM MitoQ pre-treatment effects on 500µM H_2O_2 induced necrosis presented as a line graph and bar chart. Traces are averages of 3 animals. All data shown are mean ±SEM. * p<0.05, ** p<0.01, *** p<0.001.

Figure 5.25

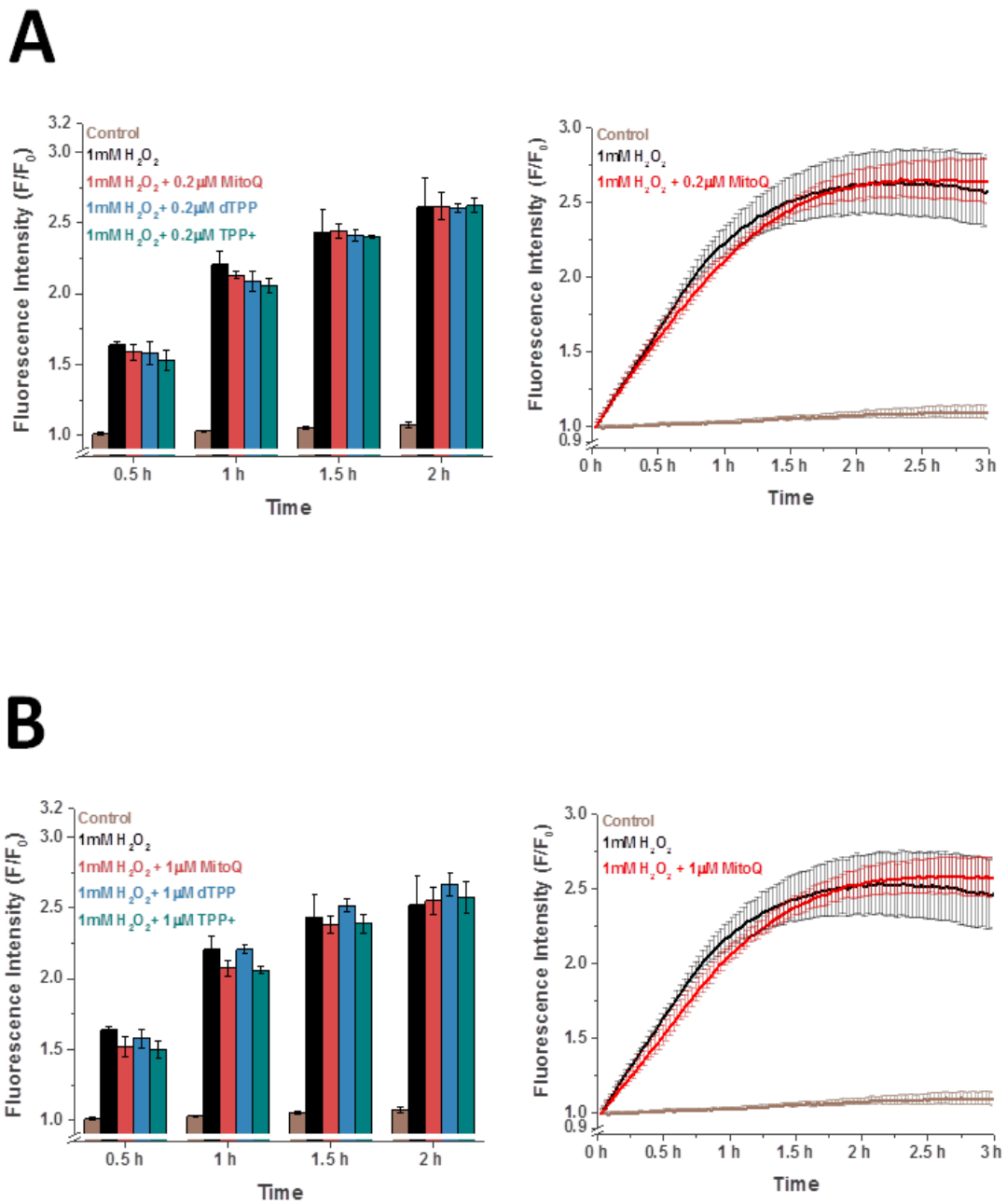

Figure 5.25. MitoQ, dTPP and TPP$^+$ had no effect on millimolar H_2O_2-induced necrosis. PI loaded cells were treated as previously described and pre-treated for 30 minutes with 0.2µM or 1µM MitoQ/dTPP/TPP$^+$. The data has been normalised to the initial fluorescence reading t=0 expressed as F/F_0. **(A)** The effects of 0.2µM MitoQ (and dTPP/TPP$^+$) on 1mM H_2O_2-induced necrosis presented as a line graph and bar chart. **(B)** The effects of 1µM MitoQ (and dTPP/TPP$^+$) on 1mM H_2O_2-induced necrosis presented as a line graph and bar chart. Traces are averages of 9 animals. All data shown are mean ±SEM.

Figure 5.26

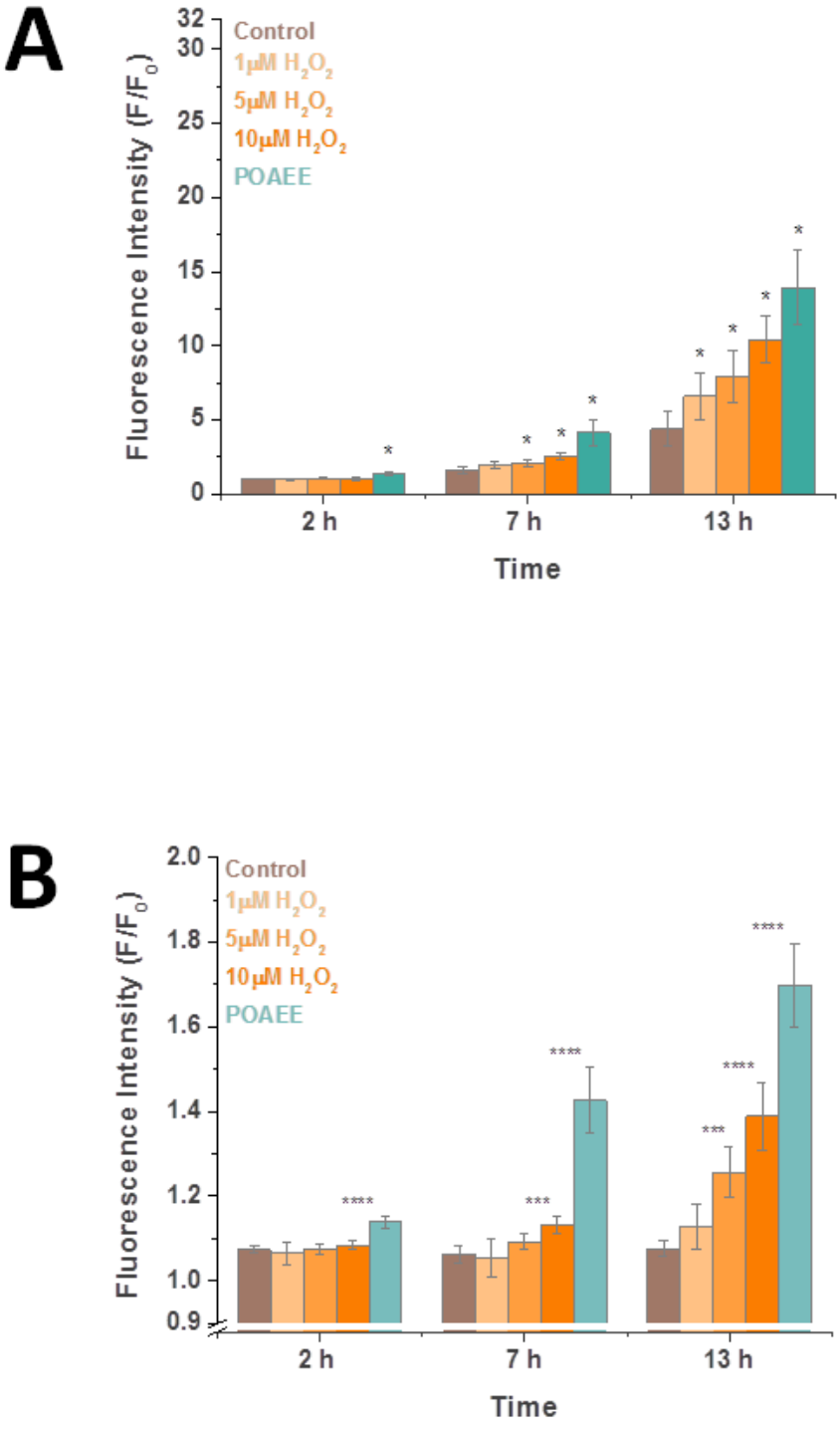

Figure 5.26. H_2O_2 and POAEE induced apoptosis and necrosis. **(A)** Comparison of 1μM, 5μM, 10μM H_2O_2, POAEE and 850mM ethanol on apoptosis, **(B)** Comparison of 1μM, 5μM, 10μM H_2O_2, POAEE and 850mM ethanol on necrosis. Traces are averages of at least 3 animals. Data has been normalised to the initial fluorescence reading t=0 expressed as F/F_0 . All data shown are mean ±SEM. * $p<0.05$, *** $p<0.001$, **** $p<0.0001$.

Discussion

ROS

Reactive oxygen species are generally thought as detrimental to cells and in disease pathology. However, it is the balance of oxidants and antioxidant status, which is critical not only to cell fate but also to the outcome of a disease. H_2O_2 is very much a Jekyll and Hyde signalling molecule. Low concentrations of the micromolar and nanomolar range play a role in signal transduction pathways (Rhee 1999; Stone et al. 2006; Millonig et al. 2012; Henriksen 2013), whereas high levels induce cellular oxidative stress, Ca^{2+} overload, mitochondrial membrane depolarisation and a depletion of ATP which would be typically followed by necrosis (Gonzalez et al. 2005; Granados et al. 2005; Bruce et al. 2007; Baggaley et al. 2008; Mankad et al. 2012). It is important to assess and understand this delicate balance in order to comprehend the consequences of antioxidant therapy and enable improved ROS mediation in oxidative stress related diseases.

H_2O_2

The action of H_2O_2 as an oxidant is generally limited to susceptible cysteine thiols and Fe-S-containing proteins. However, H_2O_2 can react with reduced iron and copper to produce $OH^{\bullet-}$ and downstream product nitric acid and peroxynitrite (Day

2011). Cellular antioxidants act to prevent elevated levels of H_2O_2 and downstream damaging effects by removing H_2O_2 and converting it to water and oxygen. This oxidant-antioxidant balance fails when oxidative stress elevates to levels the antioxidant status cannot combat and/or diminished antioxidant status. Bacteria have developed an adaptive mechanism to peroxide stress, regulating levels of Fe^{2+} to restore the equilibrium (Faulkner et al. 2011). The balance between the two factors is important in the initiation of cell-protective responses.

The mitochondria are the main source of ROS in PACs. H_2O_2 is produced in the cell via the conversion of $O_2^{\bullet-}$ either spontaneously or enzymatically by superoxide dismutases (SOD) a family of metaloenzymes (Futatsugi et al. 2005). H_2O_2 can induce apoptosis via DNA fragmentation dependent on bcl-2-like protein 4 (BAX)/BCL2-Antagonist/Killer (Bak) proteins, activation of caspase-3 and cytochrome c release (Satoh et al. 1997; Cook et al. 1999; Ryter et al. 2007). H_2O_2 can be further converted to hypochlorous acid by myeloperoxidase, a pancreatitis severity marker (Bhatia et al. 2005; Winterbourn et al. 2006). Elevated ROS production induces the activation and proliferation of immune cells particularly neutrophils, macrophages and monocytes which also produce large amounts of ROS via the NOX family, detected in patients and experimental AP models (Tsuji et al. 1994; Irani et al. 1997; Gukovskaya et al. 2002; Bedard et al. 2007).

H_2O_2 has demonstrated diverse concentration-dependent cellular effects with pathophysiological implications. H_2O_2 production is essential for normal cellular growth factor signalling and has been established as an important regulator

of cellular events in mammalian skeletal muscle. Micromolar concentrations of 30-90µM, engaged the insulin receptor substrate 1 (IRS-1)/PI3K/Protein kinase B (Akt)-dependent insulin signalling pathway and activated MAPK and p38 MAPK (Henriksen 2013). In PACs H_2O_2 (0.1-100µM) induced concentration-dependent increases in ROS production detected by CM-H_2DCFDA. Antioxidant cinnamtannin B-1 inhibited the H_2O_2-induced ROS increases and diminished both H_2O_2 and CCK induced increases in $[Ca^{2+}]_c$ demonstrating a role for H_2O_2 in Ca^{2+} mobilisation (Gonzalez et al. 2012). Heterogeneous Ca^{2+} responses have been demonstrated at <100µM H_2O_2 and inhibition of the PMCA at >50µM H_2O_2 leading to progressive increases in $[Ca^{2+}]_c$ which lead to cell necrosis (Granados et al. 2006; Baggaley et al. 2008). One millimolar H_2O_2 elicited both ER and mitochondrial Ca^{2+} release into the cytosol (Pariente et al. 2001).

In the present study we showed progressive increases in cytosolic Ca^{2+}, loss of redox potential and mitochondrial membrane depolarisation at 50-500µM. These results are complimentary to the published literature (Bruce et al. 2007; Baggaley et al. 2008). While micromolar concentrations of H_2O_2 (1µM) induced significant increases in cellular ROS over a 120 minute time period alongside an induction of apoptosis, 1µM H_2O_2 did not induce necrosis in our experiments. These results are consistent with a role of ROS in the induction of apoptosis in this cell type. Preliminary results also indicated recovery of the redox ratio with 1µM H_2O_2. Further experiments are warranted and the application of <1µM H_2O_2 could be useful to investigate specific H_2O_2 signalling pathways such as stimulation of growth factors in PACs in order to shed light on the specific role of ROS in the pancreas

(Stone et al. 2006). Application of millimolar H_2O_2 highlighted the extensive effects of overwhelming oxidant status on levels of NAD(P)H and FAD^+ critical to mitochondrial energy metabolism.

ROS and Cellular Redox Status

NAD(P)H/FAD^+ can be used as an indicator of mitochondrial redox ratio (Chance et al. 1979; Hajnóczky et al. 1995). For the first time in PACs submillimolar and millimolar H_2O_2 treatment are shown to induce mirrored concentration-dependent decreases in NAD(P)H and increases in FAD^+ levels. In isolated nerve terminals, oxidative stress induced by 50 and 100µM H_2O_2 also decreased the NAD(P)H fluorescence signal proportional to the concentration of H_2O_2 (Chinopoulos et al. 1999). H_2O_2 inhibition of the Krebs cycle enzymes was also shown to be concentration-dependent in isolated nerve terminals, inhibiting aconitase at 50µM and 100µM concentrations but α-KGDH only at the higher 100µM dose. Inhibition of aconitase by 50µM H_2O_2 had no effect on NADH(P)H levels, whereas inhibition of α-KGDH with 100µM H_2O_2 induced parallel decreases in levels of NAD(P)H (Tretter et al. 2000). The reason for this was that when α-ketoglutarate is available as a substrate, aconitase activity is not required for NAD(P)H production. Comparative TCA cycle inhibition by H_2O_2 has not yet been investigated in PACs yet. In intact cardiac mitochondria, H_2O_2 (12.5µM and 100µM) reduced NAD(P)H levels and oxygen consumption, of which NAD(P)H recovered to baseline levels with 12µM H_2O_2. These results were mirrored by reversible inhibition of succinate dehydrogenase and α-ketoglutarate dehydrogenase activity

and irreversible aconitase activity (Nulton-Persson et al. 2001). High levels of H_2O_2 were applied to rat hippocampus isolated neurons (200µM - 5mM) directly oxidising cellular NADH and $FADH_2$. In agreement with our results in PACs, 200µM-5mM H_2O_2 induced ΔΨm depolarisation (Gerich et al. 2009). Millimolar H_2O_2 treatment has also been shown to cause increases in FAD^+ in PACs, as confirmed by our results (Gonzalez et al. 2005).

MitoQ and dTPP (1µM) elicited a reduction of NAD(P)H levels in our evaluations. Here, H_2O_2 treatment exacerbated the effects of MitoQ (1µM) on the NAD(P)H/FAD^+ ratio at concentrations as low as 10µM. The effects of dTPP on NAD(P)H were also worsened by oxidant treatment. Levels of FAD^+ decreased with 10µM and 30µM H_2O_2 in combination with dTPP, not demonstrating a detectable increase until 300µM. The effect of the uncoupling agent CCCP on FAD^+ was also abolished. H_2O_2 effects on NAD(P)H/FAD^+ autofluorescence levels are in summary progressive and concentration-dependent. The effects of dTPP were non-specific and the mechanism unknown. While MitoQ has demonstrated effective protective capabilities against H_2O_2-induced ROS increases, pre-treatment proved unable to prevent oxidant induced changes to the mitochondrial redox ratio and in fact exacerbated the effects.

MPTP

MPTP opening is caused by pathological Ca^{2+} overload and leads to the non-specific permeabilisation of both inner and outer mitochondrial membranes to solutes of <1.5kDa. The resulting effects are depolarisation of the mitochondrial membrane, diminished $[Ca^{2+}]_m$ and depletion of ATP (Mukherjee et al. 2015). ATP is crucial for induction of cellular apoptosis through caspase activation and therefore ATP depletion caused by opening of the MPTP leads to necrosis (Leist et al. 1997; Nakagawa et al. 2005; Mukherjee et al. 2015). Since evidence suggests that apoptosis is a protective mechanism in AP and necrosis associated with a more severe pathology, inhibition of MPTP opening has been highlighted as a potential therapeutic target (Kaiser et al. 1995; Gukovskaya et al. 1996; Mareninova et al. 2006; Sung et al. 2009). Prevention of MPTP opening could prevent mitochondrial membrane depolarisation and ATP depletion and has been demonstrated as protective in experimental AP models (Crompton et al. 1987; Pastorino et al. 1999; Kinnally et al. 2011; Mukherjee et al. 2015). As described in the introduction chapter, the MPTP is thought to be formed between adjacent F_0 sectors of F_0F_1-ATP synthase complex dimers (Strauss et al. 2008; Bernardi 2013; Giorgio et al. 2013) and in response to Ca^{2+} overload matrix CypD regulates MPTP opening by binding to the F_0F_1-ATP synthase lateral stalk, an action requiring Pi (Bernardi 2013; Giorgio et al. 2013). Elevated levels of ROS have been suggested to further sensitise the MPTP to Ca^{2+} through cross-linking two thiol groups of adenine nucleotide translocase (ANT) near the adenine nucleotide binding site, antagonising adenine nucleotide binding to ANT (McStay et al. 2002). CypD is a non-structural pore component and

therefore a promising pharmacological target for AP drug development. Inhibition of MPTP formation in CypD KO mice and with CypD inhibitor CsA, prevented ΔΨm depolarisation, ATP depletion and necrosis induced by Ca^{2+} overload and elevated ROS levels (Baines et al. 2005; Shalbueva et al. 2013). Antioxidant treatment has also demonstrated the ability to reduce MPTP opening and cell death in kidney injury (Mitchell et al. 2011), cardiac ischemia/reperfusion injury (Hansson et al. 2015) and the isolated heart (Davidson et al. 2012). More specifically treatment with antioxidant DecylQ reduced MPTP opening which prevented dissipation of ΔΨm (Fontaine et al. 1998). More recent therapeutic approaches continue to demonstrate promise through the specific inhibition of CypD or MPTP opening.

Our results demonstrate that ΔΨm depolarisation induced by high levels of oxidative stress (1mM H_2O_2) is not reduced in CypD KO mice, suggesting that ROS do not play a pivotal role in PAC MPTP formation. 1mM H_2O_2-induced NAD(P)H depletion was very slightly worsened and increases in cellular ROS levels were elevated. H_2O_2 (1mM)-induced effects on NAD(P)H levels and ΔΨm are very rapid and have a variety of non-specific damaging effects on cellular components and membranes. Therefore it is also possible that any protection provided by inhibition of MPTP opening is not visible when applying high concentrations of H_2O_2. To date, little is known of any possible concentration-dependent effects of H_2O_2 on CypD MPTP opening. These experiments would require a more detailed assessment at lower concentrations of H_2O_2. More recent studies in mouse and human PACs demonstrate that CypD inhibition with CsA and BKA had protective effects. Both CsA and BKA treatment protected against mitochondrial impairment and necrosis

caused by TLCS and CCK-induced rises in intracellular Ca^{2+}. (Mukherjee et al. 2015). TLCS-induced rises of ROS were not different from the wild-type control and therefore ruled out as a protective mechanism through induction of apoptosis. CypD inhibition with non-immunosuppressive D-MeAla3-EtVal4-cyclosporine (Alisporivir, DEB025) (Zorov et al. 2009) and inhibition of MPTP opening with 3,5-Seco-4-nor-cholestan-5-one oxime-3-ol (TRO40303) (Schaller et al. 2010) also demonstrated protective effects of the same nature. In comparison to liver mitochondria, PAC mitochondria possess a heightened sensitivity to Ca^{2+}-induced depolarisation through MPTP opening (Odinokova et al. 2009; Gukovskaya et al. 2011). The specific mechanisms for MPTP opening in PACs could be also different to that seen in other cell types. A recent study in human embryonic kidney 293 (HEK 293T) cells has proposed that CypD is a regulator of mitochondrial gene expression (Radhakrishnan et al. 2015). The authors demonstrated CypD interaction with transcription factor B2, mitochondrial (TFB2M). Silencing of CypD lead to a down-regulation of NADH dehydrogenase 1 (ND1), cytochrome oxidase 1 (COX1) and ATP synthase subunit 6 (ATP6). Mitochondrial membrane potential was also reduced, alongside diminished oxygen consumption and results suggesting down regulation of electron transport complexes. Further work could be carried out to assess these effects of CypD KO in PACs.

Apoptosis and Necrosis

There is now strong evidence for the concentration-dependent promotion of apoptosis and necrosis by ROS in PACs. Here, low micromolar concentrations (1-10µM) of H_2O_2 favour induction of apoptosis whilst high submillimolar and millimolar concentrations (500µM-1mM) favour necrosis. The induction of both modes of cell death occurred rapidly with high submillimolar and millimolar concentrations of H_2O_2. Low micromolar concentrations promoted a gradual induction of cell death with a delayed onset. Further studies would need to be carried out to compare the number of cells undergoing apoptosis versus necrosis in comparison to the total cell count by applying the confocal assessment technique employed by Booth et al. (2011). In comparison to the effects in other cell types, Hampton et al. (1997) demonstrated that 50µM-500µM H_2O_2 had two distinct effects in Jurkat T-lymphocytes. Caspases were activated 3 hours post treatment with lower concentrations of H_2O_2 such as 50µM and led to apoptosis. In comparison, treatment with high concentrations of H_2O_2 such as 500µM did not lead to the activation of caspases or they remained inactive and necrosis occurred (Hampton et al. 1997). Building on this study, Saito et al. (2006) demonstrated that while activation of caspases-3 and -9 was observed with 50µM H_2O_2 treatment and not 500µM H_2O_2, release of cytochrome c from the mitochondria occurred under both treatment concentrations. Furthermore, in concurrence with these results, depletion of ATP, essential for apoptosome formation, occurred only with the higher concentration of 500µM H_2O_2, resulting in necrosis. A study in cultured mammalian fibroblasts treated with low micromolar concentrations of H_2O_2 (0.1 to

0.5µmol/10^7 cells caused mitogenic responses. Raising the concentration to 15 to 30µmol/10^7 cells led to apoptosis, and necrosis was caused by concentrations of over 150 to 300µmol/10^7 cells (Davies 1999).

MitoQ has demonstrated effectiveness at inhibiting H_2O_2-induced ROS increases and cell death in alternate cell types (Kelso et al. 2001; Chen et al. 2004; Dhanasekaran et al. 2004; James et al. 2005). However, MitoQ did not prevent H_2O_2-induced cell death in PACs. We have demonstrated that continuous perfusion for 30 minutes with 1mM H_2O_2 induced a large increase in ROS detectable by CM-H_2DCFDA and effectively inhibited by 1µM MitoQ (Figure 3.3). These results are confirmed in our plate reader experiments over a longer time period of 120 minutes in a concentration and pre-treatment dependent manner (Figures 5.11, 5.12 and 5.13). However, MitoQ proved ineffective at protecting against H_2O_2-induced cellular necrosis and apoptosis in PACs.

The induction of oxidative stress is also dependent on the stimulus. Toxic concentrations of CCK and EtOH induced a short term elevation of ROS levels in PACs, whereas POAEE and high concentrations of H_2O_2 induced progressive long term increases in ROS. H_2O_2 at 500µM and TLCS treatment predominantly induced necrosis. On the other hand, POAEE and CCK induced both apoptosis and necrosis, highlighting the different extent of effects between these treatments. In contrast to POAEE however, CCK-induced effects on ROS elevations were relatively short lasting

(Figure 5.14). ROS production induced by CCK (Granados et al. 2004), TLCS (Booth et al. 2011), EtOH (González et al. 2006) and POAEE (Criddle et al. 2007) has been demonstrated in PACs, although to date this study provides the first comparative assessment.

In the clinical setting, AP therapy cannot be commenced prophylactically; therefore therapeutic methods are constrained to inhibition of particular pathophysiological steps. While antioxidants have demonstrated some beneficial effects with prophylactic application in experimental AP, there was a failure to improve experimental pancreatitis severity when therapy was applied post onslaught (Demols et al. 2000). Our experiments support the lack of protection offered by antioxidants unless administered prophylactically, as MitoQ was unable to effectively inhibit high submillimolar and millimolar induced ROS increases without adequate pre-treatment.

Conclusions

In summary, this section evaluated the novel comparative effects of low micromolar to millimolar H_2O_2 on NAD(P)H/FAD^+ redox ratio, cytosolic Ca^{2+}, membrane potential, ROS levels and cell death in PACs. ROS have long been held in a negative light and thought of as deleterious detrimental by-products of mitochondrial energy production (Finkel 1998). There is now ample evidence demonstrating the crucial role of ROS in normal cellular processes such as signal transduction and induction of apoptosis, which can be protective in the development of AP (Booth et al. 2011). These effects are concentration-dependent due to the delicate oxidant/antioxidant balance in the cell and thus not only excessive oxidant levels but excessive antioxidant levels via therapeutic intervention have the potential to interfere pathologically in a detrimental manner. MitoQ provided a lack of protection against H_2O_2-induced effects and reduction of H_2O_2-induced ROS increases was not only concentration-dependent but also dependent on the time period of MitoQ pre-treatment.

Chapter 6

General Discussion

The Effects of Mitoquinone on Murine Pancreatic Acinar Cells

The effects of mitochondria-targeted antioxidant MitoQ on PACs were assessed in comparison to non-antioxidant moiety control dTPP and a basic TPP^+ derivative. This was in order to shed light on the contradictory effects of general and targeted antioxidants in experimental evaluations, with unsuccessful translation to the clinic (Uden et al. 1990; Katsinelos et al. 2005; Bjelakovic et al. 2007; Siriwardena et al. 2007; Besselink et al. 2008; Sateesh et al. 2009; Bansal et al. 2011). Oxidative stress occurs early in the development of AP. In response to known AP precipitants, oxidative stress and elevated levels of ROS in PACs have been successively and repeatedly demonstrated in a number of studies (Granados et al. 2004; González et al. 2006; Palmieri et al. 2007; Fernandez-Sanchez et al. 2009; Booth et al. 2011). An imbalance between ROS and endogenous antioxidants has been linked to an elevated disease severity (Tsai et al. 1998). However, as discussed earlier, the application of general antioxidants has shown mixed effects in isolated cells, animal models and in the clinic. This led to the development of more specific antioxidants targeted to the predominant source of ROS production, the mitochondria. These were readily diffusible with improved tissue penetration. Theoretically these targeted antioxidants would more effectively reduce elevated levels of ROS associated with the development of oxidative stress related disorders such as AP. MitoQ has to date been shown to exert protective effects in diverse disease models that are associated with oxidative stress, including colitis (Dashdorj

et al. 2013), encephalomyelitis (Davies et al. 2013), cardiac ischaemia-reperfusion injury (Chouchani et al. 2013), and sepsis (Lowes et al. 2013). However, concern has developed for MitoQ as an antioxidant therapy. This is due to limited therapeutic benefits and evidence demonstrating adverse effects at both the cellular level and in clinical trials (Gane et al. 2010; Snow et al. 2010; Reily et al. 2013). Although some recent work has investigated the adverse effects of mitochondrial targeted compounds, a deeper understanding of the effects in PACs is lacking (Reily et al. 2013; Trnka et al. 2015). Until recently, the effects of MitoQ had not been assessed in *in vivo* and *in vitro* models of acute pancreatitis (Huang et al. 2015).

MitoQ and NAD(P)H/FAD$^+$ Levels

In vitro, MitoQ effectively inhibited H_2O_2-induced ROS increases in PACs. However, there were also effects on mitochondrial bioenergetics, represented by a transient increase and progressive depletion of NAD(P)H. These results were mirrored by an elevation of oxidised FAD^+. In summary, MitoQ exhibited progressive alterations of the redox state, which were mirrored by non-antioxidant analogue dTPP. On the other hand, the MitoQ-induced elevation of FAD^+ levels was not mirrored with dTPP treatment. The differing cellular effects of the targeting component/acyl chain and antioxidant quinone group *in vitro* support our *in vivo* findings and those of recent cellular studies, which will be detailed in the remaining discussion (Huang et al. 2015; Trnka et al. 2015).

One proposal for the transient increase in NAD(P)H levels is a transient inhibition of ETC complex I, during accumulation of MitoQ and dTPP into the mitochondria. The depletion of NAD(P)H is likely to be as a result of mild uncoupling effects of the TPP^+/acyl chain leading to an increase of NAD(P)H oxidation as a compensatory mechanism. The extent of the TPP^+/acyl chain effects are thought to be dependent on the length of the acyl chain and hydrophobicity (Trnka et al. 2015). In contrast, there is also evidence for increased ETC complex I activity with both MitoQ and dTPP in articular cartilage which would lead depleted levels of NAD(P)H (Martin et al. 2012). MitoQ is continuously recycled by complex II of the ETC (Kelso et al. 2001). Therefore, the increase in oxidised FAD^+, not present with dTPP treatment, is likely due to up-regulated $FADH_2$ consumption to facilitate recycling of the antioxidant component of MitoQ.

MitoQ and $[Ca^{2+}]_i$

The transient increase in NAD(P)H with both MitoQ and dTPP treatment could also be a Ca^{2+}-dependent mechanism due to non-specific effects of the targeting component and/or the acyl chain. An increase in cytosolic Ca^{2+} leads to an uptake of Ca^{2+} by the mitochondria. The subsequent increase in $[Ca^{2+}]_m$ activates TCA cycle dehydrogenases, and is visualised by an increase in levels of NAD(P)H (Voronina et al. 2002). MitoQ and dTPP treatment caused an increase in $[Ca^{2+}]_c$ alongside a transient increase in NAD(P)H. Therefore, we assessed elevated levels of $[Ca^{2+}]_m$. However, employment of the dye Rhod-2-AM did not identify any increases

of fluorescence. This technique has been successful in detecting mitochondrial Ca^{2+} rises in PACs by several groups including our own (Gonzalez et al. 2000; Camello-Almaraz et al. 2002; Johnson et al. 2002; Voronina et al. 2002; Booth et al. 2011). The changes in $[Ca^{2+}]_c$ and NAD(P)H induced by MitoQ were very small. It is possible that any increases in $[Ca^{2+}]_m$ were not detected due to a lack of sensitivity of the Rhod-2-AM dye at detecting fluctuations of this size. Employment of a more sensitive technique such as patch clamp may highlight any increases. A transient NAD(P)H increase, could also be due to inhibitory effects by the targeting component on the mitochondrial Na^+/Ca^{2+} exchanger, as demonstrated in HeLa cells (Leo et al. 2008). This would prevent efflux of Ca^{2+} from the mitochondria leading to raised matrix Ca^{2+} concentrations and therefore NAD(P)H (Leo et al. 2008).

As mentioned, it is also possible that there is a transient inhibition of ETC complex I by MitoQ and dTPP, leading to increases in NAD(P)H, as demonstrated in PACs with complex I inhibitor rotenone (Voronina et al. 2002). ETC inhibition with rotenone can induce a rise in $[Ca^{2+}]_c$ due to a reduced electrical gradient and therefore diminished mitochondrial Ca^{2+} uptake (Johnson et al. 2002; Nguyen et al. 2009; Gravina et al. 2010; Takekawa et al. 2012). Inhibition of all four ETC complexes by lipophilic triphenylphosphonium cations has been shown in rat skeletal muscle, with a particular sensitivity of complexes I and III (Trnka et al. 2015). Therefore, the transient increase in $[Ca^{2+}]_c$ induced by both MitoQ and dTPP could be due to non-specific inhibitory effects of the targeting component on the ETC, leading to reduced uptake of Ca^{2+} into the mitochondria. While MitoQ and

dTPP caused a transient increase in $[Ca^{2+}]_c$, neither compound demonstrated any effects on ER Ca^{2+} release in response to CCK hyperstimulation. MitoQ has previously been shown to inhibit Ca^{2+} oscillations induced by CCK (Camello-Almaraz et al. 2006) and prevent MPTP opening (Lu et al. 2007; Davidson et al. 2012). These effects were suggested to be due to the antioxidant activity, however, evidence in this thesis highlight an additional mechanism of action, potentially attributed to the targeting component on the ETC, as opposed to the antioxidant ubiquinone of MitoQ.

As detailed, MitoQ and dTPP did not affect ER Ca^{2+} release in response to CCK hyperstimulation. However, ER Ca^{2+} measurements were not made during MitoQ and dTPP perfusion as previously employed for cytosolic Ca^{2+} measurements. Therefore, future experiments would analyse the effects of MitoQ and dTPP on ER Ca^{2+} to mirror the cytosolic Ca^{2+} measurements. It would then be prudent to perform experiments with $0Ca^{2+}$ in the extracellular solution during MitoQ and dTPP treatment. The aim of these experiments would be to establish if the MitoQ/dTPP-induced transient elevation in $[Ca^{2+}]_c$ is extracellular in origin due to Ca^{2+} influx across the plasma membrane. The progressive and continued increase in $[Ca^{2+}]_c$ with dTPP but not MitoQ could be due to the TPP^+ component or acyl chain and would also require investigation. Therefore, incorporating TPP^+ into further experiments would help to elucidate the specific effects. Subsequent experiments would also use $0Ca^{2+}$ media and include ER store depletion with plant sesquiterpene lactone thapsigargin prior to PAC treatment with MitoQ/dTPP/TPP^+. These

experiments could rule out or establish the ER as the source or suggest a mitochondrial or non-mitochondrial Ca^{2+} source. The application of BAPTA-AM could abolish the transient increase in NAD(P)H and therefore rule out uptake of cytosolic Ca^{2+} as a cause and support the ETC inhibition theory.

The Effects of Excessive MitoQ Accumulation

Application of both MitoQ and dTPP at 10µM caused partial mitochondrial depolarisation and eliminated any inhibitory effects of MitoQ on H_2O_2-induced ROS increases. These results support mild uncoupling effects of TPP^+ derivatives observed in alternative cell types (Echtay et al. 2002; Fink et al. 2009; Reily et al. 2013), which could indicate a protonophoric effect. However, the gradual depolarisation observed with both MitoQ and dTPP would suggest more complex metabolic effects contributing to proton leak, such as by matrix and inter-membrane space cycling or protein interactions (Ross et al. 2008; Reily et al. 2013).

The Effects of MitoQ on Apoptosis and Necrosis

All three TPP^+ derivatives assessed (MitoQ, dTPP and TPP^+) induced concentration-dependent induction of cell apoptosis and necrosis. This was initially believed to be indicative of nonspecific toxic effects due to accumulation of fatty acyl chains in the mitochondria that may relate to uncoupling actions (Borst et al.

1962; Smith et al. 2003). The justification for this proposal was that fatty acids are known to uncouple oxidative phosphorylation, and application of long-chain fatty acids to isolated PACs cause mitochondrial depolarisation, loss of NAD(P)H and ATP, leading to necrosis (Criddle et al. 2004; Criddle et al. 2006). This proposal however, did not encompass the basic TPP^+ derivative, which does not possess a fatty acyl chain. It can be suggested that the effects on pancreatic acinar cell death are likely due to the triphenylphosphonium cation. However, a role of the fatty acyl chain in the cellular effects cannot be ruled out and further experiments would need to be completed including the TPP^+ component and dUb, which does not contain the TPP^+ component. For example, the comparative effects of TPP^+ to dTPP and dUb could be assessed on membrane depolarisation and levels of NAD(P)H.

Conclusions

The proposal of a central TPP^+ involvement in the described effects of MitoQ is in concurrence with studies using a variety of TPP^+ derivatives. These results have demonstrated a sensitivity of cellular bioenergetics to the TPP^+ cation and the acyl chain, leading to inhibition of ETC complexes, mild mitochondrial uncoupling and inhibition of mitochondrial Ca^{2+} efflux (James et al. 2005; Leo et al. 2008; Fink et al. 2009; Reily et al. 2013; Trnka et al. 2015). The study by Trnka et al. (2015) showed that acyl chain containing TPP^+ derivatives inhibit all four ETC complexes with complexes I and III being most sensitive. Therefore, in PACs, cell specific effects of TPP^+, acyl chain and antioxidant group could be investigated in comparison to

known ETC inhibitors rotenone (complex I), malonate (complex II) and antimycin A (complex III). It has also been shown that the nonspecific mild uncoupling effects of the TPP^+ derivatives led to a rapid increase in proton production rate, an indicator of glycolysis. The authors proposed that the up-regulation of glycolysis is a compensatory mechanism for loss of ATP production (Reily et al. 2013). MitoQ-induced depletion of ATP has also been demonstrated in articular cartilage (Martin et al. 2012). ATP measurements could be assessed during treatment with MitoQ, dTPP and TPP^+, employing magnesium green for indirect cytosolic measurements with or without ATPase inhibitor oligomycin. It is clear from the described data that there are effects of the TPP^+ group on cellular bioenergetics with an additional specific sensitivity to the acyl linker and hydrophobicity of the conjugated chain or group. The effects of MitoQ on cellular respiration could be assessed using the Seahorse XF flux analyzer (Reily et al. 2013; Trnka et al. 2015). The above detailed effects are the main limiting factors for therapy with TPP-derived antioxidants.

Protective Capabilities of MitoQ against Toxin-Induced Effects on PACs

MitoQ has undergone two phase II clinical trials, a double-blind, placebo-controlled study in Parkinson's disease (Snow et al. 2010) and a double-blind, randomized, placebo-controlled trial in patients with a documented history of

chronic HCV infection (Gane et al. 2010). A phase II study to compare MitoQ and placebo to treat non-alcoholic fatty liver disease was terminated due to poor patient recruitment. The phase II study of hepatitis C was the first report of potential beneficial effects of MitoQ treatment in humans. Patients were randomized 1:1:1 to receive either 40mg or 80 mg MitoQ, or placebo for 28 days. Results from both treatment groups demonstrated decreased serum alanine transaminase (ALT), an indicator of liver damage. However, there was no effect on viral load, indicating MitoQ treatment reduced liver damage but with no effect on viral replication. Thirteen patients from the 80mg MitoQ group withdrew due to adverse effects compared with 1 receiving placebo and 2 from the 40mg MitoQ group (Gane et al. 2010). The large study in Parkinson's disease (PD) enrolled 128 newly diagnosed untreated PD patients and administered 40 or 80mg/day MitoQ for 12 months (Snow et al. 2010). This study showed no difference between MitoQ and placebo groups regarding disease progression as measured by the Unified Parkinson Disease Rating Scale. Over 15% of patients exhibited unexplained dose dependent nausea and vomiting not anticipated from Phase I studies or the study by Gane et al. (2010). Therefore, the study was not continued to Phase III. The primary sponsor of both trials, Antipodean Pharmaceuticals, continues product development of mitochondrial targeted antioxidant compounds which include Mitotocopherol, Mitoascorbic acid and Mitolipoic acid. More recently, the University of Delaware has sponsored a phase IV clinical trial, which commenced March 2015 to examine the effects of MitoQ on vascular function in patients with moderate to severe chronic kidney disease.

TLCS and Caerulein Models of AP

To investigate the potential efficacy of MitoQ in acute pancreatitis, two established experimental models of AP were employed: caerulein-induced (CER-AP) and bile acid TLCS-induced (TLCS-AP). Caerulein analogue CCK hyperstimulation and TLCS treatment *in vitro* have been shown to induce ROS increases and Ca^{2+} overload, although via separate mechanisms detailed earlier (Saillan-Barreau et al. 1998; Voronina et al. 2002; Granados et al. 2004; Barrow et al. 2008; Booth et al. 2011). *In vivo,* the CER-AP model is a popular non-invasive method, which induces acute interstitial acute oedematous pancreatitis, closely resembling that in humans (Lerch et al. 1994; Saluja et al. 2007; Lerch et al. 2013). CER-AP benefits from its reproducibility and convenience, although is not likely to imitate mechanisms responsible for the pathogenesis (Takacs et al. 2008; Ziegler et al. 2011). CER-AP is self-limited and reversible, characterised by sustained intracellular Ca^{2+} rises, pancreatic oedema, premature zymogen activation due to impaired cytoskeleton integrity and systemic inflammatory response (Lerch et al. 1993; Lerch et al. 1994; Halangk et al. 2000; Krüger et al. 2001; Mooren et al. 2001; Halangk et al. 2002; Lerch et al. 2002; Schnekenburger et al. 2005). Caerulein pancreatitis has also been demonstrated to induce early stress-activated protein kinases (SAPK) activation, acinar glutathione depletion, and diminished ATP and tissue necrosis (Schoenberg et al. 1991; Luthen et al. 1995; Grady et al. 1996).

In vivo, experimental biliary acute pancreatitis can be induced by infusion of retrograde ductal taurocholate into the pancreatic duct, or more acutely retrograde injection into the hepatopancreatic duct, leading to the development of haemorrhagic and necrotising pancreatitis. This model is highly reproducible and a clinical parallel to gallstone obstruction associated AP, which accounts for 30 – 50% of AP cases (Wan et al. 2012). Experimental biliary acute pancreatitis has been extensively used to investigate AP associated with multiple organ dysfunction, including lung injury, a major cause of early death in patients (Lichtenstein et al. 2000). Bile acid-induced haemorrhagic pancreatitis is characterised by zymogen degranulation, oedema, haemorrhage and rapid necrosis of the pancreatic tissue, and elevated amylase and lipase levels (Steer et al. 1991; Su et al. 2006; Wan et al. 2012).

TLCS- and CCK-Induced Apoptosis and Necrosis

While CER-AP induces a comparatively mild self-limiting disorder, TLCS-AP causes a severe necrotising, haemorrhagic pancreatitis that reaches maximal severity within 24 h post-induction in mice (Perides et al. 2010). In TLCS-induced pancreatitis, but not caerulein-induced Gpbar1 (G-protein-coupled, cell surface bile acid receptor) is expressed at the apical pole of acinar cells. Gpbar1 genetic deletion is correlated to reduced inflammation, oedema, hyperamylasemia, reduced pathological Ca^{2+} overload, intracellular activation of zymogens and PAC injury in

TLCS-induced pancreatitis, but not caerulein-induced (Perides et al. 2010). A study by Schoenberg et al. (1991) compared the pathology of CER-AP in rats (5 micrograms/kg/h) and sodium taurocholate-induced-AP by retrograde injection of 5% sodium taurocholate for 30 min, 3.5 h, and 12 h. Histological and serum enzyme levels were similar between the two models. However, the development with TLCS was more traumatic and rapid with extensive cellular necrosis and zymogen degranulation after 3.5 h and amylase levels elevated to 6 times those of the caerulein AP model. These observations are concurrent with the level and rapid increase of TLCS-induced necrosis shown in our pancreatic acinar cell suspensions, compared to near negligible TLCS-induced apoptosis. The induction of pancreatic acinar cell necrosis with CCK hyperstimulation in pancreatic acinar cell suspensions was mild and biphasic and reached a plateau within around 3-4 h with a secondary increase of necrosis at 10-13.5 h.

In the study by Schoenberg et al. (1991), CER-AP caused elevated levels of conjugated dienes and malondialdehyde, which reached their maximum after 3.5 h. At this time point, levels of interstitial oedema and intravascular granulocyte margination in the pancreatic gland were initially observed. Pronounced zymogen degranulation, tissue necrosis and granulocyte migration into the tissue was not observed until after 12 hours. In our plate reader experiments, CCK induced apoptosis in a progressive trend that reached a significant increase from the control at approximately 2 h post stimulation. Our results also compliment the study by Gukovskaya et al. (2002), which detected apoptosis through activated caspases-3, -

8, and -9 at 3 hours post stimulation. Our results are not only novel, demonstrating the contrasting effects of TLCS and CCK hyperstimulation on cell death, but provide exciting parallels to the *in vivo* observations. These results may provide further evidence for a proposed protective role of apoptosis in the severity of AP, since necrosis is reduced (Booth et al. 2011).

The Effects of MitoQ *in vivo* on TLCS-AP and CER-AP

MitoQ demonstrated no protective capabilities against AP induced by the precipitant TLCS *in vivo* and *in vitro* and mixed effects against both caerulein and analogue CCK. MitoQ partially ameliorated overall pancreatic histopathology in CER-AP, reducing pancreatic oedema and neutrophil infiltration but not biochemical markers pancreatic trypsin or serum amylase. However, these beneficial effects were also shared by non-antioxidant moiety control dTPP. In addition, dTTP unexpectedly reduced tissue necrosis, pancreatic trypsin and MPO activity. MitoQ also aggravated systemic injury, inducing concurrent increases in lung MPO and IL-6. *In vitro*, both MitoQ and dTPP abolished CCK induced NAD(P)H rises and exacerbated CCK induced cell death. In the TLCS-induced AP model MitoQ treatment was not protective (Huang et al. 2015), mirrored in the current *in vitro* experiments of this study.

The Role of Leukocyte and Neutrophil Infiltration in AP

Leukocyte and neutrophil infiltration are well known to play a central role in ROS production associated with the development of acute pancreatitis, systemic inflammatory response syndrome and lung injury (Sarr et al. 1987; Rinderknecht 1988; Guice et al. 1989; Simms et al. 1994; Inagaki et al. 1997; Rau et al. 2000; Gukovskaya et al. 2002; Mayerle 2009). Polymorphonuclear leukocytes (PMNs) are granulocytic leukocytes and have been suggested to contribute to organ dysfunction in acute pancreatitis (Sarr et al. 1987; Rinderknecht 1988; Simms et al. 1994; Oiva et al. 2013). The PMNs, which account for about 60% of leukocytes, are essential for innate immunity and one of earliest inflammatory cells to arrive at the infection/injury site (Brinkmann et al. 2007). In the experimental AP models, histology indicated that PMNs accumulated moderately within the pancreas 2 hours post induction and were abundant at 6 hours. In clinical acute pancreatitis, enrolment and infiltration of PMNs in the pancreas and distant organs are a principal feature of the disease (Mayerle 2009). PMNs may further aggravate tissue injury by releasing ROS that are generated by NAD(P)H oxidase (Gukovskaya et al. 2002) or by degranulation and release of their nuclear contents to form extracellular traps (Brinkmann et al. 2004). Serum IL-6, mainly secreted by myeloid cells including PMNs, is a cytokine known to connect pancreatic injury to distal organ damage (Zhang et al. 2013) and also serves as a severity marker for human AP (Aoun et al. 2009).

The Effects of MitoQ on PMN ROS generation

In vivo, activation of NAD(P)H oxidase in isolated PMNs was induced by 50ng/mL phorbol myristate acetate (PMA), causing a dramatic increase of ROS in the extracellular solution around PMNs. PMA is a PKC agonist and results in increased neutrophil superoxide production . The increase in ROS peaked within a few minutes and declined to a plateau after approximately 20 minutes. Application of NAD(P)H oxidase inhibitor diphenylene iodonium (DPI) reduced the PMA-induced ROS peak and abolished the plateau. MitoQ caused biphasic effects on the PMA-induced ROS production and plateau. At first a concentration-dependent inhibition of the initial ROS peak was observed. This was followed by a concentration-dependent elevation of the ROS plateau at 40 min, an action shared by dTPP only at the higher concentration (10µM). Thus, an overall increase in ROS production in the PMNs induced by MitoQ and dTPP may have facilitated lung MPO, generating hypochlorous acid and reactive oxidants, further enhancing its activity. Indeed, both MitoQ and dTPP at the doses used for the *in vivo* experiments significantly increased lung MPO activity *per se*.

The Effects of Ethanol and POAEE on Apoptosis and Necrosis

PACs metabolise alcohol to produce FAEEs at levels adequate to induce damage to the pancreas (Haber et al. 2004). Although it is evident that there is patient-specific susceptibility to excessive drinking, it is unclear why not all heavy

drinkers develop AP (Criddle 2015). Here, an improved method was developed for maintaining POAEE in aqueous solution for long term assays. This allowed for the use of a lower concentration of ethanol (85mM) and an optimised ethanol to non-oxidative metabolite POAEE ratio for maximum POAEE-derived cell death. For the first time in PACs, the comparative effects of POAEE and ethanol on apoptosis and necrosis were evaluated applying long time course plate reader experiments. POAEE substantially induced both apoptosis and necrosis over a 13 hour period. Ethanol at 850mM also induced extensive cell death of both modes.

The 850mM Ethanol and POAEE necrosis results are in agreement with a one hour end point necrosis assay, quantified by inspection of light-transmitted images (Criddle et al. 2004). POAEE was shown to induce necrosis in a Ca^{2+}-dependent manner primarily through IP_3R-mediated Ca^{2+} release from the ER (Criddle et al. 2004; Criddle et al. 2006). On the other hand, ethanol of concentrations up to 850mM showed little or no increases in $[Ca^{2+}]_i$. It was concluded that pancreatic acinar cell toxicity was mediated by nonoxidative fatty acid metabolites, rather than ethanol itself. While POAEE and POA caused Ca^{2+} toxicity via depleted ATP levels, ethanol did not (Criddle et al. 2006; Voronina et al. 2010). In addition, ethanol at 10mM did not induce apoptosis or necrosis above control values (Huang et al. 2014). Ethanol/palmitoleic acid-induced necrosis was prevented by 3-benzyl-6-chloro-2-pyrone (3-BCP), an inhibitor of carboxylester lipase (CEL), an enzyme synthesized and secreted by acinar cells (Huang et al. 2014). Non-oxidative ethanol metabolism generates FAEEs through the action of FAEE synthases such as

carboxylester lipase. FAEEs principally accumulate in PAC mitochondria where they are hydrolysed into FAs (Huang et al. 2014), in agreement with an earlier biochemical study in cardiomyocytes (Lange et al. 1983).

The Effects of MitoQ on Ethanol/POAEE-Induced Cell Death

MitoQ demonstrated some protective capabilities against POAEE-induced cell apoptosis in a dose dependent manner, offering protection at the lower concentration of 0.2µM. MitoQ also demonstrated very mild inhibition of ethanol-induced cell apoptosis in the same manner to the POAEE-induced effects. The reduction of apoptosis by MitoQ could be due to the antioxidant activity. Ethanol-induced ROS production has been demonstrated in PACs (Wittel et al. 2003; González et al. 2006). These results are in concurrence with MitoQ inhibition of TLCS-induced apoptosis demonstrated by Booth et al. (2011). As apoptosis has been highlighted as a protective mechanism in AP, inhibition by MitoQ does not suggest benefits of MitoQ targeted antioxidant therapy in alcoholic AP.

Conclusions

In summary, CER-AP is a non-invasive model of acute pancreatitis, which produces a mild, self-limiting and reversible disease. (Lerch et al. 1993; Lerch et al. 1994). Bile acid treatment induces a severe AP pathology and is characterised by tissue necrosis, leukocyte infiltration, oedema, and haemorrhage (Yagci et al. 2004).

The severity of AP correlates with the extent of necrosis, and the balance between the two modes of cell death, apoptosis and necrosis, may prove critical to the disease outcome (Gukovskaya et al. 2006). For example, the severity of caerulein-induced pancreatitis is reduced when apoptosis is enhanced. Inhibition of caspase activity and apoptosis, lead to the development of a severe necrotising pancreatitis (Bhatia et al. 1998). Our long time-course apoptosis and necrosis assay supported these *in vivo* findings. The plate reader method applied is a faster, higher throughput assay than previously employed fluorescence microscopy cell counting. The technique allows for a long time course assessment of cell death and therefore enables improved comparison to *in vivo* findings. TLCS-induced a predominantly necrotic mechanism of cell death which compliments short time point confocal experiments performed by Booth et al. (2011). MitoQ does not provide protection against mild, self-limited caerulein/CCK or severe TLCS-induced effects in AP *in vitro* or *in vivo*.

H_2O_2-Induced Effects on Pancreatic Acinar Cells

Oxidative stress plays a role in the development of a range of diseases such as neurodegenerative diseases, cardiovascular disease, cancer and lung diseases (Schulz et al. 1999; Madamanchi et al. 2005; Park et al. 2009; Uttara et al. 2009; Reuter et al. 2010). It is established that ROS and oxidative stress are involved in the development and severity of acute pancreatitis (Schoenberg et al. 1990; Tsai et al.

1998; Telek et al. 2001). Oxidative stress occurs early in the progression of AP alongside an oxidant/antioxidant imbalance (Braganza et al. 1995; Tsai et al. 1998). However, attempts to restore the depleted levels of antioxidants have produced mixed results in the clinic (Virlos et al. 2003; Siriwardena et al. 2007). It is apparent however, that ROS can bring about not only irreversible but reversible alterations to protein function in response to physiological stimuli (Weber et al. 1998; Nulton-Persson et al. 2001; Granados et al. 2004; Rigoulet et al. 2011). These actions enable ROS mediation of signalling pathways as detailed previously (Trimm et al. 1986; Suzuki et al. 1997; Denu et al. 1998; Finkel et al. 2000; Pelletier et al. 2012; Pérez et al. 2015).

It is crucial we understand this balance, as although oxidative stress has been researched to a variety of levels in oxidative stress related diseases, our understanding is still lacking, and antioxidant therapy in acute pancreatitis has been largely unsuccessful (Virlos et al. 2003; Siriwardena et al. 2007; Sateesh et al. 2009; Bansal et al. 2011). Historically, attention was predominantly focussed on the negative effects of oxidative stress and the pathophysiological role of ROS (Gerschman et al. 1954; Radi et al. 1991). The effects of oxidative stress have been commonly assessed through stimulating increased cellular oxidant production (Turrens et al. 1982; Sanfey et al. 1984; Sanfey et al. 1985).

The Role of ROS in the Development of AP

More recent redox studies *in vitro* have frequently used exogenously applied hydrogen peroxide to investigate the effects of oxidative stress. H_2O_2 is predominantly the oxidant of choice due to continuous production in the mitochondria through aerobic metabolism and because of its lack of charge, enables relatively easy diffusion across cellular membranes (Chance et al. 1979) which can be aquaporin-facilitated (Bertolotti et al. 2013; Bienert et al. 2014). Generally, these results supported clinical observations as high levels of oxidants cause extensive cellular damage. These actions are through Ca^{2+} overload, irreversible damage to nuclear and mitochondrial DNA, proteins and lipids, leading to a predominantly necrotic mode of cell death. ROS produced by PACs play a key mediatory role in inflammation and initiation of an innate immune response, recruiting leukocytes and neutrophils to the inflamed pancreas (Tsai et al. 1998; Chan 2009; Dios 2010), for example, though the activation of cytokine expression, as described earlier. These include pancreatic acinar cell produced TNF-α and activation of the transcription factor NF-κB (Norman et al. 1995; Chen et al. 2002; Ramudo et al. 2005).

ROS amplify the inflammatory cascade in AP by cross-talk with pro-inflammatory cytokines. This cross-talk is mediated by NF-κB, activator protein 1 (AP-1), Signal Transducer and Activator of Transcription 3 (STAT3), and MAPKs (Dabrowski et al. 2000; Ramnath et al. 2006; Yu et al. 2014; Pérez et al. 2015).

Leukocytes and neutrophils recruited to the pancreas then release further cytokines and potentiate tissue damage (Sandoval et al. 1996). Acute lung injury (ALI) is characterised by enhanced pulmonary vascular permeability and non-cardiogenic pulmonary oedema. The development of ALI has been linked with mediation of lung P-selectin ligation and ICAM-1 neutrophil infiltration (Folch et al. 1999; Folch et al. 2000; Grommes et al. 2011). Proteases derived from polymorphonuclear leukocytes have been associated with the development of acute respiratory distress syndrome (ARDS) (Simms et al. 1994; Lichtenstein et al. 2000; Zhou et al. 2010; Akbarshahi et al. 2012).

These responses are linked with elevated severity of acute pancreatitis, the development of infected pancreatic necrosis, systemic inflammatory response syndrome (SIRS), and with repeated incidence chronic pancreatitis (Rinderknecht 1988; Guice et al. 1989; Sandoval et al. 1996; Bhatia et al. 1998; Beger et al. 2000). Our understanding of the importance of ROS in the development of AP has been further advanced with antioxidant treatment, which typically resulted in a reduction in cellular ROS production and biomarkers *in vivo*.

ROS and Disease: Recent Developments

More recently, the roles of ROS in cellular signalling, particularly H_2O_2, have received more attention. These include the reversible activation or inhibition of

proteins and enzymes involved in signalling pathways, gene transcription, differentiation, cell survival and apoptosis. Elevated levels of oxidants in pancreatic acinar cells and AP can induce apoptosis. Evidence suggests that apoptosis can be a protective mechanism in acute pancreatitis, reducing the disease severity. This is because when a cell undergoes apoptosis rather than necrosis, the remaining cell debris is easier to clear from the affected organ, therefore leading to less inflammation (Gerschenson et al. 1992). However, it should be noted that excessive apoptosis could also be detrimental, leading to a progressive loss of pancreatic tissue. On the other hand, necrosis mediated cell destruction leads to the release of activated proteases. These cause local damage and initiate an inflammatory response in the surrounding tissue, which prevents phagocytic removal of dead cells (Bhatia et al. 1998; Bhatia 2004; Bhatia 2004). The dose-dependent effects of ROS H_2O_2 on apoptosis and necrosis have not been investigated in PACs to date.

The Effects of H_2O_2-Induced Oxidative Stress in PACs

In PACs, studies have commonly applied high micromolar and millimolar concentrations of H_2O_2 to assess the effects of oxidative stress (Dabrowski et al. 2000; Pariente et al. 2001; Rosado et al. 2002; Gonzalez et al. 2005; Weber et al. 2005; Andreolotti et al. 2006; Camello-Almaraz et al. 2006; Ohashi et al. 2006; Bruce et al. 2007; Weber et al. 2007; Weber et al. 2013). Specifically, a number of studies

have applied 1mM H_2O_2 that causes rapid and substantial cellular damage in PACs. The majority of investigations have focussed on the effects of H_2O_2 on intracellular Ca^{2+} mobilisation and responses. These results showed that high micromolar and millimolar H_2O_2 elevated ROS levels and caused large increases in cytosolic Ca^{2+} by an IP_3-receptor independent mechanism (Pariente et al. 2001). Micromolar to millimolar concentrations of H_2O_2 bring about increases in $[Ca^{2+}]_c$ through Ca^{2+} release from intracellular stores including the ER and the mitochondria (Pariente et al. 2001; Gonzalez et al. 2005; Granados et al. 2006). These sustained increases of $[Ca^{2+}]_i$ led to partial depolarisation of the $\Delta\Psi m$ and increased oxidised FAD^+ levels (Gonzalez et al. 2005). Any specific mechanisms for H_2O_2-induced mitochondrial Ca^{2+} release via the mitochondrial Na^+/Ca^{2+} exchanger have not been elucidated yet in PACs (Muallem et al. 1988; Zima et al. 2006).

A previous study highlighted that >50µM H_2O_2 induced concentration-dependent inhibition of PMCA activity, therefore preventing clearance of Ca^{2+} from the cytosol (Bruce et al. 2007; Baggaley et al. 2008). H_2O_2 mediates inhibition of Ca^{2+}-ATPases by the oxidation of sulfhydryl groups (Pariente et al. 2001). Reduction of SERCA activity occurs through oxidative modification of SERCA Cys674 (Qin et al. 2013). Our results support these findings, demonstrating progressive increases in $[Ca^{2+}]_c$ with 50µM and 500µM H_2O_2 in line with results seen with 100µM H_2O_2 (Mankad et al. 2012). H_2O_2 concentrations of <100µM have additionally demonstrated the ability to induce Ca^{2+} responses of an oscillatory manner (Granados et al. 2006; Gonzalez et al. 2012). The compiled results provide

supporting evidence for a heterogeneous nature of H_2O_2-induced effects on Ca^{2+} signalling in PACs (Bruce et al. 2007).

The Effects of Low Dose H_2O_2 in PACs

A relatively limited number of investigations have been employed in PACs to address the comparative effects of mild oxidative stress and low micromolar concentrations of H_2O_2 (<50µM) (Morgado et al. 2008; Gonzalez et al. 2012), which are likely more physiologically relevant concentrations required for H_2O_2 signalling capacity (Toledano et al. 2010; Pérez et al. 2015). The majority of studies have investigated a concentration range from mid-low micromolar (>50µM) up to high micromolar and millimolar, therefore there are still gaps in our understanding of the low micromolar and nanomolar concentration range. Our results further our understanding by demonstrating dose- and time-dependent effects of H_2O_2 in primary isolated PACs on mitochondrial function, intracellular Ca^{2+} and cell death.

The effects of H_2O_2 on NAD(P)H levels were exacerbated by nonspecific effects of both MitoQ and dTPP pre-treatment. However, while MitoQ did not affect H_2O_2-induced effects on FAD^+ levels, dTPP did. These results support the differing effects of alky chain and TPP^+ to the antioxidant group seen in our *in vivo* and *in vitro* work, as well as studies in alternative cell types (Reily et al. 2013; Huang et al. 2015; Trnka et al. 2015). The technique employed applied simultaneous

measurements of natural fluorophores, NAD(P)H and FAD^+, and can be used as an indicator of the cellular redox state. This avoided the use of a fluorescent probe, which can potentially affect cellular responses. These sensitive NAD(P)H/FAD^+ measurements enabled the novel demonstration of acute H_2O_2 effects at low micromolar concentration ranges in direct comparison to those seen on ΔΨm and $[Ca^{2+}]_c$.

The Cellular Effects of H_2O_2

Our experiments with 50µM and 500µM H_2O_2 caused partial ΔΨm depolarisation in a concentration-dependent manner, alongside mirrored increases in $[Ca^{2+}]_c$. These results were in accordance with findings from separate studies (Baggaley et al. 2008; Mankad et al. 2012). The simultaneously mirrored ΔΨm and $[Ca^{2+}]_c$ changes are in agreement with experiments strongly suggesting that ΔΨm depolarisation occurs due to large increases in cytosolic Ca^{2+} (Duchen 2000; Voronina et al. 2004). H_2O_2-induced ΔΨm depolarisation however, is likely caused by both elevated levels of Ca^{2+} and free radical-derived cellular injury. While H_2O_2 at concentrations as low as 0.1µM have demonstrated induction of Ca^{2+} oscillations and detectable ROS increases, mirrored measurements of ΔΨm have not been assessed at these concentrations. Novel findings were obtained through simultaneous measurements of ΔΨm and $[Ca^{2+}]_c$ alongside sensitive measurements of NAD(P)H. These results interestingly show that the effects of H_2O_2 on levels of NAD(P)H were more substantial than on ΔΨm and $[Ca^{2+}]_c$. 50µM induced immediate

and significant effects on NAD(P)H levels, demonstrated by a rapid decrease in fluorescence. In contrast, the effects on ΔΨm and $[Ca^{2+}]_c$ were delayed and gradual.

The Effects of H_2O_2 on NAD(P)H and FAD^+ levels

These novel results were further investigated with simultaneous measurements of NAD(P)H and FAD^+ in response to H_2O_2. Previously, Granados et al. (2005) showed that levels of 1mM H_2O_2 induce large increases in non-reduced FAD^+. These results were confirmed (Figure 5.2B) and further included measurements of NAD(P)H, demonstrating mirrored effects on NAD(P)H/FAD^+. These results indicate changes to the rate of NAD(P)H and $FADH_2$ oxidation. In summary, concentrations from 10µM to 10mM demonstrated concentration-dependent effects on levels of NAD(P)H and FAD^+. Preliminary results suggested reversible actions of 1µM H_2O_2 on NAD(P)H levels, however further experiments are required. It is interesting that 10µM H_2O_2 elicited greater effects on NAD(P)H levels than FAD^+. This could indicate less sensitivity of the FAD^+ measurement technique or H_2O_2-specific effects on the TCA cycle. The assessment of H_2O_2 effects on ETC complexes and Krebs cycle enzymes have not been performed in PACs to date. Nulton-Persson et al. (2001) have demonstrated concentration-dependent reversible inhibition of mitochondrial respiration and the activities of specific mitochondrial enzymes in isolated rat heart mitochondria. These effects were visible via a decrease in levels of NAD(P)H with 12.5µM H_2O_2. The enzymes inhibited by H_2O_2 were ETC complexes and Krebs cycle enzymes, succinate dehydrogenase

(SDH), α-KGDH, and aconitase. H_2O_2 at <50µM did not however affect complexes I, III or IV of the ETC or ATP synthase. It is possible that H_2O_2 inhibition of Kreb cycle enzymes leads to more substantial changes to levels of NAD(P)H than FAD^+ observed in more sensitive NAD(P)H responses. Alternatively, imaging of NAD(P)H autofluorescence may be more sensitive than FAD^+ measurements and therefore the technique not sensitive enough to detect H_2O_2-induced changes.

H_2O_2: ROS Generation, Apoptosis and Necrosis

Induction of ROS increases by 1-500µM H_2O_2 were demonstrated in a concentration-dependent manner. While several studies have demonstrated H_2O_2-induced ROS increases, an assessment of dose dependent H_2O_2-induction of ROS in comparison to apoptosis and necrosis has not been carried out in PACs. Concentrations of >1µM induced apoptosis and >10µM necrosis during a 13 hour period. Apoptosis was the major mode of cell death induced by 1-10µM H_2O_2, whereas mainly necrosis was induced with 500µM-1mM H_2O_2. It is extremely interesting that 1µM H_2O_2 induced apoptosis but not necrosis, consistent with prior observations in PACs showing that ROS promotes apoptosis (Criddle et al. 2006). MitoQ inhibited 500µM- and 1mM H_2O_2-induced ROS increases in a dose-dependent manner. Although MitoQ has demonstrated partial inhibition of POAEE- and ethanol-induced apoptosis, consistent with blockade of ROS, there was no protection provided against 500µM- and 1mM H_2O_2-induced apoptosis and in fact MitoQ exacerbated H_2O_2-induced necrosis. In comparison, non-targeted natural

antioxidant cinnamtannin B-1, reduced 0.1-100μM H_2O_2-induced concentration-dependent increases in ROS (Gonzalez et al. 2012) and reversed 1μM H_2O_2-induced inhibition of CCK-induced amylase secretion. Cells incubated with H_2O_2 led to a concentration-dependent reduction of cell viability from 0.1-100μM H_2O_2 in concurrence with our results. However, cinnamtannin B-1 inhibited the decrease in cell viability, while MitoQ did not in our experiments. It is likely that these results are due to the MitoQ-induced cell death independent of H_2O_2 induction.

Work has also been performed with AR42J tumorigenic cell line as a model for pancreatic acinar cell function to assess H_2O_2 -induction of apoptosis (Song et al. 2003; Weber et al. 2013). These results are in accord with the 10μM H_2O_2 results, but not those demonstrated with 1μM. Morgado et al. (2008) showed that 10μM H_2O_2 activated caspase-3 and cytochrome c release from the mitochondria to the cytosol. After 12 and 24 hours 1μM H_2O_2 did not activate caspase-3, whereas at 13 hours our results in PACs demonstrated a significant increase in apoptosis. The differences are likely to be due to the different cell types used, since AR42J cells may not accurately reflect primary isolated PACs. However, they do highlight the need to investigate further at these concentrations and down into the nanomolar range in primary isolated PACs. Interestingly, preliminary experiments measuring NAD(P)H levels with 1μM H_2O_2 treatment, showed a transient decrease which returned to basal levels during continuous perfusion. Treatment with 10μM H_2O_2 induced a decrease in NAD(P)H levels with no effect on FAD^+ levels. In a minority of experiments 10μM H_2O_2 also demonstrated an induction of mirrored NAD(P)H and

FAD^+ waves. These NAD(P)H/FAD^+ waves could be reversible inhibition of TCA dehydrogenases or a reflection of the heterogeneous effects of H_2O_2 on Ca^{2+} signalling reflected in NAD(P)H/FAD^+ changes (Bruce et al. 2007).

H_2O_2 Effects in CypD Deficient Mice

Our results with $Ppif^{-/-}$ cells indicated that oxidative stress induced by H_2O_2 is exacerbated in the absence of a functional MPTP. Both levels of ROS and depletion of NAD(P)H levels were elevated in compared to the wild type. Lower levels of H_2O_2 have not been assessed and additional investigation may provide further insights. MPTP opening is a central trigger for necrotic cell death in PACs, rather than apoptosis (Nakagawa et al. 2005; Kinnally et al. 2011; Mukherjee et al. 2015). Reversible opening of the MPTP could however restore membrane potential and ATP production (Crompton et al. 1987; Pastorino et al. 1999; Kinnally et al. 2011). Targeted antioxidant therapy can diminish cellular ROS levels in correlation to reduced MPTP opening and cell death in kidney and cardiac ischemia/reperfusion injury (Mitchell et al. 2011; Hansson et al. 2015). However, our results in $Ppif^{-/-}$ mice did not support a pivotal role for ROS in PAC MPTP opening.

Conclusions

The results obtained demonstrated novel H_2O_2 concentration-dependent effects on a variety of parameters including membrane potential, levels of NAD(P)H and FAD^+, ROS, apoptosis, necrosis and the effects of mitochondria-targeted antioxidant MitoQ. These findings contribute to our knowledge of the effects of ROS H_2O_2 in PACs, increasing our understanding for potential future studies of concentration ranges responsible for reversible oxidative effects. Further investigations into specifically <1µM H_2O_2-induced effects could provide further clarity in future work. Determination of H_2O_2 concentrations which have reversible effects on pancreatic acinar cellular bioenergetics could provide a therapeutic approach to manage ROS mediated cell signal transduction in the inflammatory response, cell death balance and development of AP and other oxidative stress related diseases.

Overall Conclusions and Future Work

The findings of this study further emphasize the unsuitability of the use of antioxidant therapy in the treatment of AP, previously highlighted by a randomised, double-blind, and placebo-controlled clinical trial (Siriwardena et al. 2007). Targeted antioxidant therapy was also not suitable for the treatment of PD (Snow et al. 2010). This study has demonstrated mixed effects of MitoQ both *in vivo* and *in vitro*. While MitoQ inhibited H_2O_2-induced ROS increases, pre-treatment offered no protection against cell death. MitoQ treatment alone caused a concentration-dependent increase of both apoptosis and necrosis. Protective effects included reducing pancreatic oedema and neutrophil infiltration in CER-AP. However, MitoQ exacerbated CCK-induced apoptosis and necrosis, systemic injury, inducing concurrent increases in lung MPO and IL-6. In contrast, the cytotoxic effects of MitoQ have however shown promise as a breast cancer treatment, through induction of autophagy and apoptosis 30-fold more than in healthy mammary cells (Rao et al. 2010).

Attempts have been made to improve the balance between reported antioxidant and pro-oxidant effects of MitoQ and facilitate improved delivery. Plastoquinonyl-decyl-triphenylphosphonium (SkQ1) was one such compound and demonstrated greater permeability across synthetic lipid bilayers. However, SkQ1 exhibited similar undesirable effects of MitoQ on cellular bioenergetics, which were attenuated by non-targeted antioxidant NAC (Smith et al. 2008; Skulachev et al. 2009; Fink et al. 2012). Further experiments could be applied to determine the

more specific effects of TPP^+ and derivatives MitoQ and dTPP on ETC inhibition and mitochondrial bioenergetics. It is unlikely that MitoQ has direct effects on Ca^{2+} levels but this might occur indirectly via antioxidant or pro-oxidant effects and due to the targeting component.

Our work, combined with evidence in other cell types, indicates mild uncoupling effects of MitoQ and TPP^+ conjugated compounds via alteration of mitochondrial bioenergetics (Reily et al. 2013). This is supported by studies in endothelial cells and mesangial cells showing an inhibitory effect of all TPP^+ derivatives on basal respiration, ATP turnover, ETC complexes and mild uncoupling of the mitochondrial membrane (Fink et al. 2012; Reily et al. 2013; Trnka et al. 2015). In C2C12 mouse myoblast cell line and rat skeletal muscle homogenate, lipophilic triphenylphosphonium cations induced proton leak, loss of mitochondrial membrane potential and inhibition of all four respiratory chain complexes in particular complexes I and III (Trnka et al. 2015). In bovine aortic endothelial cell mitochondria, MitoQ inhibited reverse electron transport to complex I and enhanced forward transport through complex I (O'Malley et al. 2006). Alternatively, MitoQ elevated mitochondrial respiration under rotenone inhibition of complex I in liver mitochondria (Kargin et al. 2008). Excessive accumulation of lipophilic cations in the mitochondria are also toxic due to disruption to ATP synthesis, (Smith et al. 2003) membrane integrity and respiration (Murphy 2008).

Further experiments could assess the actions of MitoQ, dTPP and TPP^+ on levels of NAD(P)H and FAD^+ in an inhibitor study applying ETC and ATPase inhibitors

rotenone, oligomycin and antimycin A. Induction of apoptosis is dependent on levels of ATP. Depletion of ATP can prevent apoptosis, a proposed protective mechanism in AP (Criddle et al. 2006; Booth et al. 2011). Oligomycin is a commonly used inhibitor of the ATP synthase and may be applied to assess any effects of MitoQ and TPP^+ derivatives monitored using cytosolic- or mitochondrial-targeted luciferases or magnesium green (Criddle et al. 2006; Bell et al. 2007; Voronina et al. 2010).

Prooxidant capabilities of MitoQ and ubiquinone have repeatedly been demonstrated in alternative cell types and mitochondria such as bovine heart mitochondrial membranes, human pulmonary endothelial cells, HepG2 liver hepatocellular carcinoma cells and isolated rat liver mitochondria (James et al. 2004; James et al. 2005; O'Malley et al. 2006; Doughan et al. 2007; Plecitá-Hlavatá et al. 2009). Although it is evident from these studies that MitoQ can produce superoxide, the rate of production in PACs is potentially too small and not detected in our experiments with a general oxidative stress indicator. These conclusions are supported by James et al. (2005) in *Saccharomyces cerevisiae*, where MitoQ induced superoxide production was too low to cause significant damage to mitochondrial enzymes.

It is, however, possible that applying a more specific probe (optimised with spectral analysis) such as DHE (Dihydroethidium) or MitoSOX (DHE plus TPP^+) or electron spin resonance (ESR) spectroscopy in future work may have the potential to highlight increases in superoxide production seen in other cell types (Bindokas et

al. 1996; Li et al. 2003; Rivera et al. 2005). A new antioxidant prototype based on the dietary cinnamic acid-caffeic acid conjugated to TPP^+ has also been developed (Teixeira et al. 2015). However, the effects of the triphenylphosphonium cations in PACs have not been thoroughly characterised and it may prove more fruitful to investigate novel non TPP^+ conjugated compounds or alternative therapeutic strategies. With recent accumulating evidence for ROS as signalling molecules and lack of success of management strategies attention is moving to alternative targets such as inhibition of MPTP opening. While it does not appear that MitoQ is effective, there are novel findings in this study. These provide insight into the role of ROS in AP, which is not only important in AP but also in all oxidative stress-induced diseases.

Antioxidant Therapy in the Clinic

It cannot be disputed that antioxidant application in vitro effectively reduces elevated levels of cellular ROS (Hackert et al. 2011; Assaly et al. 2012; Armstrong et al. 2013; Huang et al. 2015). Direct measurements of ROS production in the clinical setting are problematic, therefore oxidative stress is detected indirectly through the measurement of lipid peroxidation by-products, such as MPO (Holley et al. 1993; Armstrong et al. 2013; Huang et al. 2015). Elevated levels have been detected in a broad range of diseases including AP, cardiovascular diseases, cancer and neurological diseases (Dhalla et al. 2000; Chernyak et al. 2006; Uttara et al. 2009; Reuter et al. 2010; Booth et al. 2011; Berndt et al. 2013). Subsequently, ROS have

been frequently described to have a causal role, leading to a major research and treatment focussed on reducing elevated levels of ROS (Iannitti et al. 2009; Uttara et al. 2009; Esrefoglu 2012). However, there are many confounding factors, which have not been fully addressed to date. A wealth of clinical trials have applied antioxidant therapy, with inconsistent outcomes. Many trials have found no beneficial effects and only a small proportion of trials have used adequate methodologies (Gluud 2006; Bjelakovic et al. 2007). A recent meta-analysis that pooled results from 68 randomized trials, involving 232,606 patients, demonstrated that participants in the antioxidant treatment arms had a tendency for higher mortality (Madamanchi et al. 2005; Bjelakovic et al. 2007). These trials included patients with a range of diseases including coronary heart disease, alcoholic hepatitis, colorectal adenomas, PD, ischemic heart disease and additionally cigarette smokers. These concerns are further mirrored in patients with AP receiving antioxidant supplementation (Siriwardena et al. 2007). It is now becoming more widely acknowledged that antioxidant supplementation may disrupt the cellular redox balance, prevent normal cellular functions and apoptosis (Bouayed et al. 2010; Booth et al. 2011; Kinnally et al. 2011).

The area of antioxidant therapy is controversial. This thesis, while contributing to our current knowledge, also highlights that our understanding of the role of cellular oxidant levels in signalling and regulation of cellular processes is limited. Substantial cellular based in vitro and pre-clinical investigations are required in order to provide a more comprehensive understanding of what is a

highly sensitive and regulated system. Furthermore, the development of a non-invasive, reliable, quantitative method to monitor ROS production in the clinic would greatly aid investigations. Extensive, well-controlled safety studies are required to establish the long-term systemic effects (real world) of antioxidant therapy in the healthy population. A wide range of antioxidant dosages have been used in clinical trials and it is crucial that these doses are more tightly controlled and reviewed to establish a smaller effective dose range and minimise any adverse effects. Until these steps have been taken, antioxidant therapy is not recommended in a clinical setting.

Final Remarks

In this study, the effects of mitochondria-targeted antioxidant Mitoquinone were evaluated, on pancreatic acinar cell physiology and cell death, alongside the protective capabilities against the effects of AP precipitants. Briefly, MitoQ demonstrated a lack of protection and induced adverse effects on PACs in a concentration-dependent manner. These effects were caused either by MitoQ alone or in combination with bile acid TLCS, non-oxidative metabolite POAEE, CCK hyperstimulation and H_2O_2-induced oxidant elevation. Novel low micromolar to millimolar concentration-dependent effects of H_2O_2 were demonstrated on mitochondrial respiration, cell death and ROS levels in comparison to known AP precipitants and hyperstimulatory responses. MitoQ, while inhibiting H_2O_2-induced ROS increases, did not protect against H_2O_2-induced cell death or against detrimental effects on the NAD(P)H/FAD+ redox ratio. These results provide novel insights, which advance our understanding of the ROS balance in PACs.

Chapter 7

Bibliography

Adachi, T., et al. (2004). "S-Glutathiolation by peroxynitrite activates SERCA during arterial relaxation by nitric oxide." Nat Med **10**(11): 1200-1207.

Adkins, C. E., et al. (1999). "Lateral inhibition of inositol 1,4,5-trisphosphate receptors by cytosolic Ca(2+)." Curr Biol **9**(19): 1115-1118.

Adlam, V. J., et al. (2005). "Targeting an antioxidant to mitochondria decreases cardiac ischemia-reperfusion injury." FASEB J **19**(9): 1088-1095.

Adlam, V. J., et al. (2005). "Targeting an antioxidant to mitochondria decreases cardiac ischemia-reperfusion injury." The FASEB Journal **19**(9): 1088-1095.

Akbarshahi, H., et al. (2012). "Acute lung injury in acute pancreatitis--awaiting the big leap." Respir Med **106**(9): 1199-1210.

Altomare, E., et al. (1996). "Acute ethanol administration induces oxidative changes in rat pancreatic tissue." Gut **38**(5): 742-746.

Ammann, R. W. (2001). "The natural history of alcoholic chronic pancreatitis." Intern Med **40**(5): 368-375.

Andican, G., et al. (2005). "Oxidative stress and nitric oxide in rats with alcohol-induced acute pancreatitis." World J Gastroenterol **11**(15): 2340-2345.

Andreolotti, A. G., et al. (2006). "Adapter protein CRKII signaling is involved in the rat pancreatic acini response to reactive oxygen species." Journal of Cellular Biochemistry **97**(2): 359-367.

Andreyev, A. Y., et al. (2005). "Mitochondrial metabolism of reactive oxygen species." Biochemistry (Mosc) **70**(2): 200-214.

Andrzejewska, A., et al. (1999). "Nitric oxide protects the ultrastructure of pancreatic acinar cells in the course of caerulein-induced acute pancreatitis." International Journal of Experimental Pathology **80**(6): 317-324.

Aoun, E., et al. (2009). "Diagnostic Accuracy of Interleukin-6 and Interleukin-8 in Predicting Severe Acute Pancreatitis: A Meta-Analysis." Pancreatology **9**(6): 777-785.

Apte, M. V., et al. (2010). "Mechanisms of alcoholic pancreatitis." Journal of Gastroenterology and Hepatology **25**(12): 1816-1826.

Armstrong, J. A., et al. (2013). "Oxidative stress in acute pancreatitis: lost in translation?" Free Radic Res **47**(11): 917-933.

Ashby, M. C., et al. (2003). "Long distance communication between muscarinic receptors and Ca2+ release channels revealed by carbachol uncaging in cell-attached patch pipette." J Biol Chem **278**(23): 20860-20864.

Asher, G., et al. (2002). "NQO1 stabilizes p53 through a distinct pathway." Proceedings of the National Academy of Sciences **99**(5): 3099-3104.

Asin-Cayuela, J., et al. (2004). "Fine-tuning the hydrophobicity of a mitochondria-targeted antioxidant." FEBS Lett **571**(1-3): 9-16.

Asin-Cayuela, J., et al. (2004). "Fine-tuning the hydrophobicity of a mitochondria-targeted antioxidant." FEBS Letters **571**(1-3): 9-16.

Babior, B. M. (1995). "The respiratory burst oxidase." Curr Opin Hematol **2**(1): 55-60.

Baggaley, E. M., et al. (2008). "Oxidant-induced inhibition of the plasma membrane Ca2+-ATPase in pancreatic acinar cells: role of the mitochondria." Am J Physiol Cell Physiol **295**(5): C1247-1260.

Baines, C. P. (2009). "The Molecular Composition of the Mitochondrial Permeability Transition Pore." Journal of molecular and cellular cardiology **46**(6): 850-857.

Baines, C. P., et al. (2005). "Loss of cyclophilin D reveals a critical role for mitochondrial permeability transition in cell death." Nature **434**(7033): 658-662.

Banks, P. A., et al. (2013). "Classification of acute pancreatitis - 2012: Revision of the Atlanta classification and definitions by international consensus." Gut **62**(1): 102-111.

Banks, P. A., et al. (2010). "The Management of Acute and Chronic Pancreatitis." Gastroenterology & Hepatology **6**(2 Suppl 5): 1-16.

Bansal, D., et al. (2011). "Safety and efficacy of vitamin-based antioxidant therapy in patients with severe acute pancreatitis: a randomized controlled trial." Saudi J Gastroenterol **17**(3): 174-179.

Bansal, D., et al. (2011). "Safety and Efficacy of Vitamin-based Antioxidant Therapy in Patients with Severe Acute Pancreatitis: A Randomized Controlled Trial." Saudi Journal of Gastroenterology : Official Journal of the Saudi Gastroenterology Association **17**(3): 174-179.

Barrow, S. L., et al. (2008). "ATP depletion inhibits Ca2+ release, influx and extrusion in pancreatic acinar cells but not pathological Ca2+ responses induced by bile." Pflugers Archiv European Journal of Physiology **455**(6): 1025-1039.

Basso, E., et al. (2005). "Properties of the permeability transition pore in mitochondria devoid of Cyclophilin D." J Biol Chem **280**(19): 18558-18561.

Baumgartner, H. K., et al. (2007). Caspase-8-mediated apoptosis induced by oxidative stress is independent of the intrinsic pathway and dependent on cathepsins.

Baumgartner, H. K., et al. (2009). "Calcium elevation in mitochondria is the main Ca2+ requirement for mitochondrial permeability transition pore (mPTP) opening." J Biol Chem **284**(31): 20796-20803.

Baumgartner, H. K., et al. (2009). "Calcium elevation in mitochondria is the main Ca2+ requirement for mitochondrial permeability transition pore (mPTP) opening." Journal of Biological Chemistry **284**(31): 20796-20803.

Bedard, K., et al. (2007). "The NOX family of ROS-generating NADPH oxidases: physiology and pathophysiology." Physiol Rev **87**(1): 245-313.

Beger, H. G., et al. (2000). "The role of immunocytes in acute and chronic pancreatitis: When friends turn into enemies." Gastroenterology **118**(3): 626-629.

Belan, P., et al. (1997). "Distribution of Ca2+ extrusion sites on the mouse pancreatic acinar cell surface." Cell Calcium **22**(1): 5-10.

Belan, P. V., et al. (1996). "Localization of Ca2+ extrusion sites in pancreatic acinar cells." J Biol Chem **271**(13): 7615-7619.

Bell, C. J., et al. (2007). "Luciferase expression for ATP imaging: application to cardiac myocytes." Methods Cell Biol **80**: 341-352.

Bernardi, P. (2013). "The mitochondrial permeability transition pore: a mystery solved?" Front Physiol **4**: 95.

Berridge, M. J. (1981). "Phosphatidylinositol hydrolysis and calcium signaling." Adv Cyclic Nucleotide Res **14**: 289-299.

Berridge, M. J., et al. (2003). "Calcium signalling: dynamics, homeostasis and remodelling." Nat Rev Mol Cell Biol **4**(7): 517-529.

Berridge, M. J., et al. (2000). "Signal transduction. The calcium entry pas de deux." Science **287**(5458): 1604-1605.

Bertolotti, M., et al. (2013). "Tyrosine Kinase signal modulation: A matter of H2O2 membrane permeability?" Antioxidants and Redox Signaling **19**(13): 1447-1451.

Besselink, M. G., et al. (2008). "Probiotic prophylaxis in predicted severe acute pancreatitis: a randomised, double-blind, placebo-controlled trial." Lancet **371**(9613): 651-659.

Beyer, R. E., et al. (1996). "The role of DT-diaphorase in the maintenance of the reduced antioxidant form of coenzyme Q in membrane systems." Proc Natl Acad Sci U S A **93**(6): 2528-2532.

Bhatia, M. (2004). "Apoptosis of pancreatic acinar cells in acute pancreatitis: is it good or bad?" Journal of Cellular and Molecular Medicine **8**(3): 402-409.

Bhatia, M. (2004). Apoptosis versus necrosis in acute pancreatitis.

Bhatia, M. (2004). "Apoptosis versus necrosis in acute pancreatitis." American Journal of Physiology - Gastrointestinal and Liver Physiology **286**(2): G189-G196.

Bhatia, M., et al. (1998). "The effects of neutrophil depletion on a completely noninvasive model of acute pancreatitis-associated lung injury." Int J Pancreatol **24**(2): 77-83.

Bhatia, M., et al. (1998). "Induction of Apoptosis in Pancreatic Acinar Cells Reduces the Severity of Acute Pancreatitis." Biochem Biophys Res Commun **246**(2): 476-483.

Bhatia, M., et al. (2005). "Pathophysiology of acute pancreatitis." Pancreatology **5**(2-3): 132-144.

Bienert, G. P., et al. (2014). "Aquaporin-facilitated transmembrane diffusion of hydrogen peroxide." Biochimica et Biophysica Acta - General Subjects **1840**(5): 1596-1604.

Bindokas, V. P., et al. (1996). "Superoxide production in rat hippocampal neurons: selective imaging with hydroethidine." J Neurosci **16**(4): 1324-1336.

Bjelakovic, G., et al. (2007). "Mortality in randomized trials of antioxidant supplements for primary and secondary prevention: Systematic review and meta-analysis." JAMA **297**(8): 842-857.

Blaise, G. A., et al. (2005). "Nitric oxide, cell signaling and cell death." Toxicology **208**(2): 177-192.

Blanchard Ii, J. A., et al. (2001). "Antioxidants inhibit cytokine production and suppress NF-κB activation in CAPAN-1 and CAPAN-2 cell lines." Dig Dis Sci **46**(12): 2768-2772.

Booth, D. M., et al. (2011). "Calcium and reactive oxygen species in acute pancreatitis: friend or foe?" Antioxid Redox Signal **15**(10): 2683-2698.

Booth, D. M., et al. (2011). "Reactive oxygen species induced by bile acid induce apoptosis and protect against necrosis in pancreatic acinar cells." Gastroenterology **140**(7): 2116-2125.

Borst, P., et al. (1962). "Uncoupling activity of long-chian fatty acids." BBA - Biochimica et Biophysica Acta **62**(3): 509-518.

Boveris, A., et al. (1976). "Role of ubiquinone in the mitochondrial generation of hydrogen peroxide." Biochem. J. **156**: 435-444.

Boveris, A., et al. (1973). "The mitochondrial generation of hydrogen peroxide." Biochem. J. **134**: 707-716.

Braganza, J. M., et al. (1995). "Evidence for early oxidative stress in acute pancreatitis - Clues for correction." International Journal of Pancreatology **17**(1): 69-81.

Brand, M. D., et al. (1987). "Control of electron flux through the respiratory chain in mitochondria and cells." Biol. Rev. Camb. Philos. Soc. **62**: 141-193.

Braughler, J. M., et al. (1986). "The involvement of iron in lipid peroxidation. Importance of ferric to ferrous ratios in initiation." Journal of Biological Chemistry **261**(22): 10282-10289.

Brinkmann, V., et al. (2004). "Neutrophil extracellular traps kill bacteria." Science **303**(5663): 1532-1535.

Brinkmann, V., et al. (2007). "Beneficial suicide: why neutrophils die to make NETs." Nat Rev Micro **5**(8): 577-582.

Brookes, P., et al. (2002). "Hypothesis: the mitochondrial NO(*) signaling pathway, and the transduction of nitrosative to oxidative cell signals: an alternative function for cytochrome C oxidase." Free Radic Biol Med **32**(4): 370-374.

Brookes, P. S., et al. (2002). "Mitochondria: regulators of signal transduction by reactive oxygen and nitrogen species." Free Radic Biol Med **33**(6): 755-764.

Brookes, P. S., et al. (2004). "Calcium, ATP, and ROS: a mitochondrial love-hate triangle." Am J Physiol Cell Physiol **287**(4): C817-833.

Brown, G. C. (1995). "Nitric oxide regulates mitochondrial respiration and cell functions by inhibiting cytochrome oxidase." FEBS Lett **369**(2-3): 136-139.

Bruce, J. I., et al. (2007). "Oxidant-impaired intracellular Ca2+ signaling in pancreatic acinar cells: role of the plasma membrane Ca2+-ATPase." Am J Physiol Cell Physiol **293**(3): C938-950.

Bruce, J. I. E., et al. (2004). "Modulation of [Ca2+]i Signaling Dynamics and Metabolism by Perinuclear Mitochondria in Mouse Parotid Acinar Cells." Journal of Biological Chemistry **279**(13): 12909-12917.

Burdon, R. H., et al. (1989). "Free radicals and the regulation of mammalian cell proliferation." Free Radic Res Commun **6**(6): 345-358.

Burkhardt, J. K., et al. (1989). "Intracellular transport of the glycoprotein of VSV is inhibited by CCCP at a late stage of post-translational processing." Journal of Cell Science **92**(4): 633-642.

Camello-Almaraz, C., et al. (2002). "Role of mitochondria in Ca2+ oscillations and shape of Ca2+ signals in pancreatic acinar cells." Biochem Pharmacol **63**(2): 283-292.

Camello-Almaraz, M. C., et al. (2006). "Mitochondrial production of oxidants is necessary for physiological calcium oscillations." J Cell Physiol **206**(2): 487-494.

Camello-Almaraz, M. C., et al. (2006). "Mitochondrial production of oxidants is necessary for physiological calcium oscillations." J Cell Physiol **206**(2): 487-494.

Campo, G. M., et al. (2008). "Chondroitin-4-sulphate reduced oxidative injury in caerulein-induced pancreatitis in mice: the involvement of NF-kappaB translocation and apoptosis activation." Exp Biol Med (Maywood) **233**(6): 741-752.

Cancela, J. M. (2001). "Specific Ca2+ signaling evoked by cholecystokinin and acetylcholine: the roles of NAADP, cADPR, and IP3." Annu Rev Physiol **63**: 99-117.

Cancela, J. M., et al. (1999). "Coordination of agonist-induced Ca2+-signalling patterns by NAADP in pancreatic acinar cells." Nature **398**(6722): 74-76.

Cancela, J. M., et al. (2000). "Two different but converging messenger pathways to intracellular Ca(2+) release: the roles of nicotinic acid adenine dinucleotide phosphate, cyclic ADP-ribose and inositol trisphosphate." EMBO J **19**(11): 2549-2557.

Carvalho, K. M., et al. (2010). "The natural flavonoid quercetin ameliorates cerulein-induced acute pancreatitis in mice." Biol Pharm Bull **33**(9): 1534-1539.

Case, R. M. (1978). "Synthesis, intracellular transport and discharge of exportable proteins in the pancreatic acinar cell and other cells." Biol Rev Camb Philos Soc **53**(2): 211-354.

Cassone, E., et al. (1991). "Effects of allopurinol on ischemic experimental pancreatitis." International Journal of Pancreatology **8**(3): 227-234.

Castello, P. R., et al. (2006). "Mitochondrial cytochrome oxidase produces nitric oxide under hypoxic conditions: Implications for oxygen sensing and hypoxic signaling in eukaryotes." Cell Metabolism **3**(4): 277-287.

Chacko, B. K., et al. (2011). "Mitochondria-targeted ubiquinone (MitoQ) decreases ethanol-dependent micro and macro hepatosteatosis." Hepatology **54**(1): 153-163.

Chan, P. S. L. a. Y. C. (2009). "Role of Oxidative Stress in Pancreatic Inflammation." Antioxidants & Redox Signalin **11**(1): 135-166.

Chance, B., et al. (1979). "Oxidation-reduction ratio studies of mitochondria in freeze-trapped samples. NADH and flavoprotein fluorescence signals." Journal of Biological Chemistry **254**(11): 4764-4771.

Chen, K., et al. (2004). "Mitochondrial function is required for hydrogen peroxide-induced growth factor receptor transactivation and downstream signaling." Journal of Biological Chemistry **279**(33): 35079-35086.

Chen, X., et al. (2002). "NF-kappaB activation in pancreas induces pancreatic and systemic inflammatory response." Gastroenterology **122**(2): 448-457.

Cheng, G., et al. (2001). "Homologs of gp91phox: cloning and tissue expression of Nox3, Nox4, and Nox5." Gene **269**(1-2): 131-140.

Chernyak, B. V., et al. (1996). "The Mitochondrial Permeability Transition Pore is Modulated by Oxidative Agents Through Both Pyridine Nucleotides and Glutathione at Two Separate Sites." European Journal of Biochemistry **238**(3): 623-630.

Chinopoulos, C., et al. (1999). "Depolarization of In Situ Mitochondria Due to Hydrogen Peroxide-Induced Oxidative Stress in Nerve Terminals." Journal of Neurochemistry **73**(1): 220-228.

Chouchani, E. T., et al. (2013). "Cardioprotection by S-nitrosation of a cysteine switch on mitochondrial complex I." Nat Med **19**(6): 753-759.

Clapham, D. E. (2007). "Calcium signaling." Cell **131**(6): 1047-1058.

Cleeter, M. W., et al. (1994). "Reversible inhibition of cytochrome c oxidase, the terminal enzyme of the mitochondrial respiratory chain, by nitric oxide. Implications for neurodegenerative diseases." FEBS Lett **345**(1): 50-54.

Closa, D., et al. (1994). "Xanthine oxidase activation in cerulein- and taurocholate-induced acute pancreatitis in rats." Arch Int Physiol Biochim Biophys **102**(3): 167-170.

Cohen, J. J., et al. (1984). "Glucocorticoid activation of a calcium-dependent endonuclease in thymocyte nuclei leads to cell death." The Journal of Immunology **132**(1): 38-42.

Cook, S. A., et al. (1999). "Regulation of bcl-2 family proteins during development and in response to oxidative stress in cardiac myocytes: association with changes in mitochondrial membrane potential." Circ Res **85**(10): 940-949.

Criddle, D. N. (2015). "The role of fat and alcohol in acute pancreatitis: A dangerous liaison." Pancreatology.

Criddle, D. N., et al. (2007). "Importance of Reactive Oxygen Species Generation by Bile Acids and Non-Oxidative Ethanol Metabolites to Pancreatic Acinar Cell Fate." Pancreas **35**(4): 397.

Criddle, D. N., et al. (2009). "Cholecystokinin-58 and cholecystokinin-8 exhibit similar actions on calcium signaling, zymogen secretion, and cell fate in murine pancreatic acinar cells." Am J Physiol Gastrointest Liver Physiol **297**(6): G1085-1092.

Criddle, D. N., et al. (2007). "Calcium signalling and pancreatic cell death: apoptosis or necrosis?" Cell Death Differ **14**(7): 1285-1294.

Criddle, D. N., et al. (2006). "Menadione-induced reactive oxygen species generation via redox cycling promotes apoptosis of murine pancreatic acinar cells." J Biol Chem **281**(52): 40485-40492.

Criddle, D. N., et al. (2006). "Fatty acid ethyl esters cause pancreatic calcium toxicity via inositol trisphosphate receptors and loss of ATP synthesis." Gastroenterology **130**(3): 781-793.

Criddle, D. N., et al. (2004). "Ethanol toxicity in pancreatic acinar cells: mediation by nonoxidative fatty acid metabolites." Proc Natl Acad Sci U S A **101**(29): 10738-10743.

Crompton, M. (1999). "The mitochondrial permeability transition pore and its role in cell death." Biochem J **341 (Pt 2)**: 233-249.

Crompton, M., et al. (1987). "Evidence for the presence of a reversible Ca2+-dependent pore activated by oxidative stress in heart mitochondria." Biochem J **245**(3): 915-918.

Curran, F. J. M., et al. (2000). "Relationship of carotenoid and vitamins A and E with the acute inflammatory response in acute pancreatitis." British Journal of Surgery **87**(3): 301-305.

Cuzzocrea, S., et al. (2004). "Reduction in the development of cerulein-induced acute pancreatitis by treatment with M40401, a new selective superoxide dismutase mimetic." Shock **22**(3): 254-261.

Czech, M. P., et al. (1974). "Evidence for the involvement of sulfhydryl oxidation in the regulation of fat cell hexose transport by insulin." Proc Natl Acad Sci U S A **71**(10): 4173-4177.

Dabrowski, A., et al. (2000). "Reactive oxygen species activate mitogen-activated protein kinases in pancreatic acinar cells." Pancreas **21**(4): 376-384.

Dabrowski, A., et al. (1988). "Oxygen-derived free radicals in cerulein-induced acute pancreatitis." Scand J Gastroenterol **23**(10): 1245-1249.

Dabrowski, A., et al. (1996). "Jun Kinases Are Rapidly Activated by Cholecystokinin in Rat Pancreas both in Vitro and in Vivo." Journal of Biological Chemistry **271**(10): 5686-5690.

Dashdorj, A., et al. (2013). "Mitochondria-targeted antioxidant MitoQ ameliorates experimental mouse colitis by suppressing NLRP3 inflammasome-mediated inflammatory cytokines." BMC Med **11**: 178.

Dashdorj, A., et al. (2013). "Mitochondria-targeted antioxidant MitoQ ameliorates experimental mouse colitis by suppressing NLRP3 inflammasome-mediated inflammatory cytokines." BMC Med **11**(1).

Davidson, S. M. (2010). "Endothelial mitochondria and heart disease." Cardiovascular Research **88**(1): 58-66.

Davidson, S. M., et al. (2012). Slow calcium waves and redox changes precede mitochondrial permeability transition pore opening in the intact heart during hypoxia and reoxygenation.

Davidson, S. M., et al. (2012). "Slow calcium waves and redox changes precede mitochondrial permeability transition pore opening in the intact heart during hypoxia and reoxygenation." Cardiovasc Res **93**(3): 445-453.

Davies, A. L., et al. (2013). "Neurological deficits caused by tissue hypoxia in neuroinflammatory disease." Ann Neurol **74**(6): 815-825.

Davies, K. J. (1999). "The broad spectrum of responses to oxidants in proliferating cells: a new paradigm for oxidative stress." IUBMB Life **48**(1): 41-47.

Dawra, R., et al. (2011). "Intra-acinar trypsinogen activation mediates early stages of pancreatic injury but not inflammation in mice with acute pancreatitis." Gastroenterology **141**(6): 2210-2217 e2212.

Dawra, R., et al. (2007). "Development of a new mouse model of acute pancreatitis induced by administration of L-arginine." Am J Physiol Gastrointest Liver Physiol **292**(4): G1009-1018.

Day, E. V. a. A. (2011). "Hydrogen Peroxide as a Signaling Molecule." Antioxidants & Redox Signaling **15**(1): 147-151.

De Lisle, R. C., et al. (1990). "Pancreatic acinar cells in culture: Expression of acinar and ductal antigens in a growth-related manner." European Journal of Cell Biology **51**(1): 64-75.

De Waele, B., et al. (1992). "Vitamin status in patients with acute pancreatitis." Clin Nutr **11**(2): 83-86.

Del Castillo-Vaquero, A., et al. (2010). "Increased calcium influx in the presence of ethanol in mouse pancreatic acinar cells." International Journal of Experimental Pathology **91**(2): 114-124.

Demols, A., et al. (2000). "N-acetylcysteine decreases severity of acute pancreatitis in mice." Pancreas **20**(2): 161-169.

Denton, R. M., et al. (1978). "Calcium ions and the regulation of NAD+-linked isocitrate dehydrogenase from the mitochondria of rat heart and other tissues." Biochem J **176**(3): 899-906.

Denu, J. M., et al. (1998). "Specific and Reversible Inactivation of Protein Tyrosine Phosphatases by Hydrogen Peroxide: Evidence for a Sulfenic Acid Intermediate and Implications for Redox Regulation." Biochemistry **37**(16): 5633-5642.

Dhanasekaran, A., et al. (2004). "Supplementation of endothelial cells with mitochondria-targeted antioxidants inhibit peroxide-induced mitochondrial iron uptake, oxidative damage, and apoptosis." Journal of Biological Chemistry **279**(36): 37575-37587.

Dinkova-Kostova, A. T., et al. (2000). "Persuasive evidence that quinone reductase type 1 (DT diaphorase) protects cells against the toxicity of electrophiles and reactive forms of oxygen1." Free Radical Biology and Medicine **29**(3–4): 231-240.

Dios, I. D. (2010). "Inflammatory role of the acinar cells during acute pancreatitis." World Journal of Gastrointestinal Pharmacology and Therapeutics **1**(1): 15-20.

Dolman, N. J., et al. (2005). "Stable Golgi-mitochondria complexes and formation of Golgi Ca(2+) gradients in pancreatic acinar cells." J Biol Chem **280**(16): 15794-15799.

Doughan, A. K., et al. (2007). "Mitochondrial redox cycling of mitoquinone leads to superoxide production and cellular apoptosis." Antioxid Redox Signal **9**(11): 1825-1836.

Doyle, K. M., et al. (1994). "Fatty acid ethyl esters are present in human serum after ethanol ingestion." Journal of Lipid Research **35**(3): 428-437.

Droge, W. (2002). "Free radicals in the physiological control of cell function." Physiol Rev **82**(1): 47-95.

Du, W. D., et al. (2003). "Therapeutic efficacy of high-dose vitamin C on acute pancreatitis and its potential mechanisms." World J Gastroenterol **9**(11): 2565-2569.

Duchen, M. R. (1999). "Contributions of mitochondria to animal physiology: from homeostatic sensor to calcium signalling and cell death." The Journal of Physiology **516**(Pt 1): 1-17.

Duchen, M. R. (1999). "Contributions of mitochondria to animal physiology: from homeostatic sensor to calcium signalling and cell death." The Journal of Physiology **516**(1): 1-17.

Duchen, M. R. (2000). "Mitochondria and calcium: from cell signalling to cell death." J Physiol **529 Pt 1**: 57-68.

Dufour, M. C., et al. (2003). "The Epidemiology of Alcohol-Induced Pancreatitis." Pancreas **27**(4): 286-290.

Dziurkowska-Marek, A., et al. (2004). "The dynamics of the oxidant-antioxidant balance in the early phase of human acute biliary pancreatitis." Pancreatology **4**(3-4): 215-222.

Eberlein, G. A., et al. (1987). "Detection of cholecystokinin-58 in human blood by inhibition of degradation." Am J Physiol **253**(4 Pt 1): G477-482.

Echtay, K. S., et al. (2002). "Superoxide activates mitochondrial uncoupling protein 2 from the matrix side. Studies using targeted antioxidants." J Biol Chem **277**(49): 47129-47135.

Ehrenberg, B., et al. (1988). "Membrane potential can be determined in individual cells from the nernstian distribution of cationic dyes." Biophysical Journal **53**(5): 785-794.

Escobar, J., et al. (2012). "Redox signaling and histone acetylation in acute pancreatitis." Free Radical Biology and Medicine **52**(5): 819-837.

Esrefoglu, M. (2012). "Experimental and clinical evidence of antioxidant therapy in acute pancreatitis." World Journal of Gastroenterology **18**(39): 5533-5541.

Esrefoglu, M., et al. (2006). "Antioxidative effect of melatonin, ascorbic acid and N-acetylcysteine on caerulein-induced pancreatitis and associated liver injury in rats." World J Gastroenterol **12**(2): 259-264.

Esrefoglu, M., et al. (2006). "Ultrastructural clues for the protective effect of ascorbic acid and N-acetylcysteine against oxidative damage on caerulein-induced pancreatitis." Pancreatology **6**(5): 477-485.

Eu, J. P., et al. (2000). "The Skeletal Muscle Calcium Release Channel: Coupled O2 Sensor and NO Signaling Functions." Cell **102**(4): 499-509.

Faulkner, M. J., et al. (2011). "Peroxide Stress Elicits Adaptive Changes in Bacterial Metal Ion Homeostasis." Antioxid Redox Signal **15**(1): 175-189.

Favero, T. G., et al. (1995). "Hydrogen Peroxide Stimulates the Ca2+ Release Channel from Skeletal Muscle Sarcoplasmic Reticulum." Journal of Biological Chemistry **270**(43): 25557-25563.

Fernandez-Sanchez, M., et al. (2009). "Ethanol exerts dual effects on calcium homeostasis in CCK-8-stimulated mouse pancreatic acinar cells." BMC Cell Biol **10**: 77.

Feske, S., et al. (2006). "A mutation in Orai1 causes immune deficiency by abrogating CRAC channel function." Nature **441**(7090): 179-185.

Fink, B. D., et al. (2012). "Bioenergetic effects of mitochondrial-targeted coenzyme Q analogs in endothelial cells." J Pharmacol Exp Ther **342**(3): 709-719.

Fink, B. D., et al. (2009). "Mitochondrial Targeted Coenzyme Q, Superoxide, and Fuel Selectivity in Endothelial Cells." PLoS ONE **4**(1): e4250.

Finkel, T. (1998). "Oxygen radicals and signaling." Current Opinion in Cell Biology **10**(2): 248-253.

Finkel, T. (2011). "Signal transduction by reactive oxygen species." J Cell Biol **194**(1): 7-15.

Finkel, T., et al. (2000). "Oxidants, oxidative stress and the biology of ageing." Nature **408**(6809): 239-247.

Fischer, L., et al. (2007). "Phosphatidylinositol 3-kinase facilitates bile acid-induced Ca2+ responses in pancreatic acinar cells." American Journal of Physiology - Gastrointestinal and Liver Physiology **292**(3): G875-G886.

Fleury, C., et al. (2002). "Mitochondrial reactive oxygen species in cell death signaling." Biochimie **84**(2-3): 131-141.

Folch, E., et al. (1998). "Free radicals generated by xanthine oxidase mediate pancreatitis-associated organ failure." Dig Dis Sci **43**(11): 2405-2410.

Folch, E., et al. (1999). "Role of P-selectin and ICAM-1 in pancreatitis-induced lung inflammation in rats: significance of oxidative stress." Ann Surg **230**(6): 792-798; discussion 798-799.

Folch, E., et al. (2000). "H2O2 and PARS mediate lung P-selectin upregulation in acute pancreatitis." Free Radical Biology and Medicine **28**(8): 1286-1294.

Fontaine, E., et al. (1998). "A ubiquinone-binding site regulates the mitochondrial permeability transition pore." Journal of Biological Chemistry **273**(40): 25734-25740.

Fridovich, I. (1989). "Oxygen radicals from acetaldehyde." Free Radic Biol Med **7**(5): 557-558.

Frossard, J. L., et al. (2008). "Acute pancreatitis." Lancet **371**(9607): 143-152.

Fukushi, Y., et al. (2001). "Identification of Cyclic ADP-ribose-dependent Mechanisms in Pancreatic Muscarinic Ca2+ Signaling Using CD38 Knockout Mice." Journal of Biological Chemistry **276**(1): 649-655.

Fulda, S., et al. (2010). "Cellular stress responses: cell survival and cell death." Int J Cell Biol **2010**: 214074.

Futatsugi, A., et al. (2005). "IP3 receptor types 2 and 3 mediate exocrine secretion underlying energy metabolism." Science **309**(5744): 2232-2234.

Gabbita, S. P., et al. (2000). "Redox Regulatory Mechanisms of Cellular Signal Transduction." Archives of Biochemistry and Biophysics **376**(1): 1-13.

Gaiser, S., et al. (2011). "Intracellular activation of trypsinogen in transgenic mice induces acute but not chronic pancreatitis." Gut **60**(10): 1379-1388.

Galione, A., et al. (1991). "Ca^{2+}-induced Ca2+ release in sea urchin egg homogenates: modulation by cyclic ADP-ribose." Science **253**(5024): 1143-1146.

Gane, E. J., et al. (2010). "The mitochondria-targeted anti-oxidant mitoquinone decreases liver damage in a phase II study of hepatitis C patients." Liver International **30**(7): 1019-1026.

Gerasimenko, J. V., et al. (2006). "Bile acids induce Ca2+ release from both the endoplasmic reticulum and acidic intracellular calcium stores through activation of inositol trisphosphate receptors and ryanodine receptors." Journal of Biological Chemistry **281**(52): 40154-40163.

Gerasimenko, J. V., et al. (2002). "Menadione-induced apoptosis: roles of cytosolic Ca(2+) elevations and the mitochondrial permeability transition pore." J Cell Sci **115**(Pt 3): 485-497.

Gerasimenko, J. V., et al. (2002). "Menadione-induced apoptosis: Roles of cytosolic Ca2+ elevations and the mitochondrial permeability transition pore." Journal of Cell Science **115**(3): 485-497.

Gerasimenko, J. V., et al. (2003). "NAADP mobilizes Ca2+ from a thapsigargin-sensitive store in the nuclear envelope by activating ryanodine receptors." J Cell Biol **163**(2): 271-282.

Gerasimenko, O. V., et al. (2002). "The distribution of the endoplasmic reticulum in living pancreatic acinar cells." Cell Calcium **32**(5-6): 261-268.

Gerich, F., et al. (2009). "H2O2-mediated modulation of cytosolic signaling and organelle function in rat hippocampus." Pflügers Archiv - European Journal of Physiology **458**(5): 937-952.

Gerschenson, L. E., et al. (1992). "Apoptosis: a different type of cell death." The FASEB Journal **6**(7): 2450-2455.

Gerschman, R., et al. (1954). "Oxygen poisoning and x-irradiation: a mechanism in common." Science **119**(3097): 623-626.

Ghosh, A., et al. (2010). "Neuroprotection by a mitochondria-targeted drug in a Parkinson's disease model." Free Radical Biology and Medicine **49**(11): 1674-1684.

Giacomello, M., et al. (2007). "Mitochondrial Ca2+ as a key regulator of cell life and death." Cell Death Differ **14**(7): 1267-1274.

Gincel, D., et al. (2001). "Calcium binding and translocation by the voltage-dependent anion channel: a possible regulatory mechanism in mitochondrial function." Biochem J **358**(Pt 1): 147-155.

Giorgio, V., et al. (2013). "Dimers of mitochondrial ATP synthase form the permeability transition pore." Proc Natl Acad Sci U S A **110**(15): 5887-5892.

Gioscia-Ryan, R. A., et al. (2014). "Mitochondria-targeted antioxidant (MitoQ) ameliorates age-related arterial endothelial dysfunction in mice." Journal of Physiology **592**(12): 2549-2561.

Giulivi, C., et al. (1998). "Production of nitric oxide by mitochondria." J. Biol. Chem. **273**: 11038-11043.

Glancy, B., et al. (2012). "Role of mitochondrial Ca 2+ in the regulation of cellular energetics." Biochemistry **51**(14): 2959-2973.

Goldkorn, T., et al. (1998). "H2O2 acts on cellular membranes to generate ceramide signaling and initiate apoptosis in tracheobronchial epithelial cells." J Cell Sci **111 (Pt 21)**: 3209-3220.

Gonzalez, A., et al. (2005). "H2O2-induced changes in mitochondrial activity in isolated mouse pancreatic acinar cells." Mol Cell Biochem **269**(1-2): 165-173.

González, A., et al. (2006). "Ethanol impairs CCK-8-evoked amylase secretion through Ca2+-mediated ROS generation in mouse pancreatic acinar cells." Alcohol **38**(1): 51-57.

Gonzalez, A., et al. (1997). "Intracellular pH and calcium signalling in rat pancreatic acinar cells." Pflugers Archiv European Journal of Physiology **434**(5): 609-614.

Gonzalez, A., et al. (2012). "Cinnamtannin B-1, a natural antioxidant that reduces the effects of H2O2 on CCK-8-evoked responses in mouse pancreatic acinar cells." Journal of Physiology and Biochemistry **68**(2): 181-191.

Gonzalez, A., et al. (2002). "XOD-catalyzed ROS generation mobilizes calcium from intracellular stores in mouse pancreatic acinar cells." Cell Signal **14**(2): 153-159.

Gonzalez, A., et al. (2000). "Agonist-evoked mitochondrial Ca2+ signals in mouse pancreatic acinar cells." J Biol Chem **275**(49): 38680-38686.

Gough, D. R., et al. (2011). "Hydrogen peroxide: a Jekyll and Hyde signalling molecule." Cell Death and Dis **2**: e213.

Grady, T., et al. (1996). "Stress-activated protein kinase activation is the earliest direct correlate to the induction of secretagogue-induced pancreatitis in rats." Biochemical and Biophysical Research Communications **227**(1): 1-7.

Graf, D., et al. (2002). "Prevention of bile acid-induced apoptosis by betaine in rat liver." Hepatology **36**(4 I): 829-839.

Granados, M. P., et al. (2006). "Dose-dependent effect of hydrogen peroxide on calcium mobilization in mouse pancreatic acinar cells." Biochem Cell Biol **84**(1): 39-48.

Granados, M. P., et al. (2004). "Generation of ROS in response to CCK-8 stimulation in mouse pancreatic acinar cells." Mitochondrion **3**(5): 285-296.

Granados, M. P., et al. (2005). "Effect of H2O2 on CCK-8-evoked changes in mitochondrial activity in isolated mouse pancreatic acinar cells." Biology of the Cell **97**(11): 847-856.

Granados, M. P., et al. (2007). "Modulation of CCK-8-evoked intracellular Ca2+ waves by hydrogen peroxide in mouse pancreatic acinar cells." Journal of Physiology and Pharmacology **58**(3): 423-440.

Gravina, F., et al. (2010). "Role of mitochondria in contraction and pacemaking in the mouse uterus." Br J Pharmacol **161**(6): 1375-1390.

Grommes, J., et al. (2011). "Contribution of neutrophils to acute lung injury." Mol Med **17**(3-4): 293-307.

Grover, A. K., et al. (1988). "Effect of superoxide radical on Ca^{2+} pumps of coronary artery." American Journal of Physiology - Cell Physiology **255**(3).

Guice, K. S., et al. (1986). "Superoxide dismutase and catalase: a possible role in established pancreatitis." Am J Surg **151**(1): 163-169.

Guice, K. S., et al. (1989). "Neutrophil-dependent, oxygen-radical mediated lung injury associated with acute pancreatitis." Ann Surg **210**(6): 740-747.

Gukovskaya, A., et al. (1994). "Nitric oxide production regulates cGMP formation and calcium influx in pancreatic acinar cells." Am J Physiol **266**(3 Pt 1): G350-356.

Gukovskaya, A. S., et al. (2011). "Which way to die: the regulation of acinar cell death in pancreatitis by mitochondria, calcium, and reactive oxygen species." Gastroenterology **140**(7): 1876-1880.

Gukovskaya, A. S., et al. (2012). "Autophagy and pancreatitis." American Journal of Physiology - Gastrointestinal and Liver Physiology **303**(9): G993-G1003.

Gukovskaya, A. S., et al. (2002). "Cholecystokinin induces caspase activation and mitochondrial dysfunction in pancreatic acinar cells. Roles in cell injury processes of pancreatitis." J Biol Chem **277**(25): 22595-22604.

Gukovskaya, A. S., et al. (2006). "Cell death in pancreatitis: effects of alcohol." J Gastroenterol Hepatol **21 Suppl 3**: S10-13.

Gukovskaya, A. S., et al. (2002). "Ethanol metabolism and transcription factor activation in pancreatic acinar cells in rats." Gastroenterology **122**(1): 106-118.

Gukovskaya, A. S., et al. (2004). "Cell death pathways in pancreatitis and pancreatic cancer." Pancreatology **4**(6): 567-586.

Gukovskaya, A. S., et al. (1996). "Mechanisms of cell death after pancreatic duct obstruction in the opossum and the rat." Gastroenterology **110**(3): 875-884.

Gukovskaya, A. S., et al. (2002). "Neutrophils and NADPH oxidase mediate intrapancreatic trypsin activation in murine experimental acute pancreatitis." Gastroenterology **122**(4): 974-984.

Gukovsky, I., et al. (2013). "Inflammation, autophagy, and obesity: common features in the pathogenesis of pancreatitis and pancreatic cancer." Gastroenterology **144**(6): 1199-1209 e1194.

Gukovsky, I., et al. (2012). "Impaired autophagy and organellar dysfunction in pancreatitis." Journal of Gastroenterology and Hepatology **27**: 27-32.

Guyan, P. M., et al. (1990). "Heightened free radical activity in pancreatitis." Free Radical Biology and Medicine **8**(4): 347-354.

Guyan, P. M., et al. (1990). "Heightened free radical activity in pancreatitis." Free Radic Biol Med **8**(4): 347-354.

Gwack, Y., et al. (2007). "Biochemical and functional characterization of Orai proteins." J Biol Chem **282**(22): 16232-16243.

Haber, P. S., et al. (1998). "Metabolism of ethanol by rat pancreatic acinar cells." Journal of Laboratory and Clinical Medicine **132**(4): 294-302.

Haber, P. S., et al. (2004). "Non-Oxidative Metabolism of Ethanol by Rat Pancreatic Acini." Pancreatology **4**(2): 82-89.

Haber, P. S., et al. (1993). "Fatty acid ethyl esters increase rat pancreatic lysosomal fragility." The Journal of Laboratory and Clinical Medicine **121**(6): 759-764.

Hackert, T., et al. (2011). "Antioxidant therapy in acute pancreatitis: Experimental and clinical evidence." Antioxidants and Redox Signaling **15**(10): 2767-2777.

Hackert, T., et al. (2011). "Antioxidant therapy in acute pancreatitis: experimental and clinical evidence." Antioxid Redox Signal **15**(10): 2767-2777.

Hajnoczky, G., et al. (1995). "Decoding of cytosolic calcium oscillations in the mitochondria." Cell **82**(3): 415-424.

Hajnóczky, G., et al. (1995). "Decoding of cytosolic calcium oscillations in the mitochondria." Cell **82**(3): 415-424.

Halangk, W., et al. (2002). Trypsin activity is not involved in premature, intrapancreatic trypsinogen activation.

Halangk, W., et al. (2000). "Role of cathepsin B in intracellular trypsinogen activation and the onset of acute pancreatitis." J Clin Invest **106**(6): 773-781.

Halangk, W., et al. (1998). "Effect of supramaximal cerulein stimulation on mitochondrial energy metabolism in rat pancreas." Pancreas **16**(1): 88-95.

Halliwell, B. (2000). "The antioxidant paradox." The Lancet **355**(9210): 1179-1180.

Hammons, G. J., et al. (1995). "Increased DT-diaphorase activity in transformed and tumorigenic pancreatic acinar cells." Cancer Lett **96**(1): 9-14.

Hampton, M. B., et al. (1997). "Dual regulation of caspase activity by hydrogen peroxide: implications for apoptosis." FEBS Lett **414**(3): 552-556.

Han, B., et al. (1999). "Cholecystokinin induction of mob-1 chemokine expression in pancreatic acinar cells requires NF-κB activation." American Journal of Physiology - Cell Physiology **277**(1 46-1): C74-C82.

Han, B., et al. (2000). "CCK stimulates mob-1 expression and NF-κB activation via protein kinase C and intracellular Ca2+." American Journal of Physiology - Cell Physiology **278**(2 47-2): C344-C351.

Hansson, M. J., et al. (2015). "Differences in the profile of protection afforded by TRO40303 and mild hypothermia in models of cardiac ischemia/reperfusion injury." Eur J Pharmacol **760**: 7-19.

Hardman, J., et al. (2005). "Intravenous antioxidant modulation of end-organ damage in L-arginine-induced experimental acute pancreatitis." Pancreatology **5**(4-5): 380-386.

Hartman, H., et al. (2015). "Histone deacetylase regulates trypsin activation, inflammation, and tissue damage in acute pancreatitis in mice." Dig Dis Sci **60**(5): 1284-1289.

He, L., et al. (2002). "Regulated and unregulated mitochondrial permeability transition pores: a new paradigm of pore structure and function?" FEBS Lett **512**(1-3): 1-7.

Heath, D. I., et al. (1993). "Role of interleukin-6 in mediating the acute phase protein response and potential as an early means of severity assessment in acute pancreatitis." Gut **34**(1): 41-45.

Heerdt, B. G., et al. (1998). "Mitochondrial membrane potential (delta psi(mt)) in the coordination of p53-independent proliferation and apoptosis pathways in human colonic carcinoma cells." Cancer Res **58**(13): 2869-2875.

Henriksen, E. J. (2013). Effects of H2O2 on Insulin Signaling the Glucose Transport System in Mammalian Skeletal Muscle. Methods Enzymol. C. Enrique and P. Lester, Academic Press. **Volume 528:** 269-278.

Herrera, B., et al. (2001). "Reactive oxygen species (ROS) mediates the mitochondrial-dependent apoptosis induced by transforming growth factor β in fetal hepatocytes." The FASEB Journal **15**(3): 741-751.

Herst, P. M., et al. (2004). "Cell surface oxygen consumption by mitochondrial gene knockout cells." Biochim Biophys Acta **1656**(2-3): 79-87.

Higuchi, Y. (2004). "Glutathione depletion-induced chromosomal DNA fragmentation associated with apoptosis and necrosis." J Cell Mol Med **8**(4): 455-464.

Hirose, S., et al. (1974). "Disruption of charge separation followed by that of the proton gradient in the mitochondrial membrane by CCCP." Journal of Biochemistry **76**(1): 213-216.

Ho, E., et al. (1999). "Supplementation of N-acetylcysteine inhibits NFkappaB activation and protects against alloxan-induced diabetes in CD-1 mice." FASEB J **13**(13): 1845-1854.

Hong, J. H., et al. (2011). "Polarized but differential localization and recruitment of STIM1, Orai1 and TRPC channels in secretory cells." Traffic **12**(2): 232-245.

Huang, G. N., et al. (2006). "STIM1 carboxyl-terminus activates native SOC, I(crac) and TRPC1 channels." Nat Cell Biol **8**(9): 1003-1010.

Huang, W., et al. (2014). "Fatty acid ethyl ester synthase inhibition ameliorates ethanol-induced Ca2+-dependent mitochondrial dysfunction and acute pancreatitis." Gut **63**(8): 1313-1324.

Huang, W., et al. (2015). "Effects of the Mitochondria-Targeted Antioxidant Mitoquinone in Murine Acute Pancreatitis." Mediators of Inflammation **2015**: 13.

Huang, W., et al. (2015). "Effects of the mitochondria-targeted antioxidant mitoquinone in murine acute pancreatitis." Mediators of Inflammation **2015**.

Hwang, P. M., et al. (2001). "Ferredoxin reductase affects p53-dependent, 5-fluorouracil–induced apoptosis in colorectal cancer cells." Nat Med **7**(10): 1111-1117.

Iannitti, T., et al. (2009). "Antioxidant therapy effectiveness: an up to date." Eur Rev Med Pharmacol Sci **13**(4): 245-278.

Inagaki, H., et al. (1997). "Neutrophil behavior in pancreas and liver and the role of nitric oxide in rat acute pancreatitis." Pancreas **15**(3): 304-309.

Inoue, M., et al. (1999). "Cross-talk of NO, superoxide and molecular oxygen, a majesty of aerobic life." Free Radic Res **31**(4): 251-260.

Irani, K., et al. (1997). "Mitogenic signaling mediated by oxidants in Ras-transformed fibroblasts." Science **275**(5306): 1649-1652.

James, A. M., et al. (2005). "Interactions of mitochondria-targeted and untargeted ubiquinones with the mitochondrial respiratory chain and reactive oxygen species. Implications for the use of exogenous ubiquinones as therapies and experimental tools." J Biol Chem **280**(22): 21295-21312.

James, A. M., et al. (2007). "Interaction of the mitochondria-targeted antioxidant MitoQ with phospholipid bilayers and ubiquinone oxidoreductases." J Biol Chem **282**(20): 14708-14718.

James, A. M., et al. (2004). "Antioxidant and prooxidant properties of mitochondrial Coenzyme Q." Arch Biochem Biophys **423**(1): 47-56.

James, A. M., et al. (2004). "Antioxidant and prooxidant properties of mitochondrial Coenzyme Q." Archives of Biochemistry and Biophysics **423**(1): 47-56.

James, S. J., et al. (2009). "Cellular and mitochondrial glutathione redox imbalance in lymphoblastoid cells derived from children with autism." The FASEB Journal **23**(8): 2374-2383.

Jamieson, J. D., et al. (1971). "Synthesis, intracellular transport, and discharge of secretory proteins in stimulated pancreatic exocrine cells." J Cell Biol **50**(1): 135-158.

Jauslin, M. L., et al. (2003). "Mitochondria-targeted antioxidants protect Friedreich Ataxia fibroblasts from endogenous oxidative stress more effectively than untargeted antioxidants." FASEB J **17**(13): 1972-1974.

Jensen R T, J. L. R., Alpers D H, Jacobson E D, Christensen J, Walsh J H, editors. (1994). "In: Physiology of the Gastrointestinal Tract 3rd Ed." New York: Raven: 1377–1446.

Ji, B., et al. (2003). "Pancreatic gene expression during the initiation of acute pancreatitis: Identification of EGR-1 as a key regulator." Physiological Genomics **14**: 59-72.

Ji, B., et al. (2000). "Species differences between rat and mouse CCK(A) receptors determine the divergent acinar cell response to the cholecystokinin analog JMV-180." Journal of Biological Chemistry **275**(25): 19115-19120.

Ji, B., et al. (2009). "Ras activity levels control the development of pancreatic diseases." Gastroenterology **137**(3): 1072-1082, 1082 e1071-1076.

Ji, B., et al. (2009). "Ras Activity Levels Control the Development of Pancreatic Diseases." Gastroenterology **137**(3): 1072-1082.e1076.

Ji, C. (2012). "Mechanisms of Alcohol-Induced Endoplasmic Reticulum Stress and Organ Injuries." Biochemistry Research International **2012**: 216450.

Johnson, P. R., et al. (2003). "Non-uniform distribution of mitochondria in pancreatic acinar cells." Cell Tissue Res **313**(1): 37-45.

Johnson, P. R., et al. (2002). "Role of mitochondria in Ca(2+) homeostasis of mouse pancreatic acinar cells." Cell Calcium **32**(2): 59-69.

Jouaville, L. S., et al. (1999). "Regulation of mitochondrial ATP synthesis by calcium: Evidence for a long-term metabolic priming." Proc Natl Acad Sci U S A **96**(24): 13807-13812.

Kadlubar, F. F., et al. (1998). "Comparison of DNA adduct levels associated with oxidative stress in human pancreas." Mutat Res **405**(2): 125-133.

Kaiser, A. M., et al. (1995). "Relationship between severity, necrosis, and apoptosis in five models of experimental acute pancreatitis." American Journal of Physiology - Cell Physiology **269**(5 38-5): C1295-C1304.

Kamata, H., et al. (2005). "Reactive oxygen species promote TNFalpha-induced death and sustained JNK activation by inhibiting MAP kinase phosphatases." Cell **120**(5): 649-661.

Kamyar Shahedi, S. J. P., Richard Hu (2013). "Oxidative Stress and Alcoholic Pancreatitis." Journal of Gastroenterology and Hepatology **2**(1).

Kaphalia, B. S., et al. (2001). "Fatty acid ethyl esters and ethanol-induced pancreatitis." Cellular and Molecular Biology **47 Online Pub**: OL173-179.

Karch, J., et al. (2015). "Necroptosis Interfaces with MOMP and the MPTP in Mediating Cell Death." PLoS ONE **10**(6): e0130520.

Karczewski, J. M., et al. (2000). "p53-independent apoptosis induced by menadione in the human colon carcinoma cell line Caco-2." Ann N Y Acad Sci **915**: 275-278.

Kargin, V. I., et al. (2008). "Interaction of positively charged ubiquinone analog (MitoQ10) with DT-diaphorase from liver mitochondria." Biochemistry (Moscow) Supplement Series A: Membrane and Cell Biology **2**(1): 33-39.

Katsinelos, P., et al. (2005). "High-dose allopurinol for prevention of post-ERCP pancreatitis: a prospective randomized double-blind controlled trial." Gastrointest Endosc **61**(3): 407-415.

Kc, S., et al. (2005). "Vitamin C enters mitochondria via facilitative glucose transporter 1 (Glut1) and confers mitochondrial protection against oxidative injury." FASEB J **19**(12): 1657-1667.

Kelso, G. F., et al. (2001). "Selective targeting of a redox-active ubiquinone to mitochondria within cells: antioxidant and antiapoptotic properties." J Biol Chem **276**(7): 4588-4596.

Kim, H. (2008). "Cerulein pancreatitis: oxidative stress, inflammation, and apoptosis." Gut Liver **2**(2): 74-80.

Kim, J. Y., et al. (2002). "Transporter-mediated bile acid uptake causes Ca2+-dependent cell death in rat pancreatic acinar cells." Gastroenterology **122**(7): 1941-1953.

Kinnally, K. W., et al. (2011). "Is mPTP the gatekeeper for necrosis, apoptosis, or both?" Biochim Biophys Acta **1813**(4): 616-622.

Kirchgessner, A. L., et al. (1994). "NADPH diaphorase (nitric oxide synthase)-containing nerves in the enteropancreatic innervation: sources, co-stored neuropeptides, and pancreatic function." J Comp Neurol **342**(1): 115-130.

Kirichok, Y., et al. (2004). "The mitochondrial calcium uniporter is a highly selective ion channel." Nature **427**(6972): 360-364.

Kirichok, Y., et al. (2004). "The mitochondrial calcium uniporter is a highly selective ion channel." Nature **427**(6972): 360-364.

Kishimoto, T., et al. (1994). "Cytokine signal transduction." Cell **76**(2): 253-262.

Klomsiri, C., et al. (2011). "Cysteine-based redox switches in enzymes." Antioxid Redox Signal **14**(6): 1065-1077.

Kloppel, G., et al. (1993). "Pathology of acute and chronic pancreatitis." Pancreas **8**(6): 659-670.

Konturek, S. J., et al. (1993). "Role of endogenous nitric oxide in the control of canine pancreatic secretion and blood flow." Gastroenterology **104**(3): 896-902.

Kroemer, G., et al. (2007). "Mitochondrial membrane permeabilization in cell death." Physiol Rev **87**(1): 99-163.

Kroemer, G., et al. (2000). "Mitochondrial control of cell death." Nat Med **6**(5): 513-519.

Krüger, B., et al. (2001). "Effect of Hyperthermia on Premature Intracellular Trypsinogen Activation in the Exocrine Pancreas." Biochem Biophys Res Commun **282**(1): 159-165.

Kubisch, C. H., et al. (2006). "Long-term ethanol consumption alters pancreatic gene expression in rats: A possible connection to pancreatic injury." Pancreas **33**(1): 68-76.

Kuklinski, B., et al. (1992). "Anti-oxidative therapy of pancreatitis--an 18-month interim evaluation." Z Gesamte Inn Med **47**(6): 239-245.

Kuklinski, B., et al. (1995). "Decreasing mortality in acute pancreatitis with sodium selenite. Clinical results of 4 years antioxidant therapy." Med Klin (Munich) **90 Suppl 1**: 36-41.

Lamarche, F., et al. (2004). "Impact of ethanol and acetaldehyde on DNA and cell viability of cultured neurones." Cell Biol Toxicol **20**(6): 361-374.

Lambeth, J. D., et al. (2000). "Novel homologs of gp91phox." Trends Biochem Sci **25**(10): 459-461.

Lange, L. G., et al. (1983). "Mitochondrial dysfunction induced by fatty acid ethyl esters, myocardial metabolites of ethanol." Journal of Clinical Investigation **72**(2): 724-731.

Laposata, E. A., et al. (1986). "Presence of nonoxidative ethanol metabolism in human organs commonly damaged by ethanol abuse." Science **231**(4737): 497-499.

Lau, B. W., et al. (2005). "Deoxycholic acid activates protein kinase C and phospholipase C via increased Ca2+ entry at plasma membrane." Gastroenterology **128**(3): 695-707.

Lee, J. H., et al. (2012). "Prevention effects of ND-07, a novel drug candidate with a potent antioxidative action and anti-inflammatory action, in animal models of severe acute pancreatitis." Eur J Pharmacol **687**(1-3): 28-38.

Lee, M. G., et al. (1997). "Polarized expression of Ca2+ pumps in pancreatic and salivary gland cells. Role in initiation and propagation of [Ca2+]i waves." J Biol Chem **272**(25): 15771-15776.

Lee, S., et al. (2011). "Mitochondrial H_2O_2 generated from electron transport chain complex I stimulates muscle differentiation." Cell Res **21**(5): 817-834.

Lee, S., et al. (2011). "Mitochondrial H(2)O(2) generated from electron transport chain complex I stimulates muscle differentiation." Cell Research **21**(5): 817-834.

Leist, M., et al. (1997). "Intracellular adenosine triphosphate (ATP) concentration: a switch in the decision between apoptosis and necrosis." J Exp Med **185**(8): 1481-1486.

Lemasters, J. J., et al. (2007). Imaging of Mitochondrial Polarization and Depolarization with Cationic Fluorophores. Methods in Cell Biology. **80:** 283-295.

Leo, S., et al. (2008). "The mitochondrial antioxidants MitoE(2) and MitoQ(10) increase mitochondrial Ca(2+) load upon cell stimulation by inhibiting Ca(2+) efflux from the organelle." Ann N Y Acad Sci **1147**: 264-274.

Lerch, M., et al. (2002). The Role of Cysteine Proteases in Intracellular Pancreatic Serine Protease Activation. Cellular Peptidases in Immune Functions and Diseases 2. J. Langner and S. Ansorge, Springer US. **477:** 403-410.

Lerch, M. M., et al. (1993). "Experimental pancreatitis." Current Opinion in Gastroenterology **9**(5): 752-759.

Lerch, M. M., et al. (1994). "Experimental animal models of acute pancreatitis." International Journal of Pancreatology **15**(3): 159-170.

Lerch, M. M., et al. (2013). "Models of acute and chronic pancreatitis." Gastroenterology **144**(6): 1180-1193.

Letko, G., et al. (1991). "Studies on lipid peroxidation in pancreatic tissue. In vitro formation of thiobarbituric-acid-reactive substances (TBRS)." Exp Pathol **42**(3): 151-157.

Leung, P. S., et al. (2009). "Role of oxidative stress in pancreatic inflammation." Antioxid Redox Signal **11**(1): 135-165.

Lewarchik, C. M., et al. (2014). "The ryanodine receptor is expressed in human pancreatic acinar cells and contributes to acinar cell injury." American Journal of Physiology - Gastrointestinal and Liver Physiology **307**(5): G574-G581.

Li, N., et al. (2003). "Mitochondrial complex I inhibitor rotenone induces apoptosis through enhancing mitochondrial reactive oxygen species production." J Biol Chem **278**(10): 8516-8525.

Li, N., et al. (2003). "Mitochondrial Complex I Inhibitor Rotenone Induces Apoptosis through Enhancing Mitochondrial Reactive Oxygen Species Production." Journal of Biological Chemistry **278**(10): 8516-8525.

Li, Y., et al. (1995). "Dilated cardiomyopathy and neonatal lethality in mutant mice lacking manganese superoxide dismutase." Nat Genet **11**(4): 376-381.

Li, Z. D., et al. (2006). "Effect of resveratrol on pancreatic oxygen free radicals in rats with severe acute pancreatitis." World J Gastroenterol **12**(1): 137-140.

Lichtenstein, A., et al. (2000). "Acute lung injury in two experimental models of acute pancreatitis: infusion of saline or sodium taurocholate into the pancreatic duct." Crit Care Med **28**(5): 1497-1502.

Liou, J., et al. (2005). "STIM Is a Ca(2+) Sensor Essential for Ca(2+)-Store-Depletion-Triggered Ca(2+) Influx." Curr Biol **15**(13): 1235-1241.

Liu, X., et al. (1996). "Induction of apoptotic program in cell-free extracts: requirement for dATP and cytochrome c." Cell **86**(1): 147-157.

Loeffler, M., et al. (2000). "The mitochondrion in cell death control: certainties and incognita." Exp Cell Res **256**(1): 19-26.

Logsdon, C. D. (2000). "Signal transduction in pancreatic acinar cell physiology and pathophysiology." Current Opinion in Gastroenterology **16**(5): 404-409.

Logsdon, C. D., et al. (2009). "Ras activity in acinar cells links chronic pancreatitis and pancreatic cancer." Clin Gastroenterol Hepatol **7**(11 Suppl): S40-43.

Logsdon, C. D., et al. (2013). "The role of protein synthesis and digestive enzymes in acinar cell injury." Nature reviews. Gastroenterology & hepatology **10**(6): 362-370.

Lowes, D. A., et al. (2008). "The mitochondria-targeted antioxidant MitoQ protects against organ damage in a lipopolysaccharide–peptidoglycan model of sepsis." Free Radical Biology and Medicine **45**(11): 1559-1565.

Lowes, D. A., et al. (2013). "Antioxidants that protect mitochondria reduce interleukin-6 and oxidative stress, improve mitochondrial function, and reduce biochemical markers of organ dysfunction in a rat model of acute sepsis." Br J Anaesth **110**(3): 472-480.

Lu, C., et al. (2007). "Role of calcium and cyclophilin D in the regulation of mitochondrial permeabilization induced by glutathione depletion." Biochem Biophys Res Commun **363**(3): 572-577.

Lur, G., et al. (2009). "Ribosome-free terminals of rough ER allow formation of STIM1 puncta and segregation of STIM1 from IP(3) receptors." Curr Biol **19**(19): 1648-1653.

Lutgendorff, F., et al. (2008). "Probiotics enhance pancreatic glutathione biosynthesis and reduce oxidative stress in experimental acute pancreatitis." Am J Physiol Gastrointest Liver Physiol **295**(5): G1111-1121.

Luthen, R., et al. (1995). "Intrapancreatic zymogen activation and levels of ATP and glutathione during caerulein pancreatitis in rats." Am J Physiol **268**(4 Pt 1): G592-604.

Lyn-Cook, B. D., et al. (2006). "Increased levels of NAD(P)H: quinone oxidoreductase 1 (NQO1) in pancreatic tissues from smokers and pancreatic adenocarcinomas: A potential biomarker of early damage in the pancreas." Cell Biol Toxicol **22**(2): 73-80.

Ma, B., et al. (2013). "Differentially expressed kinase genes associated with trypsinogen activation in rat pancreatic acinar cells treated with taurolithocholic acid 3-sulfate." Molecular Medicine Reports **7**(5): 1591-1596.

Madamanchi, N. R., et al. (2005). "Oxidative Stress and Vascular Disease." Arteriosclerosis, Thrombosis, and Vascular Biology **25**(1): 29-38.

Maechler, P., et al. (1999). "Hydrogen Peroxide Alters Mitochondrial Activation and Insulin Secretion in Pancreatic Beta Cells." Journal of Biological Chemistry **274**(39): 27905-27913.

Mankad, P., et al. (2012). "Insulin protects pancreatic acinar cells from cytosolic calcium overload and inhibition of plasma membrane calcium pump." J Biol Chem **287**(3): 1823-1836.

Mareninova, O. A., et al. (2006). "Cell death in pancreatitis: caspases protect from necrotizing pancreatitis." J Biol Chem **281**(6): 3370-3381.

Marí, M., et al. (2009). "Mitochondrial Glutathione, a Key Survival Antioxidant." Antioxid Redox Signal **11**(11): 2685-2700.

Maroz, A., et al. (2009). "Reactivity of ubiquinone and ubiquinol with superoxide and the hydroperoxyl radical: implications for in vivo antioxidant activity." Free Radic Biol Med **46**(1): 105-109.

Martin, J. A., et al. (2012). "Mitochondrial electron transport and glycolysis are coupled in articular cartilage." Osteoarthritis and Cartilage **20**(4): 323-329.

Martindale, J. L., et al. (2002). "Cellular response to oxidative stress: signaling for suicide and survival." J Cell Physiol **192**(1): 1-15.

Mayerle, J. (2009). "A novel role for leucocytes in determining the severity of acute pancreatitis." Gut **58**(11): 1440-1441.

McCormack, J. G., et al. (1990). "Role of calcium ions in regulation of mammalian intramitochondrial metabolism." Physiological Reviews **70**(2): 391-425.

McKay, C. J., et al. (1996). "Increased monocyte cytokine production in association with systemic complications in acute pancreatitis." Br J Surg **83**(7): 919-923.

McStay, G. P., et al. (2002). "Role of critical thiol groups on the matrix surface of the adenine nucleotide translocase in the mechanism of the mitochondrial permeability transition pore." Biochem J **367**(Pt 2): 541-548.

Mehrpour, M., et al. (2010). Autophagy in health and disease. 1. Regulation and significance of autophagy: an overview.

Meissner, G. (2002). "Regulation of mammalian ryanodine receptors." Front Biosci **7**: d2072-2080.

Meissner, G. (2010). "Regulation of Ryanodine Receptor Ion Channels Through Posttranslational Modifications." Current topics in membranes **66**: 91-113.

Melino, G., et al. (2005). "How many ways to die? How many different models of cell death?" Cell Death Differ **12 Suppl 2**: 1457-1462.

Melo, C. M., et al. (2011). "Anti-inflammatory effect of alpha,beta-amyrin, a triterpene from Protium heptaphyllum, on cerulein-induced acute pancreatitis in mice." Inflamm Res **60**(7): 673-681.

Millonig, G., et al. (2012). "Sustained submicromolar H2O2 levels induce hepcidin via signal transducer and activator of transcription 3 (STAT3)." J Biol Chem **287**(44): 37472-37482.

Miquel, E., et al. (2014). "Neuroprotective effects of the mitochondria-targeted antioxidant MitoQ in a model of inherited amyotrophic lateral sclerosis." Free Radical Biology and Medicine **70**: 204-213.

Mitchell, T., et al. (2011). "The mitochondria-targeted antioxidant mitoquinone protects against cold storage injury of renal tubular cells and rat kidneys." J Pharmacol Exp Ther **336**(3): 682-692.

Mojet M.H., J., D., Keelan,J., Vergun,O. and Duchen,M.R. Oxford, UK, In Tepikin,A.V. (ed.) (2000). "Monitoring mitochondrial function in single cells " Calcium Signalling: A Practical Approach. Oxford University Press: 79–106.

Moncada, S., et al. (2002). "Does nitric oxide modulate mitochondrial energy generation and apoptosis?" Nat Rev Mol Cell Biol **3**(3): 214-220.

Moncada, S., et al. (1991). "Nitric oxide: physiology, pathophysiology, and pharmacology." Pharmacol. Rev. **43**: 109-142.

Mooren, F. C., et al. (2001). "Calcium–magnesium interactions in pancreatic acinar cells." The FASEB Journal **15**(3): 659-672.

Morgado, S., et al. (2008). "Role of intracellular calcium on hydrogen peroxide-induced apoptosis in rat pancreatic acinar AR42J cells." Journal of Applied Biomedicine **6**(4): 211-224.

Morgan, M. J., et al. (2011). "Crosstalk of reactive oxygen species and NF-kappaB signaling." Cell Res **21**(1): 103-115.

Mossner, J., et al. (1991). "Comparison between the synthetic cholecystokinin analogues caerulein and Thr28NLE31CCK25-33(CCK9) with regards to plasma bioactivity, degradation rate and stimulation of pancreatic exocrine function." Zeitschrift fur Gastroenterologie **29**(2): 59-64.

Mouret, J. (1895). "Contribution à l ' é tude des cellules glandulaires

(pancreas)." J Anat Physiol **31**: 221 – 236.

Muallem, S., et al. (1988). "Role of Na+/Ca2+ exchange and the plasma membrane Ca2+ pump in hormone-mediated Ca2+ efflux from pancreatic acini." J Membr Biol **102**(2): 153-162.

Muili, K. A., et al. (2013). "Bile acids induce pancreatic acinar cell injury and pancreatitis by activating calcineurin." Journal of Biological Chemistry **288**(1): 570-580.

Mukherjee, R., et al. (2015). "Mechanism of mitochondrial permeability transition pore induction and damage in the pancreas: inhibition prevents acute pancreatitis by protecting production of ATP." Gut.

Mukherjee, T. K., et al. (2007). "High concentration of antioxidants N-acetylcysteine and mitoquinone-Q induces intercellular adhesion molecule 1 and oxidative stress by increasing intracellular glutathione." J Immunol **178**(3): 1835-1844.

Murphy, J. A., et al. (2008). "Direct activation of cytosolic Ca2+ signaling and enzyme secretion by cholecystokinin in human pancreatic acinar cells." Gastroenterology **135**(2): 632-641.

Murphy, M. P. (2008). "Targeting lipophilic cations to mitochondria." Biochim Biophys Acta **1777**(7-8): 1028-1031.

Murphy, M. P. (2014). "Antioxidants as therapies: can we improve on nature?" Free Radical Biology and Medicine **66**(0): 20-23.

Murphy, M. P., et al. (2007). "Targeting antioxidants to mitochondria by conjugation to lipophilic cations." Annu Rev Pharmacol Toxicol **47**: 629-656.

Murphy, M. P., et al. (2000). "Drug delivery to mitochondria: the key to mitochondrial medicine." Adv Drug Deliv Rev **41**(2): 235-250.

Myoung, K. P., et al. (2002). "Slow depletion of endoplasmic reticulum Ca2+ stores and block of store-operated Ca2+ channels by 2-aminoethoxydiphenyl borate in mouse pancreatic acinar cells." Naunyn-Schmiedeberg's Archives of Pharmacology **365**(5): 399-405.

Nakagawa, T., et al. (2005). "Cyclophilin D-dependent mitochondrial permeability transition regulates some necrotic but not apoptotic cell death." Nature **434**(7033): 652-658.

Nathan, J. D., et al. (2005). "Transgenic expression of pancreatic secretory trypsin inhibitor-I ameliorates secretagogue-induced pancreatitis in mice." Gastroenterology **128**(3): 717-727.

Neuschwander-Tetri, B. A., et al. (1997). "Glutathione synthesis in the exocrine pancreas." Pancreas **14**(4): 342-349.

Ng, L. F., et al. (2014). "The mitochondria-targeted antioxidant MitoQ extends lifespan and improves healthspan of a transgenic Caenorhabditis elegans model of Alzheimer disease." Free Radic Biol Med **71**: 390-401.

Nguyen, K. T., et al. (2009). "The ψm depolarization that accompanies mitochondrial Ca 2+ uptake is greater in mutant SOD1 than in wild-type mouse motor terminals." Proc Natl Acad Sci U S A **106**(6): 2007-2011.

Nicotera, P., et al. (1998). "Intracellular ATP, a switch in the decision between apoptosis and necrosis." Toxicol Lett **102-103**: 139-142.

Niederau, C., et al. (1985). "Caerulein-induced acute necrotizing pancreatitis in mice: Protective effects of proglumide, benzotript, and secretin." Gastroenterology **88**(5 I): 1192-1204.

Niederau, C., et al. (1991). "Involvement of free radicals in the pathophysiology of chronic pancreatitis: potential of treatment with antioxidant and scavenger substances." Klin Wochenschr **69**(21-23): 1018-1024.

Nita, L., et al. (2015). "Life after the birth of the mitochondrial Na+/Ca2+ exchanger, NCLX." Science China Life Sciences **58**(1): 59-65.

Niwa, K., et al. (2003). "Redox regulation of PI3K/Akt and p53 in bovine aortic endothelial cells exposed to hydrogen peroxide." Antioxid Redox Signal **5**(6): 713-722.

Nonaka, A., et al. (1990). "Changes in lipid peroxide and oxygen radical scavengers in cerulein-induced acute pancreatitis. Imbalance between the offense and defense systems." Digestion **47**(3): 130-137.

Nonaka, A., et al. (1989). "Changes of xanthine oxidase, lipid peroxide and superoxide dismutase in mouse acute pancreatitis." Digestion **43**(1-2): 41-46.

Norman, J. G., et al. (1995). "Acute pancreatitis induces intrapancreatic tumor necrosis factor gene expression." Arch Surg **130**(9): 966-970.

Nulton-Persson, A. C., et al. (2001). "Modulation of Mitochondrial Function by Hydrogen Peroxide." Journal of Biological Chemistry **276**(26): 23357-23361.

O'Malley, Y., et al. (2006). "Reactive oxygen and targeted antioxidant administration in endothelial cell mitochondria." J Biol Chem **281**(52): 39766-39775.

Odinokova, I. V., et al. (2009). "Mechanisms regulating cytochrome c release in pancreatic mitochondria." Gut **58**(3): 431-442.

Ohashi, S., et al. (2006). "Overexpression of redox-active protein thioredoxin-1 prevents development of chronic pancreatitis in mice." Antioxidants and Redox Signaling **8**(9-10): 1835-1845.

Ohmuraya, M., et al. (2005). "Autophagic cell death of pancreatic acinar cells in serine protease inhibitor Kazal type 3-deficient mice." Gastroenterology **129**(2): 696-705.

Oiva, J., et al. (2013). "Patients with acute pancreatitis complicated by organ dysfunction show abnormal peripheral blood polymorphonuclear leukocyte signaling." Pancreatology **13**(2): 118-124.

Osera, C., et al. (2015). "Pre-exposure of neuroblastoma cell line to pulsed electromagnetic field prevents H2O2-induced ROS production by increasing MnSOD activity." Bioelectromagnetics **36**(3): 219-232.

Ostrander, J. H., et al. (2010). "Optical Redox Ratio Differentiates Breast Cancer Cell Lines Based on Estrogen Receptor Status." Cancer Research **70**(11): 4759-4766.

Oyewole, A. O., et al. (2014). "Comparing the effects of mitochondrial targeted and localized antioxidants with cellular antioxidants in human skin cells exposed to UVA and hydrogen peroxide." FASEB J **28**(1): 485-494.

Ozkan, E., et al. (2012). "Protective effects of lycopene on cerulein-induced experimental acute pancreatitis in rats." J Surg Res **176**(1): 232-238.

Packer, M. A., et al. (1996). "Superoxide production by mitochondria in the presence of nitric oxide forms peroxynitrite." Biochem. Mol. Biol. Int. **40**: 527-534.

Palade, G. (1975). "Intracellular aspects of the process of protein synthesis." Science **189**(4200): 347-358.

Palmieri, V. O., et al. (2007). "Ethanol induces secretion of oxidized proteins by pancreatic acinar cells." Cell Biol Toxicol **23**(6): 459-464.

Palty, R., et al. (2010). "NCLX is an essential component of mitochondrial Na+/Ca2+ exchange." Proceedings of the National Academy of Sciences **107**(1): 436-441.

Pan, X., et al. (2013). "The physiological role of mitochondrial calcium revealed by mice lacking the mitochondrial calcium uniporter." Nat Cell Biol **15**(12): 1464-1472.

Pandol, S. J. (2010). The Exocrine Pancreas. San Rafael (CA).

Pandol, S. J., et al. (2010). "Alcohol Abuse, Endoplasmic Reticulum Stress and Pancreatitis." Digestive Diseases **28**(6): 776-782.

Pandol, S. J., et al. (1999). "Ethanol diet increases the sensitivity of rats to pancreatitis induced by cholecystokinin octapeptide." Gastroenterology **117**(3): 706-716.

Pandol, S. J., et al. (2007). "Acute pancreatitis: bench to the bedside." Gastroenterology **132**(3): 1127-1151.

Paredes, R. M., et al. (2008). "Chemical calcium indicators." Methods **46**(3): 143-151.

Pariente, J. A., et al. (2001). "Release of calcium from mitochondrial and nonmitochondrial intracellular stores in mouse pancreatic acinar cells by hydrogen peroxide." Journal of Membrane Biology **179**(1): 27-35.

Park, H. S., et al. (2009). "Impact of oxidative stress on lung diseases." Respirology **14**(1): 27-38.

Park, J. W., et al. (1997). "Effect of carbonyl cyanide m-chlorophenylhydrazone (CCCP) on the dimerization of lipoprotein lipase." Biochimica et Biophysica Acta - Lipids and Lipid Metabolism **1344**(2): 132-138.

Park, M. K., et al. (2001). "Perinuclear, perigranular and sub-plasmalemmal mitochondria have distinct functions in the regulation of cellular calcium transport." The EMBO Journal **20**(8): 1863-1874.

Park, M. K., et al. (2000). "The endoplasmic reticulum as one continuous Ca2+ pool: Visualization of rapid Ca2+ movements and equilibration." EMBO Journal **19**(21): 5729-5739.

Pastorino, J. G., et al. (1999). "Functional consequences of the sustained or transient activation by Bax of the mitochondrial permeability transition pore." J Biol Chem **274**(44): 31734-31739.

Patel, S., et al. (2001). "Coordination of Ca2+ signalling by NAADP." Trends Biochem Sci **26**(8): 482-489.

Patron, M., et al. (2013). "The mitochondrial calcium uniporter (MCU): Molecular identity and physiological roles." Journal of Biological Chemistry **288**(15): 10750-10758.

Peery, A. F., et al. (2012). "Burden of gastrointestinal disease in the United States: 2012 update." Gastroenterology **143**(5): 1179-1187 e1171-1173.

Pelletier, M., et al. (2012). "New tricks from an old dog: mitochondrial redox signaling in cellular inflammation." Semin Immunol **24**(6): 384-392.

Pérez, S., et al. (2015). "Redox signaling in acute pancreatitis." Redox Biol **5**(0): 1-14.

Perides, G., et al. (2010). "Biliary acute pancreatitis in mice is mediated by the G-protein-coupled cell surface bile acid receptor Gpbar1." Gastroenterology **138**(2): 715-725.

Perides, G., et al. (2010). "Experimental acute biliary pancreatitis induced by retrograde infusion of bile acids into the mouse pancreatic duct." Nat Protoc **5**(2): 335-341.

Perocchi, F., et al. (2010). "MICU1 encodes a mitochondrial EF hand protein required for Ca(2+) uptake." Nature **467**(7313): 291-296.

Petersen, O. H. (1992). "Stimulus-secretion coupling: cytoplasmic calcium signals and the control of ion channels in exocrine acinar cells." J Physiol **448**: 1-51.

Petersen, O. H. (2012). "Specific mitochondrial functions in separate sub-cellular domains of pancreatic acinar cells." Pflugers Arch **464**(1): 77-87.

Petersen, O. H., et al. (1999). "Polarity in intracellular calcium signaling." Bioessays **21**(10): 851-860.

Petersen, O. H., et al. (2006). "Ca^{2+} signalling and pancreatitis: effects of alcohol, bile and coffee." Trends Pharmacol Sci **27**(2): 113-120.

Petersen, O. H., et al. (2001). "The endoplasmic reticulum: One continuous or several separate Ca2+ stores?" Trends in Neurosciences **24**(5): 271-276.

Petronilli, V., et al. (1994). "Regulation of the permeability transition pore, a voltage-dependent mitochondrial channel inhibited by cyclosporine-A." Biochimica Et Biophysica Acta-Bioenergetics **1187**(2): 255-259.

Petrov, M. S., et al. (2012). "Severity of acute pancreatitis: impact of local and systemic complications." Gastroenterology **142**(7): e20-21; author reply e21.

Pietraforte, D., et al. (2014). "Focusing at the double-edged sword of redox imbalance: signals for cell survival or for cell death?" Antioxid Redox Signal **21**(1): 52-55.

Plecitá-Hlavatá, L., et al. (2009). "Pro-oxidant mitochondrial matrix-targeted ubiquinone MitoQ10 acts as anti-oxidant at retarded electron transport or proton pumping within Complex I." The International Journal of Biochemistry & Cell Biology **41**(8–9): 1697-1707.

Ponnappa, B. C., et al. (1997). "Ethanol consumption and susceptibility of the pancreas to cerulein-induced pancreatitis." Pancreas **14**(2): 150-157.

Prakriya, M., et al. (2006). "Orai1 is an essential pore subunit of the CRAC channel." Nature **443**(7108): 230-233.

Putney, J. W., Jr. (1986). "A model for receptor-regulated calcium entry." Cell Calcium **7**(1): 1-12.

Qin, F., et al. (2013). "Hydrogen peroxide-mediated SERCA cysteine 674 oxidation contributes to impaired cardiac myocyte relaxation in senescent mouse heart." J Am Heart Assoc **2**(4): e000184.

Radhakrishnan, J., et al. (2015). "Cyclophilin-D: a resident regulator of mitochondrial gene expression." FASEB J **29**(7): 2734-2748.

Radi, R., et al. (1991). "Peroxynitrite oxidation of sulfhydryls. The cytotoxic potential of superoxide and nitric oxide." J. Biol. Chem. **266**: 4244-4250.

Rahman, S. H., et al. (2004). "Association of antioxidant enzyme gene polymorphisms and glutathione status with severe acute pancreatitis." Gastroenterology **126**(5): 1312-1322.

Rahman, S. H., et al. (2004). "Association of antioxidant enzyme gene polymorphisms and glutathione status with severe acute pancreatitis." Gastroenterology **126**(5): 1312-1322.

Ramnath, R. D., et al. (2006). "Substance P treatment stimulates chemokine synthesis in pancreatic acinar cells via the activation of NF-κB." American Journal of Physiology - Gastrointestinal and Liver Physiology **291**(6): G1113-G1119.

Ramudo, L., et al. (2005). "Biliary pancreatitis-associated ascitic fluid activates the production of tumor necrosis factor-alpha in acinar cells." Crit Care Med **33**(1): 143-148; discussion 248.

Rao, V. A., et al. (2010). "The antioxidant transcription factor Nrf2 negatively regulates autophagy and growth arrest induced by the anticancer redox agent mitoquinone." Journal of Biological Chemistry **285**(45): 34447-34459.

Raraty, M., et al. (2000). "Calcium-dependent enzyme activation and vacuole formation in the apical granular region of pancreatic acinar cells." Proc Natl Acad Sci U S A **97**(24): 13126-13131.

Rasola, A., et al. (2011). "Mitochondrial permeability transition in Ca(2+)-dependent apoptosis and necrosis." Cell Calcium **50**(3): 222-233.

Rau, B., et al. (2001). "Modulation of endogenous nitric oxide synthase in experimental acute pancreatitis: role of anti-ICAM-1 and oxygen free radical scavengers." Ann Surg **233**(2): 195-203.

Rau, B., et al. (2000). "Pathophysiologic role of oxygen free radicals in acute pancreatitis: initiating event or mediator of tissue damage?" Ann Surg **231**(3): 352-360.

Reaume, A. G., et al. (1996). "Motor neurons in Cu/Zn superoxide dismutase-deficient mice develop normally but exhibit enhanced cell death after axonal injury." Nat Genet **13**(1): 43-47.

Rebelato, E., et al. (2012). "Expression of NADPH oxidase in human pancreatic islets." Life Sci **91**(7–8): 244-249.

Reily, C., et al. (2013). "Mitochondrially targeted compounds and their impact on cellular bioenergetics." Redox Biol **1**(1): 86-93.

Reinheckel, T., et al. (1998). "Occurrence of oxidatively modified proteins: an early event in experimental acute pancreatitis." Free Radic Biol Med **24**(3): 393-400.

Reuter, S., et al. (2010). "Oxidative stress, inflammation, and cancer: How are they linked?" Free Radic Biol Med **49**(11): 1603-1616.

Rhee, S. G. (1999). "Redox signaling: hydrogen peroxide as intracellular messenger." Exp Mol Med **31**(2): 53-59.

Rhoades, R., et al. (2009). Medical physiology : principles for clinical medicine, Philadelphia ; Lippincott Williams & Wilkins, 2009.

3rd ed.

Rigoulet, M., et al. (2011). "Mitochondrial ROS generation and its regulation: Mechanisms involved in H2O2 signaling." Antioxidants and Redox Signaling **14**(3): 459-468.

Rinderknecht, H. (1988). "Fatal pancreatitis, a consequence of excessive leukocyte stimulation?" International Journal of Pancreatology **3**(2-3): 105-112.

Rivera, A., et al. (2005). "The p53-induced gene-6 (proline oxidase) mediates apoptosis through a calcineurin-dependent pathway." J Biol Chem **280**(32): 29346-29354.

Rizzuto, R., et al. (2000). "Mitochondria as all-round players of the calcium game." Journal of Physiology-London **529**(1): 37-47.

Robb-Gaspers, L. D., et al. (1998). "Integrating cytosolic calcium signals into mitochondrial metabolic responses." EMBO Journal **17**(17): 4987-5000.

Robb-Gaspers, L. D., et al. (1998). "Integrating cytosolic calcium signals into mitochondrial metabolic responses." The EMBO Journal **17**(17): 4987-5000.

Roberts, S. E., et al. (2013). "The incidence of acute pancreatitis: impact of social deprivation, alcohol consumption, seasonal and demographic factors." Aliment Pharmacol Ther **38**(5): 539-548.

Roos, J., et al. (2005). "STIM1, an essential and conserved component of store-operated Ca2+ channel function." J Cell Biol **169**(3): 435-445.

Rosado, J. A., et al. (2002). "Effects of reactive oxygen species on actin filament polymerisation and amylase secretion in mouse pancreatic acinar cells." Cellular Signalling **14**(6): 547-556.

Rosenzweig, S. A., et al. (1983). "Identification and localization of cholecystokinin-binding sites on rat pancreatic plasma membranes and acinar cells: a biochemical and autoradiographic study." J Cell Biol **96**(5): 1288-1297.

Ross, D. (1997). "Quinone reductases." In: Guengerich FP, Sipes IG, McQueen CA, Gandolfi AJ, eds. **3**: 179–177.

Ross, M. F., et al. (2005). "Lipophilic triphenylphosphonium cations as tools in mitochondrial bioenergetics and free radical biology." Biochemistry (Mosc) **70**(2): 222-230.

Ross, Meredith F., et al. (2008). Rapid and extensive uptake and activation of hydrophobic triphenylphosphonium cations within cells.

Rottenberg, H. (1979). "The measurement of membrane potential and deltapH in cells, organelles, and vesicles." Methods Enzymol **55**: 547-569.

Rutter, G. A., et al. (1988). "Regulation of NAD+-linked isocitrate dehydrogenase and 2-oxoglutarate dehydrogenase by Ca2+ ions within toluene-permeabilized rat heart mitochondria. Interactions with regulation by adenine nucleotides and NADH/NAD+ ratios." Biochemical Journal **252**(1): 181-189.

Rutter, G. A., et al. (1989). "The binding of Ca2+ ions to pig heart NAD+-isocitrate dehydrogenase and the 2-oxoglutarate dehydrogenase complex." Biochemical Journal **263**(2): 453-462.

Ryter, S. W., et al. (2007). "Mechanisms of cell death in oxidative stress." Antioxid Redox Signal **9**(1): 49-89.

Saillan-Barreau, C., et al. (1998). "Transgenic CCK-B/gastrin receptor mediates murine exocrine pancreatic secretion." Gastroenterology **115**(4): 988-996.

Saito, Y., et al. (2006). "Turning point in apoptosis/necrosis induced by hydrogen peroxide." Free Radic Res **40**(6): 619-630.

Saluja, A. K., et al. (2007). "Why does pancreatic overstimulation cause pancreatitis?" Annu Rev Physiol **69**: 249-269.

Samad, A., et al. (2014). "Insulin Protects Pancreatic Acinar Cells from Palmitoleic Acid-induced Cellular Injury." J Biol Chem **289**(34): 23582-23595.

Sameshima, H., et al. (1993). "The role of tumor necrosis factor-alpha in the aggravation of cerulein-induced pancreatitis in rats." Int J Pancreatol **14**(2): 107-115.

Sandoval, D., et al. (1996). "The role of neutrophils and platelet-activating factor in mediating experimental pancreatitis." Gastroenterology **111**(4): 1081-1091.

Sanfey, H., et al. (1984). "The role of oxygen-derived free radicals in the pathogenesis of acute pancreatitis." Ann Surg **200**(4): 405-413.

Sanfey, H., et al. (1985). "The pathogenesis of acute pancreatitis. The source and role of oxygen-derived free radicals in three different experimental models." Ann Surg **201**(5): 633-639.

Saretzki, G., et al. (2003). "MitoQ counteracts telomere shortening and elongates lifespan of fibroblasts under mild oxidative stress." Aging Cell **2**(2): 141-143.

Sarr, M. G., et al. (1987). "The role of leukocytes in the production of oxygen-derived free radicals in acute experimental pancreatitis." Surgery **101**(3): 292-296.

Sateesh, J., et al. (2009). "Effect of antioxidant therapy on hospital stay and complications in patients with early acute pancreatitis: a randomised controlled trial." Trop Gastroenterol **30**(4): 201-206.

Sato, T. (1995). "Role of free radicals on canine bile-induced pancreatitis and effect of superoxide dismutase." Nippon Geka Gakkai zasshi **96**(6): 388-395.

Satoh, T., et al. (1997). "Changes in mitochondrial membrane potential during oxidative stress-induced apoptosis in PC12 cells." J Neurosci Res **50**(3): 413-420.

Scaduto Jr, R. C., et al. (1999). "Measurement of mitochondrial membrane potential using fluorescent rhodamine derivatives." Biophysical Journal **76**(1 I): 469-477.

Schäfer, M., et al. (2003). "Role of redox signaling in the autonomous proliferative response of endothelial cells to hypoxia." Circulation Research **92**(9): 1010-1015.

Schaller, S., et al. (2010). "TRO40303, a new cardioprotective compound, inhibits mitochondrial permeability transition." J Pharmacol Exp Ther **333**(3): 696-706.

Schild, L., et al. (1999). "Induction of permeability transition in pancreatic mitochondria by cerulein in rats." Mol Cell Biochem **195**(1-2): 191-197.

Schirmer, W. J., et al. (1989). "Recombinant human tumor necrosis factor produces hemodynamic changes characteristic of sepsis and endotoxemia." Arch Surg **124**(4): 445-448.

Schmid, A., et al. (1998). "Characterization of cell volume-sensitive chloride currents in freshly prepared and cultured pancreatic acinar cells from early postnatal rats." The Journal of Physiology **513**(Pt 2): 453-465.

Schneider, A., et al. (2002). "Animal models in alcoholic pancreatitis--what can we learn?" Pancreatology **2**(3): 189-203.

Schnekenburger, J., et al. (2005). "Protein tyrosine phosphatase κ and SHP-1 are involved in the regulation of cell-cell contacts at adherens junctions in the exocrine pancreas." Gut **54**(10): 1445-1455.

Schoenberg, M. H., et al. (1991). "The involvement of oxygen radicals in acute pancreatitis." Klin Wochenschr **69**(21-23): 1025-1031.

Schoenberg, M. H., et al. (1994). "Oxygen radicals in experimental acute pancreatitis." Hepatogastroenterology **41**(4): 313-319.

Schoenberg, M. H., et al. (1990). "Oxygen free radicals in acute pancreatitis of the rat." Gut **31**(10): 1138-1143.

Schulz, H. U., et al. (1999). "Oxidative stress in acute pancreatitis." Hepatogastroenterology **46**(29): 2736-2750.

Scott, P., et al. (1993). "Vitamin C status in patients with acute pancreatitis." Br J Surg **80**(6): 750-754.

Shalbueva, N., et al. (2013). "Effects of oxidative alcohol metabolism on the mitochondrial permeability transition pore and necrosis in a mouse model of alcoholic pancreatitis." Gastroenterology **144**(2): 437-446 e436.

Siech, M., et al. (1991). "Development of acute pancreatitis in rats after single ethanol administration and induction of a pancreatic juice edema." Int J Pancreatol **8**(2): 169-175.

Siech, M., et al. (1997). "Similar morphological and intracellular biochemical changes in alcoholic acute pancreatitis and ischemic acute pancreatitis in rats." Pancreas **14**(1): 32-38.

Siegel, D., et al. (1997). "The reduction of alpha-tocopherolquinone by human NAD(P)H: quinone oxidoreductase: the role of alpha-tocopherolhydroquinone as a cellular antioxidant." Mol Pharmacol **52**(2): 300-305.

Siegel, D., et al. (2004). "NAD(P)H:Quinone Oxidoreductase 1: Role as a Superoxide Scavenger." Mol Pharmacol **65**(5): 1238-1247.

Simms, H., et al. (1994). Polymorphonuclear leukocyte dysregulation during the systemic inflammatory response syndrome.

Siriwardena, A. K., et al. (2007). "Randomised, double blind, placebo controlled trial of intravenous antioxidant (n-acetylcysteine, selenium, vitamin C) therapy in severe acute pancreatitis." Gut **56**(10): 1439-1444.

Sjödin, L., et al. (1990). "Stimulation of pancreatic amylase release is associated with a parallel sustained increase of cytoplasmic calcium." Regulatory Peptides **30**(3): 239-253.

Skulachev, V. P., et al. (2009). "An attempt to prevent senescence: a mitochondrial approach." Biochim Biophys Acta **1787**(5): 437-461.

Smith, R. A., et al. (2012). "Mitochondrial pharmacology." Trends Pharmacol Sci **33**(6): 341-352.

Smith, R. A., et al. (2010). "Animal and human studies with the mitochondria-targeted antioxidant MitoQ." Ann N Y Acad Sci **1201**: 96-103.

Smith, R. A., et al. (2003). "Delivery of bioactive molecules to mitochondria in vivo." Proc Natl Acad Sci U S A **100**(9): 5407-5412.

Smith, R. A. J., et al. (2008). Mitochondria-targeted antioxidants in the treatment of disease. Ann N Y Acad Sci. **1147:** 105-111.

Snow, B. J., et al. (2010). "A double-blind, placebo-controlled study to assess the mitochondria-targeted antioxidant MitoQ as a disease-modifying therapy in Parkinson's disease." Mov Disord **25**(11): 1670-1674.

Soderberg, B. L., et al. (2003). "Fatty Acid Ethyl Esters: Ethanol Metabolites That Reflect Ethanol Intake." American Journal of Clinical Pathology. Pathology Patterns Reviews. **119**(Suppl 1): S94-S99.

Son, Y., et al. (2011). "Mitogen-Activated Protein Kinases and Reactive Oxygen Species: How Can ROS Activate MAPK Pathways?" J Signal Transduct **2011**: 792639.

Song, J. Y., et al. (2003). "Oxidative Stress Induces Nuclear Loss of DNA Repair Proteins Ku70 and Ku80 and Apoptosis in Pancreatic Acinar AR42J Cells." Journal of Biological Chemistry **278**(38): 36676-36687.

Soubannier, V., et al. (2009). "Positioning mitochondrial plasticity within cellular signaling cascades." Biochim Biophys Acta **1793**(1): 154-170.

Starkov, A. A., et al. (2004). "Mitochondrial alpha-ketoglutarate dehydrogenase complex generates reactive oxygen species." J Neurosci **24**(36): 7779-7788.

Steer, M. L., et al. (1991). "The role of oxygen-derived free radicals in two models of experimental acute pancreatitis: effects of catalase, superoxide dismutase, dimethylsulfoxide, and allopurinol." Klin Wochenschr **69**(21-23): 1012-1017.

Stone, J. R., et al. (2006). "Hydrogen peroxide: a signaling messenger." Antioxid Redox Signal **8**(3-4): 243-270.

Straub, S. V., et al. (2000). "Calcium wave propagation in pancreatic acinar cells: functional interaction of inositol 1,4,5-trisphosphate receptors, ryanodine receptors, and mitochondria." J Gen Physiol **116**(4): 547-560.

Strauss, M., et al. (2008). "Dimer ribbons of ATP synthase shape the inner mitochondrial membrane." EMBO J **27**(7): 1154-1160.

Streb, H., et al. (1984). "Effect of inositol-1,4,5-trisphosphate on isolated subcellular fractions of rat pancreas." J Membr Biol **81**(3): 241-253.

Streb, H., et al. (1983). "Release of Ca2+ from a nonmitochondrial intracellular store in pancreatic acinar cells by inositol-1,4,5-trisphosphate." Nature **306**(5938): 67-69.

Su, K. H., et al. (2006). "Review of experimental animal models of acute pancreatitis." HPB (Oxford) **8**(4): 264-286.

Sun, J., et al. (2001). "Classes of Thiols that Influence the Activity of the Skeletal Muscle Calcium Release Channel." Journal of Biological Chemistry **276**(19): 15625-15630.

Sung, K. F., et al. (2009). "Prosurvival Bcl-2 proteins stabilize pancreatic mitochondria and protect against necrosis in experimental pancreatitis." Exp Cell Res **315**(11): 1975-1989.

Sutton, H. C., et al. (1984). "Chelated iron-catalyzed OH. formation from paraquat radicals and H2O2: Mechanism of formate oxidation." Archives of Biochemistry and Biophysics **235**(1): 106-115.

Suzuki, H., et al. (1993). "Xanthine oxidase-mediated intracellular oxidative stress in response to cerulein in rat pancreatic acinar cells." Pancreas **8**(4): 465-470.

Suzuki, Y. J., et al. (1992). "Inactivation of rabbit muscle creatine kinase by hydrogen peroxide." Free Radic Res **16**(2): 131-136.

Suzuki, Y. J., et al. (1997). "Oxidants as Stimulators of Signal Transduction." Free Radical Biology and Medicine **22**(1–2): 269-285.

Szabo, C. (2003). "Multiple pathways of peroxynitrite cytotoxicity." Toxicol Lett **140-141**: 105-112.

Szabolcs, A., et al. (2006). "Beneficial effect of resveratrol on cholecystokinin-induced experimental pancreatitis." Eur J Pharmacol **532**(1-2): 187-193.

Szalai, G., et al. (1999). "Apoptosis driven by IP(3)-linked mitochondrial calcium signals." The EMBO Journal **18**(22): 6349-6361.

Sztefko, K., et al. (2001). "Serum Free Fatty Acid Concentration in Patients with Acute Pancreatitis." Pancreatology **1**(3): 230-236.

Szuster-Ciesielska, A., et al. (2001). "Oxidative stress in blood of patients with alcohol-related pancreatitis." Pancreas **22**(3): 261-266.

Takacs, T., et al. (2008). "The clinical relevance of experimental acute pancreatitis models." Orv Hetil **149**(42): 1981-1986.

Takekawa, M., et al. (2012). "Mitochondria take up Ca2+ in two steps dependently on store-operated Ca2+ entry in mast cells." Biological and Pharmaceutical Bulletin **35**(8): 1354-1360.

Teixeira, J., et al. (2015). Bridging the Gap Between Nature and Antioxidant Setbacks: Delivering Caffeic Acid to Mitochondria. Mitochondrial Medicine. V. Weissig and M. Edeas, Springer New York. **1265:** 73-83.

Telek, G., et al. (2001). "Differential upregulation of cellular adhesion molecules at the sites of oxidative stress in experimental acute pancreatitis." J Surg Res **96**(1): 56-67.

Telek, G., et al. (2001). "The first histological demonstration of pancreatic oxidative stress in human acute pancreatitis." Hepatogastroenterology **48**(41): 1252-1258.

Telek, G., et al. (1999). "Cerium-based histochemical demonstration of oxidative stress in taurocholate-induced acute pancreatitis in rats. A confocal laser scanning microscopic study." J Histochem Cytochem **47**(9): 1201-1212.

Tenner, S., et al. (2013). "American College of Gastroenterology guideline: management of acute pancreatitis." Am J Gastroenterol **108**(9): 1400-1415; 1416.

Tinel, H., et al. (1999). Active mitochondria surrounding the pancreatic acinar granule region prevent spreading of inositol trisphosphate ‐ evoked local cytosolic Ca2+ signals.

Toledano, M. B., et al. (2010). "Reining in H2O2 for Safe Signaling." Cell **140**(4): 454-456.

Tracey, K. J., et al. (1992). "Tumor necrosis factor and regulation of metabolism in infection: role of systemic versus tissue levels." Proc Soc Exp Biol Med **200**(2): 233-239.

Tretter, L., et al. (2000). "Inhibition of Krebs cycle enzymes by hydrogen peroxide: A key role of [alpha]-ketoglutarate dehydrogenase in limiting NADH production under oxidative stress." J Neurosci **20**(24): 8972-8979.

Tretter, L., et al. (2004). "Generation of reactive oxygen species in the reaction catalyzed by alpha-ketoglutarate dehydrogenase." J Neurosci **24**(36): 7771-7778.

Trimm, J. L., et al. (1986). "Sulfhydryl oxidation induces rapid calcium release from sarcoplasmic reticulum vesicles." Journal of Biological Chemistry **261**(34): 16092-16098.

Trnka, J., et al. (2015). "Lipophilic Triphenylphosphonium Cations Inhibit Mitochondrial Electron Transport Chain and Induce Mitochondrial Proton Leak." PLoS ONE **10**(4): e0121837.

Tsai, K., et al. (1998). "Oxidative stress: an important phenomenon with pathogenetic significance in the progression of acute pancreatitis." Gut **42**(6): 850-855.

Tsai, K., et al. (1998). "Oxidative stress: an important phenomenon with pathogenetic significance in the progression of acute pancreatitis." Gut **42**(6): 850-855.

Tsuji, N., et al. (1994). "Specific interaction of pancreatic elastase and leucocytes to produce oxygen radicals and its implication in pancreatitis." Gut **35**(11): 1659-1664.

Turrens, J. F. (2003). "Mitochondrial formation of reactive oxygen species." The Journal of Physiology **552**(Pt 2): 335-344.

Turrens, J. F., et al. (1982). "Hyperoxia increases H2O2 release by lung mitochondria and microsomes." Arch. Biochem. Biophys. **217**: 411-421.

Uden, S., et al. (1990). "Antioxidant therapy for recurrent pancreatitis: placebo-controlled trial." Aliment Pharmacol Ther **4**(4): 357-371.

Ueda, S., et al. (2002). "Redox control of cell death." Antioxid Redox Signal **4**(3): 405-414.

Ueda, S., et al. (2006). "What we learnt from randomized clinical trials and cohort studies of antioxidant vitamin?: Focus on Vitamin E and cardiovascular disease." Current Pharmaceutical Biotechnology **7**(2): 69-72.

Urunuela, A., et al. (2002). "Time-course of oxygen free radical production in acinar cells during acute pancreatitis induced by pancreatic duct obstruction." Biochim Biophys Acta **1588**(2): 159-164.

Uttara, B., et al. (2009). "Oxidative Stress and Neurodegenerative Diseases: A Review of Upstream and Downstream Antioxidant Therapeutic Options." Current Neuropharmacology **7**(1): 65-74.

Viedma, J. A., et al. (1992). "Role of interleukin-6 in acute pancreatitis. Comparison with C-reactive protein and phospholipase A." Gut **33**(9): 1264-1267.

Viola, H. M., et al. (2010). "Cross-talk between L-type Ca2+ channels and mitochondria." Clinical and Experimental Pharmacology and Physiology **37**(2): 229-235.

Viola, H. M., et al. (2010). "Cross-talk between L-type Ca^{2+} channels and mitochondria." Clin Exp Pharmacol Physiol **37**(2): 229-235.

Virlos, I. T., et al. (2003). "Intravenous n‐acetylcysteine, ascorbic acid and selenium‐based anti‐oxidant therapy in severe acute pancreatitis." Scandinavian Journal of Gastroenterology **38**(12): 1262-1267.

Voronina, S., et al. (2002). "Bile acids induce calcium signals in mouse pancreatic acinar cells: implications for bile-induced pancreatic pathology." J Physiol **540**(Pt 1): 49-55.

Voronina, S., et al. (2002). "Bile acids induce calcium signals in mouse pancreatic acinar cells: Implications for bile-induced pancreatic pathology." Journal of Physiology **540**(1): 49-55.

Voronina, S., et al. (2002). "Correlation of NADH and Ca^{2+} signals in mouse pancreatic acinar cells." The Journal of Physiology **539**(Pt 1): 41-52.

Voronina, S. G., et al. (2004). "Effects of secretagogues and bile acids on mitochondrial membrane potential of pancreatic acinar cells: comparison of different modes of evaluating ΔΨm." J Biol Chem **279**(26): 27327-27338.

Voronina, S. G., et al. (2010). "Dynamic Changes in Cytosolic and Mitochondrial ATP Levels in Pancreatic Acinar Cells." Gastroenterology **138**(5): 1976-1987.e1975.

Wan, M. H., et al. (2012). "Review of experimental animal models of biliary acute pancreatitis and recent advances in basic research." HPB (Oxford) **14**(2): 73-81.

Wan, M. H., et al. (2012). "Review of experimental animal models of biliary acute pancreatitis and recent advances in basic research." HPB **14**(2): 73-81.

Ward, J. B., et al. (1995). "Is an elevated concentration of acinar cytosolic free ionised calcium the trigger for acute pancreatitis?" The Lancet **346**(8981): 1016-1019.

Ward, J. B., et al. (1996). "Progressive disruption of acinar cell calcium signaling is an early feature of cerulein-induced pancreatitis in mice." Gastroenterology **111**(2): 481-491.

Watanabe, O., et al. (1984). Supramaximal caerulein stimulation and ultrastructure of rat pancreatic acinar cell: early morphological changes during development of experimental pancreatitis.

Weber, H., et al. (2007). "Hydrogen peroxide-induced activation of defense mechanisms against oxidative stress in rat pancreatic acinar AR42J cells." Free Radical Biology and Medicine **42**(6): 830-841.

Weber, H., et al. (2005). "Calpain activation contributes to oxidative stress-induced pancreatic acinar cell injury." Biochem Pharmacol **70**(8): 1241-1252.

Weber, H., et al. (1995). "Oxygen radical generation and acute pancreatitis: effects of dibutyltin dichloride/ethanol and ethanol on rat pancreas." Pancreas **11**(4): 382-388.

Weber, H., et al. (2013). "Calpain mediates caspase-dependent apoptosis initiated by hydrogen peroxide in pancreatic acinar AR42J cells." Free Radic Res **47**(5): 432-446.

Weber, H., et al. (1998). "Increased cytosolic Ca^{2+} amplifies oxygen radical-induced alterations of the ultrastructure and the energy metabolism of isolated rat pancreatic acinar cells." Digestion **59**(3): 175-185.

Werner, J., et al. (1997). "Pancreatic injury in rats induced by fatty acid ethyl ester, a nonoxidative metabolite of alcohol." Gastroenterology **113**(1): 286-294.

Werner, J., et al. (2001). "Linkage of oxidative and nonoxidative ethanol metabolismin the pancreas and toxicity of nonoxidative ethanol metabolites for pancreatic acinar cells." Surgery **129**(6): 736-744.

Werner, J., et al. (2002). Alcoholic pancreatitis in rats: injury from nonoxidative metabolites of ethanol.

Williams, D. A., et al. (2013). Compartmentalizing genetically encoded calcium sensors. Methods in Molecular Biology. **937:** 307-326.

Wilson, J. S., et al. (2003). "Role of Alcohol Metabolism in Alcoholic Pancreatitis." Pancreas **27**(4): 311-315.

Winterbourn, C. C. (1987). "The ability of scavengers to distinguish OH· production in the iron-catalyzed Haber-Weiss reaction: Comparison of four assays for OH·." Free Radical Biology and Medicine **3**(1): 33-39.

Winterbourn, C. C. (2008). "Reconciling the chemistry and biology of reactive oxygen species." Nat Chem Biol **4**(5): 278-286.

Winterbourn, C. C., et al. (2006). "Modeling the reactions of superoxide and myeloperoxidase in the neutrophil phagosome: implications for microbial killing." J Biol Chem **281**(52): 39860-39869.

Witt, H., et al. (2000). "Mutations in the gene encoding the serine protease inhibitor, Kazal type 1 are associated with chronic pancreatitis." Nat Genet **25**(2): 213-216.

Wittel, U. A., et al. (2003). "Oxygen radical production precedes alcohol-induced acute pancreatitis in rats." Pancreas **26**(4): e74-80.

Wojtala, A., et al. (2014). "Methods to monitor ROS production by fluorescence microscopy and fluorometry." Methods Enzymol **542**: 243-262.

Wollschlager, S., et al. (1997). "[Effect of selenium administration on various laboratory parameters in patients with acute pancreatitis]." Med Klin (Munich) **92 Suppl 3**: 22-24.

Woo, H. A., et al. (2010). "Inactivation of Peroxiredoxin I by Phosphorylation Allows Localized H_2O_2 Accumulation for Cell Signaling." Cell **140**(4): 517-528.

Wu, R.-F., et al. (2010). "Nox4-Derived H_2O_2 Mediates Endoplasmic Reticulum Signaling through Local Ras Activation." Mol Cell Biol **30**(14): 3553-3568.

Wyllie, A. H., et al. (1980). "Cell death: the significance of apoptosis." Int Rev Cytol **68**: 251-306.

Xia, Y., et al. (1997). "Superoxide and peroxynitrite generation from inducible nitric oxide synthase in macrophages." Proc Natl Acad Sci U S A **94**(13): 6954-6958.

Yadav, D., et al. (2013). "The epidemiology of pancreatitis and pancreatic cancer." Gastroenterology **144**(6): 1252-1261.

Yagci, G., et al. (2004). "Beneficial effects of N-acetylcysteine on sodium taurocholate-induced pancreatitis in rats." J Gastroenterol **39**(3): 268-276.

Yakes, F. M., et al. (1997). "Mitochondrial DNA damage is more extensive and persists longer than nuclear DNA damage in human cells following oxidative stress." Proc Natl Acad Sci U S A **94**(2): 514-519.

Yamasaki, M., et al. (2004). "Organelle selection determines agonist-specific Ca^{2+} signals in pancreatic acinar and beta cells." J Biol Chem **279**(8): 7234-7240.

Yamasaki, M., et al. (2005). "Role of NAADP and cADPR in the induction and maintenance of agonist-evoked Ca2+ spiking in mouse pancreatic acinar cells." Curr Biol **15**(9): 874-878.

Yang, A. L., et al. (2008). "Epidemiology of alcohol-related liver and pancreatic disease in the United States." Archives of Internal Medicine **168**(6): 649-656.

Yang, S. R., et al. (2006). "Cigarette smoke induces proinflammatory cytokine release by activation of NF-kappaB and posttranslational modifications of histone deacetylase in macrophages." Am J Physiol Lung Cell Mol Physiol **291**(1): L46-57.

Yasar, M., et al. (2002). "Has the oxidative stress a role in late phase of experimental acute necrotizing pancreatitis?" Hepatogastroenterology **49**(48): 1692-1695.

Yu, C., et al. (2015). "Inhibition of Ras signalling reduces neutrophil infiltration and tissue damage in severe acute pancreatitis." Eur J Pharmacol **746**: 245-251.

Yu, J. H., et al. (2014). "Oxidative stress and inflammatory signaling in cerulein pancreatitis." World Journal of Gastroenterology **20**(46): 17324-17329.

Yu, J. H., et al. (2005). "NADPH oxidase mediates interleukin-6 expression in cerulein-stimulated pancreatic acinar cells." The International Journal of Biochemistry & Cell Biology **37**(7): 1458-1469.

Yu, J. H., et al. (2000). "Suppression of Cerulein-Induced Cytokine Expression by Antioxidants in Pancreatic Acinar Cells." Lab Invest **82**(10): 1359-1368.

Yule, D. I., et al. (1988). "Oscillations of cytosolic calcium in single pancreatic acinar cells stimulated by acetylcholine." FEBS Lett **239**(2): 358-362.

Zechmann, B., et al. (2008). "Subcellular immunocytochemical analysis detects the highest concentrations of glutathione in mitochondria and not in plastids." Journal of Experimental Botany **59**(14): 4017-4027.

Zhang, H., et al. (2013). "IL-6 trans-signaling promotes pancreatitis-associated lung injury and lethality." J Clin Invest **123**(3): 1019-1031.

Zhang, S. L., et al. (2006). "Genome-wide RNAi screen of Ca^{2+} influx identifies genes that regulate Ca^{2+} release-activated Ca^{2+} channel activity." Proc Natl Acad Sci U S A **103**(24): 9357-9362.

Zhou, M. T., et al. (2010). "Acute lung injury and ARDS in acute pancreatitis: mechanisms and potential intervention." World J Gastroenterol **16**(17): 2094-2099.

Zhou, Z., et al. (1998). "Cytosolic and mitochondrial Ca^{2+} signals in patch clamped mammalian ventricular myocytes." The Journal of Physiology **507**(Pt 2): 379-403.

Ziegler, K. M., et al. (2011). "Validation of a novel, physiologic model of experimental acute pancreatitis in the mouse." Am J Transl Res **3**(2): 159-165.

Zima, A. V., et al. (2006). "Redox regulation of cardiac calcium channels and transporters." Cardiovasc Res **71**(2): 310-321.

Zorov, D. B., et al. (2009). "Regulation and pharmacology of the mitochondrial permeability transition pore." Cardiovasc Res **83**(2): 213-225.

APPENDIX – RELATED PUBLICATIONS

Huang W, **Cash N**, Wen L, Szatmary P, Mukherjee R, Armstrong J, Chvanov M, Tepikin AV, Murphy MP, Sutton R & Criddle DN. (2015) **Effects of the Mitochondria-Targeted Antioxidant Mitoquinone in Murine Acute Pancreatitis.** *Mediators of Inflammation* **2015**: 901780

Armstrong JA, **Cash N**, Soares PMG, Souza MHLP, Sutton R & Criddle DN. (2013) O**xidative stress in acute pancreatitis: lost in translation?** *Free Radical Research* 47(11):917-933